# PROCEEDINGS OF THE IRE®

*Published Monthly by*

The Institute of Radio Engineers, Inc.

VOLUME 46 — *February, 1958* — NUMBER 2

## CONTENTS



## ADVERTISING SECTION



THE COVER—This reproduction of Marconi's patent specification for a 25-centimeter wavelength transmitter reveals that parabolic reflector antennas were in use as early as 1896. This is but one of a surprisingly large number of microwave antenna and waveguide techniques that were developed by early radio experimenters in the decade prior to 1900. An interesting history of these early microwave developments is presented in a paper starting on page 405 of this issue.

# Scanning the Issue

**Scanning the Transactions** (p. 510)—A new monthly feature of the PROCEEDINGS starts in this issue which will endeavor to provide readers with an informative sample of new developments drawn from current issues of the TRANSACTIONS and other IRE publications.

**Microwave Antenna and Waveguide Techniques Before 1900** (Ramsey, p. 405)—Our modern microwave technology is built largely on discoveries and developments made between 1930 and 1940. We associate with this period the beginning of the microwave era. Nevertheless, the earliest radio experimenters, in the period from Hertz's initial demonstration of radio waves in 1888 to the turn of the century, did a surprising amount of work in the microwave portion of the spectrum before it was abandoned for the then more practical and useful lower frequencies. This historical review of these many early developments in the microwave art, at wavelengths as short as 5 millimeters and high peak powers, will come as an eye-opener to most readers.

**Ghost Modes in Imperfect Waveguides** (Jaynes, p. 416)—This paper calls attention to the fact that imperfections in a waveguide, such as that caused by placing a dielectric in it, can cause so-called ghost modes in the immediate vicinity of the imperfection which can give rise to unexpected and troublesome resonance effects, especially in high-power applications. These spurious resonances may in fact arise just outside the pass band of any periodic structure that has a localized imperfection. Indeed, they are analogous to certain phenomena that have been observed in imperfect crystals of solid-state materials. While this phenomenon probably has no practical applications, it does improve our understanding of an effect which can in some cases cause an operational breakdown in a wide variety of wave propagating systems.

**High-Frequency Crystal Filter Design Techniques and Applications** (Kosowsky, p. 419)—This paper gives what is probably the first description of the use of crystals in filters at frequencies well above one megacycle. High-frequency crystal filters are now becoming commercially available in the 5 to 40 mc range which exhibit performance characteristics previously attainable only at lower frequencies, with $Q$'s ranging from 50,000 to as high as 1,000,000 and bandwidths from one cycle to several hundred kilocycles per second. These high-frequency filters will find a substantial number of uses in single sideband, AM and FM equipment. For example, FM receivers can now be designed with only a single frequency conversion and a high-frequency IF, instead of multiple frequency conversions and a lower IF, without impairing adjacent channel selectivity and with a resultant reduction of circuits. The discussion of crystal filter design techniques presented here will be of major interest to a large number of communication equipment designers, while the easily followed presentation and the many interesting applications cited will appeal to all readers.

**Experimental 8-mm Klystron Power Amplifiers** (Bridges and Curnow, p. 430—By extending the emission capabilities of oxide cathodes to 1.5 a/sq. cm it has proven possible to produce 75 watts of cw power at 8 millimeter wavelengths. This represents a six-fold increase over previous efforts and the highest power yet reported at these high frequencies.

**FM Demodulator Time-Constant Requirements for Interference Rejection** (Baghdady, p. 432)—An investigation has been made of the demands imposed on FM receiver circuits in order that they may operate satisfactorily in the presence of a high level interfering signal. It is found that these demands require that ideally the time constants of the limiter and discriminator circuits must be short enough to cope with the sharp amplitude and frequency changes that are characteristic of a disturbed signal. These ideal requirements may conflict, however, with other fundamental requirements. Some simple schemes are discussed which minimize the conflict and greatly enhance the capture performance of a FM receiver.

**A High-Power Periodically Focused Traveling-Wave Tube** (Purl, *et al.*, p. 441)—Periodically placed magnets have been widely used in beam focusing systems in order to reduce the weight and power requirements of low-power traveling-wave tubes to more practical values. However, as the power of tubes increases so do the problems of focusing the higher density beams. This paper describes a periodically focused tube that operates from 2 to 4 kmc at the kilowatt level. The achievement of such relatively high powers and wide bandwidths by means of this type of focusing is a significant step forward in making high power twt's a practical component in systems.

**Index to IRE Standards on Definitions of Terms, 1942–1957** (p. 449)—The entire technical language of the radio engineer, from "A and R Display" to "Zoning," culled from some three dozen IRE Standards on the subject, is brought together in this one alphabetical list. Approximately 3500 terms, representing 15 years of work on the part of IRE technical committees, are listed with a reference to the Standard and the PROCEEDINGS page where the definition of each term may be found. This will be an invaluable aid to the future work of individuals and committees in this field, and stands as imposing evidence of the extent to which a still young profession has advanced.

**Measurement of the Radar Cross-Section of a Man** (Schultz, *et al.*, p. 476)—This is the first disclosure of quantitative measurements of how good a radar target a man is. CW Doppler measurements were performed at five frequencies ranging from 410 mc to 9375 mc, using both vertical and horizontal polarization from various angles. It was found that the side view of a man presented the smallest radar target and the back view the greatest, and that the difference between polarizations was greatest at the lowest frequency, with horizontal polarization giving the smaller value. While the authors do not go into the applications of these experiments, it is obvious that the data will be of value in the design of military equipment for the detection of the movement of small patrols.

**IRE Standards on Television: Measurement of Luminance Signal Levels** (p. 482)—This Standard specifies the method by which operating personnel of a television transmitter may measure the relative levels of monochrome signals or of the luminance portion of color signals by means of an oscilloscope. It is a revision of a 1950 IRE Standard covering monochrome signal levels which, because it came before the adoption of color television signal standards in the U. S., was inadequate for color signal measurements.

**Theory of Networks of Linearly Variable Resistances** (Levenstein, p. 486)—The design of analog devices frequently calls for the use of potentiometers whose output voltage must vary in some special nonlinear manner as the shaft is rotated. A variety of ingenious and intricate circuits have been devised to meet these requirements, designed, of necessity, by empirical methods. The guesswork that goes into the empirical approach does not, however, result in the best possible design. In this paper, the author proposes that a network consisting simply of fixed resistances and linear rheostats driven by a common shaft be used instead of nonlinear elements, and shows that such networks are very amenable to good design techniques. Moreover, he shows that these networks can be described in a mathematical form that is analogous to that of fixed RL networks. This leads to the development of a general theory of variable resistance networks that permits them to be analyzed by the more highly developed techniques of fixed RL network theory.

# Poles and Zeros

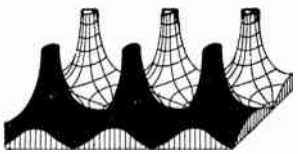

**Standards Story.** In this issue appears an index to all IRE Standards Definitions of Terms, indicating where you can find the terms defined in standard form. This should prove useful to the membership because in the past 15 years of intense IRE activity, these definitions have become scattered throughout nearly three dozen Standards publications. You may be surprised to note that the list approximates 3500 special words or definitions required to describe conditions or things in our profession. Thirty years ago there were only 277 such terms on the books. If one assumes a continued growth of terminology at this rate for the *next* thirty years, we would have 37,000 definitions. However, one can cast considerable doubt on such prediction by noting that a typical modern abridged American dictionary contains only about 60,000 words. In fact, it might be better to bet on Madison Avenue as a source of fifty per cent of our words in the next thirty years. It is also possible to conclude that at some point one has enough words available to adequately describe his activities, and then there will be those who will say we already have too many words, or at least we use them much too often.

It is interesting to note the many cases where technical words have grown out of something which started as typical American slang. To mention a few are monkey chatter, grass, blip, back porch, wow, and flutter. This seems to indicate a healthy down-to-earth view of our daily work, and it is to be hoped that electronics can continue to keep its feet on the ground.

The Standards Committee is certainly to be congratulated on the completion of an excellent job.

**Nothing New!** Immersed as we are in an industry producing things for tomorrow, it always comes as a rude shock to find that we are not nearly as modern as we had thought. Such a shock, or at least a mild thrill should come from the reading of the paper by John F. Ramsay in this issue entitled, "Microwave Antenna and Wave Guide Techniques Before 1900." To one who had the general impression that Barrow, Chu, Southworth, and a few other more or less modern investigators had discovered how to pour electromagnetic energy down the drain, this paper is deflationary. When one discovers that, prior to 1900 and Marconi, our predecessors were working in microwaves with wavelengths as short as 5 millimeters and peak powers of 70 kilowatts, one is even more hammered down in size.

When Marconi ultimately showed that the longer wavelengths seemed more suited for communication to great distances, the investigations into the microwaves of that date were dropped. We then had to wait many years for the amateurs to show the efficacy of the short waves, for radar to require development of the centimeter waves and microwave plumbing. Now we have come more than full circle to a realization that many valuable properties of the long waves have been overlooked.

A somewhat similar situation developed in the early 1920's. With the crowded radio broadcast spectrum of the time, investigators were looking into the possibilities of frequency modulation to reduce bandwidth. Carson published a paper which showed this was not possible, but which everyone interpreted as saying that frequency modulation had no value. Again, numerous years passed until Armstrong showed that there was value to the use of frequency modulation if we looked in exactly the opposite direction in which we had been looking in the early 1920's.

Apparently a scientific investigator is as easily bent as a twig in the wind.

**Students and High Schools.** One eminent engineering educator defines a vacuum tube as "something full of nothing out of which you get lots you do not expect." This might well be broadened to a definition for the whole field of electronics. Certainly the IRE STUDENT QUARTERLY, in its thorough and surprising manner, has come up with a result which was not fully expected.

While we hear much about the poor quality of our high school science educations, we actually seem to lack proof. This past fall our sister publication polled the junior and senior electrical engineering students asking their reactions towards their own high school preparations for engineering college. Many interesting comments were obtained, some of which were published in the December issue of the QUARTERLY (advertisement), but the most surprising result was that, in general, the students, about to become electronic engineers, are fairly well-satisfied with the job the high schools did on them.

To an educator interested in best utilizing the brains and intellectual man power of this country this raises a disquieting question. Are our high schools really that good, or does this mean that a student having a poor high school preparation stands no reasonable chance of reaching the junior or senior year of a modern electrical engineering curriculum? Having in the last several years talked to some hundreds of aspiring engineers who were not making it, we have a disquieting feeling that the latter conclusion may be correct. In any case, with Sputniks overhead, we have heard surprisingly little from the secondary school front as to what they are going to do about our need for better science and mathematics. As one educator has said, it is now time to start *learning* in our high schools and grade schools.—J. D. R.

# C. E. Granqvist

VICE-PRESIDENT, 1958

Carl Eric Granqvist was born on March 2, 1910 in Ljungby, Sweden. He has the Master of Art degree in electrical engineering from the Royal University of Technology in Stockholm.

Mr. Granqvist holds over twenty-five patents in the field of radio air navigation systems and devices. He has written several textbooks on radio and descriptive booklets on the aga talking beacon and the aga vhf direction finder.

As Chief Engineer of Svenska Aktiebolaget Gasaccumulator, Stockholm-Lidingo, Sweden, he was in charge of design, research and development in the electronic laboratory of that company. His present title is Director of that laboratory.

Mr. Granqvist belongs to the Swedish society, Svenska Teknologforeningen. He has also served as adviser on the Swedish Electric Committee and member of Standard Committee NK 50. He became an IRE Associate Member in 1946, and a Fellow in 1955.

# Microwave Antenna and Waveguide Techniques Before 1900*

JOHN F. RAMSAY†, ASSOCIATE MEMBER, IRE

*Summary*—Between the years 1888, when Hertz first launched electromagnetic radiation in the radio spectrum, and 1900, when Marconi was successfully establishing communication by radio, the scientific investigators of the time turned their attention to microwaves. Later, when it was found that the longer waves were more suited to long-distance communication, interest in the microwaves waned. Between 1888 and 1900, however, microwave devices and techniques had a rich development anticipating much of present-day practice. This paper reviews the antennas and waveguides of the period, with some reference to the associated microwave techniques then developed.

Apart from Hertz's dipole, with or without a plane reflector, the principal microwave antennas evolved were the cylindrical parabola, the dielectric lens, the waveguide cavity radiator, the radiating iris, and the electromagnetic horn.

Among the waveguides produced were the round, square, and rectangular forms, the open end being used as a radiator. The experimental development of these hollow pipe radiators appears to have anticipated Rayleigh's theoretical paper on waveguides by a number of years, Lodge discovering the mode property experimentally in 1894.

Many of the associated microwave components were of the "free-space" or quasi-optical type, rather than of the constrained or bounded type as common today, since the investigators between Hertz and Marconi were interested profoundly in the representation of optical phenomena at microwave frequencies. Hertz himself was the founder of "microwave optics," a classical subject being revived today.

Thus, we find the Hertzians making and using polarized mirrors, "cutoff" metal-plate gratings, quarter-wave and half-wave plates, artificial dielectrics, microwave absorbers, prisms of wax, ice, or liquid filled, or of artificial dielectric, totally reflecting prisms, lenses of sulphur, ebonite, wax, pitch, and so on, a wealth of microwave components only partly exploited today.

In the field of systems, measuring arrangements preponderated and included microwave spectrometers, interferometers, diffraction gratings plane or curved, transmission test sets, recorders, polarimeters. With the polarimeter, Bose established microwave analog physics, with macroscopic models of molecules subjected to microwave radiation. Otherwise, representations of optical phenomena were made with the enormous scale advantage arising from the use of microwaves. The properties of dielectrics, particularly anomalous dispersion, were studied and measured extensively.

All of this microwave work was carried out using spark discharge generators, often of considerable peak power, and with surprising accuracy. For detection, many devices were investigated, the most popular being the semiconducting coherer and the gaseous discharge tube.

## Introduction

In 1888, Hertz launched decimeter-wave radiation from a parabolic mirror antenna fed by a dipole. The dipole was excited by spark discharges produced by an induction coil. The radiation was received on a similar parabolic mirror antenna and the dipole was transmission line fed to a spark gap detector behind the mirror. The wavelength was 66 cm.

With this simple microwave apparatus Hertz conducted a series of experiments of great importance. First, he established action at a distance. Second, he showed the action was communicated to a distance by a wave motion exactly analogous to the known wave motion characterizing visible light. Third, he substantiated experimentally the theoretical predictions of James Clerk-Maxwell that the waves known to account for optical phenomena were electromagnetic, by the completeness of his experimental demonstrations and his accompanying theoretical analysis.

Hertz showed that his "electric waves" traveled in straight lines (although he surmised that diffraction would take place too). Shadows could be produced by obstacles. Different substances, whether solid, liquid, or gaseous, transmitted or absorbed the waves by different amounts. The waves could be reflected from walls or conducting metallic sheets. Standing waves were obtained which allowed the wavelength to be obtained. The shift of the pattern occasioned by the interposing of a dielectric obstacle allowed the properties of dielectrics to be investigated.

With oblique incidence on a conducting sheet, Hertz found the angle of reflection was equal to the angle of incidence. Using an opaque prism in the path of the radiation, the refracted waves were found to follow the optical law of refraction. The main features of geometrical optics were established.

The standing-wave experiments and the reinforcing action of a reflector behind a dipole radiator emphasized the wave nature of the radiation, being simple illustrations of interference. Just as Young had provided the first means of determining the wavelength of visible light by an interference experiment, so Hertz determined the first radio wavelength using the same principle.

In his experiments, Hertz observed from the start that the microwave radiation was strongly polarized. He pursued this feature making it both an experimental technique and an elucidation of the Maxwellian character of the waves. A new component that appeared, unknown to optics, was the grid of parallel wires, where the wire spacing was a small fraction of the wavelength. In one striking experiment, the transmitter and receiver antennas were cross-polarized and a grid introduced in the path with its wires at 45°. A response was obtained on the receiver previously inactive. "Clearly," wrote

* Original manuscript received by the IRE, September 9, 1957.
† Canadian Marconi Co., Montreal, Quebec, Canada; formerly with Marconi's Wireless Telegraph Co., Ltd., Chelmsford, Essex, England.

Hertz, "the screen resolves the advancing oscillation into two components and transmits only that component which is perpendicular to the direction of its wires. This component is inclined at 45° to the focal line of the second mirror, and may thus, after being again resolved by the mirror, act upon the secondary conductor. The phenomenon is exactly analogous to the brightening of the dark field of two crossed Nicols by the interposition of a crystalline plate in a suitable position."[1]

Hertz was fully aware that he had discovered radio-frequency optics, where the phenomenology of optics could be represented by microwaves. "It is a fascinating idea," he wrote, "that the processes in air which we have been investigating represent to us on a million-fold larger scale the same processes which go on in the neighborhood of a Fresnel mirror or between the glass plates used for exhibiting Newton's rings."[1]

It is important to notice that directive antennas played a major part in Hertz's system, providing him with a laboratory microwave link. In the path of the beam he introduced components and devices of a quasi-optical (the adjective proposed by Lodge) character which contributed to the realization of a microwave optical system as known today.

The success of Hertz's experiments attracted universal attention. Maxwell's theory was correct; light was an electromagnetic phenomenon. The scientific world, to whom electromagnetism was then the major interest, immediately took up the study of Hertz's waves and their optical implications. A school of investigators known as "the followers of Hertz," or as we may say now "the Hertzians," repeated Hertz's experiments and analytical investigations and extended the field of the work considerably. It was at this time that the divorce of optics from electromagnetism began to appear, contrary to what was expected. The electrically-minded investigators took greater interest in the generators and receivers and regarded the optical representations as well established and less important. On the other hand, physicists imbued with the long history of classical optics found in the new technique a fresh interest and the possibility of experimental verification of much that previously had been theoretical conjectures only. Of the latter group, Righi of Bologna was the most outstanding; his book, "L'Ottica delle Oscillazioni Elettriche," is a treatise on microwave optics.[2]

The young Marconi, inspired by Righi's work, conceived the idea of modulating the generator so that intelligence could be transmitted on the radio-frequency optical link. In an era of wire and cable telegraphy this was a major practical application of Hertz's apparatus, and of other components, notably the Branly-Lodge coherer detector developed by the Hertzians. Using two Hertz-type parabolic reflectors separated by a range of four miles on Salisbury Plain in England in 1897, Marconi proved to the British Post Office that his system of "wireless" telegraphy on a wavelength of 25 cm was completely successful. Marconi's consummate engineering skill dwarfed Hertz's scientific virtuosity. Today, the name Marconi is a household word; Hertz is still a textbook reference.

As time went on the followers of Hertz split. The electrically-minded joined the many followers of the youthful Marconi, the optically-minded reducing to a small minority. Other contemporary scientific advances, notably the discovery of X rays and electrons, tended to remove the scientific interest from microwave optics. Until 1900, it hardly existed as a subject. When the followers of Marconi found that longer wavelengths were more suited for communication to longer distances and that unexplained vagaries in communication at these longer wavelengths existed, microwaves vanished from wireless telegraphy, and the new problems of the longer wave radio also attracted the scientists.

With the return to microwaves in our own time, it is amazing to find the extent of the development between Hertz and Marconi. This paper illustrates the development with special reference to the directive antennas that were produced. One important nonoptical type was the hollow pipe waveguide radiator. Since antenna techniques are partly optical and partly electrical, the quasi-optical components of the Hertzians are described also.

## Parabolic Cylinder Antennas of Hertz, Righi, and Marconi

The optical properties of a parabolic reflector were well known to the Hertzians. A source at the focus would provide a "parallel" beam. Hence when Hertz found a dipole "source," he wrote, "As soon as I had succeeded in proving that the action of an electric oscillation spreads out as a wave into space, I planned experiments with the object of concentrating this action and making it perceptible at greater distances by putting the primary conductor (*i.e.*, *dipole*) in the focal line of a large concave parabolic mirror."[1] It is interesting to note that Hertz's need for an antenna was the same as Marconi's, *viz.*, to make the effects "perceptible at greater distances." Antenna gain was appreciated at a very early stage in radio!

Hertz's reflector was made of sheet zinc mounted on a timber frame (Fig. 1). The horizontal aperture was 1.2 m and the vertical aperture 2 m. The focal length was only 12.5 cm, the parabola extending forward of the focal plane to make the over-all depth of the mirror 70 cm. Since the wavelength was 66 cm, it will be appreciated that this was a very small antenna when measured in wavelengths. A most optimistic estimate of the 3-db beamwidth in the horizontal plane would be 35°;

[1] H. Hertz, "Electric Waves," Macmillan and Co., Ltd., London, Eng.; 1893.
[2] A Righi, "L'Ottica delle Oscillazioni Elettriche," N. Zanichelli, Bologna, Italy; 1897.

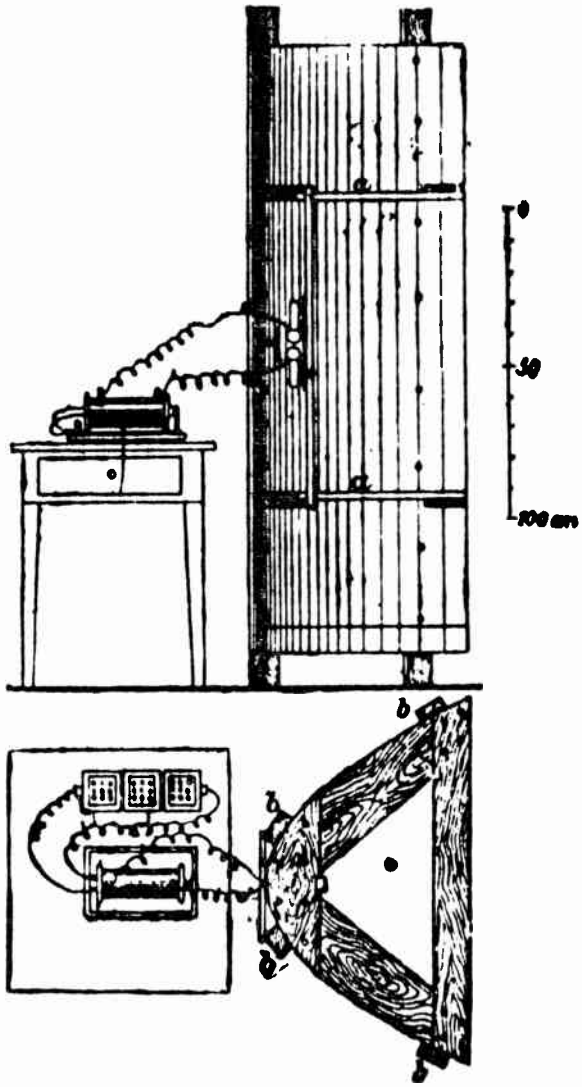


(a)

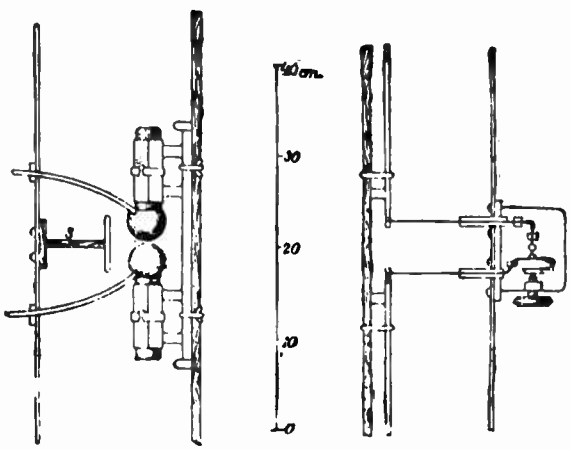


(b)

Fig. 1—(a) Hertz's parabolic reflector antenna for radiating on a wavelength of 66 cm (1888). (b) Hertz's sketches of his dipole feed arrangements for 1) transmitting and 2) receiving. (*Courtesy of Macmillan and Co., Ltd., and St. Martin's Press, Inc.*).

the beamwidth in the vertical plane would be around 80°. Such beamwidths resemble those used nowadays on "feeds" for parabolic antennas. It is surprising that Hertz was able to do so much fundamental work with these broad beams. He was often troubled by unwanted reflections from room surroundings, no doubt brought about by the use of the broad-beam antennas.

Righi, on the other hand, wishing to approach more closely to optics, worked on 3 cm and 10 cm (the *X* and *S* bands of today) with smaller parabolic cylinder reflectors.[2] Measured in wavelengths, however, the antennas were larger than those of Hertz, and very much sharper beams must have resulted. In one of Righi's illustrations he shows a parabolic cylinder used in, presumably, an *X*-band spectrometer. He did perform, however, many quasi-optical experiments in general, and must have used the parabolic cylinder antennas extensively, as in the Hertzian standing-wave experiment of Fig. 2.

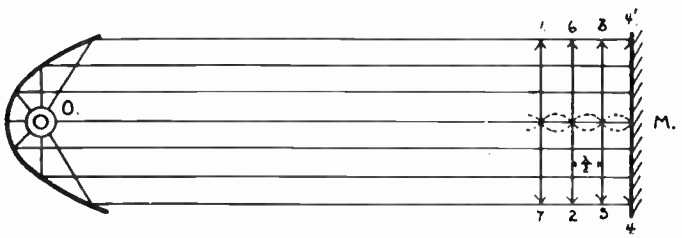


Interference by reflection from a single mirror, M. 1, 2, 3, etc., represent wave fronts differing in phase by a half period, 1 to 4 being direct and 4′ to 7 reflected and reversed in sign. The planes in which two opposite wave fronts, 4–4′, 5–3, 2–6, etc., meet are interference stripe, separated by a half wavelength, λ/2. (Poincaré.)

Fig. 2—Standing waves in free space produced by a reflecting surface. (Poincaré's drawing of Hertz's experiment.) (*Courtesy of Constable and Co., Ltd.*)

Marconi adopted the cylindrical parabola in his early 25-cm experiments, as his first patent of 1896 shows (Fig. 3).

Instead of a single spark gap, a multiple gap due to Righi was used in the focal line. Marconi had observed the need for sizeable apertures as he stated that the aperture of the antenna should be more than two wavelengths.[3]

Trouton of Dublin made copies of Hertz's apparatus, including the antennas, and repeated the optical experiments, extending the polarization analysis, and investigating the propagation into water filling a large tank made of paraffin wax.[4]

Bose of Calcutta, in 1897, was using a reflector in the form of a portion of a circular cylinder for microwave optical investigations at a wavelength of 5 mm.[5]

[3] G. Marconi, British Patent Specification No. 12039. Her Majesty's Stationery Office, June 2, 1896.

[4] F. J. Trouton, "Repetition of Hertz's experiments and determination of the vibration of light," *Nature*, vol. 39, pp. 391–393; February 21, 1889.

[5] J. C. Bose, "Collected Physical Papers," Longmans, Green and Co., New York, N. Y.; 1927.

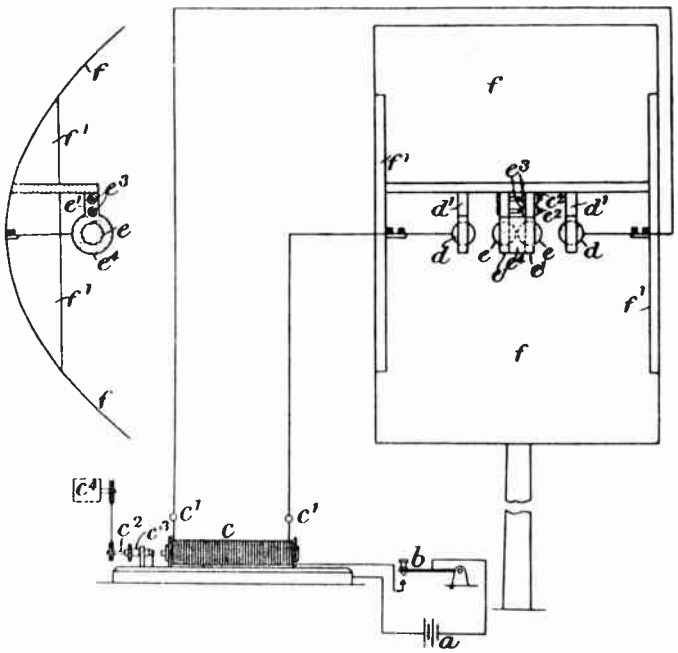


Fig. 3—Marconi's parabolic reflector antenna for transmitting information at a wavelength of 25 cm (1896). (Reproduced from Brit. Pat. Spec. No. 12039, June 2, 1896.)

The popularity of the parabolic cylinder in the 90's was no doubt due to the ease with which it could be constructed. Today in an age of improved constructional techniques, the doubly-curved paraboloidal reflector takes first place and the parallel beams the Hertzians expected but rarely obtained are now possible.

## Microwave Lenses of Lodge, Righi, Bose, and Fleming

It was natural in the early microwave optics for the investigators to consider lenses. Hertz had established refraction through a prism of pitch at radio frequencies. Lodge, who knew Hertz personally, and had translated his papers for *Nature*, in 1889 collaborated with Howard in building a cylindrical lens of pitch.[6]

Lodge's lens was 1 m square, with a focal length of 51 cm, and a thickness at the center of 21 cm. The weight was 336 pounds. As the wavelength was found to be 101 cm, this lens antenna was a very small one, measured in wavelengths. Since it was only about one wavelength square, the 3-db beamwidth would be 50° at the best. Lodge found difficulty in distinguishing any definite signs of a focus. This is not surprising, since the focal spot (or Airy disk of optics) would be nearly as large as the lens. The device was in reality a diffracting obstacle, and thus could give some antenna gain. Lodge found the received signal on a Hertzian link was increased using the "lens." Later, in 1894, he used a 9-inch-diameter glass lens on (probably) 4000 mc, where he was able to demonstrate a positive focusing action.

[6] O. J. Lodge and J. L. Howard, "On the concentration of electric radiation by lenses," *Nature*, vol. 40, p. 94; May 23, 1889.

In Italy, Righi[2] made microwave lenses of paraffin and of sulphur. These lenses were 32 cm in diameter with a focal length of 50 cm. The thickness at the center was 7 cm. He claimed to have good results. As he used wavelengths down to 3 cm, it is highly likely that his results were superior to those of Lodge due to the increased aperture in wavelengths. The optical effects would be more marked.

Bose contributed to microwave lenses in a major way in originating techniques.[5] He used 5 mm as wavelength for systematic measurements. First, using a spectrometer and the principle of total internal reflection he measured the refractive index of sulphur finding a value of 1.734.[7] Second, he was able to calculate the profiling of a sulphur lens. Third, he put the lens at the end of a tube, *i.e.*, devised a "shielded-lens" antenna (Fig. 4). Fourth, in order to avoid unwanted reflections from the inside of the tube, he made extensive investigations of materials for coating the tube, *i.e.*, looked for a suitable "microwave absorber." He found blotting paper dipped in electrolyte to be the most satisfactory absorber.

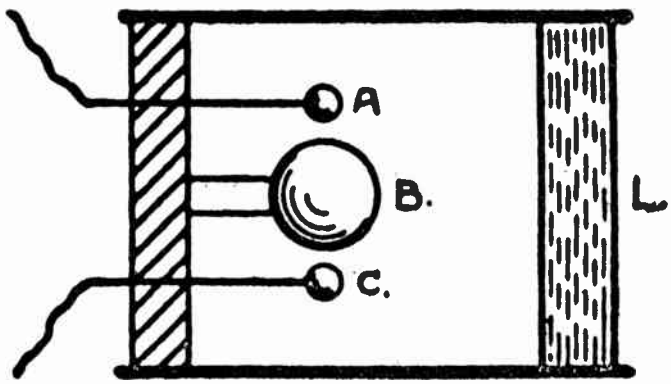


Bose's oscillator. The platinum sphere *B*, which is insulated, is the seat of the oscillations. The spheres *A* and *C* are connected to the induction coil. *L* is a cylindrical lens for concentrating the radiation. (Bose's caption.)

Fig. 4—Shielded lens antenna of Bose for radiating on wavelengths between 5 mm and 2.5 cm (1897). (*Courtesy of Longmans, Green and Co.*)

The diameter of Bose's lens was only about 1 inch so that, like many of the Hertzians, he used a relatively broad beam.

Fleming (later inventor of the thermionic diode) used a cylindrical lens of paraffin wax to demonstrate microwave optical effects.[8] As the aperture was only about 1 λ at a wavelength of 20 cm the lens action was, like Lodge's large lens, indistinct. Fleming did indeed express surprise that he succeeded in obtaining quasi-optical results at all, with such small components.

Of all the experimenters, it would appear that Righi alone succeeded in building microwave lenses of ade-

[7] J. C. Bose, "The refraction of electric waves," *Nature*, Sci. Amer. Suppl.; December 3, 1898.

[8] J. A. Fleming, "The Principles of Electric Wave Telegraphy and Telephony," Longmans, Green and Co., New York, N. Y.; 1906.

quate enough aperture to give convincing performance.

Although artificial dielectrics were devised by the followers of Hertz, and an artificial dielectric prism was actually investigated, it would appear that no one ever considered building a lens of artificial dielectric.

## Hollow Pipe Radiators of Lodge, Bose, and Fleming

The first hollow pipe or "waveguide" radiators were demonstrated at the Royal Institution in London on Friday, June 1, 1894, by Lodge in the course of his memorial lecture on "The Work of Hertz and Some of His Successors."[9]

Lodge's waveguide radiator (Fig. 5) consisted of a short length of copper tube closed at one end and open at the other. A spark gap was mounted in the tube and the leads to the induction coil were taken out through small holes in the closed end of the copper tube. Microwave radiation generated by the spark discharge was launched down the tube, and proceeded to free space from the open end. A broad radio-frequency transmitting beam was thereby obtained.

For receiving, a similar tube was used, closed at one end, a glass tube containing coarse iron filings, *i.e.*, a "coherer,"[10] replacing the spark gap of the transmitter.

Lodge called his antennas "copper hats." Referring to the mounting of the coherer tube, he said:

"Sometimes the tube is put lengthways in the hat instead of crossways, which makes it less sensitive, and has also the advantage of doing away with polarizing, or rather analyzing, power of a crossway tube."[9]

It is evident that Lodge had discovered the mode property of propagation in a hollow tube: this was to be explained later by Lord Rayleigh in 1897.[11] With the "crossway" disposition the coherer would be responsive to the $TE_{11}$ mode and therefore polarization sensitive. With the coherer lying along the axis of the tube it would be sensitive to the $TM_{01}$ mode, which has circular symmetry. The radiation pattern (for reception) for the latter mode has a null on axis. Lodge mentioned that he mounted his copper hat "with its mouth turned well askew to the source," a factor contributing to $TM_{01}$ detection at the expense of $TE_{11}$ detection.

In order to reduce the transmitter power radiated, the copper hat was "stopped down by a diaphragm plate with holes in it of varying size" clamped to it. By this artifice Lodge had secured a waveguide cavity subject to different amounts of radiation damping. Here too were some of the first radiating irises, used as attenuators. No doubt some narrowing of the spark spectrum

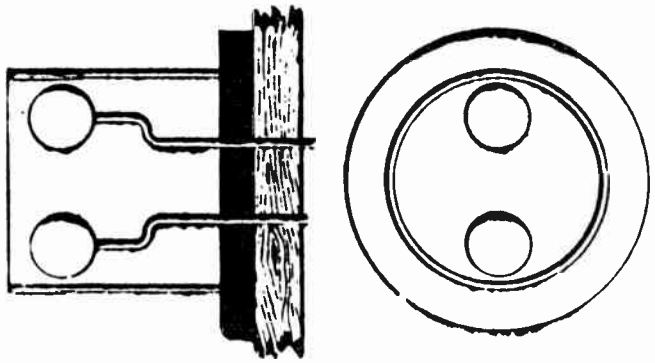

Dr. Lodge's hollow cylindrical radiator, arranged horizontally against the outside of a metal-lined box. Emitting three-inch waves. (Lodge's caption.)

(a)

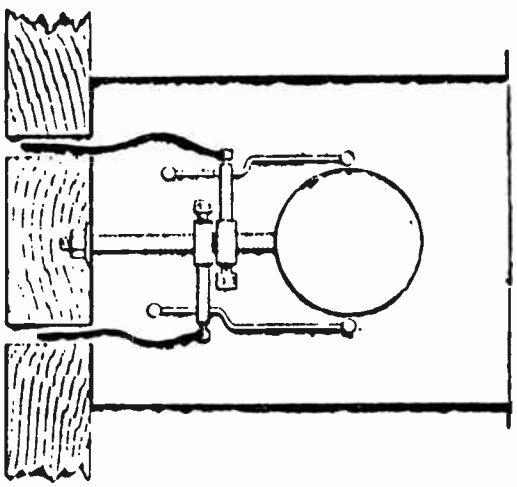

Spherical radiator for emitting a horizontal beam, arranged inside a copper hat, fixed against the outside of a metal-lined box. The wires pass into the box through glass tubes not shown. (Lodge's caption.)

(b)

Fig. 5—Hollow pipe waveguide radiators of Lodge for transmitting on centimeter wavelengths (1894). For reception a "coherer" replaced the spark gap in the tube. (*"The Electrician" Printing and Publishing Co., Ltd.*)

was also obtained by their use. In all cases, it appears a $TE_{11}$ mode was radiated from the transmitter.

Lodge used wavelengths of $7\frac{1}{2}$ cm and about 20 cm. He at one time made an estimate of 70-kw peak power as obtainable from an induction coil: this is a surprising figure. There is no doubt that power availability was not a major difficulty with the followers of Hertz. Given very good screening of the coil and all leads, microwave power was obtainable. This screening requirement may account for the appearance of waveguides.

Lodge's laboratory equipment for demonstrating microwave phenomena, using waveguide radiators for transmission and reception, is shown in Fig. 6. Note the prism of paraffin and the polarizing grid, two of Hertz's components on a much smaller scale.

Bose,[8] in India, between 1895 and 1897, used hollow tubes of either circular or square section as waveguides

[9] O. J. Lodge, "Signalling through Space without Wires," "The Electrician" Printing and Publishing Co., Ltd.; London, Eng., 1898.

[10] O. J. Lodge, "The history of the coherer principle," *Electrician;* November 12, 1897.

[11] Lord Rayleigh, "On the passage of electric waves through tubes, or the vibrations of dielectric cylinders," *Phil. Mag.*, vol. 43, pp. 125–132; February, 1897.

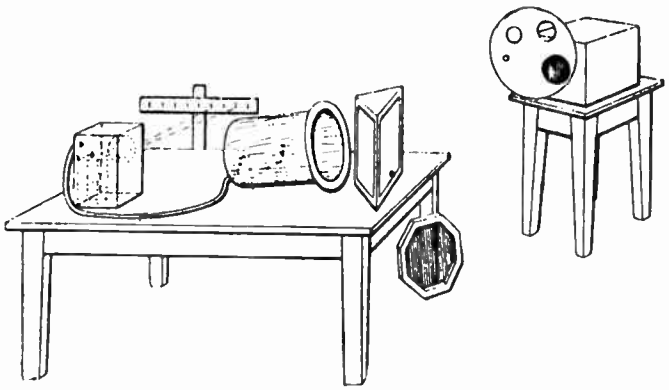

General arrangement of experiments with the copper "hat," showing metal box on a stool, inside which the radiators were fixed; the copper hat containing the coherer, with the metal box containing battery and galvanometer coil connected to it by a compo pipe conveying the wires; a paraffin prism; and a polarizing grid. (Lodge.)

Fig. 6—Microwave equipment of 1894. Lodge's drawing of his quasi-optical bench using waveguide antennas at a wavelength of about 20 cm (June 1, 1894). (*"The Electrician" Printing and Publishing Co., Ltd.*)

and waveguide radiators on wavelengths between 5 mm and 2.5 cm. Sometimes a small lens was fitted to the radiating end of the tube as has been described (Fig. 4). At Bose's lowest frequencies, his tubes would behave as slightly oversize waveguides, as the width was around 1 inch. At 5 mm, however, the tube would act more as a shield, liable to produce higher order modes, whence Bose's search for absorbent material. His adoption of hollow tubes was probably based on the use of metal tubes in telescopes and microscopes.

Fleming[8] gave lecture demonstrations on the optical features of Hertzian waves, following very closely Lodge's celebrated Royal Institution lecture of 1894. However, it is exceedingly interesting for us to find that he had replaced Lodge's round tube radiators by rectangular boxes, resembling the rectangular waveguide of the present day. Fleming used a wavelength of about 20 cm.

An inspection of the diagrams (Fig. 7) of Fleming's equipment indicates 1) that the polarization is parallel to the broad face instead of the narrow face as in a dominant-mode waveguide and 2) that the rectangular tubes would act more as cut-off attenuators than as waveguides. As, however, the spectrum of the spark would have many higher frequency components, it is likely that the boxes radiated significant power. Fleming's comment that the excellence of the quasi-optical demonstrations was surprising, having regard to the orders of magnitude in his system, may be explained, in fact, by his having very much shorter waves present.

Lodge, Bose, and Fleming must all have unconsciously used the high-pass filter property of waveguides, for the noisy sparks would be likely to have an enormous low-frequency spectral content. All three resorted to, and emphasized the need for screening the transmitting equipment.

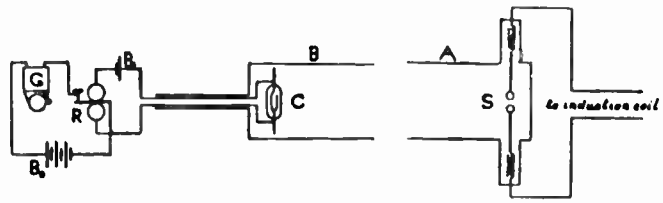


Apparatus for producing and detecting electric waves. *S*, spark balls in metal box, *A*, with open mouth; *C*, coherer in metal box; *B*, with open mouth; *R*, relay; *G*, electric bell; $B_1$, relay battery; $B_2$, electric bell battery.

(a)

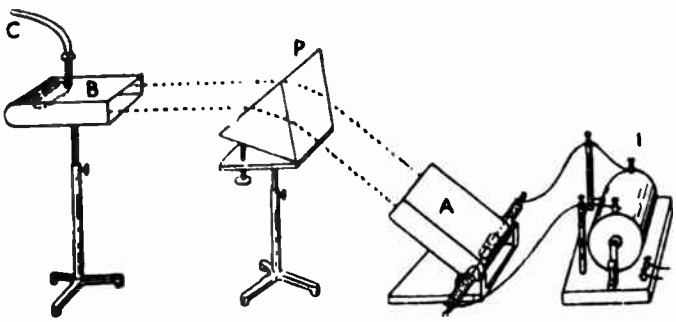


Refraction of an electric beam by a paraffin prism.

(b)

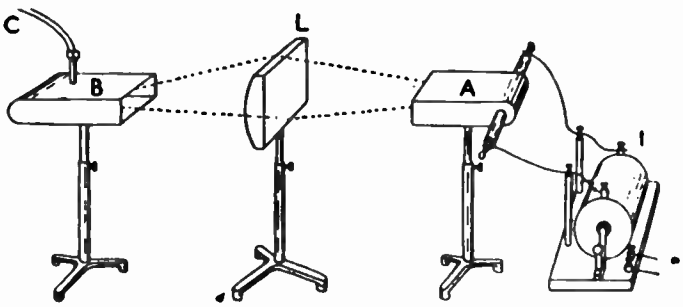


Convergence of an electric beam by a paraffin lens.

(c)

Fig. 7—Microwave-optical equipment and experiments of Fleming showing rectangular waveguide antennas used at a wavelength of 20 cm (1900). (Captions by Fleming.) (*Courtesy of Longmans, Green and Co.*)

The fact that they discovered the radiation could be led out of the transmitter box by a hollow tube represented a major step, as we now know, on the evolution of microwave transmission technique.

In radiating to free space from the open end of a hollow pipe, Lodge, Bose, and Fleming found a directive radiator unknown to optics or to Hertz. Bose was to make the next significant step.

## The Electromagnetic Horn Antenna of Bose

In 1897, Bose gave a lecture at the Royal Institution in London on the quasi-optical researches he had been carrying out with "electric waves" at a wavelength of 5 mm.[5] For demonstration purposes he had

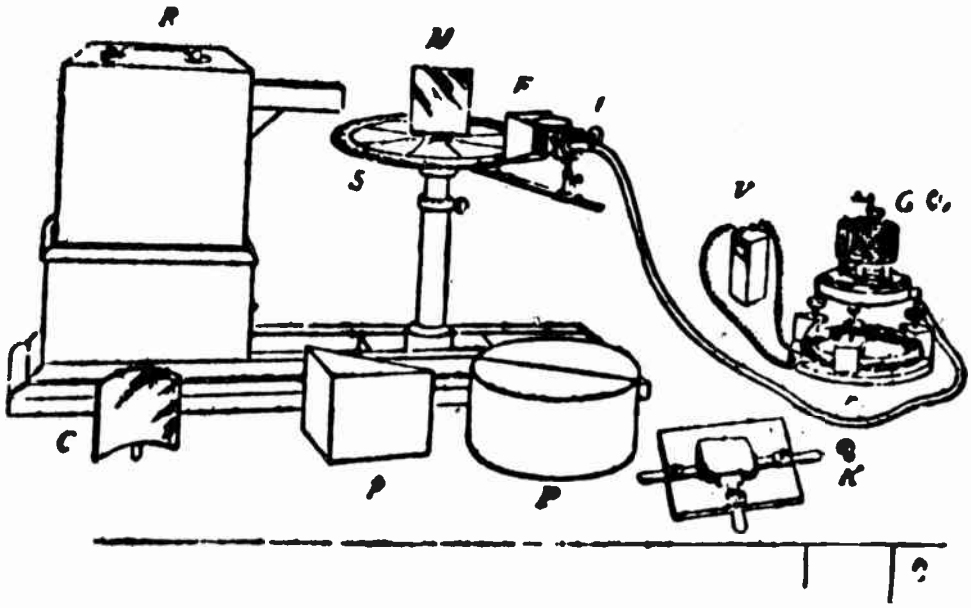

Arrangement of the apparatus. *R*, radiator; *S*, spectrometer-circle; *M*, plane mirror; *C*, cylindrical mirror; *p*, totally reflecting prism; *P*, semicylinders; *K*, crystal-holder; *F*, collecting funnel attached to the spiral spring receiver; *t*, tangent screw, by which the receiver is rotated; *V*, voltaic cell; *r*, circular rheostat; *G*, galvanometer. (Bose's caption.)

Fig. 8—Electromagnetic horn receiving antenna on microwave spectrometer used for quasi-optical demonstrations by Bose (1897). Transmitting antenna is square waveguide radiator. Wavelengths 5 mm–2.5 cm. (*Courtesy of Longmans, Green and Co.*)

brought from India a microwave spectrometer complete with screened transmitter and a receiver that rotated around the spectrometer table. Numerous quasi-optical components were also associated with this equipment for use in the demonstrations. A diagram of the equipment still exists (Fig. 8).

An inspection of Bose's receiver arrangements shows that the receiving antenna was a pyramidal electromagnetic horn, as we now call it. Bose termed his antenna a "collecting funnel," a colloquial but more vivid description. To this funnel a semiconducting detector of a multiplicity of touching spiral springs developed by Bose was connected (Fig. 9).[12]

Bose had already used waveguiding tubes—one is shown on his transmitter—so that it is natural he would conjecture that by increasing the cross section, a receiving aperture would collect more energy. This aperture could be attached to a smaller tube by tapering it down to fit, *i.e.*, by a hollow truncated pyramid construction, whence his pyramidal funnel. Thus, Bose made the first flared waveguide or small electromagnetic horn. As with so many of the components developed by the followers of Hertz, the horn was used for investigations in microwave optics as is evident in Fig. 8.

## Polarization Techniques Before 1900

Hertz initiated techniques on microwaves based on the polarization properties of electromagnetic waves. He showed that his dipole transmitter and loop receiver were linearly polarized and that the linear polarizations were substantially unaffected on reflection from plane or parabolic mirrors. He made exact studies of the polarizations in the near fields of primary and secondary radiators. His principal invention, however, was the screen or grating, a grid of parallel wires, which he described as follows:

"I next had made an octagonal frame, 2 meters high and 2 meters broad; across this were stretched copper wires 1 mm thick, the wires being parallel to each other and 3 cm apart."[1]

At a wavelength of 66 cm as used by Hertz, this screen would reflect 96 per cent of the incident power in a plane wave normally incident and polarized linearly parallel to the wires.

If however, the incident wave were polarized at right angles to the wires, most of its power would be transmitted *through* the screen. Such a device might have been called a "transflector," transmitting when the polarization was perpendicular and reflecting when the polarization was parallel to the wires.

Hertz discovered the sensitivity inherent in a "cross-polarized" link, where the transmitter and receiver polarizations are perpendicular. As referred to in the Introduction, he showed that such an arrangement resembled the crossed Nicols of optics, and in fact constituted a microwave polarimeter.

This attracted the attention of Bose who built microwave polarimeters on 5-mm wavelength with crossed gratings at the transmitter and receiver (see

[12] J. C. Bose, "On a complete apparatus for the study of the properties of electric waves," *Elec. Eng. London;* October 2, 1896.

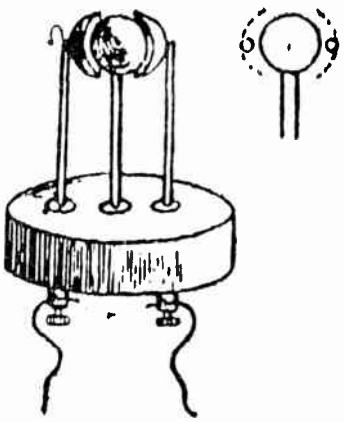

The radiator.

(a)

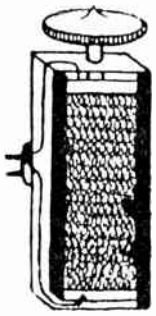

The spiral-spring receiver.

(b)

Fig. 9—(a) Spark gap arrangements for generating wavelengths down to 5 mm (Bose, 1895). Material: platinum. (b) Bose's microwave, "semi-conducting" detector consisting of rows of horizontal spiral steel springs under adjustable pressure and a small polarizing voltage (1895). (*Courtesy of Longmans, Green and Co.*)

Figs. 10–12).[13] Bose's gratings, however, were not always grids of wires but sometimes consisted of parallel strips of metal (Fig. 12) as in the cut-off metal-plate grating of today. He produced these initially in a particularly simple way by interleaving the pages of a Bradshaw railway timetable with sheets of tinfoil. (Similar virtuosity was shown by Marconi on a later occasion when he inserted parallel wires into corrugated cardboard to make a Hertzian grating.)[14] Bose had found that the leakage through a cut-off grating, as we term it, was much less than that occurring with a wire grid.

With the polarimeter, Bose investigated the properties of many natural substances and artificial devices. In the class of natural substances he studied crystals of many kinds, and vegetable fibers, in addition to strained

[13] J. C. Bose, "On a new electro-polariscope," *Electrician;* December 27, 1895.

[14] Described to the author by E. L. Payne, Marconi's Wireless Telegraph Co., Ltd., Baddow Res. Labs., Chelmsford, Essex, Eng.

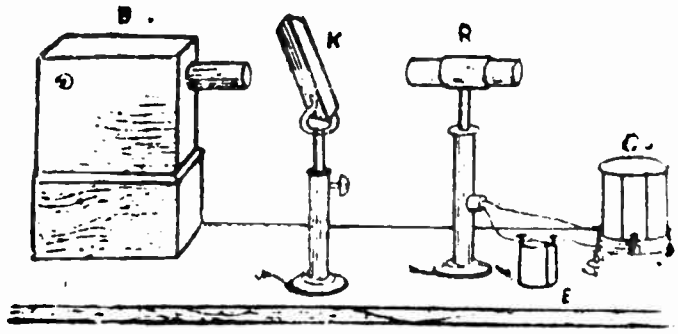


Polarization apparatus. *B*, metallic box enclosing the Ruhmkorff coil and radiator; *K*, the crystal to be examined; *E*, voltaic cell; *G*, the galvanometer; *R*, tube enclosing sensitive receiver. (Bose.)

Fig. 10—Microwave optical bench of Bose showing hollow-pipe waveguide antennas and polarization analyzer, *R* (1895). (*Courtesy of Longmans, Green and Co.*)

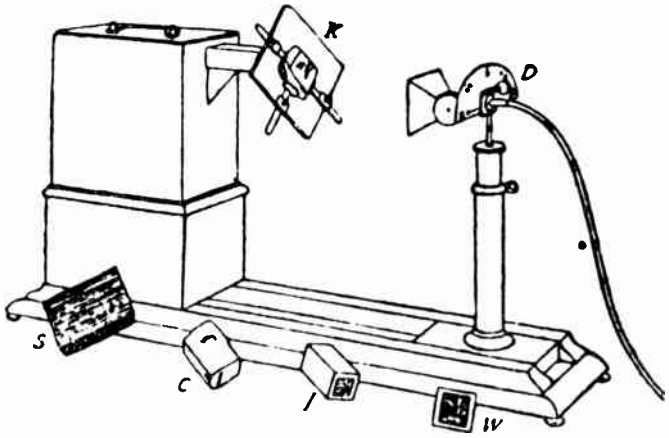


Polarization apparatus. *K*, crystal-holder; *S*, a piece of stratified rock; *C*, a crystal; *J*, jute polarizer; *W*, wire-grating polarizer; *D*, vertical graduated disk by which the rotation is measured. (Bose.)

Fig. 11—Microwave optical bench for polarization analysis. Note electromagnetic horn receiving antenna, square waveguide transmitting antenna, and Hertzian grids (Bose, 1897). (*Courtesy of Longmans, Green and Co.*)

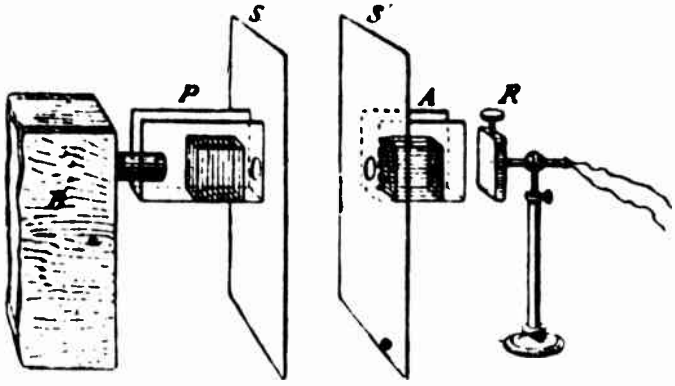


Polarization apparatus. *B*, the radiating box; *P*, the polarizer; *A*, the analyzer; *S*, *S'*, the screens; *R*, the receiver.

Fig. 12—"Cut-off waveguide" polarized mirrors as used in a polarimeter by Bose. (*Proc. Roy. Soc.*, vol. 63, p. 148; 1898.)

dielectrics as found in stratified rocks and fossils. Artificial polarizers of different forms he constructed from wires or jute fibers (Fig. 10).

One of the most remarkable applications of the microwave polarimeter developed by Bose was his use of it for analog physics.[15] Knowing that certain sugar solutions were optically active in producing polarization rotations, he conjectured that the mechanism resided in the molecule. He therefore made macroscopic or model molecules of twisted jute fibers, some with a right-hand twist, others with a left-hand twist (Fig. 13).

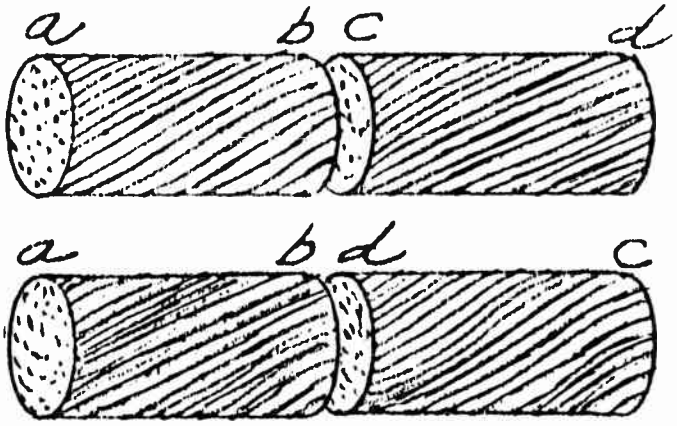


Fig. 13—Model "molecules" of twisted jute as used by Bose in 1898. (*Courtesy of Longmans, Green and Co.*)

Examined in a millimeter wave polarimeter these "molecules" gave either right or left-hand polarization twists, and jointly, no twist. Here, according to Bose, was an analog of the sugar rotations. The significant feature of this microwave technique was in its providing a macroscopic representation of the submicroscopic. Recently, in 1955, quasi-crystallographic reflections have been obtained from model crystal structures of macroscopic "atoms" when irradiated by millimeter waves.[16] The basic technique is, however, reminiscent of Bose's early experiments in microwave modeling.

Circular and elliptical polarizations of microwaves were familiar and well-understood phenomena to the followers of Hertz, the majority of whom had a trained optical background. Righi and Bose both observed the polarized structure of wood, Righi actually constructing a wooden quarter-wave plate or circular polarizer.[2] The radio half-wave plate also had its origin at this time.

Zehnder in Germany in 1894 used Hertzian grids to produce circular or elliptic polarization.[17] Lodge's description is so clear as to merit reproduction: "He takes a couple of plane polarizing grids and places them parallel to each other at a little distance apart with their wires crossed. If the two grids are close together they will act like wire-gauze, reflecting any kind of polarized radiation equally; but if the warp and woof are an eighth-wavelength apart, and the plane of the incident radiation is at 45° to the wires, the reflected radiation will be circularly polarized. A change in the circumstances will, of course, make it elliptical. Such a pair of grids acts, in fact, like a Babinet's Compensator."[9] The modern form of the arrangement consists usually of one grid spaced one-eighth wavelength from a metal sheet reflector.[18]

Garbasso and Aschkinass, by breaking up the wires of a Hertzian grid into uniform short lengths, *i.e.*, dipoles, showed that a dispersive, or frequency-sensitive, polarized mirror then existed.[19] The tuned reflector of a modern television receiving antenna is a simple case of this phenomenon. Marconi, in the first experiments in scatter communication in 1932, used parabolic mirrors of tuned elements constituting the reflectors.[20]

The optical problem to the Hertzians was to reproduce a dispersive Newtonian prism on microwaves. Such a prism was constructed from layers of dispersive dipoles by Garbasso and Aschkinass in 1894; this prism was the first component of "artificial dielectric" as we now term such a structure. The layers consisted of tinfoil strips fixed to glass plates. The wavelength was 7.5 cm (4000 mc).

It is evident that the study of the polarization properties of microwaves in microwave optics led to considerable advances in the art before 1900.

## Dielectrics in the Hertzian Epoch

Hertz's great achievement in experimentally confirming Maxwell's electromagnetic theory of light by generating, controlling, and detecting microwave radiation, arose as a by-product of a general research into the properties of dielectrics or insulators.[1]

In the years following, extensive investigations of dielectrics were carried out by the followers of Hertz. Hertz's own dielectric researches were the basis of much of the work. He developed standing-wave measurements and evolved the nodal shift technique. He was interested in secondary reradiation from dielectric masses, not ignoring the polarization characteristics. He achieved the first dielectric constant determination by refraction, using the celebrated prism of pitch. His

[15] J. C. Bose, "On the rotation of plane of polarisation of electric waves by a twisted structure," *Proc. Roy. Soc.*, vol. 63, p. 146; 1898.
[16] J. F. Ramsay and S. C. Snook, "Microwave model crystallography," *Electronic and Radio Engr.*, pp. 165–169; May, 1957.
[17] Zehnder, *Ber naturforsch. Ges. zu Freiburg i. B.*, Bd. 9, Heft 2; June 21, 1894.
[18] J. F. Ramsay, "Circular polarization for cw radar," *Marconi Rev.*, vol. 15, pp. 71–89; 2nd Quarter, 1952.
[19] Garbasso and Aschkinass, "Brechnung und Dispersion electrischer Strahlen," *Ann. der Phys.*, vol. 53, p. 534, 1894.
[20] G. Marconi, "Radio communication by means of very short electric waves," reprint, IRE Trans., vol. AP-5, pp. 90–99; January, 1957.

work is notable both for the number of substances he investigated, and in some cases for the size of the experimental samples. A list of the substances gives some idea of the thoroughness of his approach (Fig. 14).

| Solids | Liquids | Gases |
|---|---|---|
| Metals | Water | Air |
| Paraffin | Sulphuric Acid | Hydrogen |
| Shellac | Alcohol | Carbonic Acid |
| Resin | Ether | Coal Gas |
| Ebonite | Hydrochloric Acid | Chlorine |
| India-Rubber | Nitric Acid | Nitrous Oxide |
| Glass | Ammonia (Soln) | Bromine Vapor |
| Porcelain | Paraffin | Iodine Vapor |
| Earthenware | Benzole | |
| Wood | Petrol | |
| Pasteboard | Carbon Disulphide | |
| Paper | Ammonium Sulphide | |
| Ivory | Fuchsine | |
| Horn | Potassium Permanganate | |
| Hides | Nitrate of Mercury | |
| Feathers | Sodium Hyposulphite | |
| Agate | Potassium Bromide | |
| Mica | Potassium Iodide | |
| Copper Sulphate | Iron Salts | |
| Crystals | Copper Salts | |
| Topaz | Sal-Ammoniac | |
| Amethyst | Zinc Sulphate | |
| Crystallized Sugar | Common Salt | |
| Alum | Potassium Sulphate | |
| Calc-Spar | Sodium Sulphate | |
| Rock-Salt | Magnesium Sulphate | |
| Gypsum | | |
| Rock-Crystal | | |
| Smoke Glass | | |
| Quartz | | |

Fig. 14—List of substances investigated by Hertz. (*Courtesy of Macmillan and Co., Ltd., and St. Martin's Press, Inc.*)

Some of his experimental samples may be quoted.[1] His first material being paper, and the wavelength in the meter band, he "piled up books in the form of a parallelopiped 1.5 meter long, 0.5 m broad, and 1 m high." He also had cast "800 kgm of unmixed asphalt" in a block of similar size. Another block was of artificial pitch. A sulphur sample consisted of "a massive block 70 cm long, 20 cm broad and 35 cm high." As a dielectric cylinder Hertz made use of "a sandstone pillar in the building." For one liquid dielectric he used "an oak trough with 45 liters of pure paraffin."

These investigations were highly stimulating to his successors, the majority of whom used shorter waves—and smaller samples. The low-loss characteristics of paraffin and paraffin wax were known to most of the Hertzians. The liquid form was popular around the spark gap where its dielectric constant allowed greater power to be obtained. The solid form was used for components, *e.g.*, lenses and prisms, and as an insulating support. Sulphur and ebonite were used for the same purposes.

The dielectric properties of water were examined on different frequencies, both as liquid[21] and ice.[8] Alcohol, castor oil, olive oil, xylol, and petrol were also measured at microwave frequencies.[22]

Anomalous dispersion was of great interest to the followers of Hertz who, realizing the truth of the electromagnetic theory, saw a solution to the optical uncertainties. Trouton in Dublin, for example, in 1889 asked, "Would the interspersing of bodies of nearly the same period in Hertz's pitch prism alter the angle of refraction?

If so, then anomalous dispersion may yet be successfully demonstrated."[4] Today we know that he was correct and experiment has confirmed his conjecture. Trouton may be regarded as the father of artificial dielectrics; his dipole-loaded medium was the first suggestion made in this field. To the modern it is interesting to find Trouton suggested as well that the particles need not be identical. As we have seen earlier, Garbasso and Aschkinass carried out the experiment with identical dipoles in 1894.

Trouton was also aware of the need for microwave photographs and suggested molecular dissociation and ac electrolytes as possible techniques. This problem is still unsolved today.

With the current modern interest in ferrites, germanium, and powdered artificial dielectrics at microwaves, it is relevant to mention that Birkeland in 1894 made up synthetic dielectrics from paraffin and metal filings or powders.[23] His "ferro-paraffin" consisted of iron filings or chemically obtained iron powder mixed with powdered quartz in paraffin. Birkeland desired "to demonstrate in magnetic cylinders stationary magnetic waves analogous to the electric stationary waves along metallic wires." He was unsuccessful due to losses which even then were a feature of artificial dielectrics. Birkeland did observe the detuning effect in a resonant circuit of a ferro-paraffin rod, and the excessive skin depth of the current in the rod. Control experiments were also carried out with brass filings and with zinc filings in paraffin.

Bose developed lossy artificial media in his search for a microwave absorber; the blotting paper soaked in electrolyte proved the best.[5]

It is doubtful if the Faraday rotation of the plane of polarization was ever investigated by the Hertzians. It is likely however that Lodge realized that polarization rotation by a magnetic field was possible with Hertzian waves, judging from some of his experiments and papers.

Among the classical optical phenomena that were reinvestigated on centimeter and millimeter waves were total internal reflection and the evanescent field at the interface,[5] Brewster angle,[4] the quarter-wave and half-wave thickness feature of dielectric slabs,[2] polarization

[21] A. D. Cole, "Measurement of short electrical waves and their transmission through water cells," *Phys. Rev.*, vol. 7; November, 1898.

[22] E. Branly, "The transmission of Hertz waves through liquids," *Compt. Rend*, October 30, 1899.

[23] M. Birkeland, "On magnetisation produced by Hertzian currents; a magnetic dielectric," *Compt. Rend.*, June 11, 1894.

rotations,[5] double refraction,[24] and selective absorption.[5]

For these measurements and other applications, instrumentation covered microwave spectrometers,[5] interferometers,[25] diffraction gratings,[26] polarimeters,[5] all used with incoherent spark generators and (usually) coherer detectors. A notable interferometer built by Hull under the direction of Prof. A. A. Michelson at Chicago University in 1897 operated on 9.12-cm wavelength and could measure wavelength and index of refraction with an accuracy of better than 1 per cent. Fig. 15 illustrates Righi's interference experiment with Fresnel mirrors as drawn by Poincaré.[27] The wavelength was probably in $X$ band.

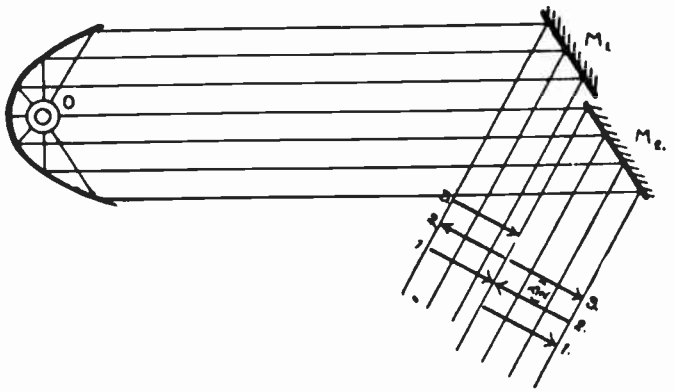


Interference between two parallel rays in the same direction. The two reflected rays have the same phase difference at all points, and the degree of interference depends upon the distance between the mirrors $M_1$ and $M_2$.

Fig. 15—Fresnel mirror experiment modelled on 3 cm by Righi (description by Poincaré). (*Courtesy of Constable and Co., Ltd.*)

## Conclusion

The above historical investigation was not written just because it provided interesting history, and to the author at least, fresh light on origins, but because in a strange way it presented a parallel with the microwave situation today.

Today, millimeter waves research is in a similar position to that existing in the 1890's. It does not know where it is going. Any objectives it seems to have are scientific, as it was with the Hertzians. Generation of the waves presents formidable difficulties, detectors are almost as crude as those of the early experimentalists. The only positive application that may appear now is hollow-pipe waveguide communications. Radar and wireless communications are beset by propagation difficulties.

Yet, every time a region of the spectrum is developed a major practical application arises. World communications arose from the so-called short-wave region, television appeared in the very-high frequency band, radar and tropospheric scatter communications exploited the centimeter waveband. "What next?" is a natural question.

It will be observed that the major practical advances tended to arise from the development of the optical features of radio waves—beam radio, line-of-sight tv, high resolution radar, scatter communications, these descriptions are optical. The closer radio techniques approach the optical, the more likely they are to yield fruitful developments. Radio astronomy is the latest example.

Therefore, the work of the Hertzians, masters of microwave optics, then points the direction in which the new microwave radio must go.

If the signposts are correct the undeveloped millimeter waveband should see a major everyday application of radio optics.

Otherwise, the millimeter waveband remains an ideal region of the spectrum for modeling devices and phenomena from other regions of the spectrum. Antennas, for example, which are too large, can be modeled as conveniently as atoms which are too small. Particularly all wave phenomena can be reproduced with a convenience not realizable in other regions of the spectrum. Optics textbooks may yet require another chapter, one on "Microwave Optics."

## Acknowledgment

The author wishes to thank the Engineer-in-Chief of Marconi's Wireless Telegraph Company Limited for permission to publish this paper. To Canadian Marconi Company special thanks are due for assistance in preparing the material for publication. Acknowledgment is also made to Dr. A. A. Oliner, Polytechnic Institute of Brooklyn, for suggesting and arranging IRE-URSI presentation of this historical review on May 23, 1957.

[24] P. Lebededev, "Double refraction of electric rays," *Electrician;* November 15, 1895.
[25] G. F. Hull, "On the use of the interferometer in the study of electric waves," *Phys. Rev.*, vol. 5, p. 231; October, 1897.
[26] J. C. Bose, "On the determination of the wavelength of electric radiation by a diffraction grating," *Proc. Roy. Soc.*, vol. 60; 1897.
[27] H. Poincaré and F. K. Vreeland, "Maxwell's Theory and Wireless Telegraphy," Constable and Co., Ltd., London, Eng.; 1905.

# Ghost Modes in Imperfect Waveguides*

E. T. JAYNES†, SENIOR MEMBER, IRE

*Summary*—**Attention is called to the existence of microwave resonances which have the unusual property that they are nonradiating, and thus have high $Q$, in spite of the fact that the fields are not enclosed completely by metallic walls. These "ghost modes" represent fields which are derived from those of the usual waveguide modes, but are "trapped" in the vicinity of imperfections in the waveguide. Their resonant frequency is slightly lower than the corresponding cutoff frequency. If one attempts to use a waveguide in its lowest mode, over a range of frequencies which includes the ghosts of higher modes, complicated resonance effects may be observed which can cause trouble in some types of microwave circuits. The same phenomenon exists in any structure which has pass bands and rejection bands, such as periodic structures or crystals.**

## Introduction

THE phenomenon described herein explains certain curious and troublesome effects observed in waveguides operating close to the cutoff frequency of a propagation mode, and it may have applications for waveguide filters. In addition, it has a certain educational value because of a mathematical analogy with the phenomenon of localized bound states due to imperfections in crystals.

## Ghost Modes Due to a Dielectric

To illustrate the simplest case, and one which can be analyzed completely, consider the structure of Fig. 1. A dielectric disk of thickness $d$, dielectric constant $\epsilon$, is placed in a cylindrical waveguide of radius $a$. Let the center of the disk be the origin of a cylindrical coordinate system $(r\theta z)$. A possible electromagnetic field is one whose transverse structure is that of the $TM_{01}$ mode, derived from the field component

$$E_z = \begin{cases} BJ_0(k_1 r)\exp\left[-(k_1^2 - k^2)^{1/2} z\right], & z > \dfrac{d}{2} \\ AJ_0(k_1 r)\cos\left[(\epsilon k^2 - k_1^2)^{1/2} z\right], & |z| < \dfrac{d}{2} \\ BJ_0(k_1 r)\exp\left[+(k_1^2 - k^2)^{1/2} z\right], & z < -\dfrac{d}{2} \end{cases} \quad (1)$$

In (1),

$$k_1 = \frac{2.405}{a} = \frac{\omega_c}{c}, \qquad k = \frac{\omega}{c},$$

where $\omega_c$ and $\omega$ are, respectively, the $TM_{01}$ cutoff frequency and an operating frequency to be determined presently. Matching solutions across the dielectric-air interfaces, we obtain the condition

$$\tan\left[(\epsilon k^2 - k_1^2)^{1/2}\frac{d}{2}\right] = \epsilon\left[\frac{k_1^2 - k^2}{\epsilon k^2 - k_1^2}\right]^{1/2}. \quad (2)$$

For any $\epsilon > 1$, (2) has at least one solution for $k$ with $k < k_1$. If $(\epsilon - 1)^{1/2} k_1 d < 2\pi$, only one such solution exists. We consider, in particular, the case where $\epsilon$ is appreciably greater than unity and $k_1 d \ll 1$. Then $k$ as determined from (2) is very close to $k_1$, and it will be a good approximation to set

$$(\epsilon k^2 - k_1^2)^{1/2} d \simeq (\epsilon - 1)^{1/2} k_1 d \ll 1,$$

so that (2) reduces to the following formula for $\omega$:

$$\omega^2 \simeq \omega_c^2\left[1 - \left(\frac{\epsilon - 1}{\epsilon}\,\frac{k_1 d}{2}\right)^2\right]. \quad (3)$$

The field derived from (1) thus represents a resonant mode with resonant frequency slightly below the cutoff frequency of the $TM_{01}$ mode, in which the fields are localized to the vicinity of the dielectric disk. The electric field configuration is sketched in Fig. 1. The longitudinal extension of this ghost mode is described by the "$1/e$ distance"

$$x_0 = \frac{1}{(k_1^2 - k^2)^{1/2}} = \frac{\lambda_c}{2\pi(1 - \omega^2/\omega_c^2)^{1/2}} \quad (4)$$

where $\lambda_c = 2\pi/k_1 = 2.6a$ is the $TM_{01}$ cutoff wavelength. Numerical values of $(x_0/\lambda_c)$ are indicated in Fig. 2. It is seen that the ghost is surprisingly well localized; for example, in the case $\omega = 0.99\,\omega_c$, $x_0$ is less than 1.5 pipe diameters. If the waveguide extends a distance three or four times $x_0$ on either side of the dielectric disk, this ghost will be essentially nonradiating and will have a very high $Q$, limited only by losses in the waveguide walls and the dielectric.

Suppose this waveguide were being operated in the $TE_{11}$ propagating mode, at frequencies near the $TM_{01}$ cutoff frequency. This is a rather common condition in practice, since the $TM_{01}$ cutoff frequency is only about 30 per cent higher than that of the $TE_{11}$ mode. In a perfect waveguide the fact that we were close to the $TM_{01}$ propagating range would not cause any trouble. However, the disk represents an "imperfection" in what would otherwise be a smooth waveguide. The slightest asymmetry in structure near the disk, or the slightest inhomogeneity in dielectric constant of the disk, can couple the ghost to the $TE_{11}$ mode and cause a large absorption of energy at the frequency given by (3). The field of the ghost can attain a magnitude several hundred times that of the propagating $TE_{11}$ mode, so that

* Original manuscript received by the IRE, September 6, 1957.
† Microwave Laboratory, Stanford University, Stanford, Calif.

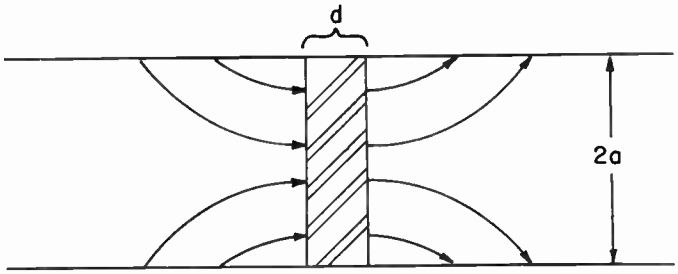


Fig. 1—$TM_{01}$ ghost mode due to a dielectric disk.

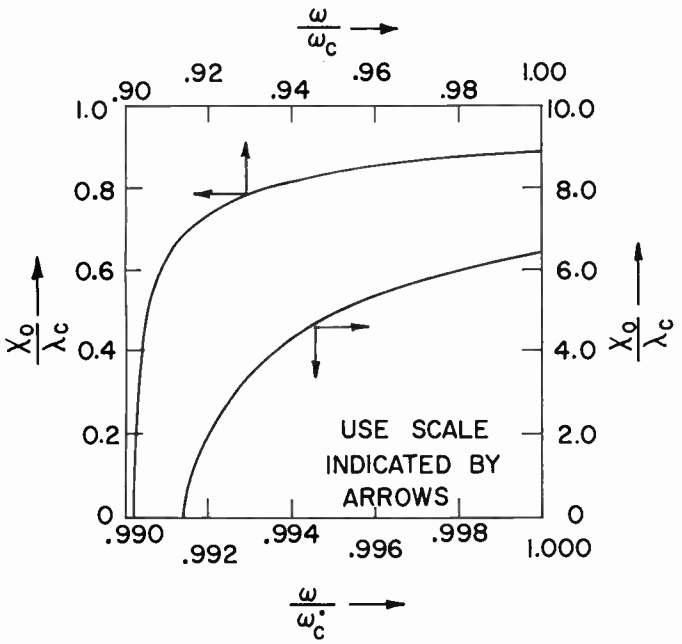


Fig. 2—"(1/e) distance" of ghost modes as a function of frequency.

in a high-power device a ghost can cause breakdown. It was, in fact, the persistent failure of ceramic windows in the output waveguides of high-powered klystrons feeding the Stanford linear electron accelerator (carrying about 20 megw at 3 kmc), which led to the recognition of ghost modes. Spurious resonances in certain ferrite devices may also be traceable to this cause.

What was said for the $TM_{01}$ mode evidently applies in general for the structure of Fig. 1; every propagation mode of the waveguide is accompanied by a ghost with the same transverse field pattern, localized to the vicinity of the disk, with a resonant frequency slightly below the corresponding cutoff frequency.

## General Ghost Modes

The presence of a dielectric is not necessary for existence of ghosts; *any* localized imperfection in a waveguide will cause them to appear. Consider first a perfect, infinitely long waveguide with zero loss, excited in one of the propagation mode patterns at exactly its cutoff frequency. It is thus a large resonant cavity with resonant frequency $\omega_c$. Let the electric and magnetic fields in the vicinity of any point $P$ on the waveguide wall be $E$, $H$. Now if $\epsilon_0 E^2 > \mu_0 H^2$, push the wall in slightly at $P$, while

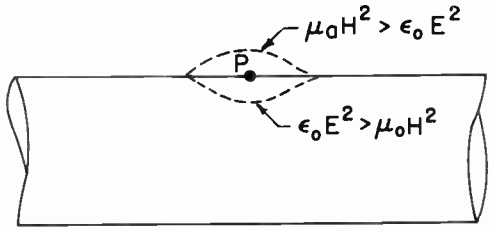


Fig. 3—Wall perturbations which create ghost modes.

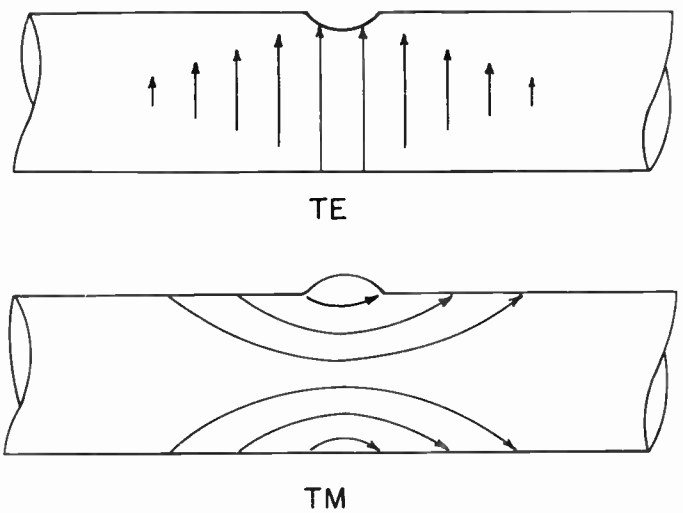


Fig. 4—Electric field lines of TE and TM ghost modes due to wall imperfections.

if $\mu_0 H^2 > \epsilon_0 E^2$, pull out a small "blister" as in Fig. 3. According to the Slater perturbation formula [1], the resonant frequency of the cavity is always lowered by this change. But at any lower frequency than $\omega_c$ the fields will be attenuated exponentially as we move away from the imperfection; thus a ghost has been created, trapped to the vicinity of the imperfection, with a resonant frequency slightly lower than $\omega_c$. Two examples are given in Fig. 4, in which only the electric field lines are sketched.

The $Q$ of a ghost mode due to a small imperfection as in Fig. 4 is given to order of magnitude by

$$Q \simeq \frac{a}{\delta} = \frac{\text{waveguide radius}}{\text{skin depth}}, \tag{5}$$

from which it is seen that values in excess of $10^4$ are easily attained. For the ghost of any mode other than the lowest one, there also will be a "loaded Q" involving the strength of coupling to propagating modes.

Crude estimates of the frequency and longitudinal extension of these ghosts, obtained from (4) and the Slater perturbation formula, are

$$\omega^2 \simeq \omega_c^2 \left[ 1 - \left( \frac{\pi \alpha \delta V}{A \lambda_c} \right)^2 \right], \tag{6}$$

$$x_0 \simeq \frac{A \lambda_c^2}{2\pi^2 \alpha \delta V}. \tag{7}$$

Here $A$ is the cross-sectional area of the waveguide, $\delta V$ is the volume added or removed by the imperfection, and $\alpha$ a dimensionless quantity of the order of magnitude unity, given by

$$\alpha = \frac{|\mu_0 H^2 - \epsilon_0 E^2|}{<\mu_0 H^2 + \epsilon_0 E^2>_{Av}} \tag{8}$$

where the fields in the numerator are values near the imperfection, while the denominator is an average over a waveguide cross section passing through the imperfection [2].

From these formulas several general conclusions may be drawn. If the imperfection is so small that

$$\delta V < \frac{A\lambda_c}{100}, \tag{9}$$

then one may expect the ghost to be separated from the cutoff frequency by less than the bandwidth $\omega_c/Q$, so that it does not appear as a well-resolved resonance, but only a slight broadening of the cutoff region. If, on the other hand,

$$\delta V > \frac{A\lambda_c}{100}, \tag{10}$$

the ghost will generally appear as a distinct resonance. The longitudinal extension $x_0$ of any well-resolved ghost will, from Fig. 2, never be more than a few times $\lambda_c$. The $\delta V$ required by (10) is so large that the usual mechanical imperfections due to machining errors, inadvertent hammer blows, etc., do not cause separation of ghosts from the waveguide modes. However, installation of almost any kind of apparatus inside a waveguide will cause them to appear, as may the presence of any twist or bend.

## Periodic Structures

What was said above for waveguides applies equally well to any periodic structure, such as those used in linear accelerators, traveling-wave tubes, or, in fact, any lumped-constant filter composed of a cascade of identical networks. By reasoning exactly like that in the preceding section, one can show that any localized imperfection in such a structure will cause a bound resonance to appear, with resonant frequency just outside the pass band of the structure. In this case, it may lie either above or below the pass band. Once again, the imperfection has to be quite large in order to cause separation of a well-resolved resonance, so that reasonable care in construction is sufficient to avoid troubles due to these ghosts.

There is an interesting, and pedagogically useful, analogy with certain well-known features of solid-state theory. Here a crystal represents a three-dimensional periodic structure, and solutions of the Schrödinger equation, in one-electron approximation, show an almost perfect mathematical analogy with those in the corresponding electrical problem [3]. In particular, the conduction bands of the crystal correspond to pass bands of the filter, and any localized imperfection in the crystal (such as a vacancy, interstitial atom, or impurity atom), results in at least one localized bound state, with an energy just above or just below the edge of a conduction band. In this way one can understand the creation of donor or acceptor impurity levels involved in $n$-type and $p$-type conductivity in semiconductors [4].

Further work on ghost modes, by M. Forrer and the writer, is being prepared for publication. Experimental results, universal curves for predicting the occurrence of ghosts, and discussion of their possible use in waveguide filters and mode convertors will be included.

## Bibliography

[1] Slater, J. C. *Microwave Electronics*, New York: D. Van Nostrand Company, Inc., 1950, p. 81.
[2] The derivation of (6) and (7) is a bit tricky, since a small change in $\delta V$ alters the "length" $x_0$ of the cavity. One must apply the Slater formula only to infinitesimal changes in $\delta V$, and integrate to obtain their cumulative effect. For this reason the frequency shift involves $(\delta V)^2$ rather than $(\delta V)$, as one might at first expect.
[3] Brillouin, L. *Wave Propagation in Periodic Structures*, New York: McGraw-Hill Book Company, Inc., 1946.
[4] Kittel, C. *Introduction to Solid-State Physics*. New York: John Wiley & Sons, Inc., 1953, Ch. 14.

# High-Frequency Crystal Filter Design Techniques and Applications*

DAVID I. KOSOWSKY†, MEMBER, IRE

*Summary*—**High-frequency crystal filters which operate to 40 mc are now being commercially produced. These filters, with bandwidths ranging from one cycle to several hundred kilocycles per second, have been made possible by new design techniques and simplified circuitry.**

**Eliminating the need for multiple frequency conversion, the small rugged filters are already beginning to find wide use in many AM, SSB, and fm receivers as well as single-sideband generators.**

**Crystal filters are normally composed of from two to eight quartz resonators in a lattice or bridge network. The filter components are characterized by high $Q$ and stability under extreme environmental conditions. Normal values of $Q$ for crystal filter components in the 1 to 40 mc range are from 50,000 to 200,000; in certain filters, element $Q$'s exceed 1,000,000.**

## Introduction

With more and more radio communication messages crowding the radio-frequency spectrum, allotment of frequency bands to various radio and radar needs has become a serious problem. New systems have been developed to aid in the economical utilization of existing frequency space. These include schemes such as single-sideband and narrow-band frequency modulation. To be successful, each of these systems must operate within a narrow, well-defined band of frequencies. As a result, filter selectivity requirements have become increasingly stringent.

At frequencies greater than a few megacycles, equipment designers up to now have been forced to resort to systems of multiple-frequency conversion in order to obtain required equipment performance. Conventional types of filters may not perform suitably for single frequency conversion. The multiple conversion process brings about increased circuit complexity, with corresponding loss in efficiency and reliability.

The high-frequency crystal filter offers a solution to the frequency conversion problem as well as other general design problems in the higher frequency ranges.

Compact filter units employing miniature quartz crystal resonators in the 5- to 40-mc range exhibit filter performance which has previously been possible only at significantly lower frequencies. The result is that multiple frequency conversions may be eliminated. Equipment simplification and size reduction can be effected, along with improved performance and reliability.

One primary reason why crystal filters perform so well at high frequencies is the inherent high $Q$ of the resonators. In a band-pass filter, high selectivity and low dissipation or insertion loss require that the $Q$'s of the critical filter components be much greater than the ratio of center frequency to bandwidth.[1] Quartz crystal resonators used in filter networks have $Q$'s that range from 10,000 to 200,000 in general. Filters have been produced with crystal $Q$'s in excess of 1,000,000. By comparison, the $Q$'s normally attainable in conventional inductances may range from 50 to 200. Nickel alloy resonators commonly employed in "mechanical" filters have $Q$'s ranging from 2000 to 10,000.[2] The advantages of using crystal resonators in filter networks have been known for over 30 years,[3] but not until recently have high-frequency filter units with controlled characteristics been made commercially available.

## Quartz Crystal Resonators

Of the hundreds of crystals that exhibit the piezoelectric effect, only the quartz crystal has been employed to any significant extent in oscillators and filters. Among other qualities, quartz crystals possess an extremely high order of stability over wide temperature variations during long time periods. In the presence of severe shock and vibration, the quartz crystal designed for filter applications does not exhibit microphonic behavior. These qualities are necessary to achieve good narrow-band filtering devices at high frequencies.

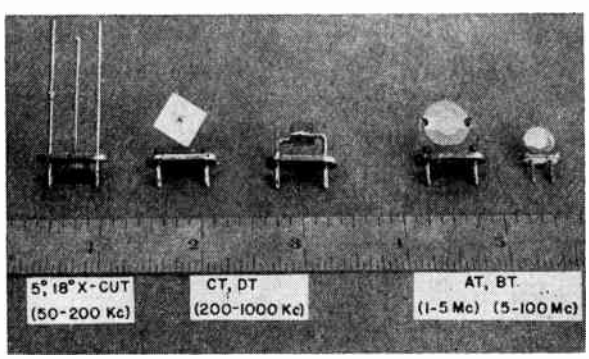


Fig. 1—Typical quartz filter crystals.

Typical quartz filter crystal resonators are shown in Fig. 1. Any plate cut from a piece of natural quartz has a number of resonant frequencies. The frequencies of resonance depend on the crystal dimensions, the vibra-

* Original manuscript received by the IRE, September 6, 1957; revised manuscript received, October 30, 1957.

† Hycon Eastern, Inc., Cambridge, Mass.

[1] E. A. Guillemin, "The effect of incidental dissipation in filters," *Electronics*, vol. 19, pp. 130–135; October, 1946.

[2] J. C. Hathaway and D. F. Babcock, "Survey of mechanical filters and their applications," PROC. IRE, vol. 45, pp. 5–16; January, 1957.

[3] W. G. Cady, "The piezo-electric resonator," PROC. IRE, vol. 10, pp. 83–114; April, 1922.

tional mode involved, and the orientation of the cut. The AT-cut crystal, which operates in a thickness shear vibrational mode, is particularly attractive because of its extremely small size at frequencies above 5 or 6 mc. Also, the AT-cut component possesses an excellent temperature coefficient. Over the temperature range of $-55°C$ to $+85°C$ the resonant frequency of a typical AT crystal will shift less than $\pm 0.005$ per cent of its nominal value.

*Equivalent Circuit*

In the vicinity of a resonant frequency, a crystal resonator may be represented by an equivalent electrical circuit[4] of the type shown in Fig. 2(a). The inductance $L_1$ and capacitance $C_1$ represent the effective mass and stiffness of the crystal, respectively. $C_0$ is the static capacitance and includes stray-wiring and holder capacitance. The resistance $R_1$ represents the frictional loss of the vibrating crystal. The crystal $Q$ is defined as the ratio of the reactance of $L_1$ at the resonant frequency to the resistance $R_1$. Because of the extremely large value of $Q$, the crystal may be considered a purely reactive network for most filter applications.

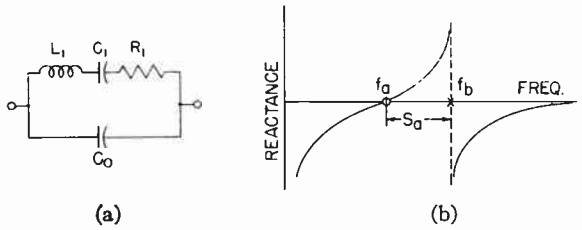


Fig. 2—Crystal resonator equivalent circuit.

The reactance curve corresponding to the lossless equivalent circuit is shown in Fig. 2(b). The resonant frequency or "zero" of the crystal unit ($f_a$) and the antiresonant frequency or "pole" ($f_b$) are related to one another by the ratio of capacitances of the crystal defined by

$$r \equiv \frac{C_0}{C_1} . \tag{1}$$

The relationship is easily seen to be:

$$f_b^2 = f_a^2\left(1 + \frac{1}{r}\right). \tag{2}$$

Because of the coupling that exists between the electrical and mechanical stresses within the crystal, there will always be a fixed ratio of capacitances for any crystal cut.[5] The lowest ratio found for quartz is 115, but because of stray-wiring and holder capacitance the minimum ratio for practical quartz cuts is approximately 125. At frequencies above one megacycle, the coupling factor associated with the AT-cut crystal increases the minimum value of $r$ to approximately 250 From (2), the zero-pole spacing [$S_a$ in Fig. 2(b)] can be approximated by

$$S_a = f_b - f_a \doteq \frac{f_a}{2r} . \tag{3}$$

$S_a$ is, therefore, a very small percentage of the crystal resonant frequency, being at most 0.4 per cent of $f_a$ at low frequencies, and 0.2 per cent of $f_a$ at high frequencies

A quartz crystal may have a number of vibrational modes in the vicinity of the desired response. However, by properly dimensioning the resonator and the electrodes which supply electrical excitation, it has been possible to produce crystals with essentially single-resonance characteristics at frequencies as high as 40 mc. Through the proper utilization of from 4 to 8 such resonators, filters are produced in which the level of undesirable or spurious responses is from 80 to 100 db below the mean pass band level.

Dimensioning a crystal resonator to suppress undesirable modes of vibration and to produce a given temperature coefficient generally limits the equivalent electrical parameters to a narrow range of values. This limitation, together with the existence of a fixed ratio of capacitances for the crystal resonator, places both theoretical and practical restrictions on the maximum bandwidth attainable with a given crystal filter configuration. Such restrictions apply even when inductances or resonant circuits are arranged in series or parallel with the crystal resonator in order to modify the resonator critical-frequency or zero-pole configuration.

These bandwidth restrictions make it desirable to utilize a design procedure which will rapidly and accurately indicate the range of filter characteristics obtainable with a given crystal resonator. A synthesis procedure developed for this purpose follows.

## Crystal Filter Circuitry

Almost all crystal filters of any significance produced in the past twenty years have been based on the symmetrical-lattice or bridge networks developed by Mason.[6] The symmetrical lattice, which is the most general form of symmetrical network, provides analytical flexibility. In addition, practical considerations peculiar to crystal filter realization often make it necessary to employ this configuration.

Several examples of crystal lattice filter circuits are illustrated in Fig. 3. Attenuation characteristics of these filters depend completely upon the arrangement of critical frequencies or zeros and poles of the series (A) and shunt (B) arms of the lattice. Fig. 3(a) and 3(b) illustrates the crystal-capacitor lattices normally designated as narrow-band filters. The bandwidth of these filters is limited directly by the zero-pole spacings

[4] K. S. Van Dyke, "The piezo-electric resonator and its equivalent network," Proc. IRE, vol. 16, pp. 742–764; June, 1928.

[5] R. A. Heising, "Quartz Crystals for Electrical Circuits," D. Van Nostrand Co., Inc., New York, N. Y., ch. 1; 1946.

[6] W. P. Mason, "Electric wave filters employing quartz crystals as elements," *Bell Sys. Tech. J.*, vol. 13, pp. 405–452; July, 1934.

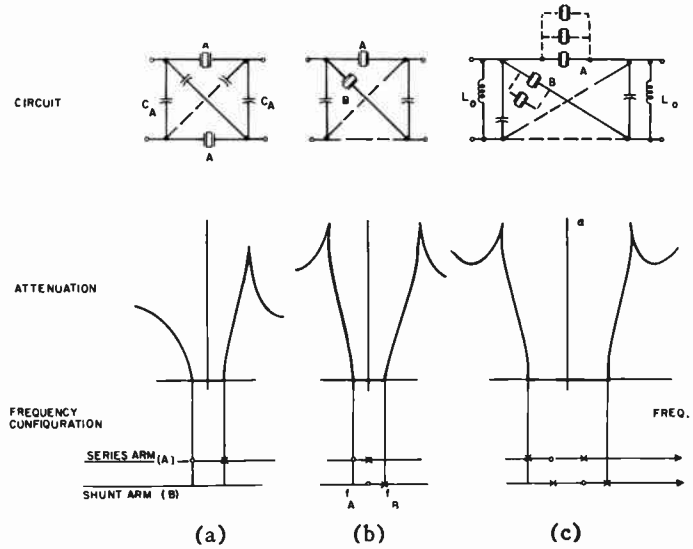


Fig. 3—Crystal lattice filter configurations.

of the associated crystals and therefore, by the ratio of capacitances ($r$). The ratio of capacitances must include the effects of external capacitance $C_A$, which may be considered to be in parallel with both series and shunt lattice arms, and will, therefore, increase the normal static capacitance $C_0$. From (3) it may be seen that the upper bandwidth limit of the narrow-band crystal filter is only a few tenths of one per cent of the filter center frequency. The lower percentage bandwidth limit, which is set by crystal dissipation and frequency tolerances, may be as small as 0.01 per cent.[7]

In order to obtain wider filter bandwidths, inductances may be placed in series or in parallel with the lattice network as shown in Fig. 3(c). The inductance $L_0$ may be considered to resonate in the vicinity of the center frequency with all or part of the crystal effective shunt capacitance ($C_0+C_A$). A number of the resultant critical frequencies of the series and shunt lattice arms may be so arranged as to provide a narrow pass band region. The remaining poles and zeros, far removed in frequency from the filter pass band, have negligible effect on the over-all characteristic.[8] The width of the pass band formed in this manner is not limited directly by the crystal ratio of capacitances. This type of filter, which will be called an intermediate-band crystal filter, may have somewhat wider bandwidths than the crystal-capacitor filter. It is highly significant that the inductances associated with the intermediate-band crystal filter need not have extremely high $Q$'s. In general, inductor $Q$'s in the order of 40–60 will be sufficient to permit bandwidths up to 2 or 3 times the bandwidth of the crystal-capacitor filter, with negligible increase in filter dissipation.

The wide-band crystal filter is obtained when all the critical frequencies resulting from an inductance-crystal combination are contained within the filter bandwidth limits, as shown in Fig. 3(c). The bandwidth range for this filter type is approximately 1.5 per cent to 10 per cent of the filter center frequency. The upper limit, which is somewhat smaller at high frequencies, is set by the crystal ratio of capacitances, while the lower limit is fixed[7] by the $Q$'s realizable for $L_0$. The dissipation present in the external inductances may be associated directly with the filter terminating impedances, producing no effect on the network attenuation characteristics other than a constant insertion loss.

The dissipation, or midband insertion loss, introduced by the filter network is only 1 or 2 db for most narrow- and intermediate-band filters. For wide-band filters, the corresponding loss depends upon filter bandwidth and external inductance $Q$. For a 5 per cent filter bandwidth and a $Q$ of 100, the filter loss is approximately 6 db.

The simple filters shown in Fig. 3 form the basic building blocks for more complicated filter networks. Greater attenuation and selectivity may be obtained either by cascading sections of the type shown, or by placing several crystals in parallel in any lattice arm as shown in Fig. 3(c) (connections shown dotted).

*Unbalanced Networks*

Until recently, the most significant application of crystal filters has been to low-frequency filters for carrier telephone systems. These filters, designed for use with balanced transmission lines, employ crystal resonators with divided electrodes[9] to obtain performance equivalent to the lattice networks shown in Fig. 3.

For vacuum tube or transistor circuitry, and at frequencies above several hundred kilocycles, it is desirable to utilize an unbalanced equivalent of the symmetrical lattice network. One of the most useful lattice equivalents is the "hybrid" network shown in Fig. 4(a).[10] The "hybrid" transformer has closely-balanced, tightly-coupled, secondary windings, and a primary winding which is uniformly coupled to the secondaries. Crystals 2A and 2B have twice the impedance of crystals A and B, respectively ($2L_1$, $C_1/2$, $C_0/2$). The inductance $L_a$ may be resonated by parallel capacitance, or it may be used as one of the inductances $L_0$ shown in Fig. 3(c).

Fig. 4(b) and 4(c) illustrates two methods of cascading hybrid-type filter networks to achieve greater attenuation and selectivity. Hybrid leakage reactance has been neglected in these circuits. Any combination of Fig. 4(a)–4(c) may be employed to provide still better performance. Alternatively, crystals placed in parallel

[7] D. I. Kosowsky, "Synthesis and Realization of Crystal Filters," Mass. Inst. Tech., Cambridge, Mass., Res. Lab. of Electronics, Tech. Rep. No. 298, pp. 38–42; June 1, 1955.

[8] See, for example, Fig. 10. The frequencies $f_1$ and $f_2$ may be closely spaced and form part of a filter pass band, while $f_3$ may be far removed from the pass band region.

[9] C. E. Lane, "Crystal channel filters for the cable carrier system," *Bell Sys. Tech. J.*, vol. 17, pp. 125–136; January, 1938.

[10] W. P. Mason, "Resistance-compensated band-pass crystal filters for unbalanced circuits," *Bell Sys. Tech. J.*, vol. 16, pp. 423–436; October, 1937.

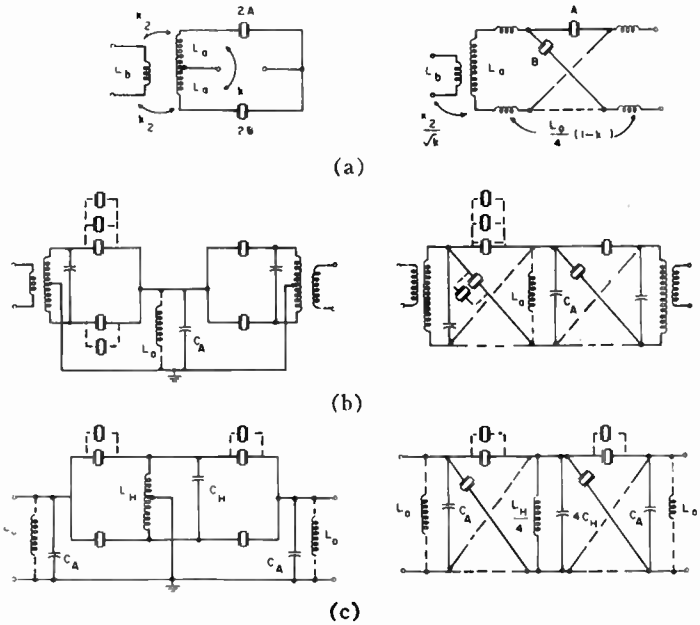

Fig. 4—"Hybrid" filter networks.

(shown dotted) in any lattice arm will accomplish the same result.

The inductances $L_0$ may be added to convert the network from the crystal-capacitor lattice [Fig. 3(b)] to the intermediate band or wide-band lattice [Fig. 3(c)]. In addition, the parallel circuit $L_0$–$C_A$ in Fig. 4(c), provides a convenient means for altering the nominal impedance level of the filter. The desired impedance transformation is easily accomplished by "tapping" $L_0$ or $C_A$ for the appropriate impedance level.

Utilizing the hybrid filter networks illustrated in Fig. 4, crystal filters have been produced throughout the frequency range of 10 kc to 40 mc, with bandwidths ranging from one cycle per second to several hundred kilocycles per second. The corresponding range of percentage bandwidths is 0.01 per cent to 7 per cent of center frequency.

## Synthesis Procedure

Design of the lattice-type crystal filter network may be accomplished by utilizing classical image-parameter synthesis techniques[6,11,12] or by considering the total insertion loss of a given filter network.[13] However, as mentioned previously, the values of the equivalent electrical parameters of the crystal resonator are not completely within the control of the filter designer. A design procedure which rapidly indicates whether a given set of filter specifications can be realized is therefore highly desirable.

Since the crystal filter is normally restricted to bandwidths which are a very small percentage of the center frequency, and because of the nature of the equations involved in the image parameter synthesis of these filters, it has been possible to develop a procedure which permits the design of even the more complicated crystal filters utilizing only simple calculations and graphical aids. This procedure is based on a normalization or approximation technique which provides solutions with accuracies that are normally well within the tolerances placed on the filter components. A complete description of the synthesis procedure is given in another report[7] and is outlined below.

As shown in Fig. 3, the pass band region of a crystal lattice filter extends from the lowest critical frequency of the series arm reactance to the highest critical frequency of the shunt arm reactance. These two frequencies, $f_A$ and $f_B$, are called the cutoff frequencies. The remaining critical frequencies of the series arm coincide with those of the shunt arm to produce a continuous pass band. For a given filter, the attenuation characteristic has a number of "infinite peaks" (bridge nulls) which can be no greater than one plus the number of "coincident" frequencies in the pass band.

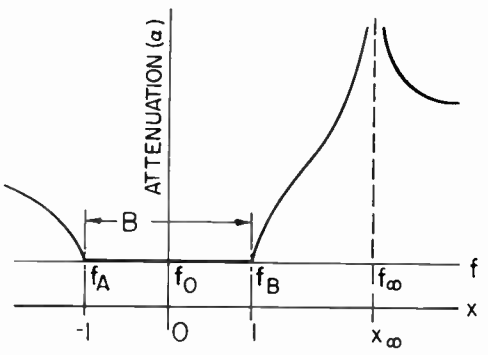


Fig. 5—"Normalized" basic section.

The simplest band-pass crystal filter [Fig. 3(a) and Fig. 5] will be referred to as the "basic" section. The characteristic of the basic section has, at most, one attenuation peak. The position of this attenuation peak may lie anywhere outside the filter pass band.

The attenuation characteristic of a filter having $n$ infinite peaks and a bandwidth $B$, is equal to the sum of the characteristics of $n$ basic sections, wherein each section has a bandwith $B$ and an attenuation peak corresponding to one of the $n$ peaks of the composite filter. The degree of complexity of a crystal filter necessary to meet a given set of specifications may, therefore, be determined through the addition of basic section characteristics.

Image attenuation of the basic section is a function of the filter cut-off frequencies, $f_A$ and $f_B$, and of the frequency of infinite attenuation $f_\infty$:

$$\alpha = \ln\left(\frac{1+p}{1-p}\right) = \text{attenuation loss} \qquad (4)$$

[11] D. Indjoudjian and P. Andrieux, "Les Filtres a Cristaux Piezo-electriques," Gauthier-Villars, Paris, France; 1953.
[12] E. A. Guillemin, "Communications Networks," John Wiley & Sons, Inc., New York, N. Y., vol. 2, ch. 10; 1935.
[13] W. Herzog, "Siebschaltungen mit Schwingkristallen," Dieterich'sche Verlagsbuchhandling, Wiesbaden, Germany; 1949.

where

$$p^2 = \left(\frac{f_\infty^2 - f_B^2}{f_\infty^2 - f_A^2}\right)\left(\frac{f^2 - f_A^2}{f^2 - f_B^2}\right). \tag{5}$$

Although (5) permits the calculation of all possible attenuation characteristics obtainable with the basic section, a complete set of characteristics would be necessary for each choice of filter relative bandwidth (ratio of bandwidth to center frequency). It is possible, however, to derive an approximation for $p$ that is independent of bandwidth and center frequency and yet introduces negligible error in practice. Referring to Fig. 5, a normalization variable defined by

$$x \equiv \frac{f - f_0}{B/2} \tag{6}$$

where

$$B \equiv f_B - f_A; \qquad f_0 \equiv \frac{f_A + f_B}{2} \tag{7}$$

is substituted into (5), resulting in

$$p^2 = \left[\frac{x_\infty - 1}{x_\infty + 1}\right]\left[\frac{x+1}{x-1}\right] \cdot \left[\frac{1 + \frac{B_r}{4}(x_\infty + 1)}{1 + \frac{B_r}{4}(x_\infty - 1)}\right]\left[\frac{1 + \frac{B_r}{4}(x-1)}{1 + \frac{B_r}{4}(x+1)}\right] \tag{8}$$

where

$$B_r = B/f_0 \text{ (relative bandwidth)} \tag{9}$$

and

$$x_\infty \equiv \frac{f_\infty - f_0}{B/2}.$$

Consideration of the values of $B_r$ and $x_\infty$ normally encountered in crystal filter design, leads to the conclusion that (8) may be closely approximated by

$$p^2 \doteq p_0^2 = \left(\frac{x_\infty - 1}{x_\infty + 1}\right)\left(\frac{x+1}{x-1}\right). \tag{10}$$

*Normalized Characteristics*

The normalized attenuation characteristic is a function only of the variable $x$ and the position of the attenuation peak ($x_\infty$). Since (10) contains neither $f_0$ nor $B$, the normalized attenuation expression will hold regardless of filter center frequency or filter bandwidth.

Reference to (8) indicates that (10) is an excellent approximation in cases of very small percentage bandwidths and small values of $x_\infty$. The set of normalized basic section characteristics shown in Fig. 6 illustrates the fact that even for the largest possible value of $x_\infty$ and for extremely wide bandwidths (for the crystal filter), the error involved in the normalization procedure is of no practical significance.

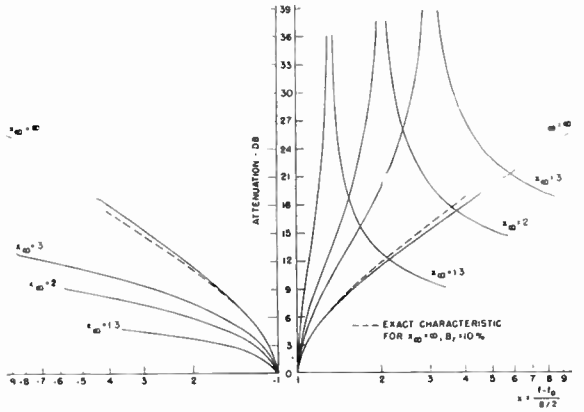


Fig. 6—"Normalized" basic section attenuation characteristics.

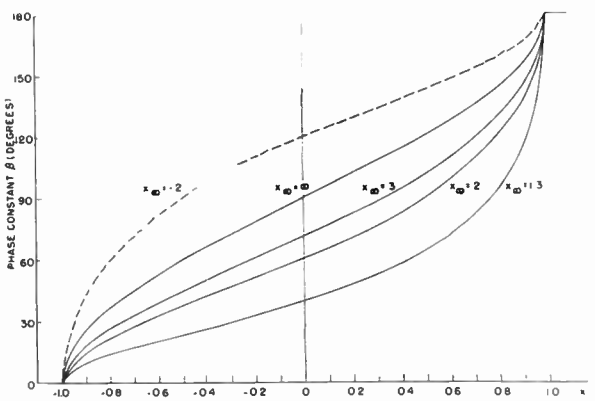


Fig. 7—Phase characteristics of basic section.

The attenuation $\alpha$ of a symmetrical network expresses the loss introduced by the network when it is terminated in its image or characteristic impedance. In practice the terminal impedances of a filter are generally fixed resistances. Image attenuation loss only approximately describes the performance of the filter. Filter termination effects, commonly called reflection and interaction losses, are of greatest importance in the filter pass band region. In this region, the attenuation loss is zero and the filter loss is primarily the result of mismatch.

To describe completely the filter transmission characteristic or insertion loss, it is necessary to determine the corresponding image impedance and phase characteristics. Fortunately, the same normalization technique may be applied to these characteristics to provide the complete insertion loss of any crystal filter.

The expression for a basic section normalized phase characteristic is given by

$$\beta_0 = 2 \tan^{-1} jp_0 \tag{11}$$

where

$\beta_0$ = normalized image phase constant.

A set of phase characteristics is shown in Fig. 7. The composite phase constant for a number of cascaded

basic sections is the sum of the phase constants for the individual sections at any value of $x$.

The image impedance characteristics of the crystal filters described above may be classified into three types depending on the nature of the cutoff frequencies $f_A$ and $f_B$. In normalized form the three types are as follows:

Type I: Zero at $f_A$ and pole at $f_B$

$$Z_{01} = R_{01}\left(\frac{1+x}{1-x}\right)^{1/2} \tag{12}$$

Type II: Zero at $f_A$ and $f_B$

$$Z_{02} = R_{02}(1-x^2)^{1/2} \tag{13}$$

Type III: Pole at $f_A$ and $f_B$

$$Z_{03} = R_{03}(1-x^2)^{-1/2} \tag{14}$$

where $R_{01}$, $R_{02}$, and $R_{03}$ are resistances whose values depend on both the relative bandwidth of the filter and the equivalent circuit parameters of the crystal resonators. Eqs. (12) and (13) are plotted in Fig. 8.

In the filter pass band region ($-1<x<+1$), the image impedance is resistive (solid line). In the attenuating region, the image impedance is reactive and the corresponding magnitude is shown by the dotted line. The Type I image impedance is characteristic of the narrow-band filter [Fig. 3(a), 3(b)], while the Type II and Type III may result when external inductances are employed in wide-band or intermediate-band filters [Fig. 3(c)].

Utilizing the data of Figs. 6–8, it is possible to construct the total insertion loss characteristic corresponding to any number of basic sections (*i.e.*, any degree of filter complexity). As an example, Fig. 9 illustrates the composite transmission characteristics of a filter consisting of 6 basic sections (peaks at $x_\infty = \pm 1.3, \pm 1.6, \infty, \infty$). These values have been chosen to provide a maximum filter attenuation of 60 db. The shape factor (ratio of 60-db bandwidth to 6-db bandwidth) is approximately 1.3:1. A Type II image impedance characteristic is assumed, and the filter is resistively terminated.

A filter of this type might be employed in a telephone carrier channel system in the vicinity of 100 kc, or in an intermediate-frequency amplifier at 10 to 15 mc where extremely high selectivity is preferred to high final attenuation. For applications requiring final attenuations of 80 to 100 db, the attenuation peaks may be placed farther from the pass band. (See Fig. 13.)

Fig. 9 illustrates the degree of approximation to "flat" pass band and linear phase characteristics which may be obtained with the crystal filter. These factors, combined with linear voltage characteristics, result in low signal distortion and contribute to good transient performance.

To complete the design of a given crystal filter, it is necessary to determine the values of the equivalent parameters of the crystal resonators from the filter insertion loss characteristic. This is accomplished first by

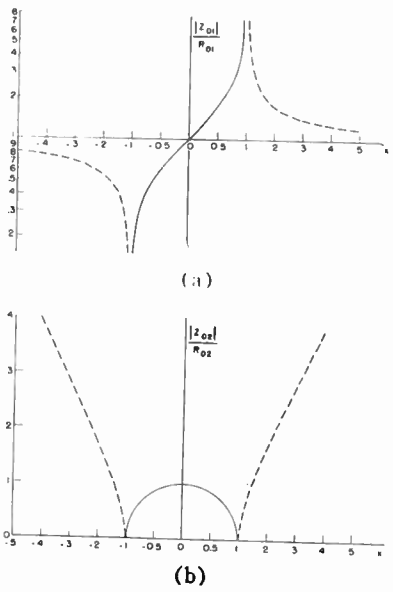


Fig. 8—Image impedance characteristics of band-pass filters. (a) Type I, (b) Type II.

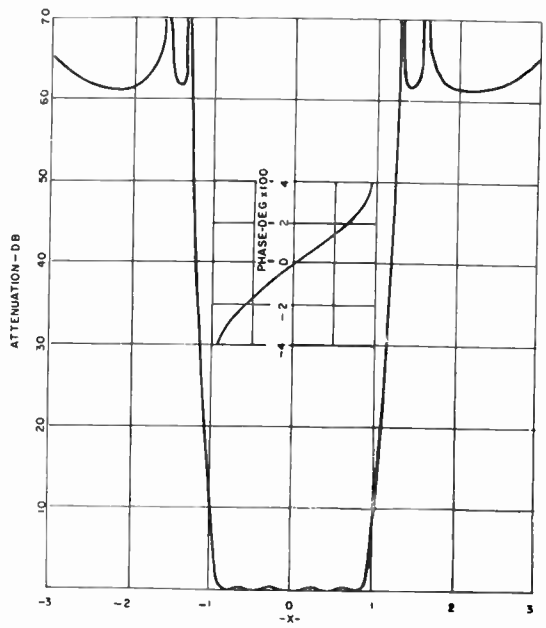


Fig. 9—Six-section transmission characteristics.

determining the locations of the pass band critical frequencies (see Fig. 3) from the attenuation peak positions, and then by calculating the element values of the filter reactances from these critical frequency configurations. It is interesting to note that even this portion of the synthesis procedure may be normalized so that the relative values of the filter elements may be determined for any given configuration without specifying filter frequency or bandwidth.

Fig. 10 illustrates the use of the normalization procedure to determine element values from zero-pole configurations. The configuration shown might represent one arm of the lattice network of Fig. 3(c). The zero and pole frequencies ($f_1$, $f_2$, $f_3$) can be derived from the attenuation frequencies of the filter utilizing conventional

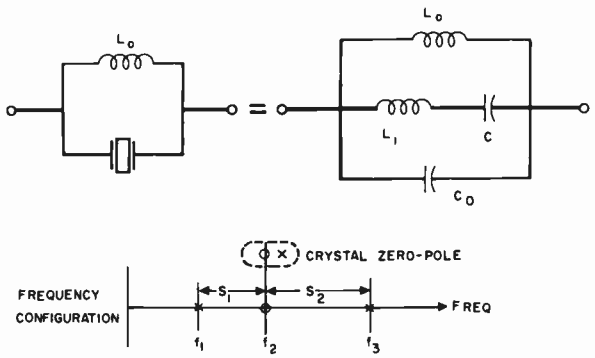


Fig. 10—Lattice-arm reactance.

synthesis techniques. On the other hand, the normalization procedure yields $S_1$ and $S_2$ directly (as functions of the filter bandwidth $B$).

Since $f_2$ is also the crystal resonant frequency, the realizability of the crystal resonator is uniquely determined by the required ratio of capacitances ($r = C_0/C_1$). If $C_0$ is chosen to determine the filter image impedance, or if $C_1$ is fixed by an available crystal unit, then the remaining element values may be determined from the ratio of capacitances and the frequency of resonance of $L_0$ and $C_0$ called $f_\alpha$. That is,

$$f_\alpha \equiv \frac{1}{2\pi(L_0C_0)^{1/2}}. \tag{15}$$

A comparison of the exact and normalized (approximate) values of $f_\alpha$ and $r$, for the network of Fig. 10 is given in (16) and (17).

| Exact | Approximate | |
|---|---|---|
| $f_\alpha = \dfrac{f_1 f_3}{f_2}$ | $f_\alpha \doteq f_2 + (S_2 - S_1)$ | (16) |
| $r = \dfrac{f_2^2}{(f_1^2 + f_3^2) - (f_\alpha^2 + f_2^2)}$ | $r \doteq \dfrac{f_2^2}{4S_1S_2}$. | (17) |

Approximations such as (16) and (17) may be written for an entire filter configuration. By the proper combination of these equations, conditions of filter realizability as well as the values of all network parameters may be described in terms of filter performance characteristics. Once equations are derived for a given filter configuration, complete filter design is accomplished by simply substituting the values of center frequency, bandwidth, and impedance level. Simple manipulation of these equations provides additional important information, such as the effects parameter variations have on the filter transmission characteristic. As a result, the normalization procedure is useful not only in filter synthesis, but also in practical considerations connected with filter realization, such as the specification of tolerances and the development of alignment techniques.

## Applications and Typical Characteristics

Without useful application, the design of high-frequency crystal filters would be to little avail. Some of the more immediately apparent applications are explored in the following paragraphs.

Bandwidth ranges from one or two cycles to several hundred kilocycles per second represent the present-day boundaries of crystal filter technique. These ranges include the majority of channel or information bands allocated to communications and navigation equipments. The ability to produce a given bandwidth at substantially higher frequencies, together with the excellent selectivity, stability, and loss characteristics of the high-frequency crystal filter, has already resulted in many interesting applications.

Crystal filters are widely applied to intermediate frequency filtering applications in AM, SSB, and fm receivers, as well as single-sideband generators. For mobile versions of these systems, filters from 10 to 30 mc are particularly attractive, offering the advantages of small size ($\frac{1}{2}$–2 cubic inches) and freedom from microphonic behavior.

Crystal filters are employed in data handling systems utilizing pulse techniques, where uniform time delay and smooth transient response characteristics are significant. Other important applications in which the crystal filter is utilized to select a band of frequencies or an entire bank of frequency bands include fixed-channel receivers at frequencies as high as 40 mc, carrier telephone systems, telemetering systems, Doppler radar, fire control and missile systems, and spectrum analysis.

### *Single-Conversion Receivers*

A single-conversion crystal-filter receiver, as shown in Fig. 11, offers the advantage of a high-frequency first IF (*i.e.*, good image rejection), combined with high adjacent channel selectivity (heretofore achieved only through multiple frequency conversion). At the same time, the elimination of multiple conversions reduces cross modulation and receiver desensitization due to mixer overload, and locally generated spurious signals.

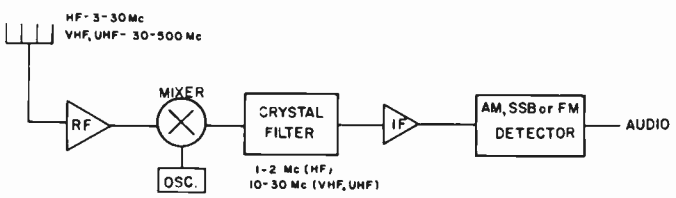


Fig. 11—Single-conversion crystal-filter receiver.

Since the frequency selection characteristics of the entire receiver are determined primarily by the crystal filter unit, it is possible to alter the receiver bandwidth and selectivity characteristics by simply changing the filter. Crystal filters designed for single conversion receivers have been produced with bandwidths ranging from 250 cps (for hf-cw telegraphy) to 50 kc (for vhf-fm or uhf-AM).

Fig. 12 illustrates the attenuation characteristics of two filters designed for single-conversion hf communica-

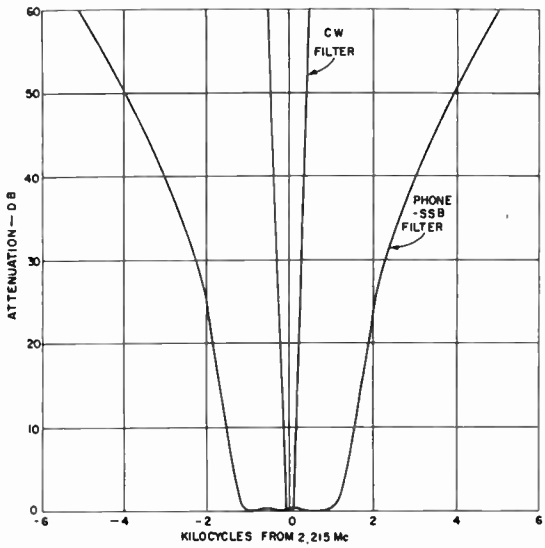


Fig. 12—Crystal filters for single conversion hf receivers.

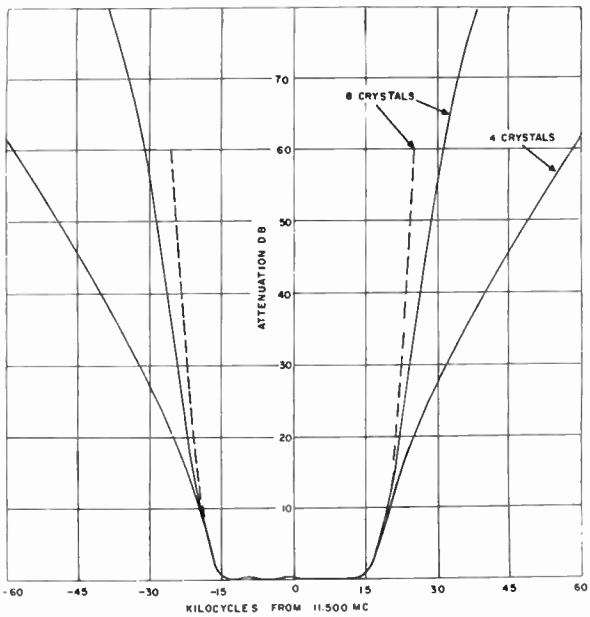


Fig. 13—Crystal filters for vhf fm receivers.

tion receivers.[14] The narrow filter has a 6-db bandwidth of 250 cps and is intended for cw telegraphy. The wider filter has a 6-db bandwidth of 2800 cps for phone-SSB reception. In both cases, the center frequency is 2.215 mc, and the shape factor (ratio of bandwidth at 60-db attenuation to bandwidth at 6-db attenuation) is slightly greater than 3:1. Pass band response variation or "ripple" is less than $\pm\frac{1}{2}$ db, while the insertion loss is less than 3 db. Each filter utilizes four crystal resonators in a hybrid configuration (Fig. 4) and is equivalent to two cascaded narrow-band lattices [Fig. 3(b)].

For vhf-fm applications, an intermediate frequency in the 10- to 15-mc range is normally chosen. Fig. 13

[14] "A selective IF amplifier for phone and cw," in "Radio Amateur's Handbook," American Radio Relay League, Inc., 34th ed., pp. 137–140; 1957.

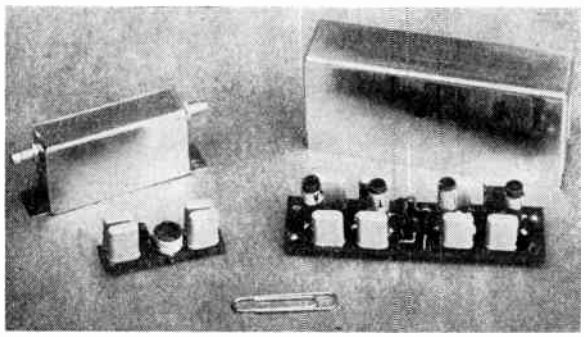

Fig. 14—Hybrid-type crystal filters.

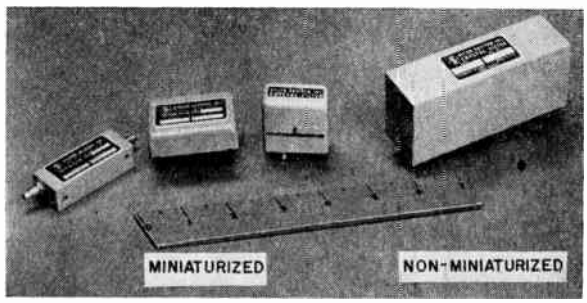


Fig. 15—High-frequency crystal filter mounting cases.

shows the attenuation characteristics of filters at 11.5 mc designed for mobile fm receivers. A comparison is made between a four-crystal filter (shape factor approximately 3.5:1) and an eight-crystal filter (shape factor approximately 1.7:1). The eight-crystal device may be made considerably more selective (*i.e.*, smaller shape factor), at the sacrifice of the final or "ultimate" attenuation reached by the filter. For example, the dotted characteristic in Fig. 13 (shape factor approximately 1.3:1) may be obtained by permitting the filter to return to an attenuation slightly greater than 60 db (see Fig. 9). The solid eight-crystal characteristic reaches an attenuation well over 80 db and represents a good compromise between final attenuation and shape factor for this application. The 6-db bandwidth for the filters shown in Fig. 13 is approximately 35 kc. For the new split-channel fm operation, filters with identical characteristics have been produced with bandwidths of 15 kc.

The filters illustrated in Fig. 13 are intermediate-band lattice networks produced in hybrid configuration. Fig. 14 shows one component arrangement for a four- and an eight-crystal filter of this type. The miniature crystal units, which occupy a volume of only 0.035 cubic inch and weigh about 1/25 of an ounce, are extremely rugged and will withstand vibration frequencies as high as 2000 cps and shock accelerations greater than 30 g.

The small size of crystal units and associated components at frequencies greater than 10 mc, makes possible extremely compact filters. Several packaging arrangements of these filters are shown in Fig. 15. The smallest of the miniaturized units ($\frac{1}{2}$ cubic inch) will accommodate a four-crystal filter. The other units may contain

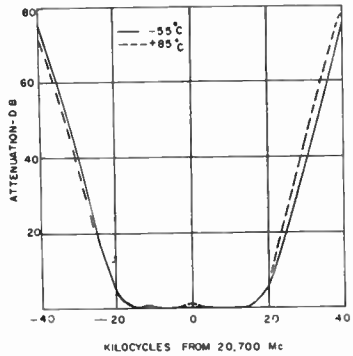


Fig. 16—Temperature performance of crystal filter.

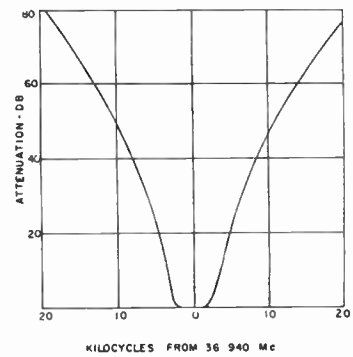


Fig. 17—Harmonic resonator filter.

up to 5 or 6 crystals, to yield characteristics lying between the 4- and 8-crystal selectivities illustrated in Fig. 13. The remaining package is nonminiaturized and accommodates the 8-crystal filter illustrated in Fig. 14.

Since the crystal filter supplies most of the selectivity of the receiver, the need for multiple-tuned interstage transformers in the IF amplifier is eliminated. Instead, the amplifier interstage networks become simple single-tuned circuits designed for maximum gain (high $Q$, high $L/C$ ratio). Furthermore, as previously mentioned, the impedance level of the crystal filter may be varied over wide limits through the use of single-tuned terminating circuits.

Therefore, one filter may be employed at a high impedance level to obtain maximum gain with vacuum tube circuitry; or it may be used at lower impedance levels to obtain maximum power transfer with transistor circuitry. In either case, the same filter is used.

Fig. 16 illustrates the attenuation characteristic of a crystal filter designed for vhf-uhf AM and fm reception. The 6-db bandwidth is approximately 40 kc and the shape factor is approximately 1.7:1. The filter characteristics at −55°C and +85°C are illustrated. Even at frequencies as high as 20 mc, the extremely high stability of the crystal resonator makes possible the realization of filters which operate over wide temperature ranges with negligible degradation of performance.

At frequencies greater than approximately 30 mc, it becomes difficult to produce crystal resonators which operate in fundamental vibrational modes. At these elevated frequencies, it is common to employ crystal

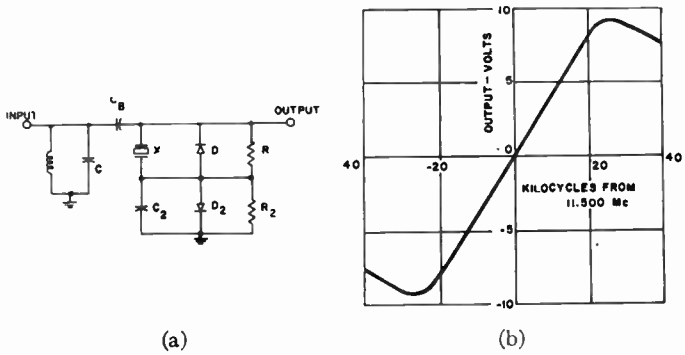


Fig. 18—Crystal discriminator.

resonators at 3rd, 5th, or 7th harmonics of their fundamental response. However, the ratio of capacitances of a harmonic resonator increases as the square of the order of the harmonic, making it difficult to obtain useful filter characteristics with such crystals. Fig. 17 shows the characteristic of a 4-crystal hybrid filter utilizing 3rd-overtone AT quartz resonators. The bandwidth of this filter is only 6 kc (0.016 per cent of center frequency).

*Crystal Discriminator*

In order to utilize the single conversion technique in fm receivers, it is necessary that fm detection be performed at the first IF. Since the first intermediate frequency may be too high to permit the realization of a conventional type of fm detector or discriminator, a crystal discriminator has been developed which possesses a stability comparable to that of the high-frequency crystal filter and which operates at the filter frequency. This device may be applied not only to fm receivers but also to automatic frequency control systems and frequency modulation generators.

The basic circuit diagram of the crystal discriminator is illustrated in Fig. 18(a). The voltage developed across the resonant circuit $L_1$–$C_1$ is transferred through bypass capacitor $C_B$, to the series crystal-capacitor circuit, $X$–$C_2$. The voltage developed across each element in this series combination is rectified by the diodes, $D_1$–$D_2$. The difference between these voltages is developed across the combination $R_1$–$R_2$, and has the form shown in Fig. 18(b). The discriminator in Fig. 18(b) is designed for use in conjunction with the filters of Fig. 13. The discriminator has a center frequency of 11.5 mc and a peak-to-peak bandwidth of approximately 50 kc. When driven from a conventional pentode limiter, which operates at a peak rf input voltage of 2 volts, the discriminator output voltage is approximately 16 volts peak-to-peak.

*Single-Sideband Generators*

In the generation of single-sideband signals by filtering techniques, the signal quality is largely dependent upon the ability of a filter to pass, with negligible distortion, one sideband of an amplitude modulated signal, and simultaneously to effectively eliminate the other

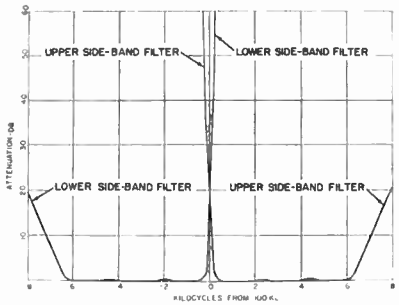


Fig. 19–Single-sideband crystal filters.

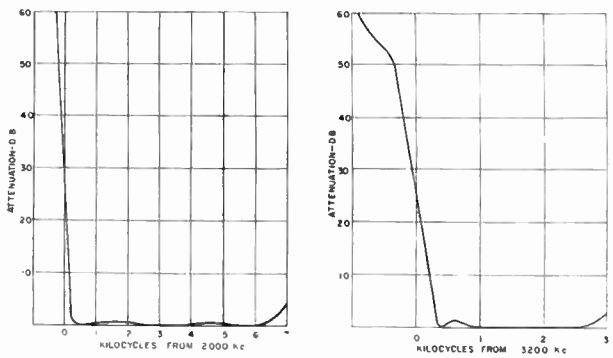


(a) (b)

Fig. 20—High-frequency SSB crystal filters.

sideband. Fig. 19 shows the attenuation characteristics of two filters designed for single-sideband generation at a frequency of 100 kc. Each filter has a bandwidth (at 2 db) of over 6 kc, and an attenuation slope which rises from 2 db to 60 db in less than 600 cps. If either filter were produced with the same steep attenuation characteristic on both sides of its pass band, the filter would have an equivalent shape factor of less than 1.2:1.

The single-sideband signal which is generated at the filter frequency is modulated onto a high frequency carrier through processes of frequency mixing or conversion, similar to those employed in the communications receiver. As was true in the receiver case, one or more frequency conversions may be eliminated by increasing the frequency of the filtering operation. To accomplish this end, crystal filters for SSB generation have been produced at frequencies as high as 16 mc.[15]

Fig. 20 (a) shows the attenuation characteristic of a single-sideband filter nearly identical with the upper-sideband filter in Fig. 19, except for a center frequency of 2 mc. The 2-mc SSB crystal filter is an intermediate-band hybrid filter.

For SSB-voice operation in the hf bands, requiring audio frequencies of 300 to 3000 cps, the attenuation characteristic shown in Fig. 20(b) is generally sufficient. This filter utilizes only 4 crystal resonators in a simple narrow-band hybrid configuration.

[15] W. E. Morrow, Jr., C. L. Mark, B. E. Nichols, and J. Leonhard, "Single-sideband techniques in uhf long-range communications," PROC. IRE, vol. 44, pp. 1854–1873; December, 1956.

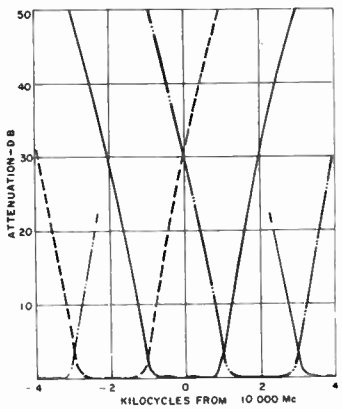


Fig. 21—"Comb" filter set.

*Fixed-Channel Receivers*

It is often desired to construct a receiver which operates on a fixed channel or small number of channels at some frequency below 30 mc. By producing a crystal filter at the given channel frequency and with the required bandwidth, a tuned radio frequency (trf) receiver may be constructed. This is equivalent to removing the rf, mixer, and oscillator stages from the crystal-filter receiver. (See Fig. 11.) For fixed-channel operation, the trf receiver, in addition to its simplicity, provides the maximum possible protection against adjacent channel interference. Any communications receiver may be converted to a fixed-channel receiver by inserting a crystal filter between the antenna and the first rf stage. In the presence of strong adjacent-channel interference in the hf bands, this technique materially reduces interference caused by intermodulation and desensitization.[16]

*Frequency Multiplexing*

Perhaps the best-known application of crystal filters is to frequency multiplexing systems, and more particularly to carrier-telephone systems.[9] Filters for this application are generally wide-band lattice filters with bandwidths of 4 kc, spaced 4 kc apart, in the range of 60–108 kc. The shape factor required is approximately 1.5:1. As illustrated in Fig. 9 and Fig. 13, it is possible to produce high-frequency as well as low-frequency crystal filters with this type of characteristic.

The close tolerances which can be maintained on the shape of a crystal filter characteristic make this device particularly well suited for frequency channelizing or "comb" filter applications. Fig. 21 illustrates part of a bank of closely-spaced filters. Each filter has a bandwidth of 2 kc in the vicinity of 10 mc, utilizes 4 crystal resonators, and occupies a volume of approximately 1 cubic inch. Filter comb sets of this type have been produced at frequencies as low as 100 kc and as high as 28 mc, for application to Doppler radar and fire control and to spectrum analysis.

[16] F. Raymond, "Reduction of Interference in the HF Range (2–32 MC) Through the Use of Bandpass Crystal Filter (Hycon Type 44)," Rome Air Dev. Center, Air Res. and Dev. Command, Tech. Memo, RADC-TM-56-33; 1957.

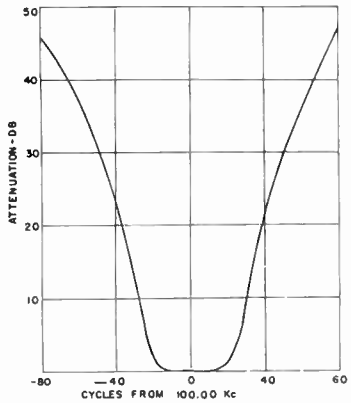


Fig. 22—Narrow-band filter for spectrum analysis.

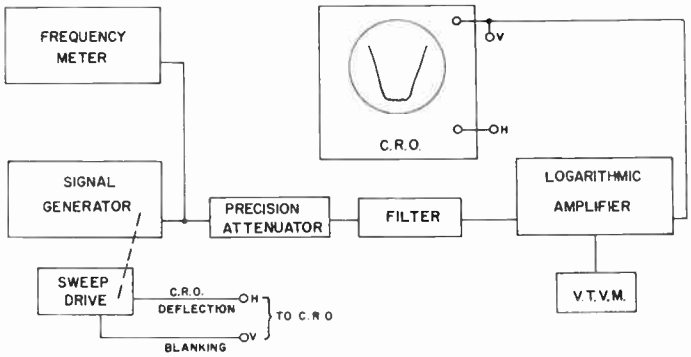


Fig. 23—Block diagram of crystal filter test facility.

In some types of spectrum analysis equipments, a single filter is made to cover an entire band of frequencies by employing the superheterodyne principle. Narrow-band crystal filters have been produced for this application with bandwidths as small as 1 cps (at a center frequency of 10 kc). Fig. 22 shows the attenuation characteristic of a 4-crystal hybrid filter at 100 kc. The bandwidth of this filter is approximately 50 cps and it has been employed in spectrum analysis equipment, in SSB equipment for carrier selection, and in channelizing equipment for pilot selection.

## Measurement of Filter Characteristics

Fig. 23 is a block diagram of the test facility which is employed for the alignment and measurement of crystal filters in the range of 10 kc to 50 mc. Basically, the filter test facility provides means of accurate frequency and attenuation-level measurements while simultaneously presenting to the operator a visual display of the entire attenuation characteristic. The attenuation display is obtained with a mechanically-swept signal generator and a logarithmic amplifier. The test circuit compresses a voltage variation of 80 db into a signal suitable for presentation on any dc oscilloscope or $X$-$Y$ plotter. A single amplifier, using several sets of plug-in inductors, covers the entire range of 10 kc to 50 mc.

The precision attenuator is operated at its proper impedance level at all times, providing accurate attenuation-level settings. The frequency meter provides accurate frequency measurement when the sweep is stopped at some chosen attenuation point. The dc output of the logarithmic amplifier is derived from an automatic gain control (agc) circuit which provides feedback around a 3-stage amplifier.

Because the crystal filter is a relatively narrow-band device compared to a conventional low-$Q$ tuned circuit, it is a simple matter to tailor the frequency characteristics of the logarithmic amplifier to have negligible effect on the attenuation characteristics of the filter. A blanking voltage, derived from the sweep drive, eliminates the effect of backlash in the drive by preventing the retrace of the filter characteristic when the direction of sweep is reversed.

Before a filter is inserted into the test facility, the output of the logarithmic amplifier is observed over the entire frequency band of interest and at a number of attenuation levels. The resulting oscilloscope display, which should be a series of evenly spaced horizontal lines, is used to check the level of the signal generator output and the flatness of the logarithmic amplifier characteristic over the frequency and attenuation ranges used in testing the crystal filter.

## Conclusion

Further progress in the development of quartz resonators may make possible the extension of crystal filter ranges to frequencies approaching 100 mc. Filter bandwidths in the order of 1 to 5 mc may be achieved, permitting the application of crystal filters to wide-band systems such as pulsed radar.

High-frequency crystal filters are beginning to play an important role in the battle to expand the number of usable channels of communication in our limited frequency spectrum. The device provides a new standard of stability and selectivity. Crystal filter units are now being produced in quantity to operate at frequencies where full advantage may be derived from their unique characteristics.

# Experimental 8-MM Klystron Power Amplifiers*

T. J. BRIDGES†, MEMBER, IRE, AND H. J. CURNOW‡

*Summary*—**Experimental klystron amplifiers, which were used to investigate the cw power obtainable at a wavelength of 8 mm, are described. Working at 5000 volts with a beam current of 0.2 a, these tubes produced an output power of 75 watts cw. Operation was limited by the maximum current density of 1.5 a/cm² which could be drawn from sprayed-oxide cathodes.**

## Introduction

A RECENT paper[1] described a klystron oscillator of the floating-drift-tube type with a cw output of 12 watts in the 8-mm wavelength band, and a life in excess of 1000 hours. It was considered that the major limitation to the output power was the cathode emission which could be obtained. At the time the only cathode available was the standard oxide-coated type and even employing special techniques, such as a 700°C bake out, the maximum emission density which could be drawn with useful life was 0.6 a/cm². However, cathodes with superior emission capabilities are now becoming available. If these were combined with the techniques referred to, a substantial increase in the output power might be possible.

To investigate this possibility, work has been carried out on klystron power amplifiers at 8-mm wavelength. The object was to discover whether the output could be increased significantly before overheating or other limitations became prohibitive. Conventional sprayed-oxide cathodes were used in these experiments since they were readily available and it was found that current densities up to 1.5 a/cm² could be drawn from them for short periods. The same electron gun as in the oscillators was used and the dc input power was increased by raising the applied voltage. As the efficiency of a klystron increases with the applied voltage and the dc input power is proportional to the 5/2 power of the voltage, it was expected that the output power would increase very rapidly as the voltage was raised. Because a floating-drift-tube oscillator is limited to a number of discrete, narrow bands of operating voltage, the tubes were constructed so that they could be used either as amplifiers or as oscillators with a phase-shifting network in the feedback loop. They were then capable of working over a wide, continuous range of voltage, and thus of dc input power.

## Description of the Tubes

The general arrangement of the tubes used in the experiments is shown in Fig. 1, while details of the resonant cavities may be seen in Fig. 2. The cavities were of the doubly re-entrant type, and the gap dimensions were such that at an operating voltage of 5000 volts the gap transit angle was 2 radians and the normalized tunnel diameter 2.8 radians. The ends of the cavity cones had different diameters to avoid multipactor effects and to shield the thin cone tips from beam interception.

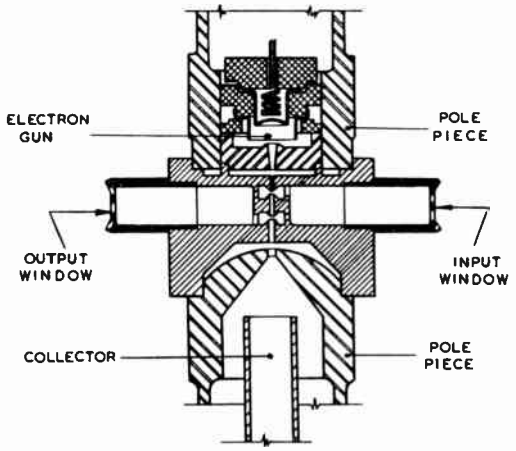


Fig. 1—General arrangement of 8-mm klystron amplifier.

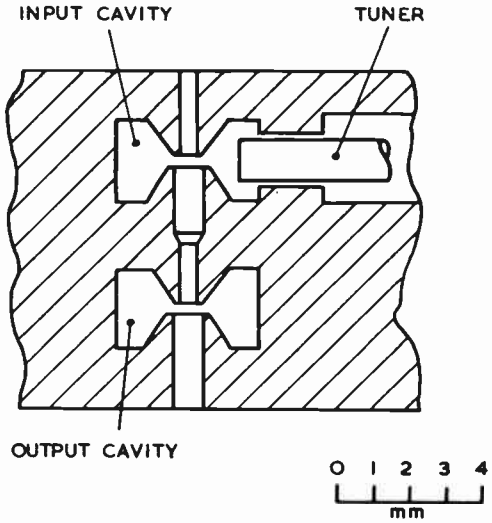


Fig. 2—Details of the resonant cavities.

The drift length between the cavities was 0.15 inch, which was about 0.16 of the effective plasma wavelength for the electron beam used. A value less than the optimum 0.25-plasma wavelength was chosen in order to reduce the length over which the focusing magnetic field had to be maintained.

The method of construction of the tubes was similar to that of the oscillators.[1] There were of course, some extra features made necessary by the different cavity arrangement. With separate cavities some means had to

* Original manuscript received by the IRE, September 18, 1957.
† Bell Telephone Labs., Inc., Murray Hill, N. J.
‡ Services Electronics Res. Lab., Baldock, Hertfordshire, Eng.
[1] R. L. Bell and M. Hillier, "An 8-mm klystron power oscillator," PROC. IRE, vol. 44, pp. 1155–1159; September, 1956.

be provided of aligning them to the same resonant frequency. The cavities were approximately tuned by adjusting the lengths of the gaps during construction. Final adjustment was made during operation by tuning the input cavity. The resonant frequency of this could be varied over a 1 per cent range by means of a fine-tuning device, which consisted of a 1-mm-diameter copper wire, shown in Fig. 2, protruding through a hole in the wall of the cavity and supported by a flexible diaphragm (not shown). Each of the cavities was coupled to a separate waveguide, the coupling being arranged to be a nominal match in the absence of the electron beam. For ease of construction the waveguides inside the tubes were circular ($TE_{11}$ mode) and simple glass windows were used. Specially designed transitions at the windows enabled a good match to be obtained directly to standard rectangular waveguide. The windows of high-melting-point aluminosilicate glass could pass a mean power of 50 watts before forced cooling became necessary.

The electron optical system was identical with that used in the oscillators, apart from the length of the tunnel. The gun had a perveance of about $0.5\times10^{-6}$ a/volt$^{3/2}$, and the current density multiplication was 100 times. A transmission efficiency of 75–80 per cent was obtained through a 0.023-inch diameter tunnel, 0.3 inch in length. The increased magnetic field required for focussing at elevated voltages was obtained with an electromagnet.

## Experimental Results

It was found that in tubes which had been baked out at 700°C, ordinary sprayed-oxide cathodes could be used at emission densities up to 1.5 a/cm$^2$. The exact conditions needed to achieve this performance were not determined, and the results varied from one cathode to another. When this emission density could be obtained it was possible to operate a tube quite consistently at 5000 volts and a beam current of 0.2 a for periods of a few hours. These conditions corresponded to a power density in the beam of 500 kw/cm$^2$.

The construction of the tubes was such that the gun could easily be replaced and satisfactory operation at 5000 volts was eventually achieved with each of four structures, with identical cavity arrangements. The low-signal gain under these conditions was 8 db. As this was so small there was no signal source available which could be used to drive the tubes to their full output. They were accordingly operated as oscillators, with an external waveguide feedback loop (see Fig. 3). The attenuation of the loop was set at about 4.5 db by the inclusion of a ring hybrid and by the loss in the waveguide components. The output power was measured with a calorimeter through a directional coupler. The phase of the feedback was adjusted with a phase shifter for optimum output. Matching stubs (not shown) were used to compensate for the mismatch caused by the presence of the electron beam across the gaps.

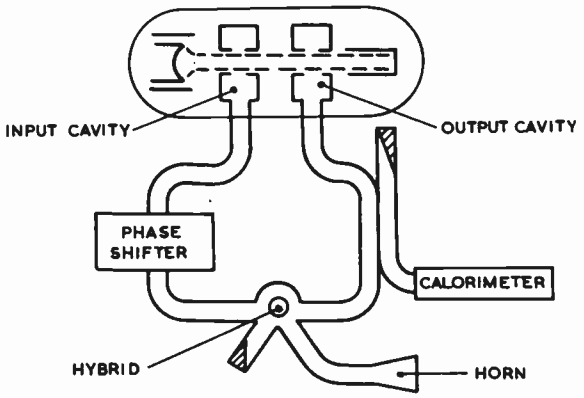


Fig. 3—Feedback loop.

Operating under the conditions described the average output power of the four tubes was 75 watts cw, corresponding to an efficiency of 7.5 per cent.

The limit to the current which could be drawn from a cathode was set by a deterioration in the transmission efficiency, causing unacceptably high dissipation on the rf structure. This was revealed by detuning the cavities, rather than by catastrophic heating effects. With better cathodes higher emission densities should be obtained before this defocusing effect occurs and the input power could then be raised even further.

## Comparison with Theory

In order to determine whether the output obtained was a fair test of the potentialities of the tubes, a comparison was made with a theoretical estimate of the power to be expected. The efficiency can be expressed in terms of the low-signal gain, the bunching angle, and the maximum rf current which can be induced in the electron stream. The low-signal gain depends on various parameters of the tube from which it can be calculated; it can also be measured directly. The maximum rf current which can be induced in an electron stream has been calculated from the theory of the bunching process. The simple theory of Webster[2] predicts that this will have an amplitude 1.16 times the beam current. A more elaborate analysis[3] suggests that the value should be rather less than this, but for the values of the parameters for these tubes the efficiency so calculated is only slightly less.

In order to work out what low-signal gain might be expected, it was necessary to know the values of the cavity resonant conductance, and the effective gap-coupling and gap-loading coefficients. These were obtained from perturbation measurements on a scaled-up model of the cavity, and from $Q$-factor measurements on the actual cavities. From the perturbation measurements the ratio $R/Q$ for the cavity was found to be 120.

[2] D. L. Webster, "Cathode ray bunching," *J. Appl. Phys.*, vol. 10, pp. 501–508; July, 1939.
[3] M. Chodorow, E. L. Ginzton, and E. J. Nalos, "Debunching of electron beams constrained by strong magnetic fields," Proc. IRE, vol. 41, pp. 999–1003; August, 1953.

$Q$-factor measurements on the cavities used in the tubes showed that the loaded $Q$ was 750. The cold-loaded conductance was therefore $1.11\times10^{-5}$ mhos. The gap-coupling and gap-loading coefficients were also calculated from the shape of the gap field given by the perturbation measurements. This was preferred to calculations based on assumed field shapes, as the gap dimensions were rather larger than those for which the common assumptions are valid. The values obtained were a mean-square coupling coefficient of 0.3 and a gap-loading conductance of $0.75\times10^{-5}$ mhos. Allowing for the effects of space-charge debunching and the mismatch introduced by the gap-loading, the low-signal gain was calculated to be 11.2 db. The experimentally observed value (8 db) was less than this. The most probable cause for this departure from theory lies in the nature of the electron stream, which certainly was not the uniform beam filling the drift tube assumed in the calculations. The effect of a smaller beam diameter would be to reduce the coupling coefficient and to increase the effect of space-charge debunching. If the observed value of the gain is used, together with the assumption of a maximum rf current 1.16 times the beam current, then the expected efficiency is 7.8 per cent, in good agreement with the observed value. Thus it may be concluded that the observed output was that which could be expected from the tubes, and no large advantage was being lost through the lack of a powerful driving source.

## Conclusion

The work carried out on these klystrons has shown that it is possible to obtain cw powers of at least 75 watts in the 8-mm wavelength band. A necessary condition for this is that the cathode must be capable of giving an emission density of 1.5 a/cm² in an electron gun with a density multiplication of 100 times. Although the power density in the beam was 500 kw/cm², the limit was not set by thermal considerations, but by cathode performance.

The actual tubes used in this investigation would be of little practical use as the life was short and the gain low. In order to produce a useful tube giving this order of output power, it would be necessary to incorporate a cathode of improved performance and to increase the gain by adding extra cavities. Neither of these operations should present any major difficulties.

## Acknowledgment

This paper is published by permission of the British Admiralty.

# FM Demodulator Time-Constant Requirements for Interference Rejection*

ELIE J. BAGHDADY†, MEMBER, IRE

*Summary*—**Under conditions of high-level interference fm receiver performance is often impaired because of improper low-frequency time constants in the limiter and discriminator circuits. The computation of the upper bounds on the permissible values of these time constants is illustrated. Severe restrictions are indicated which often conflict with other fundamental requirements. The computational results of this paper demonstrate that these severe restrictions can be alleviated by means of simple schemes that will greatly enhance the capture performance of the fm receiver.**

## I. Introduction

A BASIC requirement in fm receiver design for suppressing multipath and cochannel disturbances is the use of the proper time constants in the low-frequency parts of the limiter and discriminator circuits. The presence of an undesired signal, which is weaker than the desired one, within the linear pass band of the receiver causes the resultant signal delivered to the first limiter to exhibit severe AM and fm disturbances under conditions of high-level interference. For proper amplitude-limiting operation, the limiter circuit must be capable of following the sharp changes in the envelope of the resultant impressed signal, which may recur at a rate (in cps) equivalent to the bandwidth of the IF amplifier. In the discriminator the output circuit across which the rectified voltage is taken must be capable of following the detected instantaneous-frequency disturbance pattern. This performance is necessary in order to avert diagonal clipping and leave the variational control of the operation of the rectifying diodes entirely in the hands of the envelope of the signal delivered by the fm-to-AM-conversion section of the discriminator. Here, also, the sharp changes in the detected fm disturbance waveform may recur at a maximum rate (in cps) of one IF bandwidth. In order to insure proper

* Original manuscript received by the IRE, May 16, 1957; revised manuscript received, November 8, 1957. This work was supported in part by the U. S. Army (Signal Corps), the U. S. Air Force (Office of Sci. Res., Air Res. and Devel. Command), and the U. S. Navy (Office of Naval Res.).

† Dept. Elec. Eng. and Res. Lab. Electronics, Mass. Inst. Tech., Cambridge. Mass.

operation, it is necessary, therefore, to determine the upper bounds on the time constant of the output circuit.

After discussing briefly the properties of the disturbances caused by the interference, and of the effect of narrow-band limiting upon the fm disturbance, we shall demonstrate how certain well-known principles can be applied to the determination of the upper bounds on the limiter and discriminator time constants. These upper bounds will be quite stringent if the requirements of high-capture performance are to be met, particularly because they may conflict with other fundamental requirements. To alleviate these restrictions, the disturbances must be suppressed (or minimized) before they reach the appropriate low-frequency circuits. It is believed that, more often than not, the impairment of proper performance of most available fm receivers can be traced to improper time constants in the limiters, or discriminators—particularly in the discriminators. The present study should suggest some remedies for these difficulties.

## II. Disturbances Caused by High-Level Interference

Consider the situation in which two carriers of constant relative amplitudes 1 and $a$ ($a<1$) and of frequencies $p$ and $p+r$ rad/second ($r \ll p$) are passed simultaneously by the IF amplifier of an fm receiver. The AM and fm disturbances caused by the superposition of two such carriers have been extensively discussed in published work.[1,2] The aspects of these disturbances that are of interest in the present discussion will now be summarized.

The signals are assumed to be unmodulated in amplitude and frequency or, at worst, to have frequency modulations that are so slow, relative to the frequency difference $r$, that the signal frequencies are not appreciably changed during a period of $2\pi/r$ seconds. It will become evident presently that the severity of the interference increases with the increase in the frequency difference $r$, and is greatest, therefore, when $r$ assumes its largest possible value of one IF bandwidth (assuming, for simplicity, that this bandwidth is well defined). Thus, the assumption that $r$ is much higher than the highest modulating frequency (if any) corresponds to the situation in which the interference causes the most troublesome amplitude and frequency disturbances. This is the situation of greatest interest in the determination of the design requirements on the limiter and discriminator circuits to insure their proper operation under all possible conditions of two-signal interference.

At the input of the first amplitude limiter the resultant signal will be

$$\begin{aligned} e_{if}(t) &= \cos pt + a \cos (p+r)t \\ &= A(t) \cos [pt + \theta(t)] \end{aligned} \tag{1}$$

if time is counted from the instant at which the two signal phasors are in phase. In this expression

$$A(t) = \sqrt{1 + 2a \cos rt + a^2} \tag{2}$$

and

$$\theta(t) = \tan^{-1} \frac{a \sin rt}{1 + a \cos rt} . \tag{3}$$

The instantaneous frequency of the resultant signal is $\omega_i(t) = p + d\theta/dt$. The presence of the weaker signal within the IF pass band causes the fm demodulator (limiter-discriminator combination) to see a resultant signal whose instantaneous frequency differs from the frequency of the stronger signal by $d\theta/dt$. Therefore, $d\theta/dt$ is the fm disturbance, while $A(t)$ contains the AM disturbance. Plots of $A(t)$ and of $d\theta/dt$ are shown in Fig. 1 and Fig. 2 (next page).

It is important to observe that the average value of $d\theta/dt$ over a period of $2\pi/r$ seconds is zero. In essence, the most important step toward achieving satisfactory capture of the stronger signal is to make the instantaneous-frequency deviation of the resultant signal from the desired frequency $p$ average out to zero over one period of the frequency difference $r$, at every point in the receiver before the fm-to-AM conversion and detection process.[3,4] The outcome of this process must then be a detected disturbance waveform that is superimposed upon the output voltage which corresponds to the frequency $p$ and contributes a zero average deviation from this desired voltage. If $r$ is beyond the audible range, then the preceding requirements are necessary and sufficient, since no disturbance will be passed by the de-emphasis and audio filters. If, however, $r$ is audible, then these requirements (though necessary) will not insure complete rejection of the interference but the disturbance that gets through can be greatly reduced, if not effectively eliminated.

Two important schemes for improving the capture performance of an fm receiver will be briefly described. For the simpler scheme,[3,4] it has been shown that limiters with bandwidths of the order of the IF bandwidth will introduce significant reductions in the effectiveness of high-level interference. The reductions result from the fact that the filter sluggishness to the violent fm disturbance can cause deformation of this disturbance into milder waveforms that maintain a zero average over a frequency-difference cycle. An extremely effective scheme for suppressing the disturbance of the weaker of two fm signals can be achieved, therefore, by cascading

[1] M. S. Corrington, "Frequency-modulation distortion caused by multipath transmission," Proc. IRE, vol. 33, pp. 878–891; December, 1945.

[2] M. S. Corrington, "Frequency-modulation distortion caused by common- and adjacent-channel interference," *RCA Rev.*, vol. 7, pp. 522–560; December, 1946.

[3] E. J. Baghdady, "Frequency-modulation interference rejection with narrow-band limiters," Proc. IRE, vol. 43, pp. 51–61; January, 1955.

[4] E. J. Baghdady, "Interference Rejection in FM Receivers," Res. Lab. Electronics, M.I.T., Cambridge, Mass., Tech. Rep. 252; September 24, 1956.

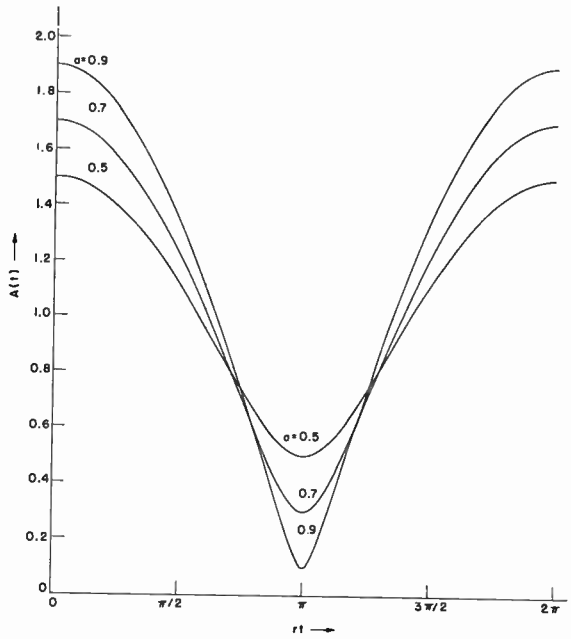


Fig. 1—Instantaneous envelope variations of the resultant of two sinusoids of relative amplitudes 1 and $a$, whose frequencies differ by $r$ rad/second.

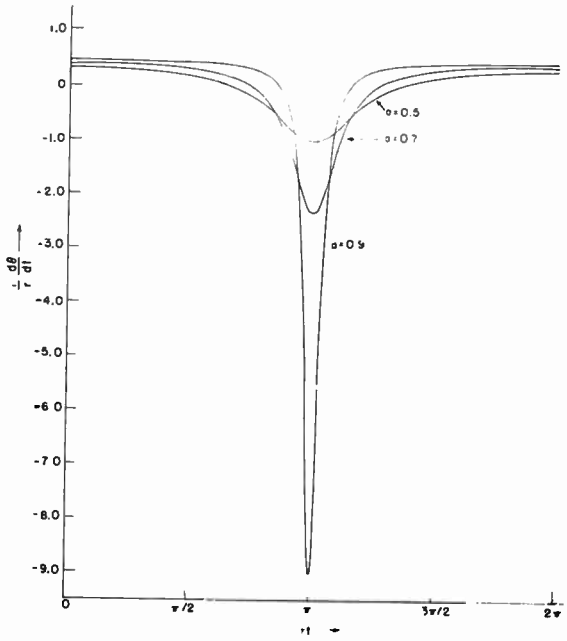


Fig. 2—Instantaneous-frequency disturbance caused by the superposition of two sinusoids of relative amplitudes 1 and $a$. The frequency of the stronger sinusoid is $p$ rad/second; the frequency of the weaker sinusoid is $p+r$ rad/second.

several stages of amplitude limiting, each of which is followed by a band-pass filter of appropriate bandwidth. With such a scheme interference is effectively suppressed, by any desired amount, ahead of the discriminator rather than after it, and requirements on the performance of a satisfactory discriminator are greatly relaxed. This has been demonstrated with conventional circuits.

The mechanism by which the cascading scheme suppresses interference is based on the fact that the first amplitude limiter spreads out the significant spectrum (which is necessary for the reproduction of the fm disturbance) over a frequency range that exceeds many times the bandwidth of the IF amplifier. The more severe the interference, the greater will be the spread of the spectrum through amplitude limiting; it will be of the order of 100 times the bandwidth of the IF amplifier if the signal strengths differ by 10 per cent of the amplitude of the stronger signal.

It follows that sizeable portions of the interference spectrum can be excluded without substantially affecting the spectrum that carries the message modulation by filtering after amplitude limiting. After one stage of limiting and filtering, a significant amount of interference will pass in a spectrum that cannot be eliminated without impairing the desired signal. Successive limiters will again spread out the interference spectrum which can be reduced further by additional filtering. As more limiter-filter units are added in cascade, more of the energy of the interference spectrum is drained off until the remaining energy is negligible. Beyond this point, the cascading of more stages of limiting and filtering is not economically justifiable.

The practical importance of the cascading scheme is enhanced significantly by the fact that the near elimination of the high-level interference (caused by undesired signals that are either delayed replicas of the desired signal, or are caused by other stations or by impulse radiation such as that from ignition systems) can be achieved with from 3 to 6 properly designed narrow-band limiters.

The greatest achievable reduction in the effective interference ratio in one stage of narrow-band limiting[5] can reduce $a$ to $(1/2)a$, when $a>0.5$. The performance of one stage of ideal narrow-band limiting with only one IF bandwidth is indicated in Fig. 3. In this plot $a_{out}$ is the output ratio of weaker-to-stronger signal amplitude (or interference ratio) and $a_{in}$ is the corresponding input ratio. The analysis leading to this plot assumes that $r>1/2(\mathrm{BW})_{if}$, and the plot only applies when $a<0.84$. It turns out, however, that this performance can be improved by various methods. One relatively simple method (which has been tested in the laboratory) is to apply positive feedback through a bandwidth of the order of the IF bandwidth from the output of the limiter to its input.[6] Under the more serious conditions of interference, this scheme results in pronounced improvement in the capture performance of the receiver. The positive feedback will increase the amplitudes of both signal and interference at the input of the limiter, but it will add more to the stronger signal than to the weaker signal. In this way, the predominance of the stronger signal is improved at the input of the limiter, and further improvement is effected by narrow-band limiting

[5] E. J. Baghdady, "Theory of stronger-signal capture in fm reception," (submitted for publication); March 15, 1957.
[6] E. J. Baghdady, "Theory of feedback around the limiter," 1957 IRE National Convention Record, Pt. 8, pp. 176–202.

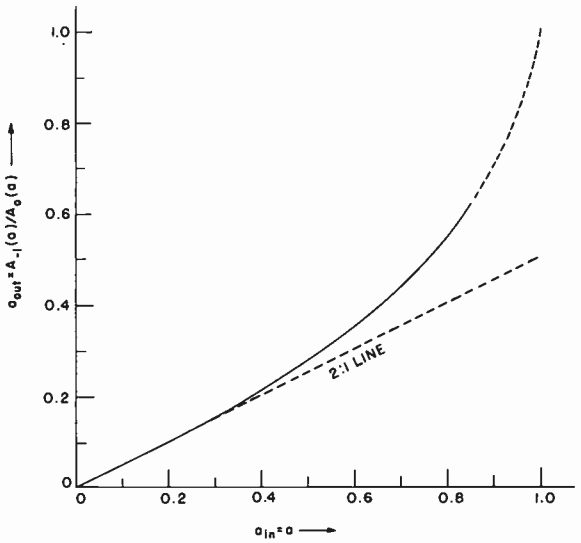


Fig. 3—Variation of the interference ratio at the output of one narrow-band limiter, whose bandwidth equals $(BW)_{if}$, with the interference ratio at the input, when the frequency difference $r=(BW)_{if}$.

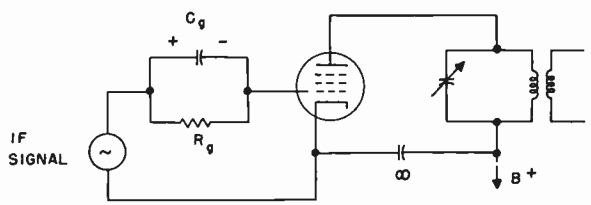


Fig. 4—Grid-circuit limiter for time-constant computation.

in the same limiter stage. The over-all improvement in one stage with band-limited positive feedback can be made equivalent to the improvement that would result from several stages that do not use feedback.

Positive feedback that causes a self-sustained oscillation in the absence of an input signal will not only cause pronounced improvement in capture performance, but it will also bring about effective interstation noise squelch, improved amplitude-limiting performance, and significant relaxation in the limiter time-constant requirements.

## III. Limiter Time-Constant Requirements

Perhaps, the only important limiter circuit that presents a time-constant problem, at present, is the grid-bias pentode limiter circuit shown in Fig. 4. It will suffice, for our purposes, to recall[7] that the operation of this limiter depends upon the control by the instantaneous amplitude of the input signal of an automatic self-rectified grid bias. This, in turn, controls the conduction angle and the height of the plate-current pulses, increasing the height and decreasing the angle with increasing signal amplitude so that the net charge delivered by each pulse to the plate-tank capacitor is kept approximately constant.

[7] L. B. Arguimbau, "Vacuum-Tube Circuits," John Wiley & Sons, Inc., New York, N.Y.; 1948.

The mechanism of the operation in the grid circuit of the grid-bias limiter lends itself to a treatment that is very similar to the usual analysis of the simple diode peak detector. In our problem there are three time-constant considerations that must be taken into account if this circuit is to be used in a receiver designed to handle a specified interference ratio $a$.

1) The product $R_gC_g$ must be sufficiently small to enable the circuit to follow the amplitude variations of a resultant two-carrier signal, and thus keep the dynamic self-bias under the exclusive control of these amplitude variations.

2) $C_g$ must be sufficiently large to bypass $R_g$ at radio frequencies and offer an impedance at radio frequencies which is much lower than the input impedance of the tube in order for the IF voltage to appear effectively between the grid and the cathode of the tube when the grid potential is on the negative swing. If $\omega_0$ is the intermediate frequency and $C_{in}$ is the input capacitance of the stage, the present requirements can be summarized as $C_gR_g \gg 1/\omega_0$ and $C_g \gg C_{in}$.

3) $R_g$ must be sufficiently large for the development of the necessary bias on the grid for effective smoothing of the envelope of the input wave. If the grid-to-cathode conduction resistance is $r_g$, then we want $R_g \gg r_g$.

Requirement 1) can be translated into an explicit condition on $R_gC_g$. Let $A(t)$ denote the instantaneous amplitude of the resultant signal impressed at the input of the grid circuit. We recognize that the magnitude of the rate at which the capacitor tends to charge (or discharge) at any instant of time must be greater than (or, at worst, equal to) the magnitude of the rate at which $A(t)$ is increasing (or decreasing), in order for the self-rectified bias on the grid to follow the amplitude variations of the input signal. For example, if $A'(t)$ is positive, the charging rate at time $t$ must be

$$\frac{A(t)}{R_gC_g} \geq A'(t).$$

Therefore the desired condition on the $RC$ time constant of the grid circuit can be written

$$R_gC_g \leq \left| \frac{A(t)}{A'(t)} \right|.$$

The quantity on the right-hand side will vary with time. Therefore if the most unfavorable situation is to be met, the condition should read

$$R_gC_g \leq \left| \frac{A(t)}{A'(t)} \right|_{min}. \tag{4}$$

Under two-signal interference conditions, $A(t)$ is given by (2). With substitution in condition (4) and evaluation of the indicated minimum, we obtain

$$R_gC_g \leq \frac{1-a^2}{ar}.$$

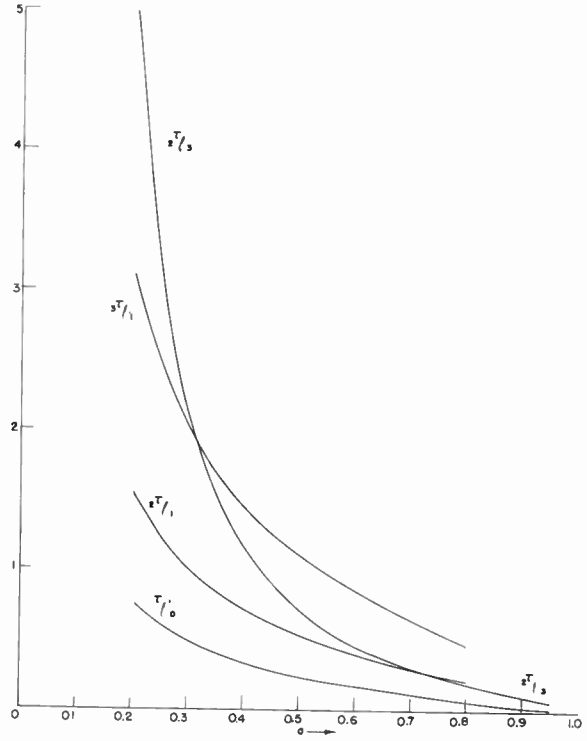


Fig. 5—Variation of the maximum permissible values of the grid-circuit time constant with the interference ratio $a$.

The frequency difference $r$ can have a maximum value, $r_{max}=2\pi W_{if}$, where $W_{if}$ denotes the IF bandwidth in cps. Therefore, under the worst interference conditions, we must have

$$\tau_{l0} = W_{if}R_gC_g \leq \frac{1-a^2}{2\pi a}. \tag{5}$$

The maximum permissible value of $\tau_{l0}$, as given by the equality sign in (5), is shown in Fig. 5 plotted against $a$. Multiplication by a scale factor appropriate to the value of $W_{if}$ will convert the normalized values of time constant to microseconds.

For conditions at the input of the second-limiter stage, which immediately follows the filter of the first limiter, the problem is greatly simplified if the filter is assumed to have idealized amplitude and phase characteristics. Thus, if we consider the filter in the plate circuit of the first grid-bias pentode limiter as an ideal filter, then the input signal of the next stage is described in terms of the worst configuration of sideband components that this filter will pass. The amplitude of the resultant of these components will not be constant since, in general, not all of the components with significant amplitudes at the output of the first limiter will be passed. The spectrum of the amplitude-limited resultant of the two input signals is given by

$$e(t) = \cos\left[pt + \theta(t)\right] = \sum_{n=-\infty}^{\infty} A_n(a)\cos(p-nr)t. \tag{6}$$

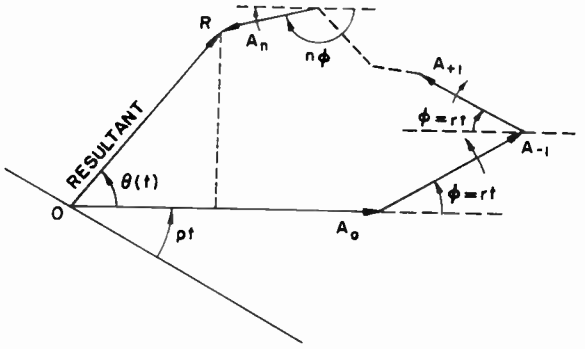


Fig. 6—Linear superposition of phasors representing the spectral components passed by the ideal-limiter filter.

This spectrum has been computed by Granlund,[8] who presented ten-place tables of $A_n(a)$. A detailed study of the properties of this spectrum has been undertaken by the author.[3,4]

If the bandwidth of the first-limiter filter is assumed to equal one IF bandwidth (as is permissible for all $a \leq 0.863$), then we know that the configuration $A_0$, $A_{-1}$ will be the worst possible spectrum for all $a$'s up to approximately 0.84, and thus, for all such cases, condition (5) is directly applicable with $a$ replaced by $A_{-1}/A_0$. Fig. 3 is a plot of $A_{-1}/A_0=a_{out}$ against $a=a_{in}$. Since $(A_{-1}/A_0)<a$, it is recognized that the highest permissible value of the time constant $R_gC_g$ is larger at the input of the second limiter than it was at the input of the first—a decided improvement in the design conditions. The extent to which improvement has been achieved is readily seen from the curve for ${}_2\tau_{l1}$, as shown in Fig. 5. Conditions at the input of the third-limiter stage are similarly computed if the second stage is assumed to be identical with the first one, and so on. Fig. 5 also shows a curve for ${}_3\tau_{l1}$ which applies to the time constant at the input of the third limiter.

When the ideal filter that follows the first limiter has three times the IF bandwidth, values of $a$ up to 0.9807 can be considered. In the critical spectrum for this bandwidth the components whose amplitudes are given by $A_1(a)$, $A_0(a)$, $A_{-1}(a)$, and $A_{-2}(a)$ are passed. These have frequencies of $p-r$, $p$, $p+r$, and $p+2r$ rad/second.

With reference to Fig. 6, we note that if the idealized limiter filter passes a spectrum made up of $M$ lower sideband components and $N$ upper sideband components, then the square of the amplitude of the resultant signal is

$$A^2(t) = \left[\sum_{n=-N}^{M} A_n\cos n\phi\right]^2 + \left[\sum_{n=-N}^{M} A_n\sin n\phi\right]^2$$

where $\phi=rt$. When the first-limiter bandwidth is three times the IF bandwidth, the most unfavorable situation arises when $M=1$, $N=2$, and $r=2\pi W_{if}$. In this case, the value of $\phi$ that gives a minimum is a root of a fifth-degree equation in $\cos\phi$. The resultant maximum

[8] J. Granlund, "Interference in Frequency-Modulation Reception," Res. Lab. Electronics, M.I.T., Cambridge, Mass., Tech. Rep. 42; January 20, 1949.

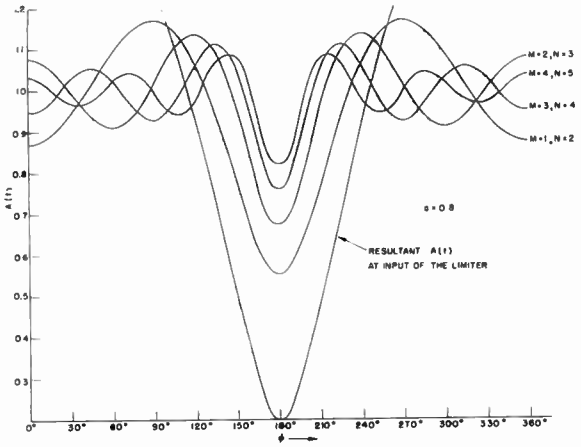


Fig. 7—Variations in the instantaneous amplitude of the resultant signal at the output of a narrow-band limiter compared with the corresponding variations at the input of the limiter.

permissible values of ${}_2\tau_{l3} \equiv W_{if} R_g C_g$ (in the grid circuit of the second limiter when the first-limiter bandwidth is three times the IF bandwidth) are plotted in Fig. 5 for comparison with the other normalized time-constant curves.

With larger values of first-limiter bandwidth, the variations in the amplitude of the most troublesome signal delivered to the second limiter become less and less severe, and the upper bound on the permissible $R_g C_g$ product at the input of the second stage becomes higher and higher. The appearance of $A(t)$ for various spectral configurations is illustrated in Fig. 7.

We may now conclude that although the action of a narrow-band limiter upon the character of the resultant signal effects only a partial reduction in the severity of the amplitude variations of the signal (instead of a complete smoothing-out process), the partial abatement of the amplitude variation is sufficient, nevertheless, to show a significant increase in the upper bound on the permissible grid-circuit time constant. Eventually, with a sufficient number of cascaded narrow-band limiters, the resultant signal amplitude is smoothed out to an essentially constant value, and the upper bound on the $RC$ product in the later stages is sufficiently high to be of no importance in the design of these stages. As for the first stage, the time-constant requirements are best relieved either by the application of regenerative feedback,[6] or by the use of a limiter whose operation does not depend upon a low-frequency time constant.

## IV. Discriminator Time-Constant Requirements

The time-constant requirements of two commonly encountered discriminator low-frequency output circuits will be discussed in the order of their simplicity. The low-frequency output circuit of many discriminators can be reduced to the forms shown in Fig. 8 and Fig. 9. In Fig. 8, the detected voltage, which ideally is proportional to the instantaneous-frequency variations of the signal at the discriminator input, appears across

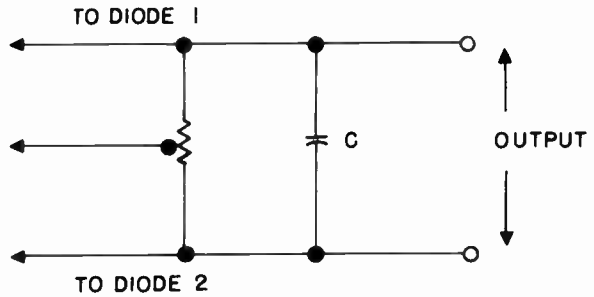


Fig. 8—Discriminator-output circuit for time-constant computation.

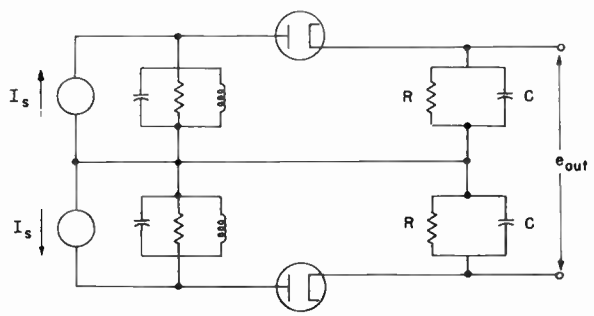


Fig. 9—Common form of balanced discriminator.

the equivalent $RC$ combination. In some circuits this $RC$ combination is a reduced form of a slightly more elaborate connection, in others $C$ is the capacitor across which the output voltage of the discriminator is taken, and $R$ either appears explicitly or consists essentially of a low equivalent output resistance that is associated with the rest of the discriminator circuit.

Let us first consider the situation in which the discriminator is either amplitude insensitive, and hence not preceded by any limiters, or amplitude sensitive but preceded by an "infinitely" wide-band ideal limiter. Assume that the discriminator has a linear over-all detection characteristic of unit slope over the whole range of the instantaneous-frequency variations of the input signal. Then, under the two-carrier interference conditions described in Section II, the voltage waveform that the output $RC$ combination must handle is given by $E_0(p) + d\theta/dt$, where $E_0(p)$ is a direct-voltage level that is dictated by the frequency $p$ of the stronger signal, and $\theta(t)$ is defined in (3). Since $d\theta/dt$ averages out to zero over $2\pi/r$ seconds, $E_0(p)$ is the only direct-voltage term that should appear at the output, inasmuch as the slow variation in this level will deliver the message of the stronger signal. If the frequency difference $r$ lies outside the range of the desired message spectrum, subsequent de-emphasis and audio (or video) filtering will yield $E_0(p)$ with no distortion from the interference.

However, failure of the voltage across the capacitor to follow the voltage variations dictated by the instantaneous frequency of the signal at the discriminator input will cause the output low-frequency voltage to have an average value (over one frequency-difference cycle) that does not correspond to the value dictated by the frequency of the stronger signal. If the average value of

the output-capacitor voltage (over a period of $2\pi/r$ seconds) is to be maintained at the value dictated by the frequency $p$, the capacitor must, at every instant of time, tend to charge or discharge at a rate that is faster than (or, at worst, just as fast as) the rate at which the impressed waveform tends to change at that instant. Equivalently, the ratio of the instantaneous value of the capacitor voltage to the $RC$ product must always exceed or, at worst, equal the time derivative of the impressed voltage evaluated at the same instant of time. This will enable the capacitor voltage to keep in step with the dictates of the instantaneous frequency of the resultant input signal, and thus ensure proper detector operation and lack of harmful diagonal clipping effects. Analogous with the problem of the limiter time constant, the restriction to be imposed on the $RC$ product is, from condition (4),

$$RC \leq \left| \frac{e(t)}{e'(t)} \right|_{\min}, \qquad e'(t) \equiv \frac{d}{dt} e(t), \tag{7}$$

where $e(t)$ is the total capacitor voltage. Evidently, $e(t)$ cannot go to zero (unless $e'(t)$ vanishes simultaneously with it). Under the aforementioned conditions,

$$e(t) = E_0(p) + \frac{1}{2} r\left[1 - \frac{1 - a^2}{1 + 2a \cos rt + a^2}\right], \tag{8}$$

where we must require that

$$E_0(p) > \frac{ar}{1 - a}. \tag{9}$$

Since $E_0(p)$ is the voltage level that corresponds to the frequency $p$, and $p$ is likely to lie on either side of the center frequency of the IF pass band, it is evident that condition (7) will define a nonzero upper bound on the $RC$ product only if the discriminator output, as seen across the $RC$ combination of Fig. 8, is not balanced to give zero voltage at the center frequency. Furthermore, values of $E_0(p)$ that do not satisfy condition (9) will cause $e(t)/e'(t)$ to have a zero minimum magnitude, and thus require that $RC$ be zero. The equality sign is excluded in condition (9) for the same reason.

With $e(t)$ as given by (8), we can show that the ratio

$$-\frac{e(t)}{e'(t)} = \frac{[E_0(1+a^2)+a^2r+a(2E_0+r)\cos\phi][1+2a\cos\phi+a^2]}{ar^2(1-a^2)\sin\phi}$$

has a minimum magnitude at the negative real root of

$$\cos^3\phi - \left[\frac{5}{2} + \frac{E_0(1+a^4)+a^4r}{2a^2(2E_0+r)}\right]\cos\phi - \left[\frac{E_0(1+a^2)+a^2r}{a(2E_0+r)} + \frac{1+a^2}{2a}\right] = 0,$$

which has a magnitude smaller than unity. An analytical expression for the resultant upper bound on the $RC$ product is available, but it is too cumbersome to be useful.

When the discriminator is preceded by one stage of narrow-band limiting whose bandwidth equals one IF bandwidth, the formulas of the preceding computation are directly applicable to the computation of the maximum permissible discriminator $RC$ product. Here, since the most unfavorable conditions at the limiter-filter output arise only when $A_0$ and $A_{-1}$ pass and $r = 2\pi W_{if}$, it is merely necessary to replace $a$ in the formulas by $(A_{-1}/A_0)$. A similar extension of the computation to the situation in which more than two limiters, each of which has a bandwidth of one $(BW)_{if}$, precede the discriminator is fairly evident.

It is of interest to observe that with a discriminator whose output across the $RC$ combination shown in Fig. 8 is balanced, the upper bound on the $RC$ product will be nonzero as long as the two signals lie symmetrically on opposite sides of the center frequency. For this situation, the upper bound is specified by

$$rCR \leq \frac{1 - a^2}{2a} \tag{10}$$

which is one half of the upper bound on the grid-circuit time constant of the limiter. Frequently, the capture ratio of a receiver is measured by simulating an interference situation in which the two (unmodulated) signals lie at opposite ends of the IF pass band. It is clear that, under this condition of measurement, a discriminator whose output is balanced about the intermediate frequency when it is observed across the $RC$ combination of Fig. 8 will appear to meet the test if its $RC$ product satisfies condition (10). Evidently, under the more general (but milder) interference conditions, it will fail.

In order to illustrate the manner in which the cascading of narrow-band limiters raises the upper bounds on the output-circuit time-constant requirements of the discriminator, we shall choose a discriminator whose characteristic goes through zero at a frequency that corresponds to a cutoff frequency of the IF amplifier. In view of condition (9), this situation is mainly of academic interest (unless the interference is effectively suppressed before it reaches the discriminator). The weaker of the two carriers will be assumed to fall at the frequency of balance. In the absence of narrow-band limiting, the voltage waveform impressed across the output capacitor is

$$e(t) = r\frac{1 + a\cos rt}{1 + 2a\cos rt + a^2}.$$

Consequently, the maximum permissible values of $\tau_{d0} = W_{if}RC$ are the values plotted in Fig. 10. If one narrow-band limiter whose bandwidth equals the IF bandwidth precedes the discriminator, the upper bounds are specified by the plotted values of ${}_1\tau_{d1}$. The curve marked

"$_2\tau_{d1}$" applies when two limiters, both of one IF bandwidth, precede the discriminator. Fig. 10 also presents a curve marked "$_1\tau_{d3}$," which applies when the discriminator is preceded by a limiter whose bandwidth equals $3(\mathrm{BW})_{if}$.

The plots of Fig. 10 show how the upper bound on the permissible time constant in the output circuit of the discriminator is raised when the discriminator is preceded by a process of narrow-band limiting. The effect produced by one narrow-band limiter will, clearly, be displayed by additional stages. After a sufficient number of stages has been cascaded, the upper bound on the maximum permissible time-constant values becomes sufficiently high, so that it exercises no important restraint on the design of the output circuit of the discriminator.

We shall now illustrate the computation of the maximum permissible time constant for the common type of discriminator circuit shown in Fig. 9. Alternative forms of this circuit (particularly, the one in which the AM-to-fm conversion is achieved through a double-tuned transformer, in which the top of the primary is connected to the center tap of the secondary) can be manipulated into the form of Fig. 9, and are, therefore, included in this treatment. The output voltage, $e_{out}$, is a superposition of the envelope of one tank-circuit response upon the other tank-circuit response with reversed polarity.

Assuming that the high-$Q$ tank circuits have the same damping factor $\alpha$, let one circuit be tuned to a frequency that is $b\alpha$ rad/second above the center frequency of operation $\omega_0$ and the other tuned to $b\alpha$ rad/second below $\omega_0$. Furthermore, let the instantaneous frequency of the excitation be deviated by $\alpha x(t)$ rad/second from the center frequency of operation. Then, if the conditions for a quasi-stationary analysis of the tuned-circuit responses are satisfied, and if the $RC$ combination of each peak detector is able to follow the envelope of the corresponding tank-circuit response, the output voltage can be normalized into the form

$$e_{out} = [1 + (x + b)^2]^{-1/2} - [1 + (x - b)^2]^{-1/2}. \quad (11)$$

For optimum linearity,[9] $b$ must be 1.225. Indeed, with this value of $b$,

$$e_{out} = kx(t), \qquad \text{for } -0.6 < x < 0.6.$$

The extent of this nearly perfect linearity is, therefore, $1.2\alpha$ rad/second centered about $x=0$, while the peak to-peak separation of the discriminator characteristic is 2.45 $\alpha$ rad/second.

Under conditions of two-signal interference, the instantaneous frequency of the amplitude-limited resultant of the two signals is

$$\omega_i(t) = \omega_{ave} - \frac{1}{2} r \frac{1 - a^2}{1 + 2a \cos rt + a^2},$$

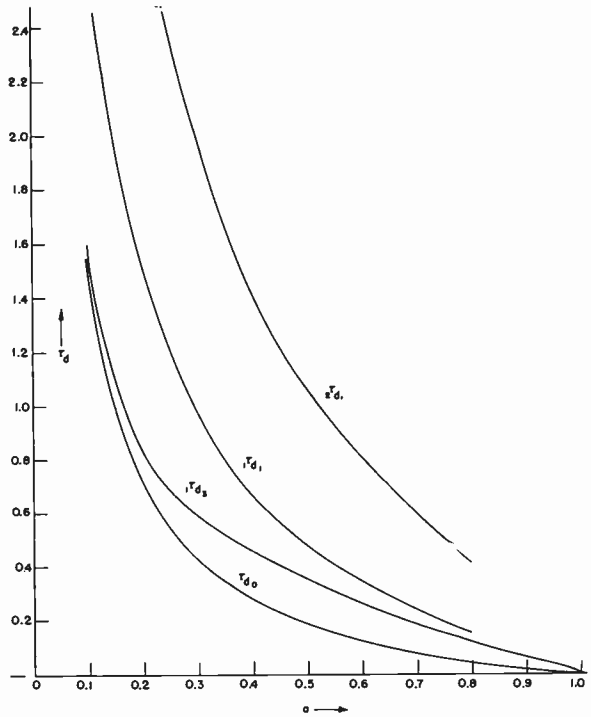


Fig. 10—Curves showing effect of cascading scheme upon the upper bounds on the time constant of Fig. 8, under the conditions of the illustrative example.

where $\omega_{ave} = p + \frac{1}{2}r$, the average of the two signal frequencies. Therefore

$$x(t) = x_{ave} - \frac{r}{2a} \frac{1 - a^2}{1 + 2a \cos rt + a^2}, \quad (12)$$

where $x_{ave} = 1/\alpha(\omega_{ave} - \omega_0)$. When the two signals are symmetrically disposed with respect to the center frequency, $x_{ave} = 0$ and

$$x(t) = -\frac{r}{2a} \frac{1 - a^2}{1 + 2a \cos rt + a^2}. \quad (13)$$

If $r$ is given its maximum value of $(\mathrm{BW})_{if}$, (13) will represent the most troublesome instantaneous-frequency deviations from $\omega_0$, measured in units of $\alpha$ rad/second.

Theory[10] shows that if

$$\frac{r}{2a} = \beta \frac{1 - a}{1 + a}, \quad (14)$$

then the conditions for quasi-stationary analysis, which justify use of (11), are satisfied if $\beta$ is bounded by the values plotted in Fig. 11. Substitution in (13) leads to

$$x(t) = \frac{-\beta(1 - a)^2}{1 + 2a \cos rt + a^2}. \quad (15)$$

The upper bound on the $RC$ product can now be found by requiring that the $RC$ combination follow the voltage waveform given by

[9] L. B. Arguimbau, "Discriminator linearity," *Electronics*, vol. 18, pp. 142–144; March, 1945.

[10] E. J. Baghdady, "Theory of Low-Distortion Transmission of FM Signals Through Linear Systems," Res. Lab. Electronics, M.I.T., Cambridge, Mass., Tech. Rep. 332; July 30, 1957. (To be published.)

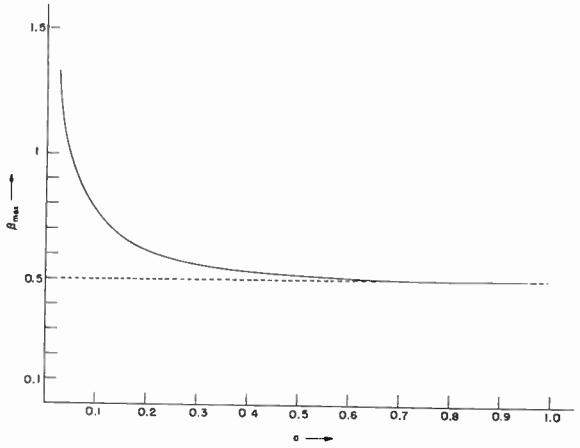


Fig. 11—The upper bounds on the value of $\beta$ in (14).

$$e(t) = 1 + \left\{ [x(t) + 1.225]^2 \right\}^{-1/2} \qquad (16)$$

$x(t)$ being given by (15). In Fig. 12 we present the results of a computation in which use was made of the values of $\beta = \beta_{max}$ that are plotted in Fig. 11. For all values of $a \leq 0.84$, the plot of Fig. 12 can be used in conjunction with the plot of Fig. 3 to determine the maximum permissible values of $\tau = W_{if}RC$ when any specified number of narrow-band limiters, each of one IF bandwidth, are cascaded ahead of the discriminator. Multiplication by a scale factor appropriate to the value of $W_{if}$ that is used will convert the dimensionless vertical scale in Fig. 12 into microseconds.

Finally, we would like to emphasize the fact that any interference suppression scheme which is used to minimize the fm disturbance before it reaches the discriminator circuit will, by virtue of its function, alleviate the low-frequency time-constant restrictions on the discriminator circuit. The results of this paper are readily adaptable to the computation of the time-constant requirements when an interference suppressor precedes the discriminator, once the manner in which the interference ratio is decreased by the suppressor has been determined.

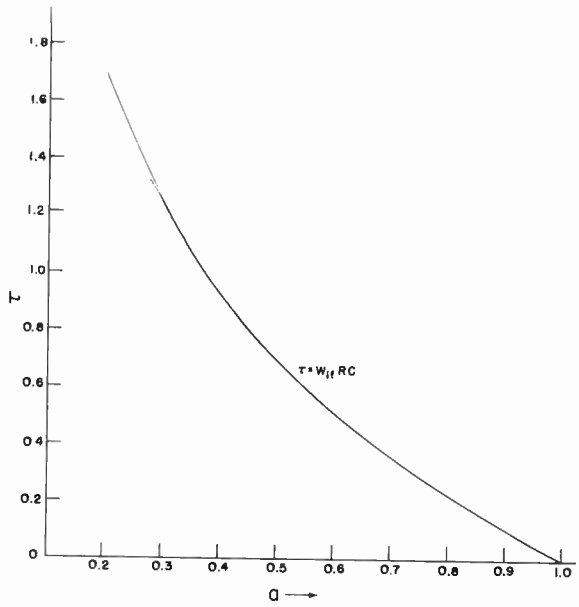


Fig. 12—Maximum permissible values of $\tau = W_{if}RC$ for each half of the balanced discriminator of Fig. 9.

# A High-Power Periodically Focused Traveling-Wave Tube*

O. T. PURL†, ASSOCIATE MEMBER, IRE, J. R. ANDERSON†, MEMBER, IRE, AND G. R. BREWER†, SENIOR MEMBER, IRE

*Summary*—**The design considerations, construction, and performance of an *S*-band, pulsed, kilowatt-level traveling-wave tube, focused by means of periodic permanent magnets are described. The tube exhibits saturated power gain in excess of 30 db, with a bandwidth of approximately 2–4 kmc and weighs 17 pounds or less, complete with package.**

**The results of studies on the electron beam defocusing effect of strong rf fields and on the effect of attenuator design on power build-up and saturation level are reported. Factors affecting the design of a high-power traveling-wave tube using periodic magnetic focusing are described in order to show the design constraints imposed by the periodic focusing system.**

## Introduction

A SERIOUS limitation to the extensive use of traveling-wave tubes in electronic systems has been the bulk and weight of the magnetic focusing system required to collimate the electron beam. This is particularly true for high-gain tubes, which frequently are too long to utilize uniform magnets efficiently. In the past few years, the use of periodic permanent magnets[1–4] for the beam-focusing system has allowed a considerable reduction to be made in the weight and power requirements for traveling-wave tubes. The use of periodic focusing, however, imposes some considerations and design limitations in addition to those for a tube focused with a uniform magnetic field. In many cases these limitations so influence the design as to make it almost imperative to consider the periodic focusing requirements from the outset.

The purpose of this paper is to present the results of work directed toward the design and development of a periodically focused *S*-band, kilowatt-level traveling-wave tube. Previous periodically focused tubes[1, 5–7] have made use of electron beams of considerably lower density than required in high-power tubes. As the power level is increased, in general, the beam current density and perveance is increased correspondingly, resulting in greater difficulty in obtaining the necessary field from existing magnet materials and in the formation and focusing of the beam. The aspects of the focusing problem peculiar to tubes of the kilowatt level or greater will be emphasized in this paper.

In the following sections, the design, construction, and electrical performance of this tube will be described in detail. In addition, the results of studies of the defocusing effect of the strong rf fields in the helix and of the rate of power build-up in the tube, as measured on a special traveling coupler, will be reported.

## General Features and Performance

A photograph of the tube package is shown in Fig. 1, in which a pulsed kilowatt-level traveling-wave tube for operation in immersed flow, as described by Caldwell and Iversen,[8] is also shown for comparison. The present periodically focused tube represents a complete redesign, which incorporates coupled-helix matches, converging beam gun, external attenuator, and shrunk glass helix to provide compatibility with the periodic permanent-magnet focusing system. In addition, the power output has been increased from 1 to 2 kw in midband and the 3-db bandwidth has been extended to the range 2200–4000 mc.

A cross-sectional drawing of the complete tube package is shown in Fig. 2. In order to obtain maximum field amplitude, the magnet outer diameter is greater than the pole piece outer diameter. The pole pieces are aligned by means of nonmagnetic spacers and the couplers and tube are mounted concentrically with the pole piece inner diameter. The collector is connected directly to the case for good thermal conductivity and no additional cooling is required for the collector.

A typical gain-frequency curve for this tube is shown in Fig. 3, exhibiting 30 db or greater (peak power output > one kw) at one watt drive from 2200–4000 mc. The large signal gain curve is quite flat ($\pm 0.5$ db from 2500–3500 mc) in spite of operation at a low $\gamma a (\gamma a \approx 1)$. The broad-band operation is achieved by optimizing the beam voltage at the upper band edge. Operation very close to saturation also contributes to the flat gain char-

* Original manuscript received by the IRE, October 1, 1957.

† Electron Tube Lab., Hughes Aircraft Co., Culver City, Calif.

[1] J. T. Mendel, C. F. Quate, and W. H. Yocom, "Electron beam focusing with periodic permanent magnet fields," PROC. IRE, vol. 42, pp. 800–810; May, 1954.

[2] A. M. Clogston and H. Heffner, "Focusing of an electron beam by periodic fields," *J. Appl. Phys.*, vol. 25, pp. 436–447; April, 1954.

[3] K. K. N. Chang, "Beam focusing by periodic and complementary fields," PROC. IRE, vol. 43, pp. 62–71; January, 1955.

[4] G. R. Brewer, "On the focusing of high-current electron beams," *J. Appl. Phys.*, vol. 25, pp. 243–251; February, 1954.

[5] K. K. N. Chang, "Periodic magnetic field focusing for low-noise traveling-wave tubes," *RCA Rev.*, vol. 16, pp. 423–431; September, 1955.

[6] W. W. Siekanowicz and F. Sterzer, "A developmental wide-band, 100-watt, 20-db, *S*-band traveling-wave amplifier utilizing periodic permanent magnets," PROC. IRE, vol. 44, pp. 55–61; January, 1956.

[7] N. Nishio, T. Nemoto, and S. Yasuda, "A package type traveling-wave amplifier for 4000 mc band," *L'Onde Elec.*, vol. 37, pp. 147–152; February, 1957.

[8] J. J. Caldwell and A. H. Iversen, "The design and performance of a kilowatt traveling-wave amplifier for pulsed operation at 3000 mc/sec," paper presented at the PGED conference, Washington, D. C.; 1955.

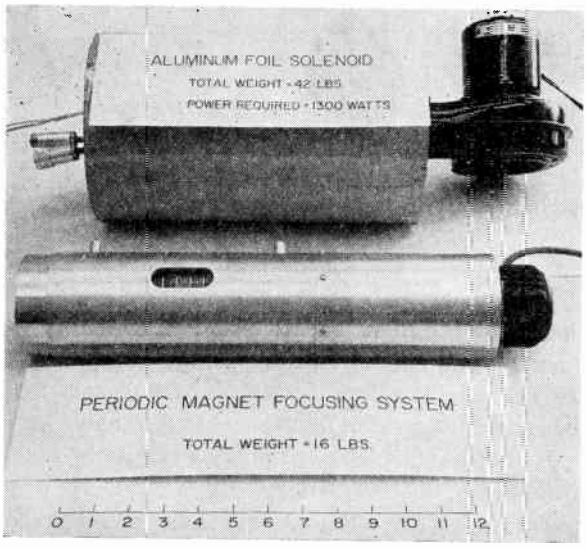


Fig. 1—Comparison of periodic-magnet and immersed-flow focusing systems for a kilowatt-level traveling-wave tube.

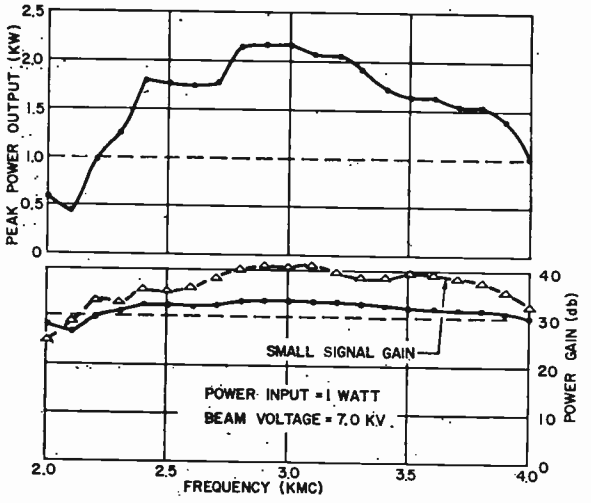


Fig. 3—Variation of power output and gain with one-watt drive power vs frequency. The small signal gain is shown also for comparison. These characteristics can be altered significantly by optimizing the attenuator to emphasize the performance feature (power output, stability, etc.) desired.

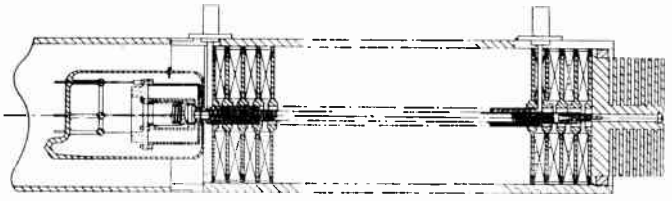

Fig. 2—Cross-sectional drawing of tube and package assembly.

acteristic. By peaking the power output at midband, 2 kw can be obtained over several hundred megacycles. The tube has operated satisfactorily at duty cycle values up to 0.006; typical values are 5-$\mu$sec pulse length, 1000 prf, and the maximum pulse length at which the tube has been operated is 16 $\mu$sec. A tube has been life tested for greater than 500 hours at 0.005 duty cycle without appreciable change in performance. It is believed that this duty cycle limit can be increased by a considerable factor by making use of more effective heat dissipation techniques; and since a tungsten-impregnated "$L$" cathode is used ($T_k \approx 1100$°C Br), the exhaustion of emission material should not occur until after a life of several times 500 hours.

Fig. 4 shows the power output as a function of power input for several frequencies. The saturation gain is 5–7 db down from that in the small signal region. This value, along with the entire shape of the curve, can be altered significantly by using different types of attenuators, as will be shown later.

The variation of power output with beam voltage is shown in Fig. 5 for both small and large signal conditions. It is seen that the optimum beam voltage is approximately 7 kv. This optimum voltage in a periodically focused tube results from a compromise between the beam transmission characteristic of the magnet system and the characteristics of the tube and is therefore more difficult to interpret than in the case of a less voltage-sensitive focusing system such as a uniform magnetic field.

A reproducible efficiency value of 20 per cent has been observed on various experimental tubes, and values as high as 30 per cent with an attenuator optimized for maximum power output. A slight increase in power output has been observed when using a uniform focusing field (from a solenoid), but this increase occurred at elevated beam voltages so that no increase in efficiency resulted. Fig. 6 shows comparative data taken with the same tube in a periodic focusing system and uniform magnetic field. The difference in the curves can be attributed to the different matches used. The gain in the uniform field will be slightly higher at a higher beam voltage.

The tube is short-circuit stable to the extent that no spurious output can be observed at a level 60 db or more down from the normal signal level. Two tubes have been operated in cascade (without intermediate matching or loss device) to give a gain of over 60 db (from one milliwatt to over a kilowatt) with the total weight of both tubes and focusing systems of 34 pounds.

## Beam Formation and Focusing

The electron gun is a converging beam type (perveance $2.2 \times 10^{-6}$), and was designed according to the method outlined by Brewer.[9] The role of the gun in successful periodic focusing should not be underestimated. It is the authors' experience that if the beam is not properly formed and injected into the periodic focusing field, no amount of magnetic field adjustment further down the tube will undo the damage. Consequently, a considerable amount of care was spent to assure correct

[9] G. R. Brewer, "Formation of high density electron beams," *J. Appl. Phys.*, vol. 28, pp. 7–15; January, 1957.

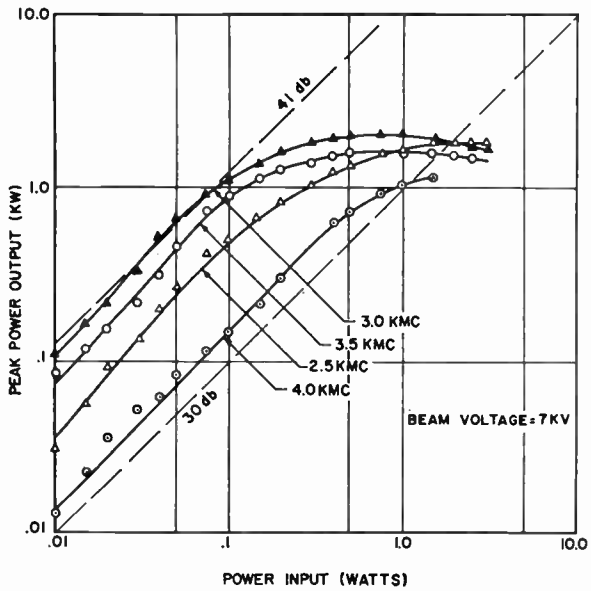


Fig. 4—Power output vs power input characteristics for several frequencies.

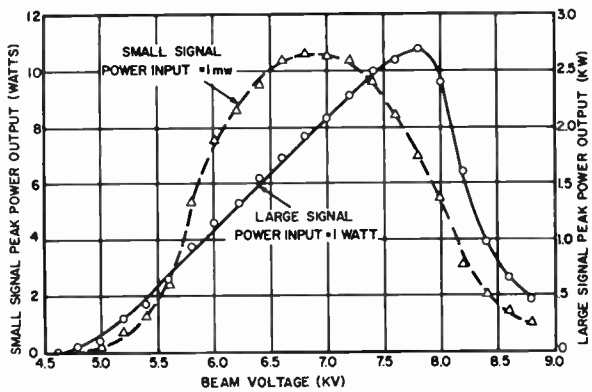


Fig. 5—Variation of output power (or gain) with beam voltage with periodic focusing and under small-signal and large-signal conditions. The equivalent curves observed in a uniform magnetic field were somewhat less peaked, and the small signal curve extended from about 6 to 9.5 kv. The beam transmission characteristic of the periodic system results in the sharp drop-off at higher voltages in these curves.

alignment of the gun parts and to shield the cathode from the stray leakage field (less than 1 per cent of the peak field has been measured at the cathode position). Entrance conditions can be designed by determining an electron trajectory from knowledge of leakage field vs axial length and matching this to the gun focusing characteristic. The use of periodic magnets, arranged with alternate polarity so that the external fields tend to cancel, results in best utilization of the magnetic material and thus corresponding compactness and light weight.

Two important focusing criteria must be satisfied for proper collimation of a periodically focused beam. First, the peak amplitude of the periodic field must be within a narrow range of values centered around that given by (1); second, the period of the field must be adjusted so that operation occurs in a "stable" region of flow.

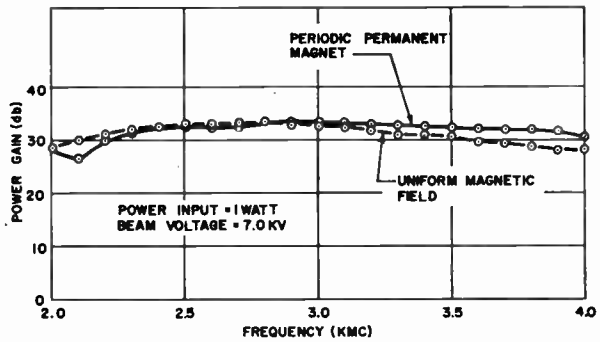


Fig. 6—Comparison of power gain for tube focused in a uniform magnetic field (Brillouin flow) and in a periodic magnetic system. Some of the difference in gain observed is due to different helix couplers used in the two tests. It is seen that the periodic focusing certainly does not degrade the tube performance.

The criterion for the amplitude of the field for minimum beam ripple is[1]

$$B_0 = 925 \frac{\sqrt{PV}}{d} \tag{1}$$

where $P$ = beam perveance in micropervs., $V$ = beam voltage in volts, $d$ = beam diameter in inches, and $B_0$ = peak amplitude of axial magnetic flux density in Gauss. Typical values for the tube are $P = 2.2 \times 10^{-6}$ $\mu$pervs, $V = 7 \times 10^3$ volts, $d = 0.100$ inch, giving required $B_0 = 1150$ Gauss. This equation expresses the condition for balance, on the average, between the outward space-charge and centrifugal forces of the beam and the inward confining force of the magnetic focusing field.

It will be illuminating to express the required field value in terms of the operating parameters of the tube. In a given design the desired power output is usually specified and an estimate of the efficiency can be made so that one can write the tube output power in terms of the beam voltage:

$$P_{\text{out}} = \text{eff } V_0 I_0 = \text{eff } V_0^{5/2} P \tag{2}$$

and

$$B_0 \sim \left[\frac{P_{\text{out}}}{\text{eff} \times V_0^{5/2} d}\right]^{1/2}. \tag{3}$$

It is seen from (3) that the desired field is proportional to the square root of the power output, so that as higher power tubes are required with reasonable beam voltages, the required field strength increases. There is an upper bound to the value $B_0$ that can be obtained in practice, arising from the maximum value of the coercive force, $H_c$, available in present-day magnetic materials and by the geometry of the tube and magnetic circuit.

Chang[10] has computed the magnetic field that can be obtained from a set of periodic ring magnets. If we take

[10] K. K. N. Chang, "Optimum design of periodic magnet structures for electron beam focusing," *RCA Rev.*, vol. 16, pp. 65–81; March, 1955.

an approximate form of his result, assuming the shim thickness is small, the peak axial flux density, $B_0$, can be written

$$B_0 \approx \frac{2H_m}{I_0\left(\frac{2\pi R_1}{L}\right)}. \quad (3a)$$

The notation follows that of Chang. $I_0$ is the zero-order modified Bessel function of the first kind.

In order to make the demagnetizing force $H_m$ as large as possible, the ratio of magnet-to-gap area is made very large so that the operating value $H_m$ is very nearly equal to $H_c$, the coercive force. However, one soon reaches a region of diminishing returns by increasing the magnet outer diameter; then one must resort to other means to increase $B_0$. With the assumption that $H_m = H_c$, (3) may be written

$$B_0 \approx \frac{2H_c}{I_0\left(2\pi \frac{R_1/d}{L/d}\right)} \quad (4)$$

where $R_1$ = pole piece inner radius, $d$ = beam diameter, and $L$ = magnet period.

The maximum magnetic field that can be obtained from a given magnet depends on the coercive force of the material and also upon the $R_1/L$ ratio. The pole piece diameter is restricted in most cases by the tube envelope or at least by the beam diameter. The period, $L$, is limited by the second consideration mentioned above; *i.e.*, by instability regions or "stop bands," expressed by the criterion[1]

$$P\left(\frac{L}{d}\right)^2 < 4.36 \times 10^{-4} \quad (5)$$

which is the mathematical expression of the theoretical condition beyond which the periodic magnet system is no longer an effective focusing system. In practice it seems necessary to remain below about 70 per cent of this value. Since there is often only a small range of variation for the ratio $L/d$, (4) indicates that it is important in most cases to reduce the ratio of pole piece inner diameter to beam diameter, $2R_1/d$, in order to utilize a given size magnet efficiently. This means that one must design the tube either with the pole piece extending through the vacuum envelope or reduce to a minimum value the radial space occupied by those tube parts between the beam and pole piece. For this reason the envelope diameter was reduced from 0.400 for the immersed-flow version to 0.250 for this tube.

The magnetic field had a period of 0.660 inch, with a peak axial value of 1200 Gauss, obtained with 3-inch od Indox magnets. The uniformity of the peaks can be maintained to within ±2 per cent by using annealed Armco iron pole pieces and selected magnets. It was found that any discontinuity in the initial part of the magnetic circuit, such as slots for couplers, etc., caused considerable decrease (10 to 15 per cent) in beam transmission, so that the input coupler is inserted between the tube envelope and first pole piece. A small-diameter coaxial line is used on the input coupler to decrease the distance from the anode to the first pole piece. A slot in the magnet for the output coupler does not cause any noticeable difficulties. Beam transmission to the collector of more than 90 per cent has been attained.

## RF Defocusing

The beam defocusing due to the action of the intense rf electric fields is more serious in a periodically focused than in a uniform-field-focused tube and the 90-per cent beam transmission observed under zero drive conditions may drop to 75 per cent with 2 kw of output power as the beam is defocused to the point of striking the helix. This defocusing can be a serious limitation on the average power capabilities of the tube. There are two reasons for the increased sensitivity of a periodically focused beam to rf fields. First, the periodic field counterbalances the space-charge field only on the average over a period, not at every point along the beam, so that radial rf fields existing in the region of zero magnetic field will have a relatively larger effect; and second, in the process of rf interaction, the axial velocity of some of the electrons is reduced to a value for which the periodic focusing is not longer effective; *i.e.*, to a velocity which corresponds to a stop band for the periodic system.

The dependence of "rf defocusing" on power level is shown in Fig. 7, where the change in helix current expressed as a percentage of the total beam current is plotted as a function of power output for different values of the focusing field period. The increase in helix current can be plotted vs $L^2$ and is shown in Fig. 8 to be roughly proportional to this quantity. Since the position of the stop band depends on $L^2$, this linear dependence would indicate that the presence of the stop band is undoubtedly a large contributor to the defocusing of the beam. For large periods, the defocusing is quite marked but by reducing the period, the helix current can be reduced considerably to compare reasonably well with the uniform field, as shown in Fig. 9. It is possible, as shown by the lower curve, to reduce the defocusing to a very small value by using a large uniform field over the entire circuit. It has also been shown that an increased field in the output region alone will suffice and that the amount of magnetic flux threading the cathode greatly influences the rf defocusing.[11]

The comparison of the rf defocusing in periodic and uniform fields is complicated by the fact that the power levels along the tube length in the two cases are different for the same applied parameters such as beam voltage, power input, etc. However, the gross behavior is clearly indicated by these curves. The rf defocusing also depends on the beam voltage as shown in Fig. 10. Lower voltage operation at the same power level results in

[11] G. R. Brewer and O. T. Purl, "Electron beam defocusing due to high intensity rf fields," paper presented at the Conference on Electron Tube Research, Boulder, Colo.; 1956.

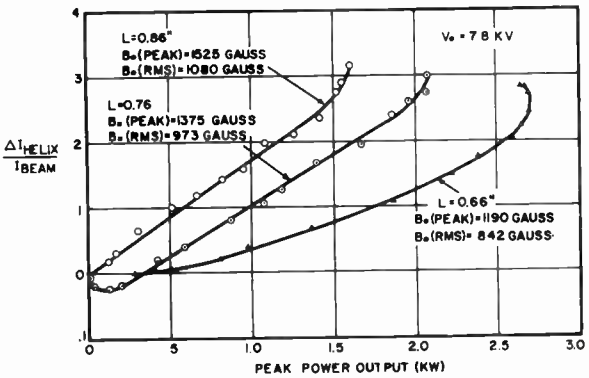


Fig. 7—Dependence of electron beam defocusing due to rf fields on power output for three values of magnet period. It is seen that the "rf defocusing" becomes greater with increase in magnet period. It is also noted that under some conditions the rf fields can focus the beam; this effect has been observed also for certain values of magnetic cathode flux with a uniform field system. (See Brewer and Purl.[11])

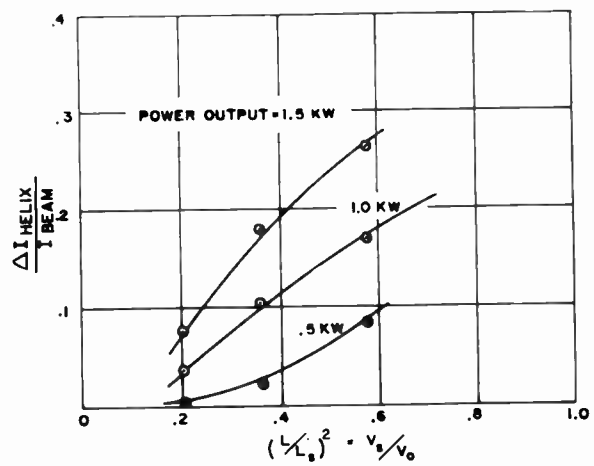


Fig. 8—Dependence of rf defocusing effect on magnet period. The abscissa scale is the square of the magnet period (data from Fig. 7) divided by the stop band period for the magnetic field used; it is also equal to the ratio of the stop band voltage to beam voltage. It is seen that the defocusing effect is roughly proportional to this quantity and that the curves appear to intersect the abscissa around 0.1.

more electrons reaching the stop-band region and becoming defocused to the helix. It is clear from the curves shown that the rf defocusing can be minimized to a great extent by operating with a smaller-period structure and at a higher beam voltage than normal. It may be worth while in certain instances to depart from maximum power output slightly by reducing the period and increasing the beam voltage in order to increase materially the possible duty cycle.

Although it is in general undesirable to collect a large percentage of the beam on the helix, the response of the beam focusing to rf fields can be utilized to provide a sensitive microwave detector tube.[12] If small duty cycle operation is permissible, the rf defocusing can be maximized and the rectified helix current will provide the detected signal. The magnitude of this effect is shown by a

[12] J. T. Mendel, "Microwave detector," PROC. IRE, vol. 44, pp. 503–508; April, 1956.

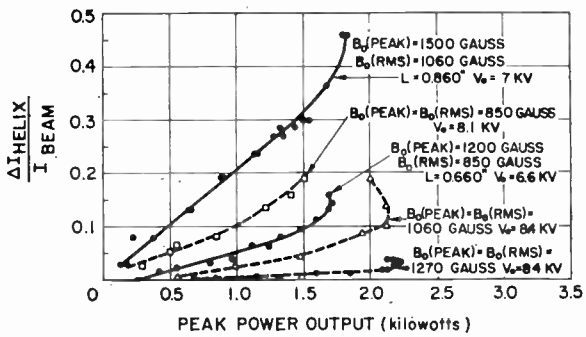


Fig. 9—Dependence of electron beam defocusing due to rf fields on power output for two values of magnet period and three values of uniform field strength. The beam voltages were adjusted for maximum power output in each case. Although the beam voltage variation slightly obscures the comparison, it is seen that periodic magnetic focusing results in considerably greater rf defocusing than use of a uniform magnetic field.

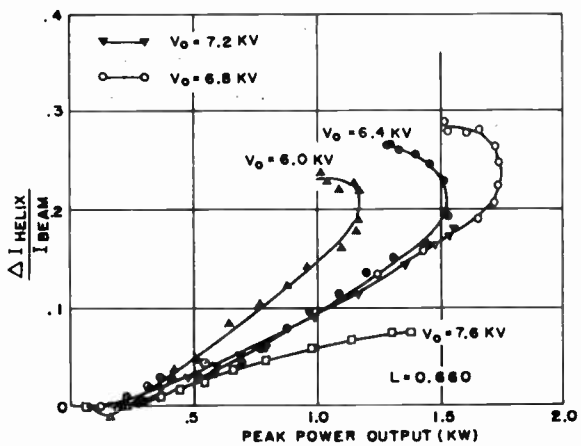


Fig. 10—Dependence of electron beam defocusing due to rf fields on power output for various values of beam voltage. As the beam voltage is reduced, the ratio $V_s/V_0$ becomes greater, resulting in larger rf defocusing, as shown in Fig. 8.

curve of helix current as a function of power input (Fig. 11). It is noted that the characteristic is relatively linear over a range of values of input power greater than ten to one.

## Components

The principal mechanical features of the tube are shown in Fig. 12, which is an exploded view of the tube, matches, and attenuator.

The match for a 50-Ω coax line to the slow-wave circuit is accomplished by using coupled helix transducers. No vacuum seal is required, and the outer helix unit can be made to occupy less than 0.050 inch of radial space. The vswr can be held to less than 2 to 1 over the 2–4 kmc band, and the insertion loss per coupler is less than 1 db at midband. The outer helix is moulded in Teflon for rigidity, and the perpendicular entry has been used for the coax connection. A termination is applied to both ends of the inner helix, but none is necessary on the outer helix. The helix structure is mounted in a precision-ground glass tube which is shrunk around the helix under vacuum to increase the heat dissipating

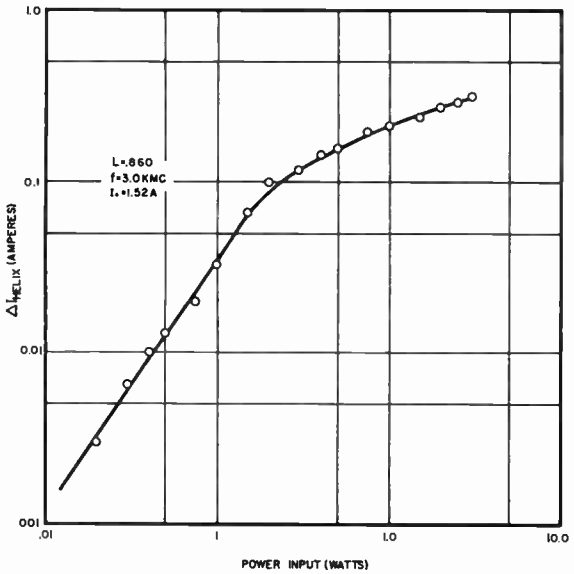


Fig. 11—Change in helix current due to rf defocusing vs input power. It is noted that the characteristic is linear up to $I_h = 0.10$ ampere so that when used as a detector, an output voltage linear up to 5 volts could be obtained with a 50-Ω load.

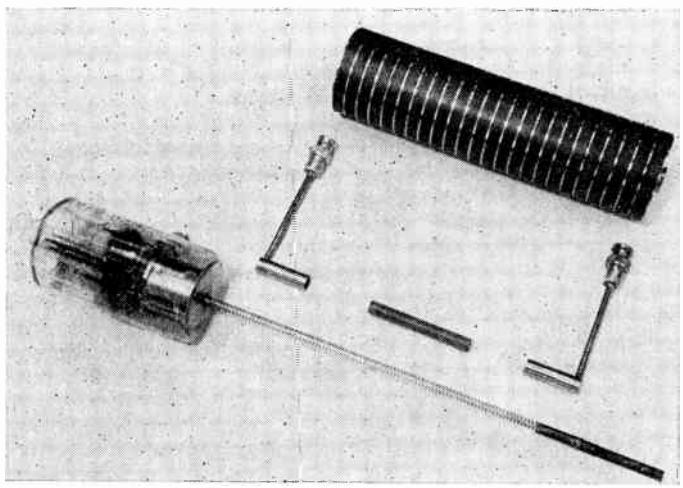

Fig. 12—Photograph of tube, coupled-helix matches, coupled-helix attenuator, and periodic-magnet stack.

quality of the circuit. Such a structure can dissipate about 9 watts per inch safely without forced air cooling. The amount of dielectric loading (DLF = 0.8) was measured by probing the field with a moving single-turn coil mounted on a carriage. The increase in loading after shrinking was found to be of the order of 2 per cent.

Several types of attenuators have been tested; *e.g.*, lossy wall attenuators of Aquadag, lossy ceramic, Teledeltos paper, and other lossy plastic materials, and coupled helix attenuators with distributed loss. The cold transmission loss as a function of frequency is shown in Fig. 13 for both types. The Teledeltos paper is molded in a layer of Teflon to keep it moisture free. The 400°C temperature, required to cure the Teflon, does not deteriorate the lossy paper. This type of attenuator has been found to be more consistent from tube to tube than spraying or painting Aquadag or other commercially available lossy materials and is capable of dissipating 12 watts of average power without any apparent damage.

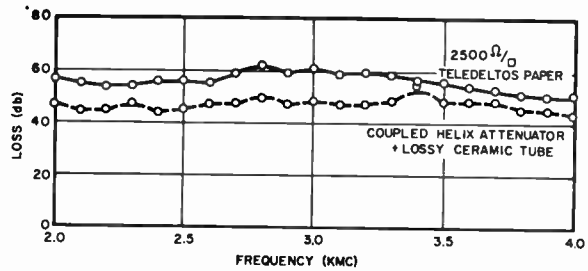


Fig. 13—Loss obtained with Teledeltos paper attenuator as compared to that with a coupled-helix plus lossy-ceramic attenuator.

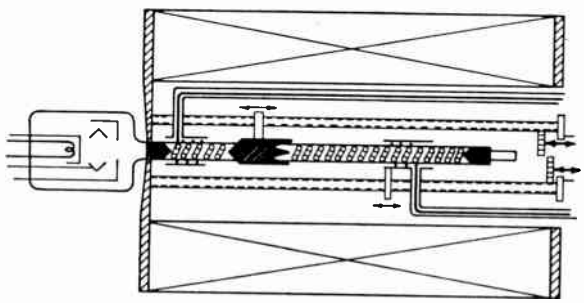

Fig. 14—Schematic drawing of movable coupler device. The input coupled-helix match is fixed in position and the attenuator and output coupled-helix match are movable independently or ganged together. The tube was operated in a uniform magnetic field for these tests.

A coupled helix attenuator has also been developed for this tube, consisting of a quadrifilar Kanthal wire helix moulded in Teflon in conjunction with a carbon impregnated ceramic tubing to provide additional loss. The saturation power output has consistently been 2–3 db lower than that with the lossy wall variety.[13]

The lossy wall attenuator has three sections—a slightly tapered input, a constant resistance center section, and a long tapered output section.

It was desirable for the tube to be short-circuit stable. For a high gain tube this imposes a stringent condition (vswr ≈ 1.04) on the match looking into the attenuator from the output. A gradual taper of the lossy material in this transition region is therefore essential and this gradual transition also apparently improves the "saturation characteristic."[14]

A program is under way to incorporate a grid in the gun which would decrease greatly the size of modulator required for the tube.

## Movable Coupler Device

In order to study further the effect of the attenuator on the tube behavior, a device was built using coupled helix matches, which allows movement of both the at-

[13] N. Rynn, "Analysis of coupled structure traveling-wave tubes," IRE Trans., vol. ED-4, pp. 172–177; April, 1957.

[14] J. J. Caldwell, "High-power traveling-wave tube gain and saturation characteristics as a function of attenuator configuration and resistivity," IRE Trans., vol. ED-4, pp. 28–32; December, 1953.

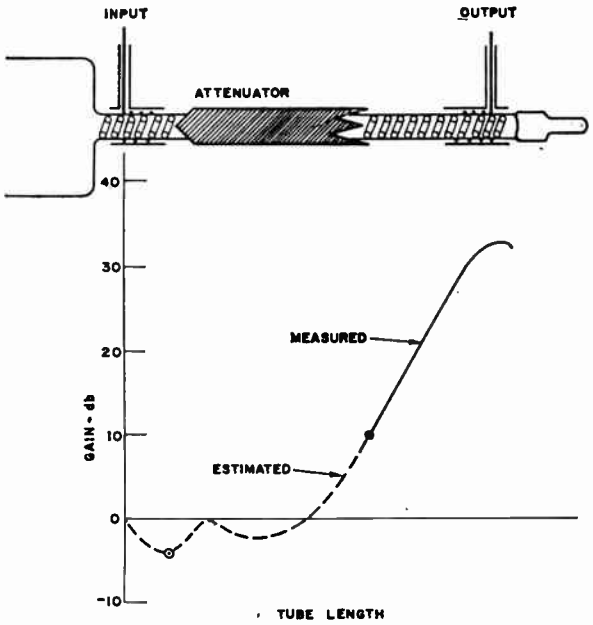


Fig. 15—Illustration of the power build-up along the tube, as determined from movable coupler measurements. The dotted parts of the curve are estimated and are therefore less accurate.

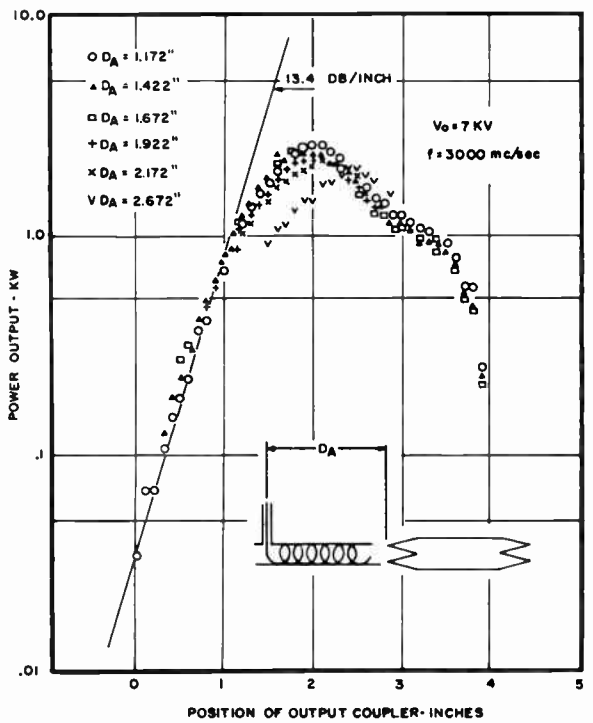


Fig. 16—Tube power output vs axial position of the output coupler for various positions of the attenuator. The zero coupler position was located at the extreme output end of the attenuator when the input end of the attenuator was $D_A = 1.172$ inches from the center line of the input coaxial line. It is seen that the power build-up after the attenuator was almost independent of attenuator position and the saturation level was highest for the attenuator in the closest position to the input.

tenuator and output match during tube operation. In contrast to probing the field, this device actually changes the electrical length of the tube during operation. A uniform field was used for focusing in these tests

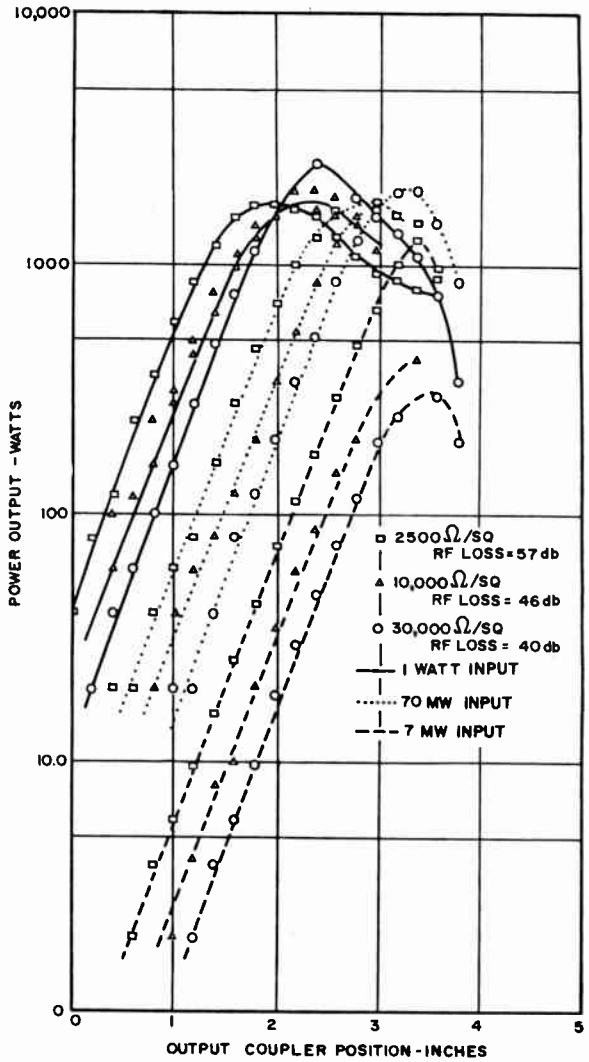


Fig. 17—Tube power output vs axial position of the output coupler for several values of attenuator resistivity and drive power levels. The attenuator was made of Teledeltos paper. $D_A = 1.172$ inches.

and the following results were observed. A schematic diagram of the apparatus is shown in Fig. 14 and an illustration of the power build-up vs position along the helix is shown in Fig. 15, as determined from these measurements. First, the position of the attenuator is not critical, as shown by the curves of Fig. 16, but for best performance should be located close to the input. The length of the input coupler is equal to 0.22 $CN$, which is close to the optimum Pierce value.[15] Second, the change in power build-up as a function of the Ω/square surface resistivity of the attenuator is shown in Fig. 17. Note that although the saturated output is higher with the higher Ω/square attenuator, a longer tube length is required to reach saturation.

The rate of power build-up can be measured rather accurately in the lossless region and is noted to be 5.6 db/$\lambda_g$. From a knowledge of $b$ and $c$, $x_1$ can be computed using this experimentally obtained value of gain per

[15] J. R. Pierce, "Traveling-Wave Tubes," D. Van Nostrand Co., Inc., New York, N. Y., p. 140; 1950.

wavelength. The resulting value obtained using $C=0.145$ and $b=1.0$, $N=11.9$ is $x_1=0.805$. The value of $x_1$ obtained by small-signal theory[16] using the above values and $QC=0.2$ gives $x_1=0.79$ to 0.80, which is within the accuracy of the curves used. The gain profile along the tube length, shown in Fig. 15, is based on the best data available from this device.

The values of the parameters $C=0.145$, $QC=0.2$, and $\gamma r_0=0.56$ are quite close to those measured by Cutler[17] to yield the optimum efficiency; from his work efficiencies of 30 per cent and greater can be expected. Efficiencies of 30 per cent have been observed, but it has been found difficult to optimize the attenuator design to achieve both maximum efficiency and maximum stability (*i.e.*, short-circuit stability).

By adjusting the attenuator it is possible to optimize the tube design to meet a variety of requirements involving the gain, power output, stability, and duty cycle. For example, if the tube is not required to operate into a bad mismatch, the attenuation can be reduced with a corresponding increase in power output and efficiency. Conversely, if a lower power and efficiency can be tolerated, the gain can be made flatter over a wider band by designing the attenuator to cause premature saturation of the tube in the midband region.

[16] C. K. Birdsall and G. R. Brewer, "Traveling-wave tube characteristics for finite values of $C$," IRE TRANS., vol. ED-1, pp. 1–11; August, 1954. These computations in turn were based on the small-signal theory of Pierce, *op. cit.*

[17] C. C. Cutler, "The nature of power saturation in traveling-wave tubes," *Bell Sys. Tech. J.*, vol. 35, pp. 841–876; July, 1956.

## Conclusion

It has been shown that a relatively high-power electron beam for use in a broad-band (essentially 2:1) traveling-wave tube can be periodically focused. Such periodic focusing does not degrade the performance of the tube but in fact can result in a tube with more diversified operating characteristics. A total of about 25 of these tubes have been built and tested, with good reproducibility of the operating characteristics. RF defocusing becomes an important factor to consider in high-power periodically focused tubes, but the effect can be reduced by proper attention to the period of the magnetic circuit and the operating voltage.

The attenuator position is not critical, but should be located near the input of the tube for maximum saturated power output. The Ω/square value used in a lossy wall attenuator can markedly affect the saturation output, and values near 2500 Ω/square seem reasonably good. A wide variety of tube requirements can be met by changing the periodic magnet circuit, the attenuator configuration, or both. It is apparent that further estensions of periodic focusing into regions of higher power will come about by either incorporating part of the magnetic circuit inside the vacuum envelope or by obtaining magnetic materials of higher coercive force.

## Acknowledgment

The assistance of T. Gorman, W. Perkins, T. Leonard, L. Toy, and B. Kesterson in the assembling and processing of these tubes is gratefully acknowledged.

# Index to IRE Standards on Definitions of Terms 1942-1957*

(58 IRE 20.S1)

## INTRODUCTION

This index covers all Standards on Definitions of Terms issued by the IRE from 1942 through July, 1957, that are still in force. It brings together in one alphabetical list approximately 3500 technical terms defined in those Standards, indicating the IRE code number of the Standard and the issue and page number of the PROCEEDINGS OF THE IRE where the definition may be found. Standards issued prior to 1949, which were published as separate reports instead of in the PROCEEDINGS, are identified by the word "separate" in the index.

In some instances the same term has been defined in more than one Standard. If the Standards are in the same field, only the last published definition is referenced in the index; if they are in different fields, all definitions are referenced.

A list of the Standards covered in the index and their IRE code numbers is given below. Reprints may be ordered at the indicated prices from IRE headquarters. Reprints of this index are also available as indicated in the footnote below.*

The IRE is greatly indebted to Chester H. Page, Vice-Chairman and Definitions Coordinator of the Standards Committee, for the substantial task of compiling this index.

## STANDARDS COVERED BY INDEX

| *Standard No.* | *Title and Where Published* | *Reprint Price* |
|---|---|---|
| 48 IRE 2, 11, 15.S1 | Standards on Antennas, Modulation Systems, and Transmitters: Definitions of Terms, 1948 (Separate Report) | $0.75 |
| 53 IRE 2.S1 | Standards on Antennas and Waveguides: Definitions of Terms, 1953 (December, 1953, PROC. IRE) | $0.75 |
| 55 IRE 2.S1 | Standards on Antennas and Waveguides: Definitions for Waveguide Components, 1955 (September, 1953, PROC. IRE) | $0.25 |
| 54 IRE 3.S1 | Standards on Audio Techniques: Definitions of Terms, 1954 (July, 1954, PROC. IRE) | $0.50 |
| 50 IRE 4.S1 | Standards on Circuits: Definitions of Terms in Network Topology, 1950 (January, 1951, PROC. IRE) | $0.50 |
| 53 IRE 4.S1 | Standards on Circuits: Definitions of Terms in the Field of Linear Varying Parameter and Nonlinear Circuits, 1953 (March, 1954, PROC. IRE) | $0.25 |
| 51 IRE 6.S1 | Standards on Electroacoustics: Definitions of Terms, 1951 (May, 1951, PROC. IRE) | $1.00 |
| 50 IRE 7.S1 | Standards on Electron Tubes: Definitions of Terms, 1950 (April, 1950, PROC. IRE) | † |
| 54 IRE 7.S1 | Standards on Electron Devices: Definitions of Terms Related to Phototubes, 1954 (August, 1954, PROC. IRE) | $0.25 |
| 54 IRE 7.S2 | Standards on Electron Devices: Definitions of Semiconductor Terms, 1954 (October, 1954, PROC. IRE) | $0.50 |
| 56 IRE 7.S3 | Standards on Electron Tubes: TR and ATR Tube Definitions, 1956 (August, 1956, PROC. IRE) | $0.50 |
| 57 IRE 7.S2 | Standards on Electron Tubes: Definitions of Terms, 1957 (July, 1957, PROC. IRE) | $1.00 |
| 50 IRE 8.S1 | Standards on Electronic Computers: Definitions of Terms, 1950 (March, 1951, PROC. IRE) | † |
| 56 IRE 8.S1 | Standards on Electronic Computers: Definitions of Terms, 1956 (September, 1956, PROC. IRE) | $0.60 |
| 42 IRE 9.S1 | Standards on Facsimile: Definitions of Terms, 1942 (Separate Report) | † |
| 56 IRE 9.S1 | Standards on Facsimile: Definitions of Terms, 1956 (June, 1956, PROC. IRE) | $0.60 |
| 55 IRE 10.S1 | Standards on Industrial Electronics: Definitions of Industrial Electronics Terms, 1955 (September, 1955, PROC. IRE) | $0.50 |
| 53 IRE 11.S1 | Standards on Modulation Systems: Definitions of Terms, 1953 (May, 1953, PROC. IRE) | $0.50 |
| 54 IRE 12.S1 | Standards on Radio Aids to Navigation: Definitions of Terms, 1954 (February, 1955, PROC. IRE) | $1.00 |
| 52 IRE 17.S1 | Standards on Receivers: Definitions of Terms, 1952 (December, 1952, PROC. IRE) | $0.60 |
| 51 IRE 20.S1 | Standards on Pulses: Definitions of Terms —Part I, 1951 (June, 1951, PROC. IRE) | $0.50 |
| 51 IRE 20.S2 | Standards on Transducers: Definitions of Terms, 1951 (August, 1951, PROC. IRE) | $0.50 |
| 52 IRE 20.S1 | Standards on Pulses: Definitions of Terms —Part II, 1952 (May, 1952, PROC. IRE) | $0.50 |
| 55 IRE 22.S1 | Standards on Television: Definitions of Color Terms, 1955 (June, 1955, PROC. IRE) | $0.60 |
| 55 IRE 23.S1 | Standards on Television: Definitions of Television Signal Measurement Terms, 1955 (May, 1955, PROC. IRE) | $1.00 |
| 45 IRE 24.S1 | Standards on Radio Wave Propagation: Definitions of Terms Relating to Guided Waves, 1945 (Separate Report) | $0.20 |
| 50 IRE 24.S1 | Standards on Wave Propagation: Definitions of Terms, 1950 (November, 1950, PROC. IRE) | $0.60 |
| 55 IRE 26.S2 | Standards on Terminology for Feedback Control Systems, 1955 (January, 1956, PROC. IRE) | $0.50 |

† Out of print.

* Reprints of this index may be purchased while available from the Institute of Radio Engineers, 1 East 79 Street, New York 21, N.Y., at $1.00 per copy. A 20 per cent discount will be allowed for 100 or more copies mailed to one address.

# PUBLISHED IRE DEFINITIONS

| | Standard | Proceedings Vol Page Mo |
|---|---|---|
| **A** | | |
| A and R Display | 54 IRE 12.S1 | 43 192 Feb |
| Absolute Delay | 54 IRE 12.S1 | 43 192 Feb |
| Absorption | 50 IRE 24.S1 | 38 1265 Nov |
| Absorption Loss | 51 IRE 6.S1 | 39 510 May |
| Absorption Modulation | 48 IRE 2,11,15.S1 | Separate |
| Accelerating Electrode | 57 IRE 7.S2 | 45 986 Jul |
| Acceleration | 51 IRE 6.S1 | 39 510 May |
| Access Time | 56 IRE 8.S1 | 44 1167 Sep |
| Accessible Terminal | 50 IRE 4.S1 | 39 27 Jan |
| Acceptor | 54 IRE 7.S2 | 42 1506 Oct |
| Accumulator | 56 IRE 8.S1 | 44 1167 Sep |
| Accuracy | 56 IRE 8.S1 | 44 1167 Sep |
| AC Erasing Head | 51 IRE 6.S1 | 39 510 May |
| AC Magnetic Biasing | 51 IRE 6.S1 | 39 510 May |
| Acetate Disks | 51 IRE 6.S1 | 39 510 May |
| Achromatic Locus | 55 IRE 22.S1 | 43 742 Jne |
| Acoustic | 51 IRE 6.S1 | 39 510 May |
| Acoustic Compliance | 51 IRE 6.S1 | 39 510 May |
| Acoustic Dispersion | 51 IRE 6.S1 | 39 510 May |
| Acoustic Generator | 51 IRE 6.S1 | 39 510 May |
| Acoustic Horn | 51 IRE 6.S1 | 39 510 May |
| Acoustic Impedance | 51 IRE 6.S1 | 39 510 May |
| Acoustic Interferometer | 51 IRE 6.S1 | 39 510 May |
| Acoustic Mass | 51 IRE 6.S1 | 39 510 May |
| Acoustic Pickup | 51 IRE 6.S1 | 39 510 May |
| Acoustic Radiating Element | 51 IRE 6.S1 | 39 510 May |
| Acoustic Radiometer | 51 IRE 6.S1 | 39 510 May |
| Acoustic Reactance | 51 IRE 6.S1 | 39 510 May |
| Acoustic Refraction | 51 IRE 6.S1 | 39 510 May |
| Acoustic Resistance | 51 IRE 6.S1 | 39 510 May |
| Acoustic Scattering | 51 IRE 6.S1 | 39 510 May |
| Acoustic Stiffness | 51 IRE 6.S1 | 39 510 May |
| Acoustic Transmission System | 51 IRE 6.S1 | 39 511 May |
| Acoustical | 51 IRE 6.S1 | 39 511 May |
| Acoustical Ohm | 51 IRE 6.S1 | 39 511 May |
| Acoustical Reciprocity Theorem | 51 IRE 6.S1 | 39 511 May |
| Acoustical Units | 51 IRE 6.S1 | 39 511 May |
| Acoustics | 51 IRE 6.S1 | 39 511 May |
| Active Transducer | 51 IRE 20.S2 | 39 898 Aug |
| Active Transducer (Audio) | 54 IRE 3.S1 | 42 1110 Jul |
| Actuating Transfer Function | 55 IRE 26.S2 | 44 108 Jan |
| ADF | 54 IRE 12.S1 | 43 192 Feb |
| A-Display | 54 IRE 12.S1 | 43 192 Feb |
| Adcock Antenna | 48 IRE 2,11,15.S1 | Separate |
| Adder | 56 IRE 8.S1 | 44 1167 Sep |
| Adder, Algebraic | 50 IRE 8.S1 | 39 272 Mar |
| Address | 56 IRE 8.S1 | 44 1167 Sep |
| Address Part | 56 IRE 8.S1 | 44 1167 Sep |
| Adjacent-Channel Attenuation | 52 IRE 17.S1 | 40 1682 Dec |
| Adjacent-Channel Interference | 52 IRE 17.S1 | 40 1682 Dec |
| Admittance | 57 IRE 7.S2 | 45 986 Jul |
| Advance Ball | 51 IRE 6.S1 | 39 511 May |
| Aeolight | 51 IRE 6.S1 | 39 511 May |
| Aerophare | 54 IRE 12.S1 | 43 192 Feb |
| AI Radar | 54 IRE 12.S1 | 43 192 Feb |
| Aided Tracking | 54 IRE 12.S1 | 43 192 Feb |
| Air Conduction | 51 IRE 6.S1 | 39 511 May |
| Airport Surface Detection Equipment (ASDE) | 54 IRE 12.S1 | 43 209 Feb |
| Air-Position Indicator (API) | 54 IRE 12.S1 | 43 207 Feb |
| Air Speed | 54 IRE 12.S1 | 43 192 Feb |
| Airborne Radar | 49 IRE 12.S1 | 37 1366 Dec |
| Airport Surveillance Radar | 54 IRE 12.S1 | 43 192 Feb |
| Alford Loop | 54 IRE 12.S1 | 43 192 Feb |
| Algebraic Adder | 50 IRE 8.S1 | 39 272 Mar |
| Alternator Transmitter | 48 IRE 2,11,15.S1 | Separate |
| Altimetric Flare-Out | 54 IRE 12.S1 | 43 192 Feb |
| Altitude | 49 IRE 12.S1 | 37 1367 Dec |
| AM to FS Converter | 56 IRE 9.S1 | 44 776 Jne |
| Ambient Temperature | 48 IRE 2,11,15.S1 | Separate |
| Ambiguity | 54 IRE 12.S1 | 43 192 Feb |
| Amplification | 54 IRE 3.S1 | 42 1110 Jul |
| Amplification Factor | 57 IRE 7.S2 | 45 986 Jul |
| Amplifier | 57 IRE 7.S2 | 45 986 Jul |
| Amplifier | 48 IRE 2,11,15.S1 | Separate |
| Amplifier Torque | 50 IRE 8.S1 | 39 272 Mar |
| Amplitude Balance Control | 54 IRE 12.S1 | 43 192 Feb |
| Amplitude Discriminator | 54 IRE 12.S1 | 43 192 Feb |
| Amplitude Distortion | 53 IRE 4.S1 | 42 554 Mar |
| Amplitude Distortion (old usage) | 48 IRE 2,11,15.S1 | Separate |
| Amplitude-Frequency Distortion | 53 IRE 4.S1 | 42 554 Mar |
| Amplitude vs Frequency Response Characteristic | 48 IRE 2,11,15.S1 | Separate |
| Amplitude-Modulated Transmitter | 48 IRE 2,11,15.S2 | Separate |
| Amplitude-Modulated Noise Level | 48 IRE 2,11,15.S1 | Separate |
| Amplitude Modulation | 53 IRE 11.S1 | 41 612 May |
| Amplitude Modulation | 52 IRE 17.S1 | 40 1682 Dec |
| Amplitude Response (Camera Tubes) | 57 IRE 7.S2 | 45 986 Jul |
| Amplitude Response Characteristic | 57 IRE 7.S2 | 45 986 Jul |
| A-N Radio Range | 54 IRE 12.S1 | 43 207 Feb |
| Analog | 56 IRE 8.S1 | 44 1167 Sep |
| Analog Computer | 56 IRE 8.S1 | 44 1167 Sep |
| And-Circuit | 56 IRE 8.S1 | 44 1167 Sep |
| And-Gate | 56 IRE 8.S1 | 44 1167 Sep |
| Angle | 57 IRE 7.S2 | 45 986 Sep |
| Angle, Maximum-Deflection | 57 IRE 7.S2 | 45 986 Jul |
| Angle Modulation | 53 IRE 11.S1 | 41 612 May |
| Angle of Elevation | 49 IRE 12.S1 | 37 1367 Dec |
| Angle or Phase of a Sine Wave | 53 IRE 11.S1 | 41 612 May |
| Angular Deviation Loss | 51 IRE 6.S1 | 39 511 May |
| Angular Deviation Sensitivity | 54 IRE 12.S1 | 43 192 Feb |
| Angular Frequency | 50 IRE 24.S1 | 38 1265 Nov |
| Angular Resolution | 54 IRE 12.S1 | 43 192 Feb |
| Angular Width | 54 IRE 12.S1 | 43 193 Feb |
| Anode (Electron Tubes) | 57 IRE 7.S2 | 45 986 Jul |
| Anode Breakdown Voltage | 57 IRE 7.S2 | 45 986 Jul |
| Anode Current | 57 IRE 7.S2 | 45 986 Jul |
| Anode Strap (Magnetrons) | 57 IRE 7.S2 | 45 986 Jul |
| Anode Voltage | 57 IRE 7.S2 | 45 986 Jul |
| Anode Voltage Drop | 57 IRE 7.S2 | 45 986 Jul |
| Antenna | 52 IRE 17.S1 | 40 1682 Dec |
| Antenna Array | 48 IRE 2,11,15.S1 | Separate |
| Antenna Cross Talk | 48 IRE 2,11,15.S1 | Separate |
| Antenna Effect | 54 IRE 12.S1 | 43 193 Feb |
| Antenna Resistance | 48 IRE 2,11,15.S1 | Separate |
| Anti-Clutter Circuits | 54 IRE 12.S1 | 43 193 Feb |
| Anti-TR Switch | 54 IRE 12.S1 | 43 193 Feb |
| Antinoise Microphone | 51 IRE 6.S1 | 39 511 May |
| Aperture | 48 IRE 2,11,15.S1 | Separate |
| Aperture Illumination | 48 IRE 2,11,15.S1 | Separate |
| Applicator (Electrodes) | 55 IRE 10.S1 | 43 1070 Sep |
| Applicator Impedance | 55 IRE 10.S1 | 43 1070 Sep |

| | Standard | Proceedings Vol Page Mo |
|---|---|---|
| Base Electrode | 54 IRE 7.S2 | 42 1506 Oct |
| Base Region | 54 IRE 7.S2 | 42 1506 Oct |
| Basic Frequency | 51 IRE 6.S1 | 39 513 May |
| Basic Repetition Rate | 54 IRE 12.S1 | 43 193 Feb |
| Baud | 53 IRE 11.S1 | 41 612 May |
| Beam Alignment | 57 IRE 7.S2 | 45 987 Jul |
| Beam Bending | 57 IRE 7.S2 | 45 987 Jul |
| Beam-Deflection Tube | 57 IRE 7.S2 | 45 987 Jul |
| Beam-Indexing Color Tube | 57 IRE 7.S2 | 45 987 Jul |
| Beam Modulation Percentage | 57 IRE 7.S2 | 45 987 Jul |
| Beam Power Tube | 57 IRE 7.S2 | 45 987 Jul |
| Bearing | 54 IRE 12.S1 | 43 193 Feb |
| Beating | 52 IRE 17.S1 | 40 1682 Dec |
| Beat Note | 52 IRE 17.S1 | 40 1682 Dec |
| Bel | 48 IRE 2,11,15.S1 | Separate |
| Bend | 54 IRE 12.S1 | 43 193 Feb |
| Bend, Waveguide | 55 IRE 2.S1 | 43 1073 Sep |
| Benito | 54 IRE 12.S1 | 43 208 Feb |
| Bias Telegraph Distortion | 48 IRE 2,11,15.S1 | Separate |
| Biconical Antenna | 48 IRE 2,11,15.S1 | Separate |
| Bidirectional Microphone | 51 IRE 6.S1 | 39 513 May |
| Bidirectional Pulse | 52 IRE 20.S1 | 40 553 May |
| Bidirectional Pulses | 48 IRE 2,11,15.S1 | Separate |
| Bidirectional Pulse Train | 52 IRE 20.S1 | 40 553 May |
| Bilateral-Area Track | 51 IRE 6.S1 | 39 513 May |
| Bilateral Transducer | 51 IRE 20.S2 | 39 898 Aug |
| Binary | 56 IRE 8.S1 | 44 1167 Sep |
| Binary Cell | 56 IRE 8.S1 | 44 1167 Sep |
| Binary-Coded-Decimal System | 56 IRE 8.S1 | 44 1167 Sep |
| Binary Digit | 50 IRE 8.S1 | 39 272 Mar |
| Binary Number System | 56 IRE 8.S1 | 44 1167 Sep |
| Binary Point | 56 IRE 8.S1 | 44 1167 Sep |
| Binder | 51 IRE 6.S1 | 39 513 May |
| Bit | 56 IRE 8.S1 | 44 1167 Sep |
| Black and White | 55 IRE 22.S1 | 43 743 Jne |
| Black Compression | 55 IRE 23.S1 | 43 620 May |
| Black Level | 55 IRE 23.S1 | 43 620 May |
| Black Peak | 55 IRE 23.S1 | 43 620 May |
| Black Recording | 56 IRE 9.S1 | 44 777 Jne |
| Black Signal | 56 IRE 9.S1 | 44 777 Jne |
| Black Transmission | 56 IRE 9.S1 | 44 777 Jne |
| Blanked Picture Signal | 55 IRE 23.S1 | 43 620 May |
| Blanking Level | 55 IRE 23.S1 | 43 620 May |
| Blanking Signal | 55 IRE 23.S1 | 43 620 May |
| Blemish | 57 IRE 7.S2 | 45 987 Jul |
| Blind Speed | 54 IRE 12.S1 | 43 193 Feb |
| Blinking | 54 IRE 12.S1 | 43 193 Feb |
| Blip (PIP) | 54 IRE 12.S1 | 43 194 Feb |
| Block | 56 IRE 8.S1 | 44 1167 Sep |
| Blocked Impedance | 51 IRE 6.S1 | 39 513 May |
| Blocking Oscillator | 48 IRE 2,11,15.S1 | Separate |
| Blooming | 54 IRE 12.S1 | 43 194 Feb |
| Bone Conduction | 51 IRE 6.S1 | 39 513 May |
| Bootstrap Circuit | 48 IRE 2,11,15.S1 | Separate |
| Boresighting | 54 IRE 12.S1 | 43 194 Feb |
| Borrow | 56 IRE 8.S1 | 44 1167 Sep |
| Boundary | 54 IRE 7.S2 | 42 1506 Oct |
| Boundary Marker | 54 IRE 12.S1 | 43 208 Feb |
| Branch (in Circuits) | 50 IRE 4.S1 | 39 27 Jan |
| Branch (in Computing) | 56 IRE 8.S1 | 44 1167 Sep |
| Branch Point | 50 IRE 4.S1 | 39 27 Jan |
| Breakdown | 57 IRE 7.S2 | 45 987 Jul |
| Breakdown Transfer Characteristic | 57 IRE 7.S2 | 45 987 Jul |
| Breakdown Voltage | 57 IRE 7.S2 | 45 987 Jul |
| Break-in-Keying | 48 IRE 2,11,15.S1 | Separate |
| Break Point | 56 IRE 8.S1 | 44 1167 Sep |
| Bridge Rectifier | 48 IRE 2,11,15.S1 | Separate |
| Bridged-T Network | 50 IRE 4.S1 | 39 27 Jan |
| Bridging | 54 IRE 3.S1 | 42 1110 Jul |
| Bridging Gain | 54 IRE 3.S1 | 42 1110 Jul |
| Bridging Loss | 54 IRE 3.S1 | 42 1110 Jul |
| Brightness | 55 IRE 22.S1 | 43 743 Jne |
| Brightness Signal | 55 IRE 22.S1 | 43 743 Jne |
| Broad-Band Tube | 57 IRE 7.S2 | 45 987 Jul |
| Broadside Array | 48 IRE 2,11,15.S1 | Separate |
| Buffer (in computors) | 56 IRE 8.S1 | 44 1167 Sep |
| Buffer Amplifier | 48 IRE 2,11,15.S1 | Separate |
| Bunching | 57 IRE 7.S2 | 45 987 Jul |
| Bunching Angle | 57 IRE 7.S2 | 45 987 Jul |
| Bunching Optimum | 57 IRE 7.S2 | 45 987 Jul |
| Bunching Parameter | 57 IRE 7.S2 | 45 987 Jul |
| Burnishing Surface | 51 IRE 6.S1 | 39 513 May |
| Bus (in Electronic Computers) | 56 IRE 8.S1 | 44 1167 Sep |
| Butt Joint | 55 IRE 2.S1 | 43 1073 Sep |
| **C** | | |
| Cable | 53 IRE 2.S1 | 41 1722 Dec |
| CCA | 54 IRE 12.S1 | 43 194 Feb |
| C-Display | 54 IRE 12.S1 | 43 197 Feb |
| Cake Wax | 51 IRE 6.S1 | 39 513 May |
| Calibration Markers | 54 IRE 12.S1 | 43 194 Feb |
| Camera Tube | 57 IRE 7.S2 | 45 987 Jul |
| Cancellation Ratio | 54 IRE 12.S1 | 43 194 Feb |
| Cancelled Video | 54 IRE 12.S1 | 43 194 Feb |
| Candle | 55 IRE 22.S1 | 43 743 Jne |
| Candlepower | 55 IRE 22.S1 | 43 743 Jne |
| Capacitance | 57 IRE 7.S2 | 45 987 Jul |
| Capacitor Pickup | 51 IRE 6.S1 | 39 513 May |
| Carbon Microphone | 51 IRE 6.S1 | 39 513 May |
| Carbon Pressure Recording | 56 IRE 9.S1 | 44 777 Jne |
| Carrier (in Modulation) | 53 IRE 11.S1 | 41 612 May |
| Carrier (in Semiconductor) | 54 IRE 7.S2 | 42 1506 Oct |
| Carrier-Amplitude Regulation | 48 IRE 2,11,15.S1 | Separate |
| Carrier Beat | 56 IRE 9.S1 | 44 777 Jne |
| Carrier-Controlled Approach | 54 IRE 12.S1 | 43 194 Feb |
| Carrier Frequency | 53 IRE 11.S1 | 41 612 May |
| Carrier-Frequency Pulse | 52 IRE 20.S1 | 40 553 May |
| Carrier-Frequency Range | 48 IRE 2,11,15.S1 | Separate |
| Carrier-Frequency Stability | 48 IRE 2,11,15.S1 | Separate |
| Carrier Noise Level | 48 IRE 2,11,15.S1 | Separate |
| Carrier Suppression | 48 IRE 2,11,15.S1 | Separate |
| Carrier-to-Noise Ratio | 53 IRE 11.S1 | 41 612 May |
| Carrier Wave | 42 IRE 9.S1 | Separate |
| Carry | 56 IRE 8.S1 | 44 1167 Sep |
| Cascade (in Circuits) | 50 IRE 4.S1 | 38 27 Jan |
| Cascaded Carry | 56 IRE 8.S1 | 44 1168 Sep |
| C-Scope | 49 IRE 12.S1 | 37 1367 Dec |
| Cathode | 57 IRE 7.S2 | 45 987 Jul |
| Cathode Coating Impedance | 57 IRE 7.S2 | 45 988 Jul |
| Cathode Current | 57 IRE 7.S2 | 45 988 Jul |
| Cathode Follower | 48 IRE 2,11,15.S1 | Separate |
| Cathode Glow | 57 IRE 7.S2 | 45 988 Jul |
| Cathode Heating Time | 57 IRE 7.S2 | 45 988 Jul |
| Cathode Interface (Layer) Capacitance | 57 IRE 7.S2 | 45 988 Jul |
| Cathode Interface (Layer) Impedance | 57 IRE 7.S2 | 45 988 Jul |
| Cathode Interface (Layer) Resistance | 57 IRE 7.S2 | 45 988 Jul |
| Cathode Luminous Sensitivity | 54 IRE 7.S1 | 42 1277 Aug |

| | Standard | Proceedings Vol | Page | Mo |
|---|---|---|---|---|
| Combination Microphone | 51 IRE 6.S1 | 39 | 514 | May |
| Command (in Computers) | 56 IRE 8.S1 | 44 | 1168 | Sep |
| Command (in Control Systems) | 55 IRE 26.S2 | 44 | 109 | Jan |
| Commutation Factor | 57 IRE 7.S2 | 45 | 989 | Jul |
| Companding | 53 IRE 11.S1 | 41 | 612 | May |
| Comparator | 50 IRE 8.S1 | 39 | 272 | Mar |
| Compass Bearing | 49 IRE 12.S1 | 37 | 1367 | Dec |
| Compass Course | 49 IRE 12.S1 | 37 | 1367 | Dec |
| Compass Heading | 49 IRE 12.S1 | 37 | 1367 | Dec |
| Compatibility | 55 IRE 22.S1 | 43 | 745 | Jne |
| Complement | 56 IRE 8.S1 | 44 | 1168 | Sep |
| Complementary Wavelength | 55 IRE 22.S1 | 43 | 745 | Jne |
| Complete Carry | 56 IRE 8.S1 | 44 | 1168 | Sep |
| Complex Target | 54 IRE 12.S1 | 43 | 194 | Feb |
| Complex Tone | 51 IRE 8.S1 | 44 | 1168 | Sep |
| Composite Color Signal | 55 IRE 22.S1 | 43 | 745 | Jne |
| Composite Color Sync | 55 IRE 22.S1 | 43 | 745 | Jne |
| Composite Controlling Voltage | 57 IRE 7.S2 | 45 | 989 | Jul |
| Composite Picture Signal | 55 IRE 23.S1 | 43 | 620 | May |
| Composite Pulse | 54 IRE 12.S1 | 43 | 194 | Feb |
| Compound Horn | 48 IRE 2,11,15.S1 | Separate | | |
| Compound Target | 54 IRE 12.S1 | 43 | 194 | Feb |
| Compression | 53 IRE 11.S1 | 41 | 612 | May |
| Compression (in Television) | 55 IRE 23.S1 | 43 | 620 | May |
| Compression Ratio | 57 IRE 7.S2 | 45 | 989 | Jul |
| Compressional Wave | 51 IRE 6.S1 | 39 | 514 | May |
| Computer | 56 IRE 8.S1 | 44 | 1168 | Sep |
| Condensed-Mercury Temperature | 57 IRE 7.S2 | 45 | 989 | Jul |
| Conditional Jump | 56 IRE 8.S1 | 44 | 1168 | Sep |
| Conditional Transfer of Control | 56 IRE 8.S1 | 44 | 1169 | Sep |
| Condor | 54 IRE 12.S1 | 43 | 208 | Feb |
| Conductance | 57 IRE 7.S2 | 45 | 989 | Jul |
| Conductance for Rectification | 57 IRE 7.S2 | 45 | 989 | Jul |
| Conduction Band | 54 IRE 7.S2 | 42 | 1506 | Oct |
| Conductivity | 54 IRE 7.S2 | 42 | 1506 | Oct |
| Conductivity Modulation | 54 IRE 7.S2 | 42 | 1506 | Oct |
| Conductivity, P-Type | 54 IRE 7.S2 | 42 | 1506 | Oct |
| Cone of Nulls | 48 IRE 2,11,15.S1 | Separate | | |
| Cone of Silence | 54 IRE 12.S1 | 43 | 194 | Feb |
| Conical Horn | 51 IRE 6.S1 | 39 | 514 | May |
| Conical Scanning | 48 IRE 2,11,15.S1 | Separate | | |
| Connected | 50 IRE 4.S1 | 38 | 27 | Jan |
| Connector Waveguide | 55 IRE 2.S1 | 43 | 1074 | Sep |
| Consol | 54 IRE 12.S1 | 43 | 208 | Feb |
| Consolan | 54 IRE 12.S1 | 43 | 208 | Feb |
| Constant Amplitude Recording | 51 IRE 6.S1 | 39 | 514 | May |
| Constant-Current Characteristic | 57 IRE 7.S2 | 45 | 989 | Jul |
| Constant-Current Modulation | 48 IRE 2,11,15.S1 | Separate | | |
| Constant-Delay Discriminator | 54 IRE 12.S1 | 43 | 194 | Feb |
| Constant Luminance Transmission | 55 IRE 22.S1 | 43 | 745 | Jne |
| Constant Velocity Recording | 51 IRE 6.S1 | 39 | 514 | May |
| Contact, High Recombination Rate | 54 IRE 7.S2 | 42 | 1506 | Oct |
| Contact, Majority Carrier | 54 IRE 7.S2 | 42 | 1506 | Oct |
| Contact Potential Difference | 57 IRE 7.S2 | 45 | 989 | Jul |
| Contact Rectifier | 48 IRE 2,11,15.S1 | Separate | | |
| Contactor, Load | 55 IRE 10.S1 | 43 | 1070 | Sep |
| Continuous-Duty Rating | 48 IRE 2,11,15.S1 | Separate | | |
| Continuous Waves or CW | 48 IRE 2,11,15.S1 | Separate | | |
| Control (in Computers) | 56 IRE 8.S1 | 44 | 1169 | Sep |
| Control Characteristic | 57 IRE 7.S2 | 45 | 989 | Jul |
| Control Circuits | 50 IRE 8.S1 | 39 | 273 | Mar |
| Control Electrode | 57 IRE 7.S2 | 45 | 989 | Jul |
| Control-Electrode Discharge Recovery Time | 57 IRE 7.S2 | 45 | 989 | Jul |
| Control Grid | 57 IRE 7.S2 | 45 | 990 | Jul |
| Control Ratio | 57 IRE 7.S2 | 45 | 990 | Jul |
| Control Track | 51 IRE 6.S1 | 39 | 514 | May |
| Controlled Carrier | 48 IRE 2,11,15.S1 | Separate | | |
| Convection Current | 57 IRE 7.S2 | 45 | 990 | Jul |
| Convection-Current Modulation | 57 IRE 7.S2 | 45 | 990 | Jul |
| Convergence | 57 IRE 7.S2 | 45 | 990 | Jul |
| Convergence, Dynamic | 57 IRE 7.S2 | 45 | 990 | Jul |
| Convergence Electrode | 57 IRE 7.S2 | 45 | 990 | Jul |
| Convergence Magnet | 57 IRE 7.S2 | 45 | 990 | Jul |
| Convergence Plane | 57 IRE 7.S2 | 45 | 990 | Jul |
| Convergence Surface | 57 IRE 7.S2 | 45 | 990 | Jul |
| Conversion Transconductance | 57 IRE 7.S2 | 45 | 990 | Jul |
| Conversion Transducer | 57 IRE 7.S2 | 45 | 990 | Jul |
| Conversion Voltage Gain | 57 IRE 7.S2 | 45 | 990 | Jul |
| Converter | 51 IRE 20.S2 | 39 | 898 | Aug |
| Converter, Facsimile | 56 IRE 9.S1 | 44 | 777 | Jne |
| Converter, Mercury Arc, Pool Cathode | 55 IRE 10.S1 | 43 | 1070 | Sep |
| Converter, Mercury Hydrogen Spark Gap | 55 IRE 10.S1 | 43 | 1070 | Sep |
| Converter Tube | 57 IRE 7.S2 | 45 | 990 | Jul |
| Converter, Quenched Spark Gap | 55 IRE 10.S1 | 43 | 1070 | Sep |
| Copy | 56 IRE 8.S1 | 44 | 1169 | Sep |
| Core | 51 IRE 6.S1 | 39 | 514 | May |
| Core Type Induction Heater or Furnace | 55 IRE 10.S1 | 43 | 1070 | Sep |
| Coreless Type Induction Heater or Furnace | 55 IRE 10.S1 | 43 | 1070 | Sep |
| Corner Reflector | 54 IRE 12.S1 | 43 | 194 | Feb |
| Corrected Compass Course | 54 IRE 12.S1 | 43 | 194 | Feb |
| Corrected Compass Heading | 54 IRE 12.S1 | 43 | 195 | Feb |
| Correction | 56 IRE 8.S1 | 44 | 1169 | Sep |
| Corrective Network (Shaping Network) | 42 IRE 9.S1 | Separate | | |
| Cosecant-Squared Pattern | 54 IRE 12.S1 | 43 | 195 | Feb |
| Count | 57 IRE 7.S2 | 45 | 990 | Jul |
| Count Down | 54 IRE 12.S1 | 43 | 195 | Feb |
| Counter | 56 IRE 8.S1 | 44 | 1169 | Sep |
| Counterpoise | 48 IRE 2,11,15.S1 | Separate | | |
| Counter Ring | 56 IRE 8.S1 | 44 | 1169 | Sep |
| Counter Tube Externally Quenched | 57 IRE 7.S2 | 45 | 990 | Jul |
| Counter Tube, Gas-Filled Radiation | 57 IRE 7.S2 | 45 | 990 | Jul |
| Counter Tube, Gas-Flow | 57 IRE 7.S2 | 45 | 990 | Jul |
| Counter Tube, Geiger-Mueller | 57 IRE 7.S2 | 45 | 990 | Jul |
| Counter-Tube, Proportional | 57 IRE 7.S2 | 45 | 990 | Jul |
| Counter Tube, Self-Quenched | 57 IRE 7.S2 | 45 | 990 | Jul |
| Counting Efficiency | 57 IRE 7.S2 | 45 | 990 | Jul |
| Counting-Rate-vs-Voltage Characteristic | 57 IRE 7.S2 | 45 | 990 | Jul |
| Coupler | 54 IRE 12.S1 | 43 | 195 | Feb |
| Coupling Aperture | 55 IRE 2.S1 | 43 | 1074 | Sep |
| Coupling (Induction Heating Usage) | 55 IRE 10.S1 | 43 | 1070 | Sep |
| Coupling Coefficient, Small Signal | 57 IRE 7.S2 | 45 | 990 | Jul |
| Coupling Loop | 55 IRE 2.S1 | 43 | 1074 | Sep |
| Coupling Probe | 55 IRE 2.S1 | 43 | 1074 | Sep |
| Course | 54 IRE 12.S1 | 43 | 195 | Feb |
| Course Error | 54 IRE 12.S1 | 43 | 195 | Feb |
| Course Error, Indicated | 54 IRE 12.S1 | 43 | 195 | Feb |
| Course Line | 54 IRE 12.S1 | 43 | 195 | Feb |
| Course Line Deviation | 54 IRE 12.S1 | 43 | 195 | Feb |
| Course (Line) Computer | 49 IRE 12.S1 | 37 | 1367 | Dec |
| Course (Line) Selector | 49 IRE 12.S1 | 37 | 1367 | Dec |
| Course Made Good | 54 IRE 12.S1 | 43 | 195 | Feb |
| Course Push (or Pull) | 54 IRE 12.S1 | 43 | 195 | Feb |
| Course Sensitivity | 54 IRE 12.S1 | 43 | 195 | Feb |
| Course Softening | 54 IRE 12.S1 | 43 | 195 | Feb |
| Course Width | 54 IRE 12.S1 | 43 | 195 | Feb |

| | Standard | Proceedings Vol Page Mo |
|---|---|---|
| Deviation from Pulse Flatness | 54 IRE 12.S1 | 43 196 Feb |
| Deviation Distortion | 52 IRE 17.S1 | 40 1682 Dec |
| Deviation Ratio | 53 IRE 11.S1 | 41 613 May |
| Deviation Sensitivity (in FM) | 52 IRE 17.S1 | 40 1682 Dec |
| Deviation Sensitivity (in Navigation Aids) | 54 IRE 12.S1 | 43 196 Feb |
| Deviation Sensitivity Angular | 54 IRE 12.S1 | 43 196 Feb |
| Diagnostic Routine | 56 IRE 8.S1 | 44 1169 Sep |
| Dielectric Antenna | 48 IRE 2,11,15.S1 | Separate |
| Dielectric Dissipation Factor | 55 IRE 10.S1 | 43 1070 Sep |
| Dielectric Heating | 55 IRE 10.S1 | 43 1070 Sep |
| Dielectric Phase Angle | 55 IRE 10.S1 | 43 1070 Sep |
| Dielectric Power Factor | 55 IRE 10.S1 | 43 1070 Sep |
| Dielectric Strength | 55 IRE 10.S1 | 43 1070 Sep |
| Dielectric Waveguide | 53 IRE 2.S1 | 41 1723 Dec |
| Difference Detector | 54 IRE 12.S1 | 43 196 Feb |
| Difference in Depth of Modulation (DDM) | 54 IRE 12.S1 | 43 196 Feb |
| Difference Limen | 51 IRE 6.S1 | 39 515 May |
| Difference Transfer Function | 55 IRE 26.S2 | 44 108 Jan |
| Differential Gain | 55 IRE 23.S1 | 43 620 May |
| Differential Gain Control | 54 IRE 12.S1 | 43 196 Feb |
| Differential Phase | 55 IRE 23.S1 | 43 620 May |
| Differentiating Network | 48 IRE 2,11,15.S1 | Separate |
| Differentiator | 53 IRE 11.S1 | 41 613 May |
| Differentiator (in Electronic Computers) | 56 IRE 8.S1 | 44 1169 Sep |
| Diffracted Wave | 51 IRE 6.S1 | 39 515 May |
| Diffraction | 51 IRE 6.S1 | 39 515 May |
| Diffuse Sound | 51 IRE 6.S1 | 39 515 May |
| Diffuse Transmission Density | 51 IRE 6.S1 | 39 515 May |
| Diffusion Constant | 54 IRE 7.S2 | 42 1506 Oct |
| Diffusion Length | 54 IRE 7.S2 | 42 1506 Oct |
| Digit | 56 IRE 8.S1 | 44 1169 Sep |
| Digit, Binary | 50 IRE 8.S1 | 39 273 Mar |
| Digit, Sign | 50 IRE 8.S1 | 39 273 Mar |
| Digital Computer | 56 IRE 8.S1 | 44 1169 Sep |
| Diode Characteristic | 57 IRE 7.S2 | 45 992 Jul |
| Diode (Electron Tube) | 57 IRE 7.S2 | 45 991 Jul |
| Diode, Semiconductor | 54 IRE 7.S2 | 42 1506 Oct |
| Diplex Radio Transmission | 48 IRE 2,11,15.S1 | Separate |
| Dipole Antenna | 48 IRE 2,11,15.S1 | Separate |
| Direct-Coupled Attenuation | 57 IRE 7.S2 | 45 992 Jul |
| Direct-Current Amplifier | 48 IRE 2,11,15.S1 | Separate |
| Direct Grid Bias | 57 IRE 7.S2 | 45 992 Jul |
| Direct Radiator Loudspeaker | 51 IRE 6.S1 | 39 515 May |
| Direct Recording | 56 IRE 9.S1 | 44 777 Jne |
| Direct Wave | 50 IRE 24.S1 | 38 1265 Nov |
| Directed Reference Flight | 54 IRE 12.S1 | 43 196 Feb |
| Direction | 54 IRE 12.S1 | 43 196 Feb |
| Direction Finder (DF) | 54 IRE 12.S1 | 43 196 Feb |
| Direction Finder Deviation | 54 IRE 12.S1 | 43 196 Feb |
| Direction of Polarization | 50 IRE 24.S1 | 38 1265 Nov |
| Direction of Propagation | 53 IRE 2.S1 | 41 1723 Dec |
| Directional Antenna | 48 IRE 2,11,15.S1 | Separate |
| Directional Coupler | 55 IRE 2.S1 | 43 1074 Sep |
| Directional Gain | 55 IRE 23.S1 | 43 620 May |
| Directional Homing | 54 IRE 12.S1 | 43 196 Feb |
| Directional Microphone | 51 IRE 6.S1 | 39 515 May |
| Directive Gain | 48 IRE 2,11,15.S1 | Separate |
| Directivity | 48 IRE 2,11,15.S1 | Separate |
| Directivity Factor | 51 IRE 6.S1 | 39 515 May |
| Directivity Index | 51 IRE 6.S1 | 39 515 May |
| Directivity Pattern | 51 IRE 6.S1 | 39 515 May |
| Director | 48 IRE 2,11,15.S1 | Separate |

| | Standard | Proceedings Vol Page Mo |
|---|---|---|
| Discharge | 57 IRE 7.S2 | 45 992 Jul |
| Discrete Sentence Intelligibility | 51 IRE 6.S1 | 39 515 May |
| Discrete Word Intelligibility | 51 IRE 6.S1 | 39 516 May |
| Discriminator (General) | 54 IRE 12.S1 | 43 196 Feb |
| Discriminator (Specific) | 53 IRE 11.S1 | 41 613 May |
| Discriminator Constant Delay | 54 IRE 12.S1 | 43 196 Feb |
| Discriminator, Pulse Duration | 54 IRE 12.S1 | 43 196 Feb |
| Dish | 54 IRE 12.S1 | 43 196 Feb |
| Disk Recorder | 51 IRE 6.S1 | 39 516 May |
| Dispatcher | 50 IRE 8.S1 | 39 273 Mar |
| Display | 54 IRE 12.S1 | 43 196 Feb |
| Display Primaries | 55 IRE 22.S1 | 43 745 Jne |
| Dissector Tube | 57 IRE 7.S2 | 45 992 Jul |
| Dissymmetrical Transducer | 51 IRE 20.S2 | 39 898 Aug |
| Distance Mark | 54 IRE 12.S1 | 43 199 Feb |
| Distance Measuring Equipment | 54 IRE 12.S1 | 43 208 Feb |
| Distance Resolution | 54 IRE 12.S1 | 43 199 Feb |
| Distortion | 53 IRE 4.S1 | 42 554 Mar |
| Distortion | 52 IRE 17.S1 | 40 1682 Dec |
| Distortion Barrel | 57 IRE 7.S2 | 45 992 Jul |
| Distortion, Keystone | 57 IRE 7.S2 | 45 992 Jul |
| Distortion, Pincushion | 57 IRE 7.S2 | 45 992 Jul |
| Distortion, S | 57 IRE 7.S2 | 45 992 Jul |
| Distortion, Spiral | 57 IRE 7.S2 | 45 992 Jul |
| Distributed Constant | 53 IRE 2.S1 | 41 1723 Dec |
| Distribution Coefficients | 55 IRE 22.S1 | 43 745 Jne |
| Disturbance | 55 IRE 26.S2 | 44 109 Jan |
| Divergence Loss | 51 IRE 6.S1 | 39 516 May |
| Dividing Network | 51 IRE 6.S1 | 39 516 May |
| Doherty Amplifier | 48 IRE 2,11,15.S1 | Separate |
| Domestic Induction Heater | 55 IRE 10.S1 | 43 1070 Sep |
| Dominant Mode of Propagation | 53 IRE 2.S1 | 41 1723 Dec |
| Dominant Wave | 53 IRE 2.S1 | 41 1723 Dec |
| Dominant Wavelength | 55 IRE 22.S1 | 43 745 Jne |
| Donor | 54 IRE 7.S2 | 42 1506 Oct |
| Doping | 54 IRE 7.S2 | 42 1506 Oct |
| Doping Compensation | 54 IRE 7.S2 | 42 1506 Oct |
| Doppler Effect | 51 IRE 6.S1 | 39 516 May |
| Doppler Shift | 51 IRE 6.S1 | 39 516 May |
| Doppler System | 54 IRE 12.S1 | 43 199 Feb |
| Doppler System, Pulsed | 54 IRE 12.S1 | 43 199 Feb |
| Dot-Sequential | 55 IRE 22.S1 | 53 745 Jne |
| Double-Length Number | 56 IRE 8.S1 | 44 1169 Sep |
| Double Pole-Piece Magnetic Head | 51 IRE 6.S1 | 39 516 May |
| Double-Precision Number | 56 IRE 8.S1 | 44 1169 Sep |
| Double-Sideband Transmitter | 48 IRE 2,11,15.S1 | Separate |
| Downward Modulation | 52 IRE 17.S1 | 40 1682 Dec |
| Drift Angle | 54 IRE 12.S1 | 43 199 Feb |
| Drift Correction Angle | 54 IRE 12.S1 | 43 199 Feb |
| Drift Mobility | 54 IRE 7.S2 | 42 1506 Oct |
| Drift Rate | 57 IRE 7.S2 | 45 992 Jul |
| Drift Space | 57 IRE 7.S2 | 45 992 Jul |
| Drive Pattern | 56 IRE 9.S1 | 44 777 Jne |
| Drive Pin | 51 IRE 6.S1 | 39 516 May |
| Drive-Pin Hole | 51 IRE 6.S1 | 39 516 May |
| Driving-Point Admittance | 57 IRE 7.S2 | 45 992 Jul |
| Driving Signals (in Television) | 55 IRE 23.S1 | 43 620 May |
| Drum Speed | 56 IRE 9.S1 | 44 777 Jne |
| Dual Frequency Induction Heater or Furnace | 55 IRE 10.S1 | 43 1070 Sep |
| Dual Modulation | 56 IRE 9.S1 | 44 777 Jne |
| Dual Networks | 50 IRE 4.S1 | 39 27 Jan |
| Dubbing | 51 IRE 6.S1 | 39 516 May |
| Dummy Antenna | 52 IRE 17.S1 | 40 1682 Dec |
| Dummy Load | 52 IRE 17.S1 | 40 1682 Dec |

| | Standard | Proceedings Vol | Page | Mo |
|---|---|---|---|---|
| Duplex Cavity | 54 IRE 12.S1 | 43 | 199 | Feb |
| Duplex Operation | 48 IRE 2,11,15.S1 | Separate | | |
| Duplexing Assembly | 54 IRE 12.S1 | 43 | 199 | Feb |
| Duty Cycle | 48 IRE 2,11,15.S1 | Separate | | |
| Duty Factor | 48 IRE 2,11,15.S1 | Separate | | |
| Duty Ratio | 54 IRE 12.S1 | 43 | 199 | Feb |
| Dynamic Characteristic | 57 IRE 7.S2 | 45 | 992 | Jul |
| Dynamic Sequential Control | 50 IRE 8.S1 | 39 | 273 | Mar |
| Dynatron Oscillation | 48 IRE 2,11,15.S1 | Separate | | |
| Dynatron Oscillator | 48 IRE 2,11,15.S1 | Separate | | |
| Dynode | 57 IRE 7.S2 | 45 | 992 | Jul |
| Dynode Current | 57 IRE 7.S2 | 45 | 992 | Jul |
| Dynode Spots | 57 IRE 7.S2 | 45 | 992 | Jul |
| **E** | | | | |
| E-Display | 54 IRE 12.S1 | 43 | 199 | Feb |
| E Layer | 50 IRE 24.S1 | 38 | 1265 | Nov |
| E-plane Bend | 55 IRE 2.S1 | 43 | 1074 | Sep |
| E-plane Tee Junction | 55 IRE 2.S1 | 43 | 1074 | Sep |
| E Region | 50 IRE 24.S1 | 38 | 1265 | Nov |
| E-H Tee | 55 IRE 2.S1 | 43 | 1074 | Sep |
| E-H Tuner | 55 IRE 2.S1 | 43 | 1074 | Sep |
| Earphone | 51 IRE 6.S1 | 39 | 516 | May |
| Earphone Coupler | 51 IRE 6.S1 | 39 | 516 | May |
| Eccentric Groove | 51 IRE 6.S1 | 39 | 516 | May |
| Eccentricity | 51 IRE 6.S1 | 39 | 516 | May |
| Echo (in Electroacoustics) | 51 IRE 6.S1 | 39 | 516 | May |
| Echo (in Facsimile) | 56 IRE 9.S1 | 44 | 777 | Jne |
| Echo (in Navigation Aids) | 54 IRE 12.S1 | 43 | 199 | Feb |
| Echo Box | 54 IRE 12.S1 | 43 | 199 | Feb |
| Echo, Second-Time Around | 54 IRE 12.S1 | 43 | 199 | Feb |
| Echo Suppressor | 54 IRE 12.S1 | 43 | 199 | Feb |
| Effective Acoustic Center | 51 IRE 6.S1 | 39 | 516 | May |
| Effective Area | 48 IRE 2,11,15.S1 | Separate | | |
| Effective Band (in Facsimile) | 56 IRE 9.S1 | 44 | 777 | Jne |
| Effective Bandwidth | 48 IRE 2,11,15.S1 | Separate | | |
| Effective Bunching Angle | 57 IRE 7.S2 | 45 | 992 | Jul |
| Effective Height | 48 IRE 2,11,15.S1 | Separate | | |
| Effective Percentage Modulation | 48 IRE 2,11,15.S1 | Separate | | |
| Effective Radius of the Earth | 50 IRE 24.S1 | 38 | 1265 | Nov |
| Effective Sound Pressure | 51 IRE 6.S1 | 39 | 516 | May |
| Efficiency | 57 IRE 7.S2 | 45 | 992 | Jul |
| Efficiency (Radiation Counter Tubes) | 57 IRE 7.S2 | 45 | 992 | Jul |
| Efficiency, Load Circuit | 55 IRE 10.S1 | 43 | 1070 | Sep |
| Efficiency, Over-all Electrical | 55 IRE 10.S1 | 43 | 1070 | Sep |
| Electra | 54 IRE 12.S1 | 43 | 208 | Feb |
| Electric Dipole | 48 IRE 2,11,15.S1 | Separate | | |
| Electric Displacement Density | 50 IRE 24.S1 | 38 | 1265 | Nov |
| Electric Field | 50 IRE 24.S1 | 38 | 1265 | Nov |
| Electric Field Strength | 50 IRE 24.S1 | 38 | 1265 | Nov |
| Electric (Magnetic) Field Strength | 52 IRE 17.S1 | 40 | 1682 | Dec |
| Electric Field Vector | 53 IRE 2.S1 | 41 | 1723 | Dec |
| Electric Flux Density | 50 IRE 24.S1 | 38 | 1265 | Nov |
| Electric Transducer | 51 IRE 20.S2 | 39 | 898 | Aug |
| Electrical Distance | 54 IRE 12.S1 | 43 | 199 | Feb |
| Electrical Function Switch | 50 IRE 8.S1 | 39 | 273 | Mar |
| Electrical Length | 53 IRE 2.S1 | 41 | 1723 | Dec |
| Electrical Length | 50 IRE 24.S1 | 38 | 1265 | Nov |
| Electrical Noise | 48 IRE 2,11,15.S1 | Separate | | |
| Electroacoustic Transducer | 51 IRE 6.S1 | 39 | 516 | May |
| Electroacoustic Transducer | 51 IRE 20.S2 | 39 | 898 | Aug |
| Electroacoustical Reciprocity Theorem | 51 IRE 6.S1 | 39 | 516 | May |
| Electrochemical Recording | 56 IRE 9.S1 | 44 | 777 | Jne |
| Electrode (Electron Tubes) | 57 IRE 7.S2 | 45 | 992 | Jul |
| Electrode (Semiconductor) | 54 IRE 7.S2 | 42 | 1506 | Oct |
| Electrode Admittance | 57 IRE 7.S2 | 45 | 992 | Jul |
| Electrode Capacitance | 57 IRE 7.S2 | 45 | 993 | Jul |
| Electrode Characteristic | 57 IRE 7.S2 | 45 | 993 | Jul |
| Electrode Conductance | 57 IRE 7.S2 | 45 | 993 | Jul |
| Electrode Current | 57 IRE 7.S2 | 45 | 993 | Jul |
| Electrode-Current Averaging Time | 57 IRE 7.S2 | 45 | 993 | Jul |
| Electrode Dark Current | 57 IRE 7.S2 | 45 | 993 | Jul |
| Electrode Dissipation | 57 IRE 7.S2 | 45 | 993 | Jul |
| Electrode Impedance | 57 IRE 7.S2 | 45 | 993 | Jul |
| Electrode Resistance | 57 IRE 7.S2 | 45 | 993 | Jul |
| Electrode Voltage | 57 IRE 7.S2 | 45 | 993 | Jul |
| Electrolytic Recording | 56 IRE 9.S1 | 44 | 777 | Jne |
| Electromagnetic Wave | 50 IRE 24.S1 | 38 | 1265 | Nov |
| Electromagnetic Wave | 53 IRE 2.S1 | 41 | 1723 | Dec |
| Electromechanical Recording | 56 IRE 9.S1 | 44 | 777 | Jne |
| Electromechanical Transducer | 51 IRE 6.S1 | 39 | 517 | May |
| Electromechanical Transducer | 51 IRE 20.S2 | 39 | 898 | Aug |
| Electrometer Tube | 57 IRE 7.S2 | 45 | 993 | Jul |
| Electron-Beam Tube | 57 IRE 7.S2 | 45 | 993 | Jul |
| Electron-Coupled Oscillator | 48 IRE 2,11,15.S1 | Separate | | |
| Electron Device | 57 IRE 7.S2 | 45 | 993 | Jul |
| Electron Emission | 57 IRE 7.S2 | 45 | 993 | Jul |
| Electron Gun | 57 IRE 7.S2 | 45 | 993 | Jul |
| Electron-Gun Density Multiplication | 57 IRE 7.S2 | 45 | 993 | Jul |
| Electron Multiplier | 57 IRE 7.S2 | 45 | 993 | Jul |
| Electron-Stream Potential | 57 IRE 7.S2 | 45 | 993 | Jul |
| Electron-Stream Transmission Efficiency | 56 IRE 7.S1 | 44 | 347 | Mar |
| Electron Tube | 57 IRE 7.S2 | 45 | 993 | Jul |
| Electron-Wave Tube | 57 IRE 7.S2 | 45 | 993 | Jul |
| Electrons, Conduction | 54 IRE 7.S2 | 42 | 1506 | Oct |
| Electronic | 57 IRE 7.S2 | 45 | 993 | Jul |
| Electronic Efficiency | 57 IRE 7.S2 | 45 | 993 | Jul |
| Electronic Gap Admittance | 57 IRE 7.S2 | 45 | 993 | Jul |
| Electronic Keying | 48 IRE 2,11,15.S1 | Separate | | |
| Electronic Line Scanning | 56 IRE 9.S1 | 44 | 777 | Jne |
| Electronic Microphone | 51 IRE 6.S1 | 39 | 517 | May |
| Electronic Raster Scanning | 56 IRE 9.S1 | 44 | 777 | Jne |
| Electronics | 57 IRE 7.S2 | 45 | 993 | Jul |
| Electrophonic Effect | 51 IRE 6.S1 | 39 | 517 | May |
| Electrostatic Actuator | 51 IRE 6.S1 | 39 | 517 | May |
| Electrostatic Focusing | 57 IRE 7.S2 | 45 | 993 | Jul |
| Electrostatic Loudspeaker | 51 IRE 6.S1 | 39 | 517 | May |
| Electrostatic Memory | 50 IRE 8.S1 | 39 | 273 | Mar |
| Electrostatic Memory Tube | 50 IRE 8.S1 | 39 | 273 | Mar |
| Electrostatic Microphone | 51 IRE 6.S1 | 39 | 517 | May |
| Electrostatic Recording | 56 IRE 9.S1 | 44 | 777 | Jne |
| Electrothermal Recording | 56 IRE 9.S1 | 44 | 777 | Jne |
| Element (of a Circuit) | 50 IRE 4.S1 | 39 | 27 | Jan |
| Element (Semiconductor) | 54 IRE 7.S2 | 42 | 1506 | Oct |
| Element (of a Tube) | 57 IRE 7.S2 | 45 | 993 | Jul |
| Elemental Area | 56 IRE 9.S1 | 44 | 777 | Jne |
| Elements of a Fix | 54 IRE 12.S1 | 43 | 199 | Feb |
| Elliptically Polarized Wave | 53 IRE 2.S1 | 41 | 1723 | Dec |
| Ellipticity | 53 IRE 2.S1 | 41 | 1723 | Dec |
| Elongation | 42 IRE 9.S1 | Separate | | |
| Embossing Stylus | 51 IRE 6.S1 | 39 | 517 | May |
| Emission | 57 IRE 7.S2 | 45 | 993 | Jul |
| Emission Characteristic | 57 IRE 7.S2 | 45 | 994 | Jul |
| Emitter, Majority | 54 IRE 7.S2 | 42 | 1506 | Oct |
| Emitter, Minority | 54 IRE 7.S2 | 42 | 1506 | Oct |
| Enabling Pulse | 54 IRE 12.S1 | 43 | 199 | Feb |
| Encoder | 56 IRE 8.S1 | 44 | 1169 | Sep |
| End-Around Carry | 56 IRE 8.S1 | 44 | 1169 | Sep |
| End-Fire Array | 48 IRE 2,11,15.S1 | Separate | | |
| End-of-Copy Signal | 56 IRE 9.S1 | 44 | 778 | Jne |

| | Standard | Proceedings Vol Page Mo |
|---|---|---|
| End Shield (Magnetrons) | 57 IRE 7.S2 | 45 994 Jul |
| Energy Gap | 54 IRE 7.S2 | 42 1506 Oct |
| Envelope Delay | 56 IRE 9.S1 | 44 778 Jne |
| Envelope Delay | 50 IRE 24.S1 | 38 1265 Nov |
| Envelope Delay Distortion | 56 IRE 9.S1 | 44 778 Jne |
| Equal-Energy Source | 55 IRE 22.S1 | 43 745 Jne |
| Equalizing Pulses | 55 IRE 23.S1 | 43 620 May |
| Equally Tempered Scale | 51 IRE 6.S1 | 39 517 May |
| Equation Solver | 50 IRE 8.S1 | 39 273 Mar |
| Equiphase Surface | 50 IRE 24.S1 | 38 1265 Nov |
| Equiphase Zone | 54 IRE 12.S1 | 43 199 Feb |
| Equipotential Cathode | 57 IRE 7.S2 | 45 994 Jul |
| Equisignal Localizer | 54 IRE 12.S1 | 43 199 Feb |
| Equisignal Zone | 49 IRE 12.S1 | 37 1368 Dec |
| Equivalent Conductance | 57 IRE 7.S2 | 45 994 Jul |
| Equivalent Dark-Current Input | 57 IRE 7.S2 | 45 994 Jul |
| Equivalent Diode | 57 IRE 7.S2 | 45 994 Jul |
| Equivalent Noise Conductance | 57 IRE 7.S2 | 45 994 Jul |
| Equivalent Noise Current | 57 IRE 7.S2 | 45 994 Jul |
| Equivalent Noise Resistance | 57 IRE 7.S2 | 45 994 Jul |
| Erase | 57 IRE 7.S2 | 45 994 Jul |
| Erasing Head | 51 IRE 6.S1 | 39 517 May |
| Erasing Speed (in Charge-Storage Tubes) | 57 IRE 7.S2 | 45 994 Jul |
| Error | 56 IRE 8.S1 | 44 1169 Sep |
| Error-Detecting Code | 56 IRE 8.S1 | 44 1169 Sep |
| Error, Height | 54 IRE 12.S1 | 43 199 Feb |
| Error, Instrumental | 54 IRE 12.S1 | 43 199 Feb |
| Error, Round-Off | 50 IRE 8.S1 | 39 273 Mar |
| Error, Sky | 54 IRE 12.S1 | 43 199 Feb |
| Error, Truncation | 50 IRE 8.S1 | 39 273 Mar |
| Eureka | 54 IRE 12.S1 | 43 208 Feb |
| Excess-Three Code | 56 IRE 8.S1 | 44 1169 Sep |
| Excitation (Drive) | 48 IRE 2,11,15.S2 | Separate |
| Excitation Purity | 55 IRE 22.S1 | 43 745 Jne |
| Excited Field Loudspeaker | 51 IRE 6.S1 | 39 517 May |
| Exciter | 48 IRE 2,11,15.S1 | Separate |
| Expansion | 53 IRE 11.S1 | 41 613 May |
| Exponential Flare-Out | 54 IRE 12.S1 | 43 199 Feb |
| Exponential Horn | 51 IRE 6.S1 | 39 517 May |
| Exponential Transmission | 53 IRE 2.S1 | 41 1723 Dec |
| External Termination | 57 IRE 7.S2 | 45 994 Jul |
| Externally Quenched Counter Tube | 57 IRE 7.S2 | 45 994 Jul |
| Extract | 56 IRE 8.S1 | 44 1169 Sep |
| Extract Instruction | 50 IRE 8.S1 | 39 273 Mar |
| Extraordinary-Wave Component | 50 IRE 24.S1 | 38 1266 Nov |
| Extrinsic Properties | 54 IRE 7.S2 | 42 1506 Oct |

**F**

| | | |
|---|---|---|
| F-Display | 54 IRE 12.S1 | 43 200 Feb |
| F Layer | 50 IRE 24.S1 | 38 1266 Nov |
| F Region | 50 IRE 24.S1 | 38 1266 Nov |
| FS to AM Converter | 56 IRE 9.S1 | 44 778 Jne |
| FTC | 54 IRE 12.S1 | 43 200 Feb |
| Facsimile (in Electrical Communications) | 56 IRE 9.S1 | 44 778 Jne |
| Facsimile Receiver | 42 IRE 9.S1 | Separate |
| Facsimile Recorder | 42 IRE 9.S1 | Separate |
| Facsimile Signal (Picture Signal) | 56 IRE 9.S1 | 44 778 Jne |
| Facsimile-Signal Level | 56 IRE 9.S1 | 44 778 Jne |
| Facsimile System | 56 IRE 9.S1 | 44 778 Jne |
| Facsimile Transient | 56 IRE 9.S1 | 44 778 Jne |
| Facsimile Transmission | 56 IRE 9.S1 | 44 778 Jne |
| Facsimile Transmitter | 42 IRE 9.S1 | Separate |
| Factor | 57 IRE 7.S2 | 45 994 Jul |
| **Fading** | 50 IRE 24.S1 | 38 1266 Nov |
| False Course | 54 IRE 12.S1 | 43 199 Feb |
| Fan Beam | 54 IRE 12.S1 | 43 200 Feb |
| Fan Marker | 54 IRE 12.S1 | 43 208 Feb |
| Fanned-Beam Antenna | 48 IRE 2,11,15.S1 | Separate |
| Fast Groove | 51 IRE 6.S1 | 39 517 May |
| Fast-Time-Constant Circuit | 54 IRE 12.S1 | 43 200 Feb |
| Fault Electrode Current | 57 IRE 7.S2 | 45 994 Jul |
| Feedback | 48 IRE 2,11,15.S1 | Separate |
| Feedback Control Loop | 55 IRE 26.S2 | 44 108 Jan |
| Feedback Control System | 55 IRE 26.S2 | 44 108 Jan |
| Feedback Control System Linear | 56 IRE 26.S2 | 44 108 Jan |
| Feedback Control System Nonlinear | 56 IRE 26.S2 | 44 109 Jan |
| Feedback Control System, Quasi-Linear | 56 IRE 26.S2 | 44 109 Jan |
| Feedback Oscillator | 48 IRE 2,11,15.S1 | Separate |
| Feedback Path | 56 IRE 26.S2 | 44 108 Jan |
| Feedback Regulator | 56 IRE 26.S2 | 44 109 Jan |
| Feedback Transfer Function | 56 IRE 26.S2 | 44 108 Jan |
| Fermi Level | 54 IRE 7.S2 | 42 1506 Oct |
| Fidelity | 52 IRE 17.S1 | 40 1682 Dec |
| Fidelity | 48 IRE 2,11,15.S1 | Separate |
| Field (in Television) | 55 IRE 23.S1 | 43 620 May |
| Field Emission | 57 IRE 7.S2 | 45 994 Jul |
| Field-Enhanced Photoelectric Emission | 57 IRE 7.S2 | 45 994 Jul |
| Field-Enhanced Secondary Emission | 57 IRE 7.S2 | 45 994 Jul |
| Field-Free Emission Current | 57 IRE 7.S2 | 45 994 Jul |
| Field Frequency | 55 IRE 23.S1 | 43 620 May |
| Field Sequential | 55 IRE 22.S1 | 43 746 Jne |
| Field Strength, Electric or Magnetic | 52 IRE 17.S1 | 40 1682 Dec |
| Field Strength Meter | 55 IRE 10.S1 | 43 1070 Sep |
| Filament | 57 IRE 7.S2 | 45 994 Jul |
| Filament Current | 50 IRE 7.S1 | 38 433 Apr |
| Filament Voltage | 50 IRE 7.S1 | 38 433 Apr |
| Filler | 51 IRE 6.S1 | 39 517 May |
| Fine Chrominance Primary | 55 IRE 22.S1 | 43 746 Jne |
| Fired Tube | 57 IRE 7.S2 | 45 994 Jul |
| Firing Time, High-Level | 57 IRE 7.S2 | 45 995 Jul |
| Fishbone Antenna | 48 IRE 2,11,15.S1 | Separate |
| Fix | 54 IRE 12.S1 | 43 200 Feb |
| Fixed-Frequency Transmitter | 48 IRE 2,11,15.S1 | Separate |
| Fixed-Point System | 56 IRE 8.S1 | 44 1169 Sep |
| Fixed Transmitter | 48 IRE 2,11,15.S1 | Separate |
| Flag Alarm | 54 IRE 12.S1 | 43 200 Feb |
| Flare-Out | 54 IRE 12.S1 | 43 200 Feb |
| Flat Leakage Power | 57 IRE 7.S2 | 45 995 Jul |
| Flat Spot | 54 IRE 12.S1 | 43 200 Feb |
| Flection-Point Emission Current | 57 IRE 7.S2 | 45 995 Jul |
| Flicker | 55 IRE 22.S1 | 43 746 Jne |
| Flight Path | 54 IRE 12.S1 | 43 200 Feb |
| Flight Path Computer | 54 IRE 12.S1 | 43 200 Feb |
| Flight Path Deviation | 54 IRE 12.S1 | 43 200 Feb |
| Flight-Path-Deviation Indicator | 54 IRE 12.S1 | 43 200 Feb |
| Flight-Path-Reference Flight | 54 IRE 12.S1 | 43 200 Feb |
| Flight Track | 54 IRE 12.S1 | 43 200 Feb |
| Flip-Flop | 56 IRE 8.S1 | 44 1169 Sep |
| Floating-Point System | 56 IRE 8.S1 | 44 1169 Sep |
| Flood Projection | 56 IRE 9.S1 | 44 778 Jne |
| Flow Diagram (in Electronic Computers) | 56 IRE 8.S1 | 44 1169 Sep |
| Flowed Wax | 51 IRE 6.S1 | 39 517 May |
| Flutter | 52 IRE 17.S1 | 40 1683 Dec |
| **Flutter Echo** | 51 IRE 6.S1 | 39 517 May |

| | Standard | Proceedings Vol | Page | Mo |
|---|---|---|---|---|
| Gill-Morrell Oscillator | 48 IRE 2,11,15.S1 | Separate | | |
| Glide-Path | 54 IRE 12.S1 | 43 | 200 | Feb |
| Glide-Slope | 54 IRE 12.S1 | 43 | 200 | Feb |
| Glide-Slope Angle | 54 IRE 12.S1 | 43 | 200 | Feb |
| Glide-Slope Deviation | 54 IRE 12.S1 | 43 | 200 | Feb |
| Glide-Slope Facility | 54 IRE 12.S1 | 43 | 200 | Feb |
| Glide-Slope Sector | 54 IRE 12.S1 | 43 | 200 | Feb |
| Glow Discharge | 57 IRE 7.S2 | 45 | 996 | Jul |
| Glow-Discharge Cold-Cathode Tube | 50 IRE 7.S1 | 38 | 434 | Apr |
| Glow-Discharge Tube | 57 IRE 7.S2 | 45 | 996 | Jul |
| Glue Line Heating | 55 IRE 10.S1 | 43 | 1070 | Sep |
| Gradient Microphone | 51 IRE 6.S1 | 39 | 518 | May |
| Grain | 51 IRE 6.S1 | 39 | 518 | May |
| Graininess | 51 IRE 6.S1 | 39 | 518 | May |
| Grass | 54 IRE 12.S1 | 43 | 200 | Feb |
| Grating Reflector | 48 IRE 2,11,15.S1 | Separate | | |
| Grid (of a Tube) | 57 IRE 7.S2 | 45 | 996 | Jul |
| Grid Bearing | 49 IRE 12.S1 | 37 | 1368 | Dec |
| Grid Bias | 57 IRE 7.S2 | 45 | 996 | Jul |
| Grid Characteristic | 57 IRE 7.S2 | 45 | 996 | Jul |
| Grid-Controlled Mercury-Arc Rectifier | 48 IRE 2,11,15.S1 | Separate | | |
| Grid Course | 49 IRE 12.S1 | 37 | 1368 | Dec |
| Grid Current | 57 IRE 7.S2 | 45 | 996 | Jul |
| Grid-Drive Characteristic | 57 IRE 7.S2 | 45 | 996 | Jul |
| Grid Driving Power | 57 IRE 7.S2 | 45 | 996 | Jul |
| Grid Emission | 57 IRE 7.S2 | 45 | 996 | Jul |
| Grid Heading | 49 IRE 12.S1 | 37 | 1368 | Dec |
| Grid Modulation | 48 IRE 2,11,15.S1 | Separate | | |
| Grid Neutralization | 48 IRE 2,11,15.S1 | Separate | | |
| Grid North | 49 IRE 12.S1 | 37 | 1368 | Dec |
| Grid Pulse Modulation | 48 IRE 2,11,15.S1 | Separate | | |
| Grid Voltage | 57 IRE 7.S2 | 45 | 996 | Jul |
| Groove | 51 IRE 6.S1 | 39 | 518 | May |
| Groove Angle | 51 IRE 6.S1 | 39 | 518 | May |
| Groove Shape | 51 IRE 6.S1 | 39 | 518 | May |
| Groove Speed | 51 IRE 6.S1 | 39 | 518 | May |
| Ground-Controlled Approach | 49 IRE 12.S1 | 37 | 1368 | Dec |
| Ground Clutter | 54 IRE 12.S1 | 43 | 200 | Feb |
| Ground Distance | 54 IRE 12.S1 | 43 | 200 | Feb |
| Ground Equalizer Inductors | 48 IRE 2,11,15.S1 | Separate | | |
| Ground Noise | 51 IRE 6.S1 | 39 | 519 | May |
| Ground-Position Indicator | 49 IRE 12.S1 | 37 | 1368 | Dec |
| Ground Return (Radar) | 54 IRE 12.S1 | 43 | 200 | Feb |
| Ground Speed | 54 IRE 12.S1 | 43 | 200 | Feb |
| Ground Surveillance Radar | 49 IRE 12.S1 | 37 | 1368 | Dec |
| Ground System of an Antenna | 48 IRE 2,11,15.S1 | Separate | | |
| Ground Wave | 50 IRE 24.S1 | 38 | 1266 | Nov |
| Grounded-Cathode Amplifier | 48 IRE 2,11,15.S1 | Separate | | |
| Grounded-Grid Amplifier | 48 IRE 2,11,15.S1 | Separate | | |
| Grounded-Plate Amplifier | 48 IRE 2,11,15.S1 | Separate | | |
| Grouping (in Recording) | 51 IRE 6.S1 | 39 | 519 | May |
| Grouping (in Facsimile) | 56 IRE 9.S1 | 44 | 778 | Jne |
| Group Velocity | 50 IRE 24.S1 | 38 | 1266 | Nov |
| Guard Circle | 51 IRE 6.S1 | 39 | 519 | May |
| Guided Wave | 50 IRE 24.S1 | 38 | 1266 | Nov |

## H

| | | | | |
|---|---|---|---|---|
| H | 54 IRE 12.S1 | 43 | 208 | Feb |
| H and D Curve | 51 IRE 6.S1 | 39 | 519 | May |
| H-Display | 54 IRE 12.S1 | 43 | 201 | Feb |
| H Network | 50 IRE 4.S1 | 39 | 27 | Jan |
| H-plane Bend | 55 IRE 2.S1 | 43 | 1074 | Sep |
| H-plane Tee Junction | 55 IRE 2.S1 | 43 | 1074 | Sep |
| Half Adder | 56 IRE 8.S1 | 44 | 1170 | Sep |
| Half-Power Width of a Radiation Lobe | 48 IRE 2,11,15.S1 | Separate | | |
| Halftone Characteristic | 56 IRE 9.S1 | 44 | 778 | Jne |
| Hall Constant | 54 IRE 7.S2 | 42 | 1506 | Oct |
| Harmonic | 53 IRE 4.S1 | 42 | 554 | Mar |
| Harmonic Conversion Transducer | 51 IRE 20.S2 | 39 | 898 | Aug |
| Harmonic Conversion Transducer | 57 IRE 7.S2 | 45 | 996 | Jul |
| Harmonic Distortion | 53 IRE 4.S1 | 42 | 554 | Mar |
| Harmonic Distortion | 52 IRE 17.S1 | 40 | 1683 | Dec |
| Harmonic Leakage Power | 57 IRE 7.S2 | 45 | 996 | Jul |
| Harmonic Series of Sounds | 51 IRE 6.S1 | 39 | 519 | May |
| Hartley Oscillator | 48 IRE 2,11,15.S1 | Separate | | |
| Heading | 54 IRE 12.S1 | 43 | 201 | Feb |
| Hearing Loss | 51 IRE 6.S1 | 39 | 519 | May |
| Hearing Loss for Speech | 51 IRE 6.S1 | 39 | 519 | May |
| Heat Loss | 53 IRE 2.S1 | 41 | 1723 | Dec |
| Heater | 57 IRE 7.S2 | 45 | 996 | Jul |
| Heater Coil | 55 IRE 10.S1 | 43 | 1070 | Sep |
| Heater Current | 50 IRE 7.S1 | 38 | 434 | Apr |
| Heater Voltage | 50 IRE 7.S1 | 38 | 434 | Apr |
| Heater Warm-Up Time | 57 IRE 7.S2 | 45 | 996 | Jul |
| Heating Pattern | 55 IRE 10.S1 | 43 | 1070 | Sep |
| Heating Station | 55 IRE 10.S1 | 43 | 1070 | Sep |
| Heating Time | 57 IRE 7.S2 | 45 | 997 | Jul |
| Height Error | 54 IRE 12.S1 | 43 | 201 | Feb |
| Height Error, Ionospheric | 54 IRE 12.S1 | 43 | 201 | Feb |
| Height Markers (Radar) | 54 IRE 12.S1 | 43 | 201 | Feb |
| Heptode | 57 IRE 7.S2 | 45 | 997 | Jul |
| Heterodyne Conversion Transducer | 57 IRE 7.S2 | 45 | 997 | Jul |
| Heterodyne Conversion Transducer (Converter) | 51 IRE 20.S2 | 39 | 898 | Aug |
| Hexadecimal | 56 IRE 8.S1 | 44 | 1170 | Sep |
| Hexode | 57 IRE 7.S2 | 45 | 997 | Jul |
| High-Frequency Induction Heater or Furnace | 55 IRE 10.S1 | 43 | 1070 | Sep |
| High-Level Firing Time | 57 IRE 7.S2 | 45 | 997 | Jul |
| High-Level Modulation | 48 IRE 2,11,15.S1 | Separate | | |
| High-Level Radio-Frequency Signal | 57 IRE 7.S2 | 45 | 997 | Jul |
| High-Level VSWR | 57 IRE 7.S2 | 45 | 997 | Jul |
| High-Speed Carry | 56 IRE 8.S1 | 44 | 1170 | Sep |
| High-Velocity Scanning | 57 IRE 7.S2 | 45 | 997 | Jul |
| Hold | 57 IRE 7.S2 | 45 | 997 | Jul |
| Holding Beam | 50 IRE 8.S1 | 39 | 274 | Mar |
| Hole | 54 IRE 7.S2 | 42 | 1506 | Oct |
| Homing | 54 IRE 12.S1 | 43 | 201 | Feb |
| Horizontal Ring Induction Furnace | 55 IRE 10.S1 | 43 | 1071 | Sep |
| Horizontally Polarized Wave | 50 IRE 24.S1 | 38 | 1266 | Nov |
| Horn Loudspeaker | 51 IRE 6.S1 | 39 | 519 | May |
| Horn Mouth | 51 IRE 6.S1 | 39 | 519 | May |
| Horn Radiator | 48 IRE 2,11,15.S1 | Separate | | |
| Horn Throat | 51 IRE 6.S1 | 39 | 519 | May |
| Hot Cathode | 57 IRE 7.S2 | 45 | 997 | Jul |
| Hot-Cathode Tube | 57 IRE 7.S2 | 45 | 997 | Jul |
| Hot-Wire Microphone | 51 IRE 6.S1 | 39 | 519 | May |
| Hue | 55 IRE 22.S1 | 43 | 746 | Jne |
| Hum | 52 IRE 17.S1 | 40 | 1683 | Dec |
| Hum Modulation | 52 IRE 17.S1 | 40 | 1683 | Dec |
| Hybrid Electromagnetic Wave | 53 IRE 2.S1 | 41 | 1727 | Dec |
| Hybrid Junction | 55 IRE 2.S1 | 43 | 1074 | Sep |
| Hybrid Tee | 55 IRE 2.S1 | 43 | 1074 | Sep |
| Hydrophone | 51 IRE 6.S1 | 39 | 519 | May |
| Hyperbolic Flare-Out | 54 IRE 12.S1 | 43 | 201 | Feb |
| Hysteresis (of an Oscillation) | 57 IRE 7.S2 | 45 | 997 | Jul |
| Hysteresis (Radiation-Counter) | 57 IRE 7.S2 | 45 | 997 | Jul |
| Hysteresis Heater | 55 IRE 10.S1 | 43 | 1071 | Sep |

| | Standard | Proceedings Vol Page Mo |
|---|---|---|
| Ionization Time | 57 IRE 7.S2 | 45 998 Jul |
| Ionizing Event | 57 IRE 7.S2 | 45 998 Jul |
| Ionosphere | 50 IRE 24.S1 | 38 1266 Nov |
| Ionospheric Error | 54 IRE 12.S1 | 43 201 Feb |
| Ionospheric Height Error | 54 IRE 12.S1 | 43 201 Feb |
| Ionospheric Wave | 50 IRE 24.S1 | 38 1266 Nov |
| Ion Spot | 50 IRE 7.S1 | 38 434 Apr |
| Ion Spot (Camera Tube) | 57 IRE 7.S2 | 45 998 Jul |
| Ion Spot (Picture Tube) | 57 IRE 7.S2 | 45 998 Jul |
| Iris | 55 IRE 2.S1 | 43 1074 Sep |
| **J** | | |
| J Antenna | 48 IRE 2,11,15.S1 | Separate |
| J-Display | 54 IRE 12.S1 | 43 201 Feb |
| Jitter | 54 IRE 12.S1 | 43 201 Feb |
| Jitter (in Facsimile) | 56 IRE 9.S1 | 44 778 Jne |
| Johnson Noise | 57 IRE 7.S2 | 45 998 Jul |
| Jump | 56 IRE 8.S1 | 44 1170 Sep |
| Junction | 54 IRE 7.S2 | 42 1507 Oct |
| Junction, Alloy | 54 IRE 7.S2 | 42 1507 Oct |
| Junction, Collector | 54 IRE 7.S2 | 42 1507 Oct |
| Junction, Diffused | 54 IRE 7.S2 | 42 1507 Oct |
| Junction, Doped | 54 IRE 7.S2 | 42 1507 Oct |
| Junction Emitter | 54 IRE 7.S2 | 42 1507 Oct |
| Junction, Fused | 54 IRE 7.S2 | 42 1507 Oct |
| Junction, Grown | 54 IRE 7.S2 | 42 1507 Oct |
| Junction, *N-N* | 54 IRE 7.S2 | 42 1507 Oct |
| Junction, *P-N* | 54 IRE 7.S2 | 42 1507 Oct |
| Junction, *P-P* | 54 IRE 7.S2 | 42 1507 Oct |
| Junction Point | 50 IRE 4.S1 | 38 27 Jan |
| Junction, Rate-Grown | 54 IRE 7.S2 | 42 1507 Oct |
| Just Scale | 51 IRE 6.S1 | 39 519 May |
| **K** | | |
| K-Display | 54 IRE 12.S1 | 43 201 Feb |
| Keep-Alive | 57 IRE 7.S2 | 45 998 Jul |
| Keep-Alive Circuit | 54 IRE 12.S1 | 43 201 Feb |
| Kendall Effect | 56 IRE 9.S1 | 44 778 Jne |
| Keyer | 48 IRE 2,11,15.S1 | Separate |
| Keying | 53 IRE 11.S1 | 41 613 May |
| Kink | 54 IRE 12.S1 | 43 201 Feb |
| Knee of Transfer Characteristic | 57 IRE 7.S2 | 45 998 Jul |
| **L** | | |
| LANAC (Laminar Navigation, Anti-Collision) | 54 IRE 12.S1 | 43 208 Feb |
| L-Display | 54 IRE 12.S1 | 43 201 Feb |
| L Network | 50 IRE 4.S1 | 38 27 Jan |
| LOP | 54 IRE 12.S1 | 43 202 Feb |
| Lacquer Disks | 51 IRE 6.S1 | 39 520 May |
| Lacquer Original | 51 IRE 6.S1 | 39 520 May |
| Lacquer Recording | 51 IRE 6.S1 | 39 520 May |
| Ladder Network | 50 IRE 4.S1 | 38 28 Jan |
| Lag | 57 IRE 7.S2 | 45 998 Jul |
| Lambert | 55 IRE 22.S1 | 43 746 Jne |
| Laminated Record | 51 IRE 6.S1 | 39 520 May |
| Landing, Poor | 57 IRE 7.S2 | 45 998 Jul |
| Land | 51 IRE 6.S1 | 39 520 May |
| Lane | 54 IRE 12.S1 | 43 201 Feb |
| Language | 56 IRE 8.S1 | 44 1170 Sep |
| Lapel Microphone | 51 IRE 6.S1 | 39 520 May |
| Lateral Recording | 51 IRE 6.S1 | 39 520 May |
| Lattice | 54 IRE 12.S1 | 43 201 Feb |
| Lattice Network | 50 IRE 4.S1 | 38 28 Jan |
| Lead-In Groove | 51 IRE 6.S1 | 39 520 May |
| Lead-Out Groove | 51 IRE 6.S1 | 39 520 May |
| Lead-Over Groove | 51 IRE 6.S1 | 39 520 May |
| Leader Cable | 54 IRE 12.S1 | 43 201 Feb |
| Leading Edge | 55 IRE 23.S1 | 43 620 May |
| Leading Edge Pulse Time | 51 IRE 20.S1 | 39 625 Jne |
| Leading Edge Pulse Time | 55 IRE 23.S1 | 43 621 May |
| Leakage Power | 57 IRE 7.S2 | 45 998 Jul |
| Leakage Radiation | 48 IRE 2,11,15.S1 | Separate |
| Left-Handed Polarized Wave | 50 IRE 24.S1 | 38 1266 Nov |
| Length of Scanning Line | 42 IRE 9.S1 | Separate |
| Lens | 48 IRE 2,11,15.S1 | Separate |
| Level (in Audio) | 54 IRE 3.S1 | 42 1111 Jul |
| Level (in Charge-Storage Tubes) | 57 IRE 7.S2 | 45 998 Jul |
| Level (in Television) | 55 IRE 23.S1 | 43 621 May |
| Level Above Threshold | 51 IRE 6.S1 | 39 520 May |
| Lifetime, Volume | 54 IRE 7.S2 | 42 1507 Oct |
| Light | 55 IRE 22.S1 | 43 746 Jne |
| Light-Beam Pickup | 51 IRE 6.S1 | 39 520 May |
| Light Carrier Injection | 56 IRE 9.S1 | 44 778 Jne |
| Light-Microsecond | 54 IRE 12.S1 | 43 201 Feb |
| Light Modulation | 42 IRE 9.S1 | Separate |
| Light Modulator | 51 IRE 6.S1 | 39 520 May |
| Light Value | 51 IRE 6.S1 | 39 520 May |
| Limited Signal | 54 IRE 12.S1 | 43 201 Feb |
| Limited Stability | 53 IRE 4.S1 | 42 555 Mar |
| Limiter | 48 IRE 2,11,15.S1 | Separate |
| Limiter | 52 IRE 17.S1 | 40 1683 Dec |
| Limiting | 52 IRE 17.S1 | 40 1683 Dec |
| Line Frequency | 55 IRE 23.S1 | 43 621 May |
| Line Hydrophone | 51 IRE 6.S1 | 39 520 May |
| Line Microphone | 51 IRE 6.S1 | 39 520 May |
| Line of Position | 54 IRE 12.S1 | 43 202 Feb |
| Line or Trace | 57 IRE 7.S2 | 45 998 Jul |
| Line Stretcher | 55 IRE 2.S1 | 43 1074 Sep |
| Linear Array | 48 IRE 2,11,15.S1 | Separate |
| Linear Power Amplifier | 48 IRE 2,11,15.S1 | Separate |
| Linear Rectifier | 48 IRE 2,11,15.S1 | Separate |
| Linear Transducer | 51 IRE 20.S2 | 39 898 Aug |
| Linear Varying-Parameter Network | 53 IRE 4.S1 | 42 555 Mar |
| Linearity Region | 54 IRE 12.S1 | 43 202 Feb |
| Linearly Polarized Wave | 50 IRE 24.S1 | 38 1266 Nov |
| Lin-Log Receiver | 54 IRE 12.S1 | 43 202 Feb |
| Lip Microphone | 51 IRE 6.S1 | 39 520 May |
| Live Room | 51 IRE 6.S1 | 39 520 May |
| Load (General) | 54 IRE 3.S1 | 42 1111 Jul |
| Load (Induction Heating) | 55 IRE 10.S1 | 43 1071 Sep |
| Load (of a Tube) | 57 IRE 7.S2 | 45 999 Jul |
| Load (Dynamic) Characteristic | 57 IRE 7.S2 | 45 999 Jul |
| Load Circuit (Induction Heating) | 55 IRE 10.S1 | 43 1071 Sep |
| Load Circuit (in Transmitters) | 48 IRE 2,11,15.S1 | Separate |
| Load-Circuit Efficiency (Induction Heating) | 55 IRE 10.S1 | 43 1071 Sep |
| Load-Circuit Efficiency | 48 IRE 2,11,15.S1 | Separate |
| Load-Circuit Power Input (Transmitters) | 48 IRE 2,11,15.S1 | Separate |
| Load Coil | 55 IRE 10.S1 | 43 1071 Sep |
| Load Impedance | 54 IRE 3.S1 | 42 1111 Jul |
| Load Impedance Diagram | 57 IRE 7.S2 | 45 999 Jul |
| Load Leads | 55 IRE 10.S1 | 43 1071 Sep |
| Load Matching | 55 IRE 10.S1 | 43 1071 Sep |
| Load Matching Network | 55 IRE 10.S1 | 43 1071 Sep |
| Load Matching Switch | 55 IRE 10.S1 | 43 1071 Sep |
| Load Switch | 55 IRE 10.S1 | 43 1071 Sep |
| Load Transfer Switch | 55 IRE 10.S1 | 43 1071 Sep |
| Loaded Applicator Impedance | 55 IRE 10.S1 | 43 1071 Sep |
| Loaded Impedance | 51 IRE 6.S1 | 39 520 May |
| Loaded Q | 57 IRE 7.S2 | 45 999 Jul |
| Lobe Switching | 54 IRE 12.S1 | 43 202 Feb |

| | Standard | Proceedings Vol | Page | Mo |
|---|---|---|---|---|
| Maximum Keying Frequency (Facsimile) | 56 IRE 9.S1 | 44 | 778 | Jne |
| Maximum Modulating Frequency (Facsimile) | 56 IRE 9.S1 | 44 | 778 | Jne |
| Maximum Output | 52 IRE 17.S1 | 40 | 1683 | Dec |
| Maximum Sensitivity | 52 IRE 17.S1 | 40 | 1683 | Dec |
| Maximum Sound Pressure | 51 IRE 6.S1 | 39 | 521 | May |
| Maximum System Deviation | 52 IRE 17.S1 | 40 | 1683 | Dec |
| Maximum Usable Frequency | 50 IRE 24.S1 | 38 | 1266 | Nov |
| Maximum Undistorted Output | 52 IRE 17.S1 | 40 | 1684 | Dec |
| MCW | 48 IRE 2,11,15.S1 | Separate | | |
| M-Display | 54 IRE 12.S1 | 43 | 202 | Feb |
| Mean Free Path | 51 IRE 6.S1 | 39 | 521 | May |
| Mean Pulse Time | 51 IRE 20.S1 | 39 | 625 | Jne |
| Mechanical Phonograph Recorder | 51 IRE 6.S1 | 39 | 521 | May |
| Mechanical Transmission System | 51 IRE 6.S1 | 39 | 521 | May |
| Meissner Oscillator | 48 IRE 2,11,15.S1 | Separate | | |
| Mel | 51 IRE 6.S1 | 39 | 522 | May |
| Melting Channel | 55 IRE 10.S1 | 43 | 1071 | Sep |
| Memory | 56 IRE 8.S1 | 44 | 1171 | Sep |
| Memory Capacity | 50 IRE 8.S1 | 39 | 274 | Mar |
| Memory Capacity | 56 IRE 8.S1 | 44 | 1171 | Sep |
| Memory Circulating | 50 IRE 8.S1 | 39 | 274 | Mar |
| Memory, Delay-Line | 50 IRE 8.S1 | 39 | 274 | Mar |
| Memory, Electrostatic | 50 IRE 8.S1 | 39 | 274 | Mar |
| Memory Tube | 57 IRE 7.S2 | 45 | 999 | Jul |
| Memory Tube, Electrostatic | 50 IRE 8.S1 | 39 | 274 | Mar |
| Mercury Arc Converter, Pool Cathode | 55 IRE 10.S1 | 43 | 1071 | Sep |
| Mercury Hydrogen Spark Gap Converter | 55 IRE 10.S1 | 43 | 1071 | Sep |
| Mercury Vapor Tube | 57 IRE 7.S2 | 45 | 999 | Jul |
| Mesh | 50 IRE 4.S1 | 38 | 28 | Jan |
| MEW (Microwave Early Warning) | 54 IRE 12.S1 | 43 | 208 | Feb |
| Microbar | 51 IRE 6.S1 | 39 | 522 | May |
| Microphone | 51 IRE 6.S1 | 39 | 522 | May |
| Microphone | 52 IRE 17.S1 | 40 | 1684 | Dec |
| Microphonism | 57 IRE 7.S2 | 45 | 999 | Jul |
| Middle Marker | 54 IRE 12.S1 | 43 | 208 | Feb |
| Minimum Distance | 54 IRE 12.S1 | 43 | 202 | Feb |
| Minimum Firing Power | 57 IRE 7.S2 | 45 | 999 | Jul |
| Minor Cycle | 56 IRE 8.S1 | 44 | 1171 | Sep |
| Minor Lobe | 48 IRE 2,11,15.S1 | Separate | | |
| Minority Carrier | 54 IRE 7.S2 | 42 | 1507 | Oct |
| Mistake | 56 IRE 8.S1 | 44 | 1171 | Sep |
| Mixed Highs | 55 IRE 22.S1 | 43 | 747 | Jne |
| Mixer | 51 IRE 6.S1 | 38 | 522 | May |
| Mixer Tube | 57 IRE 7.S2 | 45 | 999 | Jul |
| Mixing Point | 55 IRE 26.S2 | 44 | 108 | Jan |
| Mobile Transmitter | 48 IRE 2,11,15.S1 | Separate | | |
| Mobility | 54 IRE 7.S2 | 42 | 1507 | Oct |
| Mobility, Hall | 54 IRE 7.S2 | 42 | 1507 | Oct |
| Mode | 57 IRE 7.S2 | 45 | 999 | Jul |
| Mode Filter | 55 IRE 2.S1 | 43 | 1074 | Sep |
| Mode of an Oscillator | 57 IRE 7.S2 | 45 | 999 | Jul |
| Mode of Propagation | 53 IRE 2.S1 | 41 | 1723 | Dec |
| Mode Purity | 57 IRE 7.S2 | 45 | 999 | Jul |
| Mode of Resonance | 53 IRE 2.S1 | 41 | 1723 | Dec |
| Mode Separation | 57 IRE 7.S2 | 45 | 999 | Jul |
| Mode Transducer | 53 IRE 2.S1 | 41 | 1723 | Dec |
| Mode Transducer | 51 IRE 20.S2 | 39 | 898 | Aug |
| Mode Transformer | 51 IRE 20.S2 | 39 | 898 | Aug |
| Moder | 49 IRE 12.S1 | 37 | 1369 | Dec |
| Modes, Degenerate | 57 IRE 7.S2 | 45 | 999 | Jul |
| Modified Index of Refraction | 50 IRE 24.S1 | 38 | 1266 | Nov |
| Modulated Wave | 48 IRE 2,11,15.S1 | Separate | | |
| Modulating Electrode | 50 IRE 7.S1 | 38 | 435 | Apr |
| Modulating Signal | 52 IRE 17.S1 | 40 | 1684 | Dec |
| Modulating Wave | 53 IRE 11.S1 | 41 | 613 | May |
| Modulation | 53 IRE 11.S1 | 41 | 613 | May |
| Modulation | 52 IRE 17.S1 | 40 | 1684 | Dec |
| Modulation Capability | 48 IRE 2,11,15.S1 | Separate | | |
| Modulation Factor | 53 IRE 11.S1 | 41 | 613 | May |
| Modulation Factor | 52 IRE 17.S1 | 40 | 1684 | Dec |
| Modulation Index | 53 IRE 11.S1 | 41 | 614 | May |
| Modulation Noise | 51 IRE 6.S1 | 39 | 522 | May |
| Modulated Amplifier | 48 IRE 2,11,15.S1 | Separate | | |
| Modulator | 53 IRE 11.S1 | 41 | 614 | May |
| Moire | 57 IRE 7.S2 | 45 | 999 | Jul |
| Moire | 55 IRE 22.S1 | 43 | 747 | Jne |
| Mold | 51 IRE 6.S1 | 39 | 522 | May |
| Monochromatic | 55 IRE 22.S1 | 43 | 747 | Jne |
| Monochrome | 55 IRE 22.S1 | 43 | 747 | Jne |
| Monochrome Signal | 55 IRE 22.S1 | 43 | 747 | Jne |
| Monochrome Transmission | 55 IRE 22.S1 | 43 | 747 | Jne |
| Monoscope | 57 IRE 7.S2 | 45 | 999 | Jul |
| Monoscope | 52 IRE 17.S1 | 40 | 1684 | Dec |
| Motional Impedance | 51 IRE 6.S1 | 39 | 522 | May |
| Motor Effect | 55 IRE 10.S1 | 43 | 1071 | Sep |
| Motor Field Induction Heater | 55 IRE 10.S1 | 43 | 1071 | Sep |
| Mount | 57 IRE 7.S2 | 45 | 999 | Jul |
| Moving-Coil Loudspeaker | 51 IRE 6.S1 | 39 | 522 | May |
| Moving-Coil Microphone | 51 IRE 6.S1 | 39 | 522 | May |
| Moving-Coil Pickup | 51 IRE 6.S1 | 39 | 522 | May |
| Moving-Conductor Loudspeaker | 51 IRE 6.S1 | 39 | 522 | May |
| Moving-Conductor Microphone | 51 IRE 6.S1 | 39 | 522 | May |
| Moving Target Indicator (MTI) | 54 IRE 12.S1 | 43 | 202 | Feb |
| MTI | 54 IRE 12.S1 | 43 | 202 | Feb |
| MTI Subclutter Visibility | 54 IRE 12.S1 | 43 | 202 | Feb |
| MTI Target Visibility | 54 IRE 12.S1 | 43 | 202 | Feb |
| MTR (Multiple Track Range) | 54 IRE 12.S1 | 43 | 208 | Feb |
| Mu-($\mu$) Factor | 57 IRE 7.S2 | 45 | 1000 | Jul |
| Multicavity Magnetron | 51 IRE 7.S2 | 45 | 1000 | Jul |
| Multicellular Horn | 51 IRE 6.S1 | 39 | 522 | May |
| Multichannel Radio Transmitter | 48 IRE 2,11,15.S1 | Separate | | |
| Multielectrode Tube | 57 IRE 7.S2 | 45 | 1000 | Jul |
| Multifrequency Transmitter | 48 IRE 2,11,15.S1 | Separate | | |
| Multipath | 56 IRE 9.S1 | 44 | 779 | Jne |
| Multipath Transmission (Multipath) | 56 IRE 9.S1 | 44 | 779 | Jne |
| Multiple-Address | 50 IRE 8.S1 | 39 | 274 | Mar |
| Multiple-Address Code | 56 IRE 8.S1 | 44 | 1171 | Sep |
| Multiple Course | 54 IRE 12.S1 | 43 | 202 | Feb |
| Multiple Modulation | 53 IRE 11.S1 | 41 | 614 | May |
| Multiple Sound Track | 51 IRE 6.S1 | 39 | 522 | May |
| Multiple Spot Scanning | 56 IRE 9.S1 | 44 | 779 | Jne |
| Multiple Tube Counts | 57 IRE 7.S2 | 45 | 1000 | Jul |
| Multiple-Tuned Antenna | 48 IRE 2,11,15.S1 | Separate | | |
| Multiple-Unit Tube | 57 IRE 7.S2 | 45 | 1000 | Jul |
| Multiplex Radio Transmission | 48 IRE 2,11,15.S1 | Separate | | |
| Multiplication Point | 56 IRE 26.S2 | 44 | 108 | Jan |
| Multiplier | 56 IRE 8.S1 | 44 | 1171 | Sep |
| Multiplier Phototube | 57 IRE 7.S2 | 45 | 1000 | Jul |
| Multisegment Magnetron | 57 IRE 7.S2 | 45 | 1000 | Jul |
| Multitrack Recording System | 51 IRE 6.S1 | 39 | 522 | May |
| Multivibrator | 48 IRE 2,11,15.S1 | Separate | | |
| Musa Antenna | 48 IRE 2,11,15.S1 | Separate | | |
| Musical Echo | 51 IRE 6.S1 | 39 | 522 | May |

N

| | | | | |
|---|---|---|---|---|
| Narrow-Band Axis | 55 IRE 22.S1 | 43 | 747 | Jne |
| Navaglobe | 54 IRE 12.S1 | 43 | 209 | Feb |
| Navar | 54 IRE 12.S1 | 43 | 209 | Feb |

| | Standard | PROCEEDINGS Vol Page Mo |
|---|---|---|
| Paraboloidal Reflector | 48 IRE 2,11,15.S1 | Separate |
| Parallel Arithmetic Unit | 50 IRE 8.S1 | 39 275 Mar |
| Parallel Digital Computer | 56 IRE 8.S1 | 44 1171 Sep |
| Parallel Elements | 50 IRE 4.S1 | 39 28 Jan |
| Parallel (in Computers) | 56 IRE 8.S1 | 44 1171 Sep |
| Parallel Transmission | 50 IRE 8.S1 | 39 275 Mar |
| Parallel Two-Terminal Pair Networks | 50 IRE 4.S1 | 39 28 Jan |
| Parasitic Element | 48 IRE 2,11,15.S1 | Separate |
| Parasitic Oscillations | 48 IRE 2,11,15.S1 | Separate |
| Parity Check | 57 IRE 8.S1 | 44 1171 Sep |
| Partial | 51 IRE 6.S1 | 39 523 May |
| Partial Carry | 56 IRE 8.S1 | 44 1171 Sep |
| Partial Velocity | 51 IRE 6.S1 | 39 523 May |
| Passive Transducer | 51 IRE 20.S2 | 39 898 Aug |
| Passive Transducer | 54 IRE 3.S1 | 42 1111 Jul |
| Path | 54 IRE 12.S1 | 43 203 Feb |
| P-Display | 54 IRE 12.S1 | 43 203 Feb |
| Peak Alternating Gap Voltage | 57 IRE 7.S2 | 45 1001 Jul |
| Peak Cathode Current | 57 IRE 7.S2 | 45 1001 Jul |
| Peak Electrode Current | 57 IRE 7.S2 | 45 1001 Jul |
| Peak Forward Anode Voltage | 57 IRE 7.S2 | 45 1001 Jul |
| Peak Inverse Anode Voltage | 57 IRE 7.S2 | 45 1001 Jul |
| Peak Power Output | 48 IRE 2,11,15.S1 | Separate |
| Peak Pulse Amplitude | 56 IRE 23.S1 | 43 621 May |
| Peak Pulse Amplitude | 51 IRE 20.S1 | 39 625 Jne |
| Peak Pulse Power | 52 IRE 20.S1 | 40 553 May |
| Peak Pulse Power Carrier Frequency | 52 IRE 20.S1 | 40 553 May |
| Peak-Signal Level | 42 IRE 9.S1 | Separate |
| Peak Sound Pressure | 51 IRE 6.S1 | 39 523 May |
| Pencil Beam | 54 IRE 12.S1 | 43 203 Feb |
| Pencil-Beam Antenna | 48 IRE 2,11,15.S1 | Separate |
| Penetration Frequency | 50 IRE 24.S1 | 38 1267 Nov |
| Pentode | 57 IRE 7.S2 | 45 1001 Jul |
| Per Cent Hearing | 51 IRE 6.S1 | 39 523 May |
| Per Cent Hearing Loss | 51 IRE 6.S1 | 39 523 May |
| Per Cent Ripple | 48 IRE 2,11,15.S1 | Separate |
| Percentage Modulation | 53 IRE 11.S1 | 41 614 May |
| Percentage Modulation | 52 IRE 17.S1 | 40 1684 Dec |
| Percentage Modulation | 48 IRE 2,11,15.S1 | Separate |
| Performance Chart | 57 IRE 7.S2 | 45 1001 Jul |
| Periodic Electromagnetic Wave | 50 IRE 24.S1 | 38 1267 Nov |
| Periodic Pulse Train | 52 IRE 20.S1 | 40 553 May |
| Permanent Echo | 54 IRE 12.S1 | 43 203 Feb |
| Permanent Magnet Loudspeaker | 51 IRE 6.S1 | 39 523 May |
| Perpendicular Magnetization | 51 IRE 6.S1 | 39 523 May |
| Persistence Characteristic | 57 IRE 7.S2 | 45 1001 Jul |
| Persistence Characteristic (Camera Tubes) | 57 IRE 7.S2 | 45 1001 Jul |
| Perveance | 57 IRE 7.S2 | 45 1001 Jul |
| Phanton Target | 54 IRE 12.S1 | 43 203 Feb |
| Phase Constant | 53 IRE 2.S1 | 41 1724 Dec |
| Phase Delay | 56 IRE 9.S1 | 44 779 Jne |
| Phase Deviation | 53 IRE 11.S1 | 41 614 May |
| Phase Distortion | 53 IRE 4.S1 | 42 555 Mar |
| Phase Distortion | 56 IRE 9.S1 | 44 779 Jne |
| Phase-Frequency Distortion | 53 IRE 4.S1 | 42 555 Mar |
| Phase-Frequency Distortion | 56 IRE 9.S1 | 44 779 Jne |
| Phase-Frequency Response Characteristic | 48 IRE 2,11,15.S1 | Separate |
| Phase Localizer | 54 IRE 12.S1 | 43 203 Feb |
| Phase-Modulated Transmitter | 48 IRE 2,11,15.S1 | Separate |
| Phase Modulation (PM) | 53 IRE 11.S1 | 41 614 May |
| Phase Modulation | 52 IRE 17.S1 | 40 1684 Dec |
| Phase-Propagation Ratio | 50 IRE 24.S1 | 38 1267 Nov |
| Phase-Recovery Time | 57 IRE 7.S2 | 45 1001 Jne |
| Phase-Shift Microphone | 51 IRE 6.S1 | 39 523 May |
| Phase-Shift Oscillator | 48 IRE 2,11,15.S1 | Separate |
| Phase Shifter Waveguide | 55 IRE 2.S1 | 43 1074 Sep |
| Phase-Tuned Tube | 57 IRE 7.S2 | 45 1001 Jul |
| Phaser | 42 IRE 9.S1 | Separate |
| Phase Velocity | 50 IRE 24.S1 | 38 1267 Nov |
| Phase Velocity | 53 IRE 2.S1 | 41 1724 Dec |
| Phasing | 56 IRE 9.S1 | 44 779 Jne |
| Phasing Line | 42 IRE 9.S1 | Separate |
| Phasing Signal | 56 IRE 9.S1 | 44 779 Jne |
| Phi ($\Phi$) Polarization | 48 IRE 2,11,15.S1 | Separate |
| Phon | 51 IRE 6.S1 | 39 523 May |
| Phonograph Pickup | 51 IRE 6.S1 | 39 524 May |
| Phosphor | 50 IRE 7.S1 | 38 436 Apr |
| Photocathode | 57 IRE 7.S2 | 45 1001 Jul |
| Photoelectric Emission | 57 IRE 7.S2 | 45 1001 Jul |
| Photographic Emulsion | 51 IRE 6.S1 | 39 524 May |
| Photographic Recording | 42 IRE 9.S1 | Separate |
| Photographic Sound Recorder | 51 IRE 6.S1 | 39 524 May |
| Photographic Sound Reproducer | 51 IRE 6.S1 | 39 524 May |
| Photographic Transmission Density | 51 IRE 6.S1 | 39 524 May |
| Photometry | 55 IRE 22.S1 | 43 747 Jne |
| Photomultiplier | 57 IRE 7.S2 | 45 1001 Jul |
| Photosensitive Recording | 56 IRE 9.S1 | 44 779 Jne |
| Phototube | 57 IRE 7.S2 | 45 1001 Jul |
| Photovaristor | 54 IRE 7.S2 | 42 1507 Oct |
| (Pi) $\pi$-Mode | 57 IRE 7.S2 | 45 1002 Jul |
| Pi Network | 50 IRE 4.S1 | 39 28 Jan |
| Pickup | 52 IRE 17.S1 | 40 1684 Dec |
| Pickup Arm | 51 IRE 6.S1 | 39 524 May |
| Pickup Cartridge | 51 IRE 6.S1 | 39 524 May |
| Pickup Spectral Characteristic | 55 IRE 22.S1 | 43 747 Jne |
| Pickup Tube | 57 IRE 7.S2 | 45 1001 Jul |
| Picture Black (or "Black") | 42 IRE 9.S1 | Separate |
| Picture Frequencies | 56 IRE 9.S1 | 44 779 Jne |
| Picture Inversion | 56 IRE 9.S1 | 44 779 Jne |
| Picture Signal (Facsimile) | 56 IRE 9.S1 | 44 779 Jne |
| Picture Signal (TV) | 55 IRE 23.S1 | 43 621 May |
| Picture Tube | 50 IRE 7.S1 | 38 436 Apr |
| Picture White (Facsimile) | 42 IRE 9.S1 | Separate |
| Pierce Oscillator | 48 IRE 2,11,15.S1 | Separate |
| Pill-Box Antenna | 48 IRE 2,11,15.S1 | Separate |
| Pilotage | 54 IRE 12.S1 | 43 203 Feb |
| Pinch Effect | 55 IRE 10.S1 | 43 1072 Sep |
| PIP | 54 IRE 12.S1 | 43 203 Feb |
| PIP Matching | 54 IRE 12.S1 | 43 203 Feb |
| PIP-Matching Display | 54 IRE 12.S1 | 43 199 Feb |
| Pistonphone | 51 IRE 6.S1 | 39 524 May |
| Pitch | 51 IRE 6.S1 | 39 524 May |
| Pitch Attitude | 49 IRE 12.S1 | 37 1369 Dec |
| Place | 56 IRE 8.S1 | 44 1171 Sep |
| Plan Position Indicator (PPI) | 54 IRE 12.S1 | 43 203 Feb |
| Planar Network | 50 IRE 4.S1 | 39 28 Jan |
| Planckian Locus | 55 IRE 22.S1 | 43 747 Jne |
| Plane Earth Factor | 50 IRE 24.S1 | 38 1267 Nov |
| Plane of Polarization | 50 IRE 24.S1 | 38 1267 Nov |
| Plane Polarized Wave | 50 IRE 24.S1 | 38 1267 Nov |
| Plane Wave | 50 IRE 24.S1 | 38 1267 Nov |
| Plan Position Indicator | 49 IRE 12.S1 | 37 1369 Dec |
| Plate | 57 IRE 7.S2 | 45 1002 Jul |
| Plate Characteristic | 57 IRE 7.S2 | 45 1002 Jul |
| Plate Current | 57 IRE 7.S2 | 45 1002 Jul |
| Plate (Anode) Efficiency | 48 IRE 2,11,15.S1 | Separate |
| Plate Keying | 48 IRE 2,11,15.S1 | Separate |

| | Standard | Proceedings Vol | Page | Mo |
|---|---|---|---|---|
| Pulse Frequency Spectrum | 51 IRE 20.S1 | 39 | 626 | Jne |
| Pulse, Ghost | 54 IRE 12.S1 | 43 | 203 | Feb |
| Pulse Interleaving | 51 IRE 20.S1 | 39 | 626 | Jne |
| Pulse Interrogation | 52 IRE 20.S1 | 40 | 553 | May |
| Pulse Interval | 51 IRE 20.S1 | 39 | 626 | Jne |
| Pulse-Interval Modulation | 51 IRE 20.S1 | 39 | 626 | Jne |
| Pulse-Interval Modulation | 53 IRE 11.S1 | 41 | 614 | May |
| Pulse Jitter | 52 IRE 20.S1 | 40 | 553 | May |
| Pulse-Length Modulation | 51 IRE 20.S1 | 39 | 626 | Jne |
| Pulse Mode | 52 IRE 20.S1 | 40 | 553 | May |
| Pulse-Mode Multiplex | 52 IRE 20.S1 | 40 | 553 | May |
| Pulse Mode, Spurious | 52 IRE 20.S1 | 40 | 553 | May |
| Pulse-Moder | 54 IRE 12.S1 | 43 | 203 | Feb |
| Pulse Modulation | 52 IRE 20.S1 | 40 | 553 | May |
| Pulse Modulation | 53 IRE 11.S1 | 41 | 614 | May |
| Pulse Modulator | 48 IRE 2,11,15.S1 | Separate | | |
| Pulse Multiplex | 52 IRE 20.S1 | 40 | 553 | May |
| Pulse Packet | 54 IRE 12.S1 | 43 | 203 | Feb |
| Pulse-Phase Modulation | 52 IRE 20.S1 | 40 | 553 | May |
| Pulse-Position Modulation | 53 IRE 11.S1 | 41 | 614 | May |
| Pulse-Position Modulation | 51 IRE 20.S1 | 39 | 626 | Jne |
| Pulse Power, Carrier-Frequency, Peak | 52 IRE 20.S1 | 40 | 553 | May |
| Pulse Power, Peak | 52 IRE 20.S1 | 40 | 553 | May |
| Pulse, Radio-Frequency | 51 IRE 20.S1 | 39 | 626 | Jne |
| Pulse Rate | 54 IRE 12.S1 | 43 | 203 | Feb |
| Pulse Regeneration | 51 IRE 20.S1 | 39 | 626 | Jne |
| Pulse Repeater (Transponder) | 48 IRE 2,11,15.S1 | Separate | | |
| Pulse Repetition Frequency | 54 IRE 12.S1 | 43 | 203 | Feb |
| Pulse Repetition Frequency | 51 IRE 20.S1 | 39 | 626 | Jne |
| Pulse Repetition Period | 51 IRE 20.S1 | 39 | 626 | Jne |
| Pulse Repetition Rate | 51 IRE 20.S1 | 39 | 626 | Jne |
| Pulse Repetition Rate (PRF) | 54 IRE 12.S1 | 43 | 203 | Feb |
| Pulse Reply | 52 IRE 20.S1 | 40 | 554 | May |
| Pulse Rise Time | 51 IRE 20.S1 | 39 | 626 | Jne |
| Pulse Separation | 52 IRE 20.S1 | 40 | 554 | May |
| Pulse Shaper | 52 IRE 20.S1 | 40 | 554 | May |
| Pulse Shaping | 52 IRE 20.S1 | 40 | 554 | May |
| Pulse, Single-Polarity | 52 IRE 20.S1 | 40 | 554 | May |
| Pulse Spacing | 51 IRE 20.S1 | 39 | 626 | Jne |
| Pulse Spectrum | 51 IRE 20.S1 | 39 | 626 | Jne |
| Pulse Spike | 51 IRE 20.S1 | 39 | 626 | Jne |
| Pulse Spike Amplitude | 52 IRE 20.S1 | 40 | 554 | May |
| Pulse Tilt | 55 IRE 23.S1 | 43 | 621 | May |
| Pulse Tilt | 52 IRE 20.S1 | 40 | 554 | May |
| Pulse Time, Leading Edge | 51 IRE 20.S1 | 39 | 626 | Jne |
| Pulse Time, Mean | 51 IRE 20.S1 | 39 | 626 | Jne |
| Pulse-Time Modulation | 53 IRE 11.S1 | 41 | 614 | May |
| Pulse-Time Modulation | 51 IRE 20.S1 | 39 | 626 | Jne |
| Pulse Time, Trailing Edge | 51 IRE 20.S1 | 39 | 626 | Jne |
| Pulse Train | 51 IRE 20.S1 | 39 | 626 | Jne |
| Pulse Train, Bidirectional | 52 IRE 20.S1 | 40 | 554 | May |
| Pulse Train, Periodic | 52 IRE 20.S1 | 40 | 554 | May |
| Pulse-Train Spectrum | 52 IRE 20.S1 | 40 | 554 | May |
| Pulse Train, Undirectional | 52 IRE 20.S1 | 40 | 554 | May |
| Pulse Transmitter | 48 IRE 2,11,15 S1 | Separate | | |
| Pulse Undirectional | 51 IRE 20.S1 | 39 | 626 | Jne |
| Pulse Valley | 52 IRE 20.S1 | 40 | 554 | May |
| Pulse Width | 55 IRE 23.S1 | 43 | 621 | May |
| Pulse Width | 52 IRE 20.S1 | 40 | 554 | May |
| Pulse-Width Modulation | 51 IRE 20.S1 | 39 | 626 | Jne |
| Pulsed Doppler System | 54 IRE 12.S1 | 43 | 203 | Feb |
| Pulsed Oscillator | 48 IRE 2,11,15.S1 | Separate | | |
| Pulsed Oscillator | 52 IRE 20.S1 | 40 | 554 | May |
| Pulsed-Oscillator Starting Time | 52 IRE 20.S1 | 40 | 554 | May |
| Pulses Equalizing | 52 IRE 20.S1 | 40 | 554 | May |
| Purity | 55 IRE 22.S1 | 43 | 747 | Jne |
| Purple Boundary | 55 IRE 22.S1 | 43 | 747 | Jne |
| Push-Pull Currents (Balanced Currents) | 53 IRE 2.S1 | 41 | 1724 | Dec |
| Push-Pull Microphone | 51 IRE 6.S1 | 39 | 525 | May |
| Push-Pull Oscillator | 48 IRE 2,11,15.S1 | Separate | | |
| Push-Pull Voltages | 53 IRE 2.S1 | 41 | 1724 | Dec |
| Pushing Figure (of an Oscillator) | 57 IRE 7.S2 | 45 | 1002 | Jul |
| Push-Push Circuit | 48 IRE 2,11,15.S1 | Separate | | |
| Push-Push Currents | 53 IRE 2.S1 | 41 | 1724 | Dec |
| Push-Push Voltages | 53 IRE 2.S1 | 41 | 1724 | Dec |
| Pyramidal Horn | 48 IRE 2,11,15.S1 | Separate | | |
| Pythagorean Scale | 51 IRE 6.S1 | 39 | 525 | May |
| **Q** | | | | |
| Quadripole | 50 IRE 4.S1 | 39 | 28 | Jan |
| Quadrantal Error | 49 IRE 12.S1 | 37 | 1369 | Dec |
| Quantization | 53 IRE 11.S1 | 41 | 614 | May |
| Quantization Distortion | 53 IRE 11.S1 | 41 | 614 | May |
| Quantization Level | 53 IRE 11.S1 | 41 | 614 | May |
| Quantization Noise | 53 IRE 11.S1 | 41 | 614 | May |
| Quantized Pulse Modulation | 53 IRE 11.S1 | 41 | 614 | May |
| Quantum Efficiency | 57 IRE 7.S2 | 45 | 1002 | Jul |
| Quenched Spark Gap Converter | 55 IRE 10.S1 | 43 | 1072 | Sep |
| Quenching | 57 IRE 7.S2 | 45 | 1002 | Jul |
| Quieting Sensitivity | 52 IRE 17.S1 | 40 | 1685 | Dec |
| **R** | | | | |
| Racon | 54 IRE 12.S1 | 43 | 209 | Feb |
| Radar | 54 IRE 12.S1 | 43 | 203 | Feb |
| Radar Equation | 54 IRE 12.S1 | 43 | 203 | Feb |
| Radar Performance Figure | 54 IRE 12.S1 | 43 | 203 | Feb |
| Radar Pilotage Equipment | 54 IRE 12.S1 | 43 | 204 | Feb |
| Radar Range Equation | 54 IRE 12.S1 | 43 | 204 | Feb |
| Radar Relay | 54 IRE 12.S1 | 43 | 204 | Feb |
| Radar Shadow | 54 IRE 12.S1 | 43 | 204 | Feb |
| Radar Transmitter | 48 IRE 2,11,15.S1 | Separate | | |
| Radial | 54 IRE 12.S1 | 43 | 204 | Feb |
| Radial Time Base Display | 54 IRE 12.S1 | 43 | 204 | Feb |
| Radial Transmission Line | 53 IRE 2.S1 | 41 | 1724 | Dec |
| Radiance | 55 IRE 22.S1 | 43 | 747 | Jne |
| Radiant Flux | 55 IRE 22.S1 | 43 | 747 | Jne |
| Radiant Intensity | 55 IRE 22.S1 | 43 | 747 | Jne |
| Radiant Sensitivity (of a Photo-Tube) | 54 IRE 7.S1 | 42 | 1277 | Aug |
| Radiating Element | 48 IRE 2,11,15.S1 | Separate | | |
| Radiation Counter | 57 IRE 7.S2 | 45 | 1002 | Jul |
| Radiation-Counter Tube | 57 IRE 7.S2 | 45 | 1002 | Jul |
| Radiation Efficiency | 48 IRE 2,11,15.S1 | Separate | | |
| Radiation Intensity | 48 IRE 2,11,15.S1 | Separate | | |
| Radiation Lobe | 48 IRE 2,11,15.S1 | Separate | | |
| Radiation Loss | 53 IRE 2.S1 | 41 | 1724 | Dec |
| Radiation (Nuclear) | 57 IRE 7.S2 | 45 | 1002 | Jul |
| Radiation Pattern | 48 IRE 2,11,15.S1 | Separate | | |
| Radiation Resistance | 48 IRE 2,11,15.S1 | Separate | | |
| Radio-Autopilot Coupler | 49 IRE 12.S1 | 37 | 1369 | Dec |
| Radio Beacon | 54 IRE 12.S1 | 43 | 204 | Feb |
| Radio Broadcasting | 48 IRE 2,11,15.S1 | Separate | | |
| Radio Channel | 52 IRE 17.S1 | 40 | 1685 | Dec |
| Radio Communication Circuit | 48 IRE 2,11,15.S1 | Separate | | |
| Radio Direction Finding | 54 IRE 12.S1 | 43 | 204 | Feb |
| Radio Field Strength | 50 IRE 24.S1 | 38 | 1267 | Nov |
| Radio Frequency | 50 IRE 24.S1 | 38 | 1267 | Nov |
| Radio Frequency | 52 IRE 17.S1 | 40 | 1685 | Dec |
| Radio-Frequency Alternator | 48 IRE 2,11,15.S1 | Separate | | |
| Radio-Frequency Converter | 55 IRE 10.S1 | 43 | 1072 | Sep |

| | *Standard* | *PROCEEDINGS Vol Page Mo* |
|---|---|---|
| Radio-Frequency Generator-Electron Tube Type | 55 IRE 10.S1 | 43 1072 Sep |
| Radio-Frequency Pulse | 51 IRE 20.S1 | 39 626 Jne |
| Radio-Frequency Signal, High Level | 57 IRE 7.S2 | 45 1002 Jul |
| Radio-Frequency Signal, Low-Level | 57 IRE 7.S2 | 45 1003 Jul |
| Radio Horizon | 50 IRE 24.S1 | 38 1267 Nov |
| Radio Magnetic Indicator (RMI) | 54 IRE 12.S1 | 43 204 Feb |
| Radio Navigation | 49 IRE 12.S1 | 37 1370 Dec |
| Radio Proximity Fuze | 48 IRE 2,11,15.S1 | Separate |
| Radio Range | 54 IRE 12.S1 | 43 204 Feb |
| Radio Receiver | 52 IRE 17.S1 | 40 1685 Dec |
| Radio Transmitter | 48 IRE 2,11,15.S1 | Separate |
| Radio Wave Propagation | 50 IRE 24.S1 | 38 1267 Nov |
| Radiolocation | 54 IRE 12.S1 | 43 204 Feb |
| Radiophare | 54 IRE 12.S1 | 43 204 Feb |
| Radiosonde | 48 IRE 2,11,15.S1 | Separate |
| Radix | 56 IRE 8.S1 | 44 1172 Sep |
| Radix Point | 50 IRE 8.S1 | 39 276 Mar |
| Radome | 48 IRE 2,11,15.S1 | Separate |
| Radux | 54 IRE 12.S1 | 43 209 Feb |
| Rain Return | 54 IRE 12.S1 | 43 204 Feb |
| Ramark | 54 IRE 12.S1 | 43 209 Feb |
| Random Errors | 54 IRE 12.S1 | 43 204 Feb |
| Random Noise | 48 IRE 2,11,15.S1 | Separate |
| Range | 54 IRE 12.S1 | 43 204 Feb |
| Range Mark | 54 IRE 12.S1 | 43 204 Feb |
| Range Resolution | 54 IRE 12.S1 | 43 204 Feb |
| Range, Visual-Aural | 54 IRE 12.S1 | 43 204 Feb |
| Range, Visual Radio | 54 IRE 12.S1 | 43 204 Feb |
| Rank | 50 IRE 4.S1 | 39 28 Jan |
| Raster | 57 IRE 7.S2 | 45 1003 Jul |
| Raster Burn | 57 IRE 7.S2 | 45 1003 Jul |
| Rate of Decay | 51 IRE 6.S1 | 39 525 May |
| Ratio | 57 IRE 7.S2 | 45 1003 Jul |
| Raydist | 54 IRE 12.S1 | 43 209 Feb |
| Rayleigh Disk | 51 IRE 6.S1 | 39 525 May |
| R-C Oscillator | 48 IRE 2,11,15.S1 | Separate |
| RDF-Radio Direction Finding | 54 IRE 12.S1 | 43 204 Feb |
| Reactance Modulator | 48 IRE 2,11,15.S1 | Separate |
| Read | 56 IRE 8.S1 | 44 1172 Sep |
| Read (in Charge-Storage Tubes) | 57 IRE 7.S2 | 45 1003 Jul |
| Read-Around Number | 57 IRE 7.S2 | 45 1003 Jul |
| Read-Around Ratio | 57 IRE 7.S2 | 45 1003 Jul |
| Read Number | 57 IRE 7.S2 | 45 1003 Jul |
| Reading Speed | 57 IRE 7.S2 | 45 1003 Jul |
| Ready-To-Receive Signal | 56 IRE 9.S1 | 44 779 Jne |
| Rebecca | 54 IRE 12.S1 | 43 209 Feb |
| Recalescent Point | 55 IRE 10.S1 | 43 1072 Sep |
| Receiver, Facsimile | 56 IRE 9.S1 | 44 779 Jne |
| Receiver Gating | 54 IRE 12.S1 | 43 204 Feb |
| Receiver Primaries | 55 IRE 22.S1 | 43 748 Jne |
| Receiver Pulse Delay | 52 IRE 20.S1 | 40 554 May |
| Receiving Converter, Facsimile (FS to AM Converter) | 56 IRE 9.S1 | 44 779 Jne |
| Reciprocal Transducer | 51 IRE 20.S2 | 39 989 Aug |
| Recombination Rate, Surface | 54 IRE 7.S2 | 42 1507 Oct |
| Recombination Rate, Volume | 54 IRE 7.S2 | 42 1507 Oct |
| Recombination Velocity | 54 IRE 7.S2 | 42 1507 Oct |
| Record Medium | 56 IRE 9.S1 | 44 779 Jne |
| Record Sheet | 56 IRE 9.S1 | 44 779 Jne |
| Recorded Spot | 56 IRE 9.S1 | 44 779 Jne |
| Recorded Spot X Dimension | 56 IRE 9.S1 | 44 779 Jne |
| Recorded Spot Y Dimension | 56 IRE 9.S1 | 44 779 Jne |
| Recorder, Facsimile | 56 IRE 9.S1 | 44 779 Jne |
| Recording Channel | 51 IRE 6.S1 | 39 525 May |
| Recording (in Facsimile) | 56 IRE 9.S1 | 44 779 Jne |
| Recording Loss | 51 IRE 6.S1 | 39 525 May |
| Recording Spot (in Facsimile) | 56 IRE 9.S1 | 44 779 Jne |
| Recording Stylus | 51 IRE 6.S1 | 39 525 May |
| Recovery Time | 57 IRE 7.S2 | 45 1003 Jul |
| Recovery Time (ATR Tubes) | 56 IRE 7.S3 | 44 1039 Aug |
| Recovery Time (Gas Tubes) | 57 IRE 7.S2 | 45 1003 Jul |
| Recovery Time (Geiger-Mueller Counters) | 57 IRE 7.S2 | 45 1003 Jul |
| Recovery Time (TR and Pre-TR Tubes) | 57 IRE 7.S2 | 45 1003 Jul |
| Rectangular Scanning | 48 IRE 2,11,15.S1 | Separate |
| Rectification Factor | 57 IRE 7.S2 | 45 1003 Jul |
| Rectifier | 48 IRE 2,11,15.S1 | Separate |
| Rectilinear Scanning | 42 IRE 9.S1 | Separate |
| Recurrence Rate | 54 IRE 12.S1 | 43 204 Feb |
| Redistribution | 57 IRE 7.S2 | 45 1003 Jul |
| Redundancy Check | 56 IRE 8.S1 | 44 1172 Sep |
| Reference Black Leve | 55 IRE 23.S1 | 43 621 May |
| Reference Direction | 49 IRE 12.S1 | 37 1370 Dec |
| Reference Line | 49 IRE 12.S1 | 37 1370 Dec |
| Reference Volume | 54 IRE 3.S1 | 42 1111 Jul |
| Reference White | 55 IRE 22.S1 | 43 748 Jne |
| Reference White Level | 55 IRE 23.S1 | 43 621 May |
| Reflected Wave | 53 IRE 2.S1 | 41 1724 Dec |
| Reflection Coefficient | 53 IRE 2.S1 | 41 1724 Dec |
| Reflection Coefficient (of Transmission Medium) | 53 IRE 2.S1 | 41 1724 Dec |
| Reflection Color-Tube | 57 IRE 7.S2 | 45 1003 Jul |
| Reflection Error | 54 IRE 12.S1 | 43 204 Feb |
| Reflection Loss | 53 IRE 2.S1 | 41 1724 Dec |
| Reflector (Antenna) | 48 IRE 2,11,15.S1 | Separate |
| Reflector (in Tubes) | 57 IRE 7.S2 | 45 1003 Jul |
| Reflex Baffle | 51 IRE 6.S1 | 39 525 May |
| Reflex Bunching | 57 IRE 7.S2 | 45 1003 Jul |
| Refracted Wave | 53 IRE 2.S1 | 41 1724 Dec |
| Refracted Wave | 50 IRE 24.S1 | 38 1267 Nov |
| Refraction Error | 54 IRE 12.S1 | 43 204 Feb |
| Refraction Loss | 51 IRE 6.S1 | 39 525 May |
| Refractive Index | 50 IRE 24.S1 | 38 1267 Nov |
| Refractive Modulus | 50 IRE 24.S1 | 38 1267 Nov |
| Regeneration (in Charge-Storage Tubes) | 57 IRE 7.S2 | 45 1003 Jul |
| Regeneration (in Computers) | 56 IRE 8.S1 | 44 1172 Sep |
| Regeneration (in Transmitters) | 48 IRE 2,11,15.S1 | Separate |
| Regenerative Repeater | 53 IRE 11.S1 | 41 614 May |
| Region, Geiger-Mueller | 57 IRE 7.S2 | 45 1003 Jul |
| Region of Limited Proportionality | 57 IRE 7.S2 | 45 1003 Jul |
| Region, Proportional | 57 IRE 7.S2 | 45 1003 Jul |
| Register | 56 IRE 8.S1 | 44 1172 Sep |
| Register, Delay-Line | 50 IRE 8.S1 | 39 276 Mar |
| Register Length | 56 IRE 8.S1 | 44 1172 Sep |
| Register, Static | 50 IRE 8.S1 | 39 276 Mar |
| Regulation (Gas Tubes) | 57 IRE 7.S2 | 45 1003 Jul |
| Reignition | 57 IRE 7.S2 | 45 1003 Jul |
| Rejection Band | 53 IRE 2.S1 | 41 1724 Dec |
| Relative Bearing | 54 IRE 12.S1 | 43 204 Feb |
| Relative Course | 49 IRE 12.S1 | 37 1370 Dec |
| Relative Heading | 49 IRE 12.S1 | 37 1370 Dec |
| Relative Luminosity | 55 IRE 22.S1 | 43 748 Jne |
| Relative Plateau Slope | 57 IRE 7.S2 | 45 1003 Jul |
| Relative Refractive Index | 50 IRE 24.S1 | 38 1267 Nov |
| Relative Response | 51 IRE 6.S1 | 39 525 May |
| Relative Velocity | 51 IRE 6.S1 | 39 525 May |
| Relaxation Oscillator | 48 IRE 2,11,15.S1 | Separate |
| Relay Radar | 54 IRE 12.S1 | 43 204 Feb |
| Remote Control | 48 IRE 2,11,15.S1 | Separate |

| | Standard | Proceedings Vol Page Mo |
|---|---|---|
| Repeatability | 57 IRE 7.S2 | 45 1003 Jul |
| Repeller | 57 IRE 7.S2 | 45 1004 Jul |
| Repetition Frequency | 54 IRE 12.S1 | 43 204 Feb |
| Repetition Rate | 54 IRE 12.S1 | 43 204 Feb |
| Repetition Rate, Basic | 54 IRE 12.S1 | 43 204 Feb |
| Repetition Rate, Specific | 54 IRE 12.S1 | 43 204 Feb |
| Reply | 54 IRE 12.S1 | 43 204 Feb |
| Reply Efficiency, Transponder | 54 IRE 12.S1 | 43 204 Feb |
| Reproducing Stylus | 51 IRE 6.S1 | 39 525 May |
| Reproduction Speed | 56 IRE 9.S1 | 44 779 Jne |
| Re-Recording | 51 IRE 6.S1 | 39 525 May |
| Re-Recording System | 51 IRE 6.S1 | 39 525 May |
| Reset | 56 IRE 8.S1 | 44 1172 Sep |
| Residual Error | 54 IRE 12.S1 | 43 204 Feb |
| Resistance | 57 IRE 7.S2 | 45 1004 Jul |
| Resolution | 49 IRE 12.S1 | 37 1370 Dec |
| Resolution | 57 IRE 7.S2 | 45 1004 Jul |
| Resolution, Structural | 57 IRE 7.S2 | 45 1004 Jul |
| Resolver | 50 IRE 8.S1 | 39 276 Mar |
| Resolving Power | 48 IRE 2,11,15.S1 | Separate |
| Resolving Time | 57 IRE 7.S2 | 45 1004 Jul |
| Resolving Time | 54 IRE 12.S1 | 43 204 Feb |
| Resonant Gap | 57 IRE 7.S2 | 45 1004 Jul |
| Resonant-Line Oscillator | 48 IRE 2,11,15.S1 | Separate |
| Resonant Modes in Cylindrical Cavities | 45 IRE 24.S1 | Separate |
| Resonant Window (Switching Tubes) | 56 IRE 7.S3 | 44 1038 Aug |
| Resonator Mode | 57 IRE 7.S2 | 45 1004 Jul |
| Resonator, Waveguide | 55 IRE 2.S1 | 43 1074 Sep |
| Responder | 54 IRE 12.S1 | 43 204 Feb |
| Responder Beacon | 54 IRE 12.S1 | 43 204 Feb |
| Response | 57 IRE 7.S2 | 45 1004 Jul |
| Retained Image | 57 IRE 7.S2 | 45 1004 Jul |
| Retarding-Field (Position-Grid) Oscillator | 48 IRE 2,11,15.S1 | Separate |
| Retention Time, Maximum | 57 IRE 7.S2 | 45 1004 Jul |
| Retrace Line | 52 IRE 17.S1 | 40 1685 Dec |
| Return Loss | 53 IRE 2.S1 | 41 1724 Dec |
| Return Transfer Function | 55 IRE 26.S2 | 44 108 Jan |
| Reverberation | 51 IRE 6.S1 | 39 525 May |
| Reverberation Chamber | 51 IRE 6.S1 | 39 525 May |
| Reverberation Time | 51 IRE 6.S1 | 39 525 May |
| Reverberation Time Meter | 51 IRE 6.S1 | 39 525 May |
| Reverse Emission | 57 IRE 7.S2 | 45 1004 Jul |
| Rewrite | 56 IRE 8.S1 | 44 1172 Sep |
| Rho Theta | 54 IRE 12.S1 | 43 204 Feb |
| Rhombic Antenna | 48 IRE 2,11,15.S1 | Separate |
| Ribbon Microphone | 51 IRE 6.S1 | 39 525 May |
| Rieke Diagram | 57 IRE 7.S2 | 45 1004 Jul |
| Right-Handed (Clockwise) Polarized Wave | 50 IRE 24.S1 | 38 1267 Nov |
| Ring Around | 54 IRE 12.S1 | 43 205 Feb |
| Ring Counter | 56 IRE 8.S1 | 44 1172 Sep |
| Ring Head | 51 IRE 6.S1 | 39 525 May |
| Ring Oscillator | 48 IRE 2,11,15.S1 | Separate |
| Ring Time | 54 IRE 12.S1 | 43 205 Feb |
| Ringing (in Facsimile) | 56 IRE 9.S1 | 44 780 Jne |
| Ringing (in Receivers) | 52 IRE 17.S1 | 40 1685 Dec |
| Ripple | 52 IRE 17.S1 | 40 1685 Dec |
| Ripple Voltage | 48 IRE 2,11,15.S1 | Separate |
| Rising-Sun Magnetron | 57 IRE 7.S2 | 45 1004 Jul |
| RMI | 54 IRE 12.S1 | 43 205 Feb |
| RMS (Effective) Pulse Amplitude | 51 IRE 20.S1 | 39 626 Jne |
| Roll Out | 50 IRE 8.S1 | 39 276 Mar |
| Root-Sum Square | 52 IRE 17.S1 | 40 1685 Dec |
| Rotary Generator | 55 IRE 10.S1 | 43 1072 Sep |
| Rotating Joint | 55 IRE 2.S1 | 43 1074 Sep |
| Round-Off | 50 IRE 8.S1 | 39 276 Mar |
| Round-Off Error | 50 IRE 8.S1 | 39 276 Mar |
| Routine | 56 IRE 8.S1 | 44 1172 Sep |
| RT Box | 54 IRE 12.S1 | 43 205 Feb |
| Rumble | 51 IRE 6.S1 | 39 525 May |
| Rumble, Turntable | 52 IRE 17.S1 | 40 1685 Dec |
| **S** | | |
| Sabin | 51 IRE 6.S1 | 39 526 May |
| Sampling Gate | 54 IRE 12.S1 | 43 205 Feb |
| Saturated Signal | 54 IRE 12.S1 | 43 205 Feb |
| Saturating Signal | 54 IRE 12.S1 | 43 205 Feb |
| Saturation | 55 IRE 22.S1 | 43 748 Jne |
| SBA (Standard Beam Approach) | 54 IRE 12.S1 | 43 209 Feb |
| Scale | 51 IRE 6.S1 | 39 526 May |
| Scale Factor | 50 IRE 8.S1 | 39 276 Mar |
| Scanner | 56 IRE 9.S1 | 44 780 Jne |
| Scanning (Antenna) | 48 IRE 2,11,15.S1 | Separate |
| Scanning Antenna Mount | 48 IRE 2,11,15.S1 | Separate |
| Scanning, High-Velocity | 57 IRE 7.S2 | 45 1004 Jul |
| Scanning (in Facsimile) | 56 IRE 9.S1 | 44 780 Jne |
| Scanning (in Navigation Aids) | 49 IRE 12.S1 | 37 1370 Dec |
| Scanning Line Frequency | 56 IRE 9.S1 | 44 780 Jne |
| Scanning Line Length | 56 IRE 9.S1 | 44 780 Jne |
| Scanning Loss | 48 IRE 2,11,15.S1 | Separate |
| Scanning Low-Velocity | 57 IRE 7.S2 | 45 1004 Jul |
| Scanning Spot X Dimension | 56 IRE 9.S1 | 44 780 Jne |
| Scanning Spot Y Dimension | 56 IRE 9.S1 | 44 780 Jne |
| Scatterband | 54 IRE 12.S1 | 43 205 Feb |
| Scattering Loss | 51 IRE 6.S1 | 39 526 May |
| Schottky Emission | 57 IRE 7.S2 | 45 1004 Jul |
| Scintillation | 54 IRE 12.S1 | 43 205 Feb |
| Scope | 54 IRE 12.S1 | 43 205 Feb |
| Scoring System | 51 IRE 6.S1 | 39 526 May |
| Screen | 57 IRE 7.S2 | 45 1004 Jul |
| Screen Grid | 57 IRE 7.S2 | 45 1004 Jul |
| Screen-Grid Characteristic | 57 IRE 7.S2 | 45 1004 Jul |
| Screen-Grid Current | 57 IRE 7.S2 | 45 1004 Jul |
| Screen-Grid Modulation | 48 IRE 2,11,15.S1 | Separate |
| Sea Return | 54 IRE 12.S1 | 43 205 Feb |
| Searchlighting | 54 IRE 12.S1 | 43 205 Feb |
| Search Radar | 54 IRE 12.S1 | 43 205 Feb |
| Secondary Emission | 57 IRE 7.S2 | 45 1004 Jul |
| Secondary-Emission Ratio | 57 IRE 7.S2 | 45 1004 Jul |
| Secondary Grid Emission | 57 IRE 7.S2 | 45 1004 Jul |
| Secondary Radar | 54 IRE 12.S1 | 43 205 Feb |
| Second-Channel Attenuation | 52 IRE 17.S1 | 40 1685 Dec |
| Second-Channel Interference | 52 IRE 17.S1 | 40 1685 Dec |
| Second-Time-Around Echo | 54 IRE 12.S1 | 43 205 Feb |
| Sectionalized Vertical Antenna | 48 IRE 2,11,15.S1 | Separate |
| Sectoral Horn | 48 IRE 2,11,15.S1 | Separate |
| Sector Display | 54 IRE 12.S1 | 43 205 Feb |
| Sector Scanning | 48 IRE 2,11,15.S1 | Separate |
| Selectance | 52 IRE 17.S1 | 40 1685 Dec |
| Selection Check | 56 IRE 8.S1 | 44 1172 Sep |
| Selective Fading | 50 IRE 24.S1 | 38 1267 Nov |
| Selectivity | 52 IRE 17.S1 | 40 1685 Dec |
| Selector Pulse | 54 IRE 12.S1 | 43 205 Feb |
| Self-Checking Code | 56 IRE 8.S1 | 44 1172 Sep |
| Self-instructed Carry | 50 IRE 8.S1 | 39 276 Mar |
| Self-Pulse Modulation | 48 IRE 2,11,15.S1 | Separate |
| Self-Quenched Counter Tube | 57 IRE 7.S2 | 45 1004 Jul |
| Semiconductor | 54 IRE 7.S2 | 42 1507 Oct |
| Semiconductor, Compensated | 54 IRE 7.S2 | 42 1507 Oct |

| | Standard | Proceedings Vol Page Mo |
|---|---|---|
| Slope Deviation | 49 IRE 12.S1 | 37 1370 Dec |
| Slot Antenna | 48 IRE 2,11,15.S1 | Separate |
| Slug Tuner | 55 IRE 2.S1 | 43 1074 Sep |
| Slug Tuning | 48 IRE 2,11,15.S1 | Separate |
| Small-Signal Forward Transadmittance | 57 IRE 7.S2 | 45 1006 Jul |
| Soft Spot | 54 IRE 12.S1 | 43 206 Feb |
| Sonar | 54 IRE 12.S1 | 43 206 Feb |
| Sone | 51 IRE 6.S1 | 39 526 May |
| Sonne | 54 IRE 12.S1 | 43 209 Feb |
| Sound | 51 IRE 6.S1 | 39 526 May |
| Sound Absorption | 51 IRE 6.S1 | 39 526 May |
| Sound Absorption Coefficient | 51 IRE 6.S1 | 39 526 May |
| Sound Analyzer | 51 IRE 6.S1 | 39 526 May |
| Sound Articulation | 51 IRE 6.S1 | 39 526 May |
| Sound Energy | 51 IRE 6.S1 | 39 526 May |
| Sound-Energy Density | 51 IRE 6.S1 | 39 526 May |
| Sound-Energy Flux | 51 IRE 6.S1 | 39 527 May |
| Sound Field | 51 IRE 6.S1 | 39 527 May |
| Sound Intensity | 51 IRE 6.S1 | 39 527 May |
| Sound Level | 51 IRE 6.S1 | 39 527 May |
| Sound Level Meter | 51 IRE 6.S1 | 39 527 May |
| Sound Power of a Source | 51 IRE 6.S1 | 39 527 May |
| Sound Pressure Level | 51 IRE 6.S1 | 39 527 May |
| Sound Probe | 51 IRE 6.S1 | 39 528 May |
| Sound Recording System | 51 IRE 6.S1 | 39 528 May |
| Sound Reflection Coefficient | 51 IRE 6.S1 | 39 528 May |
| Sound Reproducing System | 51 IRE 6.S1 | 39 528 May |
| Sound Track | 51 IRE 6.S1 | 39 528 May |
| Sound Transmission Coefficient | 51 IRE 6.S1 | 39 528 May |
| Source | 54 IRE 3.S1 | 42 1112 Jul |
| Source Impedance | 54 IRE 3.S1 | 42 1112 Jul |
| Space Charge | 57 IRE 7.S2 | 45 1006 Jul |
| Space-Charge Debunching | 57 IRE 7.S2 | 45 1006 Jul |
| Space-Charge Density | 57 IRE 7.S2 | 45 1006 Jul |
| Space-Charge Grid | 57 IRE 7.S2 | 45 1006 Jul |
| Space-Charge-Limited Current | 57 IRE 7.S2 | 45 1006 Jul |
| Space-Charge Region | 54 IRE 7.S2 | 42 1508 Oct |
| Space Pattern | 55 IRE 23.S1 | 43 621 May |
| Spacing Wave (Back Wave) | 48 IRE 2,11,15.S1 | Separate |
| Spark-Gap Modulation | 48 IRE 2,11,15.S1 | Separate |
| Spark Transmitter | 48 IRE 2,11,15.S1 | Separate |
| Speaker | 52 IRE 17.S1 | 40 1685 Dec |
| Specific Acoustic Impedance | 51 IRE 6.S1 | 39 528 May |
| Specific Acoustic Reactance | 51 IRE 6.S1 | 39 528 May |
| Specific Acoustic Resistance | 51 IRE 6.S1 | 39 528 May |
| Specific Repetition Rate | 54 IRE 12.S1 | 43 206 Feb |
| Spectral Characteristic | 57 IRE 7.S2 | 45 1006 Jul |
| Spectral Characteristic | 55 IRE 22.S1 | 43 748 Jne |
| Spectral Sensitivity Characteristic | 57 IRE 7.S2 | 45 1006 Jul |
| Spectrum Locus | 55 IRE 22.S1 | 43 748 Jne |
| Spherical-Earth Factor | 50 IRE 24.S1 | 38 1267 Nov |
| Spherical Hyperbola | 54 IRE 12.S1 | 43 206 Feb |
| Spherical Wave | 50 IRE 24.S1 | 38 1267 Nov |
| Spike Leakage Energy | 57 IRE 7.S2 | 45 1006 Jul |
| Spill | 57 IRE 7.S2 | 45 1006 Jul |
| Spinner | 54 IRE 12.S1 | 43 206 Feb |
| Spiral Scanning | 48 IRE 2,11,15.S1 | Separate |
| Split-Anode Magnetron | 57 IRE 7.S2 | 45 1006 Jul |
| Split Hydrophone | 51 IRE 6.S1 | 39 528 May |
| Split Projector | 51 IRE 6.S1 | 39 528 May |
| Spot | 50 IRE 7.S1 | 38 437 Apr |
| Spot Projection | 56 IRE 9.S1 | 44 780 Jne |
| Spot Speed | 56 IRE 9.S1 | 44 780 Jne |
| Spurious Pulse Mode | 52 IRE 20.S1 | 40 554 May |
| Spurious Radiation | 48 IRE 2,11,15.S1 | Separate |
| Spurious Response Ratio | 52 IRE 17.S1 | 40 1685 Dec |
| Spurious Tube Counts | 57 IRE 7.S2 | 45 1006 Jul |
| Sputtering | 51 IRE 6.S1 | 39 528 May |
| Square Wave | 52 IRE 17.S1 | 40 1685 Dec |
| Square-Wave Response | 57 IRE 7.S2 | 45 1006 Jul |
| Square-Wave Response Characteristic | 57 IRE 7.S2 | 45 1006 Jul |
| Squeezable Waveguide | 54 IRE 12.S1 | 43 206 Feb |
| Squeeze Track | 51 IRE 6.S1 | 39 528 May |
| Squelch | 52 IRE 17.S1 | 40 1685 Dec |
| Squint | 54 IRE 12.S1 | 43 206 Feb |
| Squitter | 54 IRE 12.S1 | 43 206 Feb |
| SRE (Surveillance Radar Element) | 54 IRE 12.S1 | 43 209 Feb |
| Stabilization | 54 IRE 12.S1 | 43 206 Feb |
| Stabilized Feedback | 48 IRE 2,11,15.S1 | Separate |
| Stabilized Flight | 54 IRE 12.S1 | 43 206 Feb |
| Stable Element | 54 IRE 12.S1 | 43 206 Feb |
| Stage Efficiency | 48 IRE 2,11,15.S1 | Separate |
| Stagger | 56 IRE 9.S1 | 44 780 Jne |
| Stalo | 54 IRE 12.S1 | 43 206 Feb |
| Stamper | 51 IRE 6.S1 | 39 528 May |
| Standard Microphone | 51 IRE 6.S1 | 39 528 May |
| Standard Observer | 55 IRE 22.S1 | 43 748 Jne |
| Standard Pitch | 51 IRE 6.S1 | 39 528 May |
| Standard Propagation | 50 IRE 24.S1 | 38 1267 Nov |
| Standard Refraction | 50 IRE 24.S1 | 38 1267 Nov |
| Standard Sea Water Conditions | 51 IRE 6.S1 | 39 529 May |
| Standard Volume Indicator | 54 IRE 3.S1 | 42 1112 Jul |
| Standing-on-Nines Carry | 56 IRE 8.S1 | 44 1173 Sep |
| Standing Wave | 50 IRE 24.S1 | 38 1268 Nov |
| Standing Wave | 53 IRE 2.S1 | 41 1725 Dec |
| Standing-Wave Loss Factor | 53 IRE 2.S1 | 41 1725 Dec |
| Standing-Wave Ratio | 53 IRE 2.S1 | 41 1725 Dec |
| Star Chain | 54 IRE 12.S1 | 43 206 Feb |
| Star Network | 50 IRE 4.S1 | 38 28 Jan |
| Start Record Signal | 56 IRE 9.S1 | 44 780 Jne |
| Start Signal | 56 IRE 9.S1 | 44 780 Jne |
| Starter | 57 IRE 7.S2 | 45 1006 Jul |
| Starter Breakdown Voltage | 57 IRE 7.S2 | 45 1006 Jul |
| Starter Gap | 57 IRE 7.S2 | 45 1006 Jul |
| Starter Voltage Drop | 57 IRE 7.S2 | 45 1006 Jul |
| Starting Current of an Oscillator | 57 IRE 7.S2 | 45 1006 Jul |
| Static Characteristic | 57 IRE 7.S2 | 45 1006 Jul |
| Static Pressure | 51 IRE 6.S1 | 39 529 May |
| Static Register | 50 IRE 8.S1 | 39 276 Mar |
| Staticizer | 56 IRE 8.S1 | 44 1173 Sep |
| STC | 54 IRE 12.S1 | 43 206 Feb |
| Steady-State Oscillation | 51 IRE 6.S1 | 39 529 May |
| Steerable Antenna | 48 IRE 2,11,15.S1 | Separate |
| Stereophonic Sound System | 51 IRE 6.S1 | 39 529 May |
| Sticking Picture | 57 IRE 7.S2 | 45 1006 Jul |
| Stirring Effect | 55 IRE 10.S1 | 43 1072 Sep |
| Stop Record Signal | 56 IRE 9.S1 | 44 780 Jne |
| Stop Signal | 56 IRE 9.S1 | 44 780 Jne |
| Storage | 56 IRE 8.S1 | 44 1173 Sep |
| Storage Capacity | 56 IRE 8.S1 | 44 1173 Sep |
| Storage Element | 57 IRE 7.S2 | 45 1006 Jul |
| Storage Time | 57 IRE 7.S2 | 45 1006 Jul |
| Storage Tube | 57 IRE 7.S2 | 45 1006 Jul |
| Storage Tube | 50 IRE 8.S1 | 39 277 Mar |
| Store | 56 IRE 8.S1 | 44 1173 Sep |
| Streaming | 51 IRE 6.S1 | 39 529 May |
| Strength of a Sound Source | 51 IRE 6.S1 | 39 529 May |
| Striation Technique | 51 IRE 6.S1 | 39 529 May |
| Stroke Speed (Scanning or Recording Line Frequency) | 56 IRE 9.S1 | 44 780 Jne |

| | Standard | PROCEEDINGS Vol Page Mo |
|---|---|---|
| Tracking (Navigation) | 49 IRE 12.S1 | 37 1370 Dec |
| Tracking (Receivers) | 52 IRE 17.S1 | 40 1685 Dec |
| Tracking Error | 51 IRE 6.S1 | 39 530 May |
| Trailing Edge | 55 IRE 23.S1 | 43 622 May |
| Trailing Edge Pulse Time | 51 IRE 20.S1 | 39 626 Jne |
| Transadmittance | 57 IRE 7.S2 | 45 1007 Jul |
| Transadmittance Forward | 57 IRE 7.S2 | 45 1007 Jul |
| Transmittance Compression Ratio | 57 IRE 7.S2 | 45 1007 Jul |
| Transconductance | 57 IRE 7.S2 | 45 1007 Jul |
| Transcriber | 56 IRE 8.S1 | 44 1173 Sep |
| Transducer | 54 IRE 3.S1 | 42 1112 Jul |
| Transducer | 57 IRE 7.S2 | 45 1007 Jul |
| Transducer | 51 IRE 20.S2 | 39 898 Aug |
| Transducer Equivalent Noise Pressure | 51 IRE 6.S1 | 39 530 May |
| Transducer Gain | 54 IRE 3.S1 | 42 1112 Jul |
| Transducer Gain | 51 IRE 20.S2 | 39 899 Aug |
| Transducer Gain | 57 IRE 7.S2 | 45 1008 Jul |
| Transducer Loss | 54 IRE 3.S1 | 42 1112 Jul |
| Transducer Loss | 51 IRE 20.S2 | 39 899 Aug |
| Transducer Pulse Delay | 52 IRE 20.S1 | 40 554 May |
| Transfer | 56 IRE 8.S1 | 44 1173 Sep |
| Transfer Admittance | 42 IRE 9.S1 | Separate |
| Transfer Admittance | 57 IRE 7.S2 | 45 1008 Jul |
| Transfer Characteristic | 57 IRE 7.S2 | 45 1008 Jul |
| Transfer Characteristic | 52 IRE 17.S1 | 40 1685 Dec |
| Transfer Check | 56 IRE 8.S1 | 44 1173 Sep |
| Transfer, Conditional | 50 IRE 8.S1 | 39 277 Mar |
| Transfer Control | 56 IRE 8.S1 | 44 1173 Sep |
| Transfer Current | 57 IRE 7.S2 | 45 1008 Jul |
| Transfer Function | 55 IRE 26.S2 | 44 108 Jan |
| Transfer Ratio | 42 IRE 9.S1 | Separate |
| Transfer Ratio | 55 IRE 26.S2 | 44 108 Jan |
| Transfer, Unconditional | 50 IRE 8.S1 | 39 277 Mar |
| Transformer Loss | 54 IRE 3.S1 | 42 1112 Jul |
| Transformer, Waveguide | 55 IRE 2.S1 | 43 1074 Sep |
| Transient Motion | 51 IRE 6.S1 | 39 530 May |
| Transistor | 54 IRE 7.S2 | 42 1508 Oct |
| Transistor, Conductivity Modulation | 54 IRE 7.S2 | 42 1508 Oct |
| Transistor, Filamentary | 54 IRE 7.S2 | 42 1508 Oct |
| Transistor, Junction | 54 IRE 7.S2 | 42 1508 Oct |
| Transistor, Point-Contact | 54 IRE 7.S2 | 42 1508 Oct |
| Transistor, Point-Junction | 54 IRE 7.S2 | 42 1508 Oct |
| Transistor, Unipolar | 54 IRE 7.S2 | 42 1508 Oct |
| Transit Angle | 57 IRE 7.S2 | 45 1008 Jul |
| Transit-Time Mode | 57 IRE 7.S2 | 45 1008 Jul |
| Transition Frequency | 51 IRE 6.S1 | 39 530 May |
| Transition Loss (in Audio Systems and Components) | 54 IRE 3.S1 | 42 1112 Jul |
| Transition Region | 54 IRE 7.S2 | 42 1508 Oct |
| Transitron Oscillator | 48 IRE 2,11,15.S1 | Separate |
| Translation Loss | 51 IRE 6.S1 | 39 530 May |
| Translator | 56 IRE 8.S1 | 44 1173 Sep |
| Transmission | 51 IRE 6.S1 | 39 530 May |
| Transmission Band | 53 IRE 2.S1 | 41 1725 Dec |
| Transmission Coefficient | 53 IRE 2.S1 | 41 1725 Dec |
| Transmission Gain | 42 IRE 9.S1 | Separate |
| Transmission Level | 48 IRE 2,11,15.S1 | Separate |
| Transmission Level | 42 IRE 9.S1 | Separate |
| Transmission Line | 53 IRE 2.S1 | 41 1725 Dec |
| Transmission Loss | 53 IRE 2.S1 | 41 1725 Dec |
| Transmission Loss (or "Loss") | 42 IRE 9.S1 | Separate |
| Transmission Primaries | 55 IRE 22.S1 | 43 748 Jne |
| Transmitted Wave | 53 IRE 2.S1 | 41 1725 Dec |
| Transmitted Wave | 50 IRE 24.S1 | 38 1268 Nov |
| Transmitter, Facsimile | 56 IRE 9.S1 | 44 780 Jne |
| Transmitter Pulse Delay | 52 IRE 20.S1 | 40 554 May |
| Transmitting Converter, Facsimile (AM to FS Converter) | 56 IRE 9.S1 | 44 780 Jne |
| Transmitting Current Response | 51 IRE 6.S1 | 39 530 May |
| Transmitting Efficiency | 51 IRE 6.S1 | 39 531 May |
| Transmitting Power Response | 51 IRE 6.S1 | 39 531 May |
| Transmitting Voltage Response | 51 IRE 6.S1 | 39 531 May |
| Trans-u Factor | 57 IRE 7.S2 | 45 1008 Jul |
| Transponder | 54 IRE 12.S1 | 43 207 Feb |
| Transponder Beacon | 54 IRE 12.S1 | 43 207 Feb |
| Transponder Crossband | 54 IRE 12.S1 | 43 207 Feb |
| Transponder Reply Efficiency | 54 IRE 12.S1 | 43 207 Feb |
| Transportable Transmitter | 48 IRE 2,11,15.S1 | Separate |
| Transrectification Factor | 57 IRE 7.S2 | 45 1008 Jul |
| Transverse-Beam Traveling-Wave Tube | 57 IRE 7.S2 | 45 1008 Jul |
| Transverse Electric Wave | 53 IRE 2.S1 | 41 1725 Dec |
| Transverse Electric Wave | 50 IRE 24.S1 | 38 1268 Nov |
| Transverse Electromagnetic Wave | 50 IRE 24.S1 | 38 1268 Nov |
| Transverse Electromagnetic Wave | 53 IRE 2.S1 | 41 1725 Dec |
| Transverse-Field Traveling Wave Tube | 57 IRE 7.S2 | 45 1008 Jul |
| Transverse Magnetic Wave | 53 IRE 2.S1 | 41 1725 Dec |
| Transverse Magnetic Wave | 50 IRE 24.S1 | 38 1268 Nov |
| Transverse Magnetization | 51 IRE 6.S1 | 39 531 May |
| Traveling Plane Wave | 53 IRE 2.S1 | 41 1725 Dec |
| Traveling Plane Wave | 50 IRE 24.S1 | 38 1268 Nov |
| Traveling-Wave Magnetron | 57 IRE 7.S2 | 45 1008 Jul |
| Traveling-Wave Magnetron Oscillations | 57 IRE 7.S2 | 45 1008 Jul |
| Traveling-Wave Tube | 57 IRE 7.S2 | 45 1008 Jul |
| Traveling-Wave Tube Interaction Circuit | 57 IRE 7.S2 | 45 1008 Jul |
| Tree | 50 IRE 4.S1 | 38 29 Jan |
| Triad | 54 IRE 12.S1 | 43 207 Feb |
| Tricon | 54 IRE 12.S1 | 43 209 Feb |
| Trigatron | 54 IRE 12.S1 | 43 207 Feb |
| Trigger Level | 54 IRE 12.S1 | 43 207 Feb |
| Triode | 57 IRE 7.S2 | 45 1008 Jul |
| Triplet | 54 IRE 12.S1 | 43 207 Feb |
| Tristimulus Values | 55 IRE 22.S1 | 43 748 Jne |
| Troposphere | 50 IRE 24.S1 | 38 1268 Nov |
| Tropospheric Wave | 50 IRE 24.S1 | 38 1268 Nov |
| Trouble-Location Problem | 50 IRE 8.S1 | 39 277 Mar |
| True Bearing | 49 IRE 12.S1 | 37 1370 Dec |
| True Course | 49 IRE 12.S1 | 37 1370 Dec |
| True Heading | 49 IRE 12.S1 | 37 1370 Dec |
| True Homing | 49 IRE 12.S1 | 37 1370 Dec |
| Truncation Error | 50 IRE 8.S1 | 39 277 Mar |
| Tube | 57 IRE 7.S2 | 45 1008 Jul |
| Tube | 52 IRE 17.S1 | 40 1685 Dec |
| Tube Count | 57 IRE 7.S2 | 45 1009 Jul |
| Tube Heating Time | 57 IRE 7.S2 | 45 1009 Jul |
| Tube, Vacuum | 52 IRE 17.S1 | 40 1685 Dec |
| Tube Voltage Drop | 57 IRE 7.S2 | 45 1009 Jul |
| Tuned-Grid Oscillator | 48 IRE 2,11,15.S1 | Separate |
| Tuned-Grid Tuned-Plate Oscillator | 48 IRE 2,11,15.S1 | Separate |
| Tuned-Plate Oscillator | 48 IRE 2,11,15.S1 | Separate |
| Tuner, Waveguide | 55 IRE 2.S1 | 43 1074 Sep |
| Tuning, Electronic | 57 IRE 7.S2 | 45 1009 Jul |
| Tuning Probe | 55 IRE 2.S1 | 43 1074 Sep |
| Tuning Range | 57 IRE 7.S2 | 45 1009 Jul |
| Tuning Range, Electronic | 57 IRE 7.S2 | 45 1009 Jul |

| | Standard | PROCEEDINGS Vol Page Mo |
|---|---|---|
| Wave Front | 42 IRE 9.S1 | Separate |
| Waveguide | 50 IRE 24.S1 | 38 1268 Nov |
| Waveguide | 53 IRE 2.S1 | 41 1725 Dec |
| Waveguide Wavelength | 53 IRE 2.S1 | 41 1725 Dec |
| Wave Heating | 55 IRE 10.S1 | 43 1072 Sep |
| Wave Interference | 50 IRE 24.S1 | 38 1268 Nov |
| Wavelength | 50 IRE 24.S1 | 38 1268 Nov |
| Wave Normal | 53 IRE 2.S1 | 41 1725 Dec |
| Wave Normal | 50 IRE 24.S1 | 38 1268 Nov |
| Wave Tail | 42 IRE 9.S1 | Separate |
| Wax | 51 IRE 6.S1 | 39 532 May |
| Wax Original | 51 IRE 6.S1 | 39 532 May |
| Way Point | 54 IRE 12.S1 | 43 207 Feb |
| Weighting | 48 IRE 2,11,15.S1 | Separate |
| White | 55 IRE 22.S1 | 43 748 Jne |
| White Compression (White Saturation) | 55 IRE 23.S1 | 43 622 May |
| White Object | 55 IRE 22.S1 | 43 748 Jne |
| White Peak | 55 IRE 23.S1 | 43 622 May |
| White Recording | 56 IRE 9.S1 | 44 781 Jne |
| White Signal | 56 IRE 9.S1 | 44 781 Jne |
| White-to-Black Frequency Swing | 42 IRE 9.S1 | Separate |
| White-to-Black Amplitude Range | 42 IRE 9.S1 | Separate |
| White Transmission | 56 IRE 9.S1 | 44 781 Jne |
| Whole Tone | 51 IRE 6.S1 | 39 532 May |
| Wide-Band Axis | 55 IRE 22.S1 | 43 748 Jne |
| Wide-Band Improvement | 48 IRE 2,11,15.S1 | Separate |
| Wide-Band Ratio | 48 IRE 2,11,15.S1 | Separate |
| Williams-Tube Storage | 56 IRE 8.S1 | 44 1173 Sep |
| Word | 56 IRE 8.S1 | 44 1173 Sep |
| Word Time | 56 IRE 8.S1 | 44 1173 Sep |
| Work Coil | 55 IRE 10.S1 | 43 1072 Sep |
| Work Function | 57 IRE 7.S2 | 45 1010 Jul |
| Wow | 52 IRE 17.S1 | 40 1685 Dec |
| Write | 56 IRE 8.S1 | 44 1173 Sep |
| Write | 57 IRE 7.S2 | 45 1010 Jul |
| Writing Speed | 57 IRE 7.S2 | 45 1010 Jul |
| Wye Junction | 55 IRE 2.S1 | 43 1074 Sep |
| **X** | | |
| X Wave | 50 IRE 24.S1 | 38 1268 Nov |
| **Y** | | |
| Y Network | 51 IRE 4.S1 | 39 29 Jan |
| **Z** | | |
| Z (Zone) Marker | 54 IRE 12.S1 | 43 209 Feb |
| Zero-Subcarrier Chromaticity | 55 IRE 22.S1 | 43 748 Jne |
| Zero Time Reference | 54 IRE 12.S1 | 43 207 Feb |
| Zone (Z) Marker | 49 IRE 12.S1 | 37 1371 Dec |
| Zone Leveling | 54 IRE 7.S2 | 42 1508 Oct |
| Zone Purification | 54 IRE 7.S2 | 42 1508 Oct |
| Zoning | 48 IRE 2,11,15.S1 | Separate |

# Measurement of the Radar Cross Section of a Man*

F. V. SCHULTZ†, SENIOR MEMBER, IRE, R. C. BURGENER‡, ASSOCIATE MEMBER, IRE, AND S. KING§, SENIOR MEMBER, IRE

*Summary*—Both the monostatic and the bistatic radar cross sections[1] of a man were measured at the five frequencies 410, 1120, 2890, 4800, and 9375 mc. The measurements were made using both horizontal and vertical polarizations, and for various directions of facing, or aspects, of the man being used as a target. The cw Doppler method[2] was used in making the measurements. The man whose cross section was measured weighed about 200 pounds and he was six feet tall.

It was found that the man's cross section varied as follows, depending primarily upon polarization of the incident wave and aspect of the man:

| | |
|---|---|
| 410 mc | 0.033 to 2.33 square meters |
| 1120 mc | 0.098 to 0.997 square meters |
| 2890 mc | 0.140 to 1.05 square meters |
| 4800 mc | 0.368 to 1.88 square meters |
| 9375 mc | 0.495 to 1.22 square meters. |

A few measurements were made with men of different sizes, and these indicate that the cross section is approximately proportional to the weight of the man.

* Original manuscript received by the IRE, June 6, 1957; revised manuscript received, October 21, 1957. This work was conducted by Project Michigan under Department of the Army Contract, DA-36-039 SC-52654, administered by the U.S. Army Signal Corps, operating under a tri-service charter.

† School of Elec. Eng., Purdue Univ., Lafayette, Ind. Formerly with the Dept. of Elec. Eng., Univ. of Tennessee, Knoxville, Tenn.

‡ Battelle Memorial Inst., Columbus, Ohio. Formerly with the Dept. of Elec. Eng., Univ. of Tennessee, Knoxville, Tenn.

§ Hughes Aircraft Co., Fullerton, Calif. Formerly with the Dept. of Elec. Eng., Univ. of Tennessee, Knoxville, Tenn.

[1] The bistatic radar cross section is measured when the transmitter and receiver are not located on the same radial from the target. The monostatic cross section is a special case of the bistatic cross section. The monostatic value is obtained when the transmitter and receiver are at the same location, and thus on the same radial.

[2] D. D. King and H. Scharfman, "Antenna scattering measurements by modulation of the scatterer," PROC. IRE, vol. 42, pp. 854–858; May, 1954.

## I. Introduction

OFTEN in making radar cross section measurements indicated above, it is desirable to utilize modeling techniques which make possible the use of indoor laboratory facilities for carrying out the measurements. Since a human being is neither a perfect conductor nor a perfect dielectric, it was considered unwise to attempt to use a modeling technique which would involve a modeling of the electrical properties of the target as well as of its size. Consequently full-scale measuring techniques were used.

## II. Experimental Procedure

Since a cw Doppler system was used in making the measurements, it was necessary to impart radial motion (relative to the Doppler transmitter and receiver) to the target in order to obtain a Doppler signal. This was accomplished by constructing a test stand consisting of a wooden A frame that supported a swinging platform on which the man stood. A 16-inch sphere and one with a diameter of 10 inches served as standard targets for calibration purposes, and these were hung from the cross member of the test stand. Nylon cord, with a diameter of about 3/32 inch and a test strength of 190 pounds, supported the swinging platform as well as the standard spheres. No detectable Doppler signal was generated by the motion of these nylon supporting cords.

In order to reduce satisfactorily the Doppler return signal from the swinging platform on which the man stood, it was necessary to erect in front of the platform a barrier of microwave absorbing material. A block of Styrofoam was placed on top of the swinging wooden platform in order that a full view of the man standing thereon would be seen by the Doppler measuring system. The unwanted Doppler return was satisfactorily reduced by these techniques. The test stand was sufficiently rigid that no detectable Doppler return was generated by it. Multiple reflections involving various stationary objects and the swinging targets were believed to be of no consequence since cross checks on the measured cross sections obtained for the two different spheres, used as standards, were very satisfactory.

Each of the transmitters used consisted of a suitable cw generator coupled to an appropriate antenna, which could be rotated about a horizontal axis. This made possible the emission of either horizontally or vertically polarized waves. At the receiver an antenna identical to the transmitting antenna was coupled to a superheterodyne-type receiver. During operation the Doppler-shifted signal from the target and the leakage signal from the transmitter passed through the receiver and produced a Doppler beat signal at the output of the second detector of the receiver. This signal was fed through a variable band-pass audio filter to reduce the noise, and then finally used to drive the pen of a recording oscillograph. The pen deflections were proportional to the voltage of the Doppler signal returned by the target, the linearity of the system having been verified over the operating range. Typical tape records taken on the oscillograph are illustrated in Fig. 1(a) and 1(b).

A series of measurements commenced with setting the transmitter and receiver side by side at the correct distance from the test stand and directly in front of the test stand. Measurements were first made of the Doppler signals returned by each of the two spheres used as standards. After these calibration recordings the man was placed on the movable platform of the test stand and the Doppler signal returned by the swinging man was recorded with the man facing the Doppler transmitter and receiver. Further measurements were made of the signal returned by the man after he was rotated 45° about a vertical axis, then a 90° rotation (side view), next 135°, and finally 180° (rear view). Returns for five different aspects of the man were thus obtained. Following the recordings of the man's returns, calibration recordings of the two standards were made again. The entire process was then repeated, so that at least two series of records were obtained for each set of conditions. These measurements yielded the monostatic radar cross section of the man for one particular frequency and polarization.

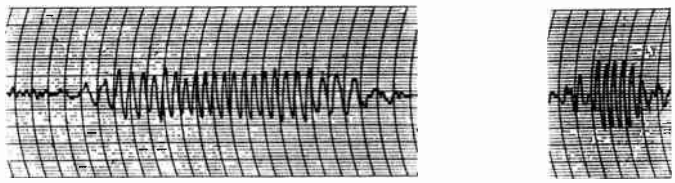

(a) (b)

Fig. 1—(a) Recording of the 16-inch standard sphere made at 9375 mc, a bistatic angle of 30°, and horizontal polarization. The voltage scale is 10 mv per mm, and the recording speed was 125 mm per second. (b) Recording of man's return at 45° front aspect with all conditions as above, except that the recording tape speed was 25 mm per second.

In order to measure the bistatic cross section, the transmitter was first moved 15° clockwise, considering the test stand and the line of motion of the swinging target platform as references, and the Doppler receiver was moved 15° counterclockwise. The measuring process described in the preceding paragraph was repeated and thus the 30° bistatic-angle radar cross section of the man was obtained. In the same way the 60° and 90° bistatic-angle cross sections were measured.

Since it was not feasible to elevate the Doppler system and the target sufficiently above the ground to eliminate the ground-reflected waves, it was necessary to take steps to reduce sufficiently the variation of field intensity over the surface of the man, this variation being caused by the interference between the direct wave from the transmitter and the ground-reflected wave. A similar phenomenon existed, of course, for the

propagation path from the target to the receiving antenna. The most satisfactory means of reducing this effect proved to be the use of diffracting screens[3,4] placed on the ground between the transmitter and target and between the target and receiver. By this method it was possible to reduce the measured field variation in the area occupied by the target to approximately plus or minus 1 db.

Since the cw Doppler system employed for the measurements detects all moving objects, noise caused by moving vegetation and insects entered the system along with the return from the desired target. The effect of this noise was satisfactorily reduced by taking three steps. First, a band-pass filter centered at the frequency of the target return was connected to the output of the second detector of the receiver to eliminate the portion of the clutter return that was not at the target frequency. Second, vegetation was removed as much as possible. Third, the transmitter and receiver were moved as close as allowable to the target so that a return of sufficient magnitude to override the clutter might be received from the target.

The third step mentioned above could not be carried to an extreme because of the requirement that the phase-front curvature of the rf wave over the target be satisfactorily small. A number of workers in the microwave measurements field have developed experimental and theoretical criteria for the minimum range necessary in radar cross section measurements in order to minimize the errors resulting from the curvature of the wave phase front at the target.[2-5] For the present measurements the criterion for allowable phase-front curvature was set at $\pi/16$ radian. The minimum range for the measurements as developed from this criterion is $R=4D^2/\lambda$, where $R$ is the minimum permissible range, $D$ is the major dimension of the target, and $\lambda$ is the wavelength at which the measurements are being made. Computations from the above equation, with $D$ equal to six feet, give the results shown in Table I. No allowance was made here for phase shifts introduced by the ground-reflected wave.

At 4800 mc and 9375 mc, it was not possible to obtain adequately large return signals from the target for target-transmitter separations of greater than 400 feet because of extraneous signal return from moving vegetation. The phase-front curvature over the target for this separation of 400 feet and for 4800 and 9375 mc is of course greater than $\pi/16$ radian, selected as the maximum allowable. Consequently it was necessary to determine as well as possible the results of this condition. In order to do this, an experiment was undertaken

TABLE I

MINIMUM ALLOWABLE SEPARATION ($R$) BETWEEN TRANSMITTER AND TARGET FOR A MAXIMUM PHASE-FRONT VARIATION OVER THE TARGET OF $\pi/16$ RADIAN. TARGET HEIGHT IS 6 FEET

| Frequency | $R$ |
|---|---|
| 410 mc | 60 feet |
| 1120 mc | 164 feet |
| 2890 mc | 422 feet |
| 4800 mc | 702 feet |
| 9375 mc | 1370 feet |

to evaluate this effect of phase-front curvature on the measured cross section of a man. This experiment was conducted at a frequency of 1120 mc and consisted of identical measurements made at three different ranges. The first range used (71 feet) was chosen because it produced the same phase variation over the target as occurred during the 9375-mc measurements made at a range of 400 feet. The second range (104 feet) simulated the conditions of phase variation during the 4800-mc measurements, while the third range (200 feet) insured a phase variation of less than the $\pi/16$-radian criterion. In all three measurements the diffracting screens were used to make the signal strength over the target uniform. It was not possible to scale the target, so the measurements were not completely definitive, but the results did indicate that an error of probably not more than about 20 per cent was introduced in the 9375-mc measurements, and one of probably not more than about 5 per cent in the 4800-mc results.

## III. DATA REDUCTION

As mentioned previously, the Doppler beat signal generated by the moving target was traced on paper tape by a recording oscillograph. Sample tape recordings are shown in Fig. 1(a) and 1(b), and, as stated before, the deflections are proportional to the voltage of the Doppler beat signal. The measurement procedure has also been described earlier in the paper; this consisted of first obtaining calibration recordings of the two standard spheres, then recordings of the human target, and finally check recordings of the two spheres. The entire procedure was then repeated once or twice.

The first step in the data reduction consisted of reading the deflections recorded on the tapes. This was done by drawing straight lines through the average peak values and the average through values attained by the deflections, after the Doppler beat signal had settled down to a fairly steady tone. The averaging process was done visually. These total swings on the tapes were read and recorded for both the human target and the spheres. The two sets of values obtained on the spheres, one set at the beginning of an experiment and the other at the end, were averaged. In no case were these two sets of values sufficiently different to indicate a systematic drift in the characteristics of the complete measurement system.

[3] H. E. Bussey, "Reflected ray suppression," PROC. IRE, vol. 38, p. 1453; December, 1950.
[4] C. C. Cutler, A. P. King, and W. E. Kock, "Microwave antenna measurements," PROC. IRE, vol. 35, pp. 1469-1470; December, 1947.
[5] D. R. Rhodes, "On minimum range for radiation patterns," PROC. IRE, vol. 42, pp. 1408-1410; September, 1954.

TABLE II
CALCULATED RADAR CROSS SECTIONS IN SQUARE METERS OF THE STANDARD SPHERES

| Sphere | Frequency | Horizontal Polarization | | | | Vertical Polarization | | | |
|---|---|---|---|---|---|---|---|---|---|
| | | Bistatic Angle in Degrees | | | | Bistatic Angle in Degrees | | | |
| | | 0° | 30° | 60° | 90° | 0° | 30° | 60° | 90° |
| 10 inches | 410 mc | 0.17886 | 0.15720 | 0.10073 | 0.04017 | 0.17886 | 0.17915 | 0.17162 | 0.15300 |
| 16 inches | 1120 mc | 0.16911 | 0.09064 | 0.17965 | 0.11448 | 0.16911 | 0.14704 | 0.20315 | 0.23490 |
| 16 inches | 2890 mc | 0.12901 | 0.12901 | 0.12901 | 0.12901 | 0.12901 | 0.12901 | 0.12901 | 0.12901 |
| 16 inches | 4800 mc | 0.12888 | 0.12888 | 0.12888 | 0.12888 | 0.12888 | 0.12888 | 0.12888 | 0.12888 |
| 16 inches | 9375 mc | 0.12888 | 0.12888 | 0.12888 | 0.12888 | 0.12888 | 0.12888 | 0.12888 | 0.12888 |

Since the targets were swung through a distance of never less than about two wavelengths, the error due to changing target velocity, as discussed by Ruze,[6] should never exceed about 10 per cent.

After all the tape deflection readings for the signal return from the human target were recorded, they were smoothed by the use of a least-squares technique and these final regression values were used for calculating the radar cross sections.

The radar cross section of the human target, corresponding to each final regression value of tape deflection, was calculated by using the following:

$$\sigma_m = \left[\frac{R_m}{R_s}\right]^2 \sigma_s.$$

Here

$\sigma_m$ = radar cross section, in square meters, of the man.

$R_m$ = tape deflection, in millimeters, corresponding to Doppler signal generated by human target.

$R_s$ = tape deflection, in millimeters, corresponding to Doppler signal generated by sphere used as standard for calibration.

$\sigma_s$ = calculated radar cross section, in square meters, of the sphere used as a standard.

In all cases, except at 410 mc, the 16-inch sphere was used as a standard and the readings obtained on the 10-inch sphere were used as a check of the system accuracy. The calculated and the measured values of the cross section of this 10-inch sphere differed by an average of about 0.5 db, or about 12 per cent.

The radar cross sections of the spheres at the lower frequencies were calculated by using the exact electromagnetic solution.[7] At the higher frequencies the geometrical optics values were used. The calculated cross sections of the spheres are listed in Table II. It should be mentioned that the average diameter of the 16-inch sphere was 15.95 inches and that of the 10-inch sphere was 9.88 inches. The sphericity of both spheres was excellent, various diameters differing by only 3/32 inch, or less.

## IV. Results Obtained

The values of the radar cross section of the man are listed in Tables III–VII, inclusive, for the various frequencies, polarizations, bistatic angles, and aspect angles used in the experiment. It is an easy matter to see from the tables how the radar cross section of the man varies with aspect angle and with bistatic angle for a given frequency and a given polarization, but the variations with frequency and with polarization are somewhat more difficult to observe. For this reason Fig. 2–Fig. 6 have been prepared. Values of the cross section, averaged over bistatic angle, are shown in Fig. 2 and in normalized form in Fig. 3. For Fig. 4 and Fig. 5 the values of cross section were averaged over target aspect for given values of polarization, frequency, and bistatic angle. The curves then give indications of how, for a given polarization and frequency, the man's cross section varies with bistatic angle. In order to obtain Fig. 6, the cross section values corresponding to a given polarization and frequency were averaged over bistatic angle and aspect of the target. Fig. 6 then indicates how these average values of cross section vary with frequency for each of the two polarizations.

## V. Conclusion

As shown in the Summary, the measured radar cross section of the man used varies from 0.033 square meter to 2.33 square meters. These extreme values were obtained at 410 mc, the smaller for horizontal polarization and a side view of the man, the larger for vertical polarization and a rear view of the man. These results might be expected for a quasi-cylindrical target such as a man. As the frequency was increased the cross section differed less and less between the two polarizations.

Examination of Tables III–VII reveals that, in general, the cross section is least for a side view of the man and

[6] J. Ruze, "Errors in Radar Cross-Section Reflection Measurements," Air Force Cambridge Field Station, Cambridge, Mass., Rep. No. 4-24; July 30, 1947.

[7] D. E. Kerr, "Propagation of Short Radio Waves," McGraw-Hill Book Co., New York, N. Y., pp. 445–454; 1951.

TABLE III

RADAR CROSS SECTIONS IN SQUARE METERS FOR 410 MC

| Target Aspect | Horizontal Polarization | | | | Vertical Polarization | | | |
|---|---|---|---|---|---|---|---|---|
| | Bistatic Angle in Degrees | | | | Bistatic Angle in Degrees | | | |
| | 0° | 30° | 60° | 90° | 0° | 30° | 60° | 90° |
| Front | 0.897 | 0.641 | 0.795 | 0.464 | 1.127 | 0.939 | 1.628 | 2.163 |
| 45° Front | 0.197 | 0.108 | 0.264 | 0.196 | 0.312 | 0.217 | 0.613 | 0.941 |
| Side | 0.083 | 0.033 | 0.157 | 0.136 | 0.161 | 0.095 | 0.397 | 0.681 |
| 45° Rear | 0.321 | 0.197 | 0.367 | 0.251 | 0.464 | 0.346 | 0.816 | 1.174 |
| Rear | 1.091 | 0.796 | 0.931 | 0.529 | 1.343 | 1.138 | 1.880 | 2.327 |

TABLE IV

RADAR CROSS SECTIONS IN SQUARE METERS FOR 1120 MC

| Target Aspect | Horizontal Polarization | | | | Vertical Polarization | | | |
|---|---|---|---|---|---|---|---|---|
| | Bistatic Angle in Degrees | | | | Bistatic Angle in Degrees | | | |
| | 0° | 30° | 60° | 90° | 0° | 30° | 60° | 90° |
| Front | 0.718 | 0.359 | 0.410 | 0.388 | 0.879 | 0.718 | 0.608 | 0.997 |
| 45° Front | 0.322 | 0.156 | 0.124 | 0.154 | 0.433 | 0.344 | 0.224 | 0.447 |
| Side | 0.281 | 0.135 | 0.098 | 0.131 | 0.386 | 0.305 | 0.187 | 0.391 |
| 45° Rear | 0.518 | 0.256 | 0.259 | 0.268 | 0.656 | 0.531 | 0.410 | 0.719 |
| Rear | 0.718 | 0.359 | 0.410 | 0.388 | 0.879 | 0.718 | 0.608 | 0.997 |

TABLE V

RADAR CROSS SECTIONS IN SQUARE METERS FOR 2890 MC

| Target Aspect | Horizontal Polarization | | | | Vertical Polarization | | | |
|---|---|---|---|---|---|---|---|---|
| | Bistatic Angle in Degrees | | | | Bistatic Angle in Degrees | | | |
| | 0° | 30° | 60° | 90° | 0° | 30° | 60° | 90° |
| Front | 0.409 | 0.665 | 0.471 | 0.322 | 0.496 | 0.774 | 0.564 | 0.400 |
| 45° Front | 0.228 | 0.427 | 0.275 | 0.165 | 0.294 | 0.516 | 0.347 | 0.221 |
| Side | 0.198 | 0.386 | 0.242 | 0.140 | 0.260 | 0.471 | 0.310 | 0.192 |
| 45° Rear | 0.268 | 0.481 | 0.318 | 0.198 | 0.339 | 0.574 | 0.395 | 0.260 |
| Rear | 0.613 | 0.920 | 0.688 | 0.506 | 0.719 | 1.048 | 0.800 | 0.602 |

TABLE VI

RADAR CROSS SECTIONS IN SQUARE METERS FOR 4800 MC

| Target Aspect | Horizontal Polarization | | | | Vertical Polarization | | | |
|---|---|---|---|---|---|---|---|---|
| | Bistatic Angle in Degrees | | | | Bistatic Angle in Degrees | | | |
| | 0° | 30° | 60° | 90° | 0° | 30° | 60° | 90° |
| Front | 1.499 | 1.404 | 1.320 | 1.039 | 1.745 | 1.643 | 1.552 | 1.247 |
| 45° Front | 0.858 | 0.786 | 0.724 | 0.521 | 1.047 | 0.968 | 0.898 | 0.670 |
| Side | 0.658 | 0.596 | 0.542 | 0.368 | 0.825 | 0.755 | 0.694 | 0.495 |
| 45° Rear | 0.940 | 0.865 | 0.799 | 0.585 | 1.137 | 1.054 | 0.982 | 0.742 |
| Rear | 1.624 | 1.525 | 1.438 | 1.144 | 1.881 | 1.774 | 1.680 | 1.361 |

TABLE VII

RADAR CROSS SECTIONS IN SQUARE METERS FOR 9375 MC

| Target Aspect | Horizontal Polarization | | | | Vertical Polarization | | | |
|---|---|---|---|---|---|---|---|---|
| | Bistatic Angle in Degrees | | | | Bistatic Angle in Degrees | | | |
| | 0° | 30° | 60° | 60° | 0° | 30° | 60° | 90° |
| Front | 1.018 | 0.749 | 0.933 | 0.799 | 1.003 | 0.736 | 0.919 | 0.786 |
| 45° Front | 0.858 | 0.612 | 0.780 | 0.658 | 0.845 | 0.601 | 0.767 | 0.647 |
| Side | 0.730 | 0.505 | 0.658 | 0.547 | 0.718 | 0.495 | 0.647 | 0.536 |
| 45° Rear | 0.905 | 0.652 | 0.825 | 0.700 | 0.891 | 0.641 | 0.812 | 0.688 |
| Rear | 1.215 | 0.919 | 1.122 | 0.975 | 1.199 | 0.905 | 1.106 | 0.961 |

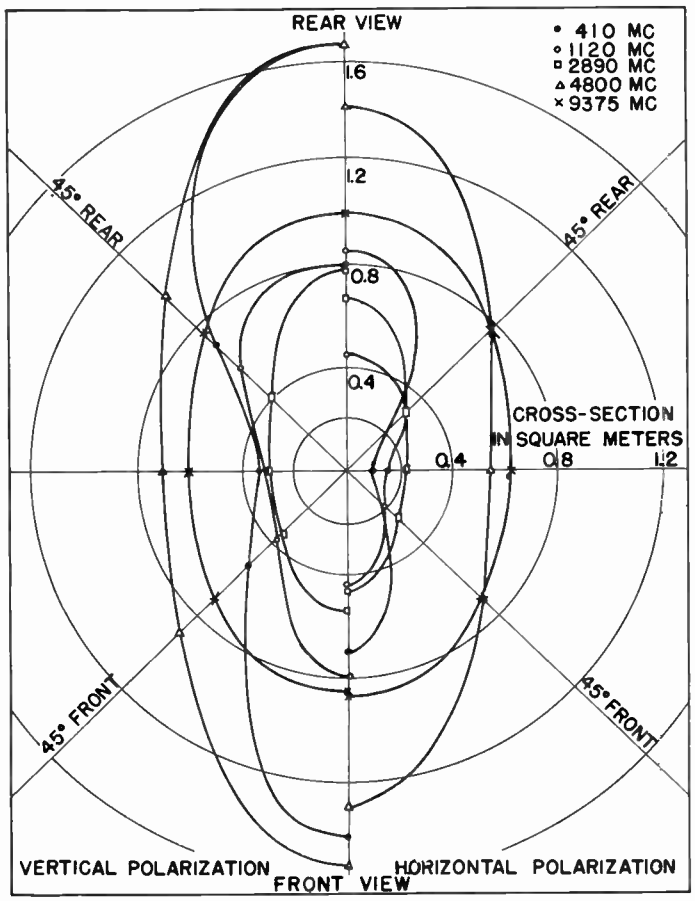


Fig. 2—Average bistatic radar cross section of a man as a function of target aspect angle, with frequency and polarization as parameters.

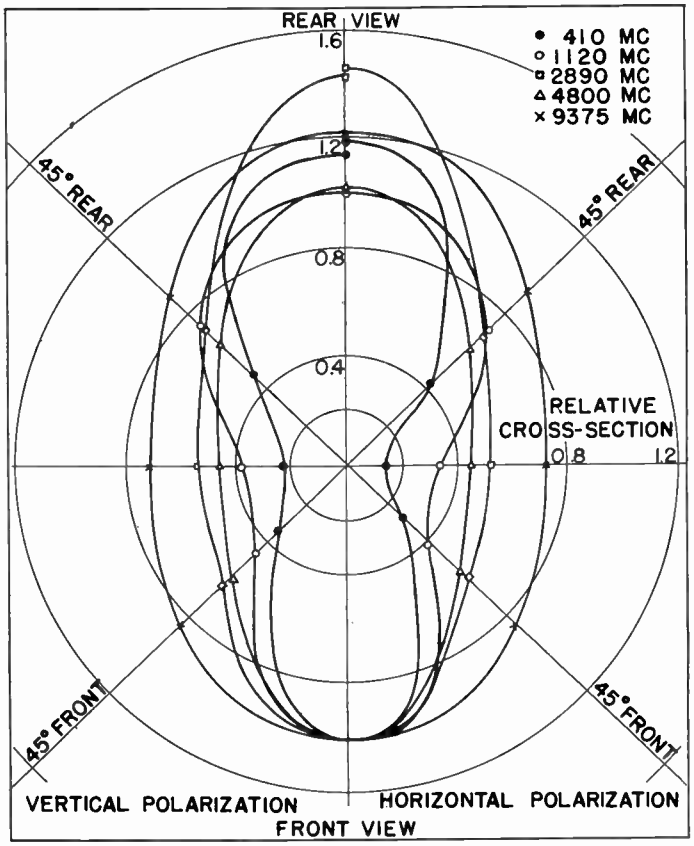


Fig. 3—Average relative bistatic radar cross section of a man as a function of target aspect angle, with frequency and polarization as parameters. (The curves are normalized with respect to the radar cross section of the front aspect.)

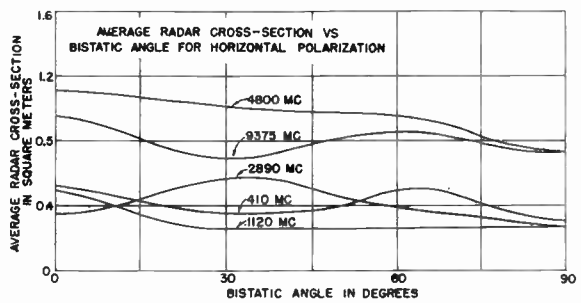


Fig. 4—Average bistatic radar cross section of a man as a function of bistatic angle, for horizontal polarization with frequency as a parameter.

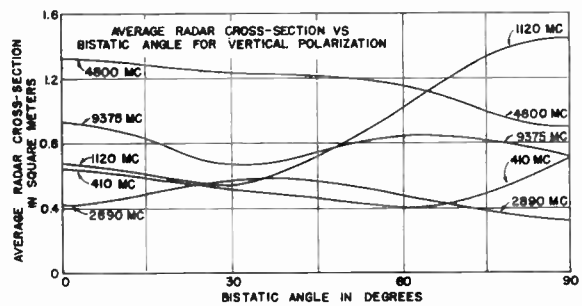


Fig. 5—Average bistatic radar cross section of a man as a function of bistatic angle, for vertical polarization with frequency as a parameter.

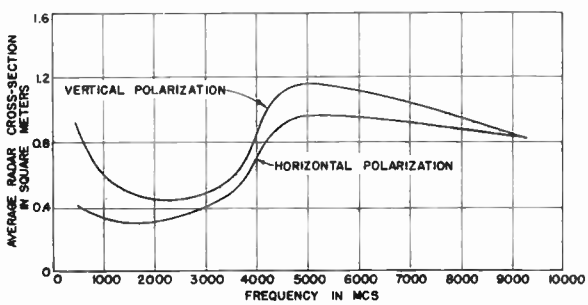


Fig. 6—Average radar cross section of a man as a function of frequency, with polarization as a parameter.

somewhat greater for a rear view than a front view. Fig. 4 and Fig. 5 show that the cross section varies but little with bistatic angle, except for vertical polarization at 410 mc, where the cross section increases about twice as the bistatic angle goes from 0° to 90°. These are not unexpected results.

Fig. 6 illustrates the over-all variation of the cross section with frequency. The general decrease in polarization dependence as the frequency is increased is, of course, to be anticipated. Because of the complex nature of the object being measured, however, no explanation is offered for the other characteristics of the two curves contained in this figure.

# IRE Standards on Television: Measurement of Luminance Signal Levels, 1958*

(58 IRE 23. S1)

## COMMITTEE PERSONNEL

### Subcommittee on Video Signal Transmission Methods of Measurement
1957–1958

J. M. BARSTOW, *Chairman*

M. H. Diehl
A. B. Ettlinger
H. P. Kelly
H. Mate
R. M. Morris
J. R. Popkin-Clurman
E. B. Pores
E. H. Schreiber
L. Staschover
J. W. Wentworth
W. B. Whalley

### Committee on Video Techniques
1957–1958

S. DOBA, JR., *Chairman*
G. L. FREDENDALL, *Vice-Chairman*

I. C. Abrahams
S. W. Athey
A. J. Baracket
J. M. Barstow
J. H. Battison
E. E. Benham
K. B. Benson
E. M. Coan
L. B. Davis
V. J. Duke
J. R. Hefele
J. L. Jones
R. T. Petruzzelli
W. J. Poch

### Standards Committee
1957–1958

M. W. BALDWIN, JR., *Chairman*
C. H. PAGE, *Vice-Chairman*
R. F. SHEA, *Vice-Chairman*
L. G. CUMMING, *Vice-Chairman*

J. Avins
W. R. Bennett
J. G. Brainerd
D. R. Brown
T. J. Carroll
P. S. Carter
A. G. Clavier
G. A. Deschamps
S. Doba, Jr.
J. E. Eiselein
D. Frezzolini
E. A. Gerber
A. B. Glenn
H. Goldberg
V. M. Graham
R. A. Hackbusch
H. C. Hardy
D. E. Harnett
A. G. Jensen
I. M. Kerney
J. G. Kreer, Jr.
W. A. Lynch
A. A. Macdonald
Wayne Mason
D. E. Maxwell
H. R. Mimno
G. A. Morton
J. H. Mulligan, Jr.
W. Palmer
R. L. Pritchard
P. A. Redhead
R. Serrell
H. R. Terhune
W. E. Tolles
J. E. Ward
E. Weber
W. T. Wintringham

### Measurements Coordinator

R. F. SHEA

* Approved by IRE Standards Committee, September 12, 1957. Reprints of this Standard, 58 IRE 23. S1, may be purchased while available from the Institute of Radio Engineers, 1 East 79th Street, New York, N. Y., at $0.60 per copy. A 20 per cent discount will be allowed for 100 or more copies mailed to one address.

## 1.0 Introduction

This Standard is a revision of Part 1 of Standard 50 IRE 23. S1 and replaces in all respects this previously issued part of the Standard. The need for the revision stems from the standardization of color television signals in the USA, and the inadequacy of the earlier Standard in providing methods of measuring the luminance component of the color signal. The revision consists primarily of a change in the response characteristics of the oscilloscopes to insure adequate suppression of the color subcarrier. Other minor changes in wording and in the associated figures have been made to bring the standard into accord with present terminology and practice.

### *1.1 Description*

This Standard describes methods of measuring the significant amplitude levels of a monochrome or color television signal, either composite or noncomposite. It is concerned with measurements at points in transmission systems where the signals are at video frequency. The methods described in this Standard are limited to those involving the use of oscilloscopes, and are primarily directed to specifying means of measuring television signal levels for operating purposes.

For the purposes of this Standard, the levels which are significant are the levels of monochrome signals or the levels of the luminance portion of color signals. The peak amplitude excursion of a color signal may exceed, by substantial amounts, the peak amplitude excursions of the luminance portion of the signal, but since subjective brightness is more nearly proportional to the luminance signal than to any other quantity, it is most desirable from the operating standpoint to control and adjust levels using the luminance signal as a gauge. When this is done, monochrome and color signals, interspersed in a given program sequence, will produce approximately the same brightness and contrast when viewed on color or monochrome monitors without supplementary adjustments.

In the succeeding paragraphs of this Standard, the words "luminance signal" will refer to either a monochrome signal or to the luminance portion of a color signal.

Six significant amplitude levels of a composite luminance signal have been defined as follows.[1] These are shown in the right-hand portion of Fig. 1.

**Reference White Level.** The picture signal level corresponding to a specified maximum limit for *White Peaks.*

**White Peak.** A peak excursion of the picture signal in the white direction.

**Black Peak.** A peak excursion of the picture signal in the black direction.

[1] Cf. "IRE standards on television: Definitions of television signal measurement terms, 1955 (55 IRE 23. S1)," Proc. IRE, vol. 43, pp. 619–622; May, 1955.

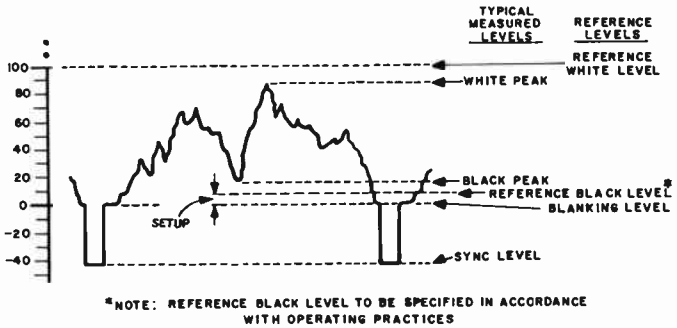


Fig. 1—Significant levels and details of IRE standard scale.

**Reference Black Level.** The picture signal level corresponding to a specified maximum limit for *Black Peaks.*

**Blanking Level.** That level of a composite picture signal which separates the range containing picture information from the range containing synchronizing information.

*Note:* The setup region is regarded as picture information.

**Sync Level.** The level of the peaks of the sync signal.

This Standard specifies a method of measuring the differences between these levels in a manner permitting ready correlation between the measurements at different parts of a system, regardless of the nominal voltages at the points of measurement.

### *1.2 Theory of Measurements*

*1.2.1 General:* The method of level measurement prescribed in this Standard is based on the provision of oscilloscopes of standardized characteristics, with a linear scale for indicating the various levels. The scale is the same on all oscilloscopes, but each oscilloscope is calibrated with a voltage related to the nominal signal level at the point where the measurements are to be made. If the gains or losses between two measuring points on a system are normal, therefore, similar scale readings should be obtained for all the significant levels on oscilloscopes at both points regardless of differences in the voltages at the two points.

*1.2.2 Scale:* The standard scale is shown in the left-hand portion of Fig. 1, together with an illustrative luminance signal to show the relation between the scale and the oscilloscope presentation. It will be observed that the zero or reference point of the scale is placed at the blanking level. The upper part of this scale is marked from 0 to 100 with 100 corresponding to the reference white level. The scale is linear and two additional points (at 110 and 120) are provided to permit reading abnormally high *White Peaks.* The various levels of the picture signal are read on this scale above zero. The lower part of the scale is marked in linear steps from 0 to −50 and on it are read the levels of the sync signal.

Where other scales are used for specific purposes,

such as modulation monitoring at broadcast transmitters, the standard scale should be added to any existing scales to permit correlation with measurements at other points in the system. The standard level scale should be placed with the 0 and 100 markings corresponding to the normal *Blanking* and *Reference White Levels*, respectively, of the other scale.

## 2.0 Apparatus Required

### *2.1 List of Equipment*

A suitable oscilloscope is required for these measurements. Its specifications are given below and form a part of this Standard.

### *2.2 Specifications of Standard Oscilloscope for Level Measurements*

*2.2.1 Measurement Accuracy:* An oscilloscope which is suitable for this application should be capable of television level measurements with errors not exceeding 2.5 units on the scale. Factors which contribute to error include:

Spot size and brightness,
Deflection amplitude,
Amplifier linearity,
Readability of scales or markers, including a reasonable allowance for parallax,
Calibration accuracy, and stability of calibration.

*2.2.2 Bandwidth:* The oscilloscope response characteristic should be such as to introduce negligible measurement errors due to low-frequency distortion or overshoot. The response characteristics should be standardized so that uniform measurements are obtained with different oscilloscopes. The bandwidth should be great enough to yield satisfactory luminance signal level readings and narrow enough that the readings are negligibly affected by the subcarrier portion of a color signal. To meet these requirements, this Standard prescribes that the response shall be monotonic and within the limits indicated in Fig. 2. This provides 20-db attenuation (−3 db or +5 db) at 3.58 mc with respect to the low frequencies and a rise time on the order of 0.3 μsec.

The specified characteristic may be obtained by adding a suitable network to an oscilloscope of wider bandwidth. For example, Fig. 3 shows a one-stage four-terminal network that may be used for this purpose with an oscilloscope having a bandwidth much wider than the specified characteristic. By arranging to remove the network, the oscilloscope can be made available for other uses where its full bandwidth is needed, such as 1) to measure color burst amplitude in terms of IRE scale units or 2) to check the amplitude of chrominance signal peaks on a color test signal. Fig. 3 also shows the circuit constants of an idealized three-stage amplifier having the specified nominal characteristics. For oscilloscopes having intermediate bandwidth, the prescribed responses may be attained with a smaller number of interstage networks or with different constants in the three networks.

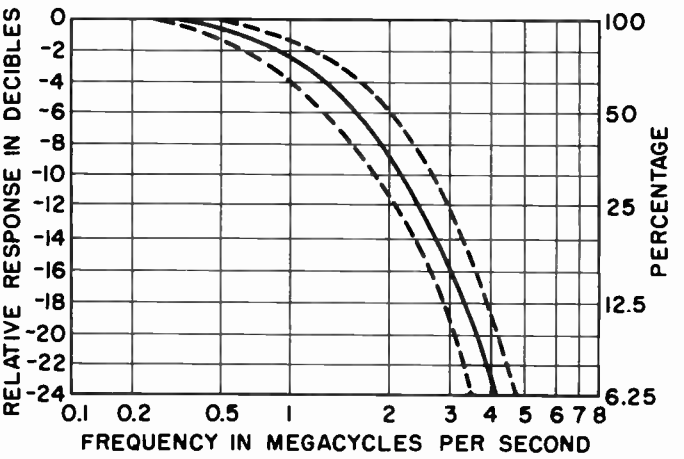


Fig. 2—Frequency response for standard oscilloscope (IRE roll-off).

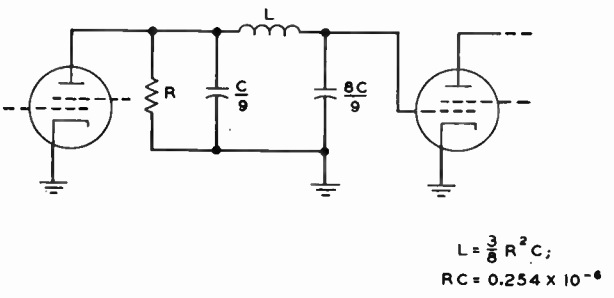


(a)

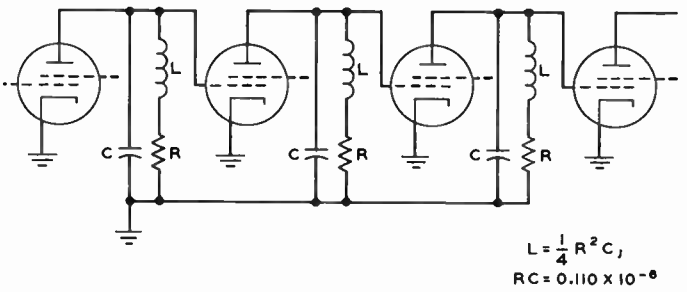


(b)

Fig. 3—Idealized networks for standard oscilloscope, R in ohms, L in henrys, and C in farads. (a) One-stage four-terminal network and (b) three-stage RCL network.

There should be no sudden break in the response curve above 3.58 mc and the maximum response above 5 mc should be at least 20 db down with respect to that of 100 kc. The oscilloscope should indicate less than 2 per cent tilt in a 60-cps symmetrical square wave.

*2.2.3 Scale:* The oscilloscope shall be provided with the standard scale shown in Fig. 1 and described in 1.2.2 of this Standard.

*2.2.4 Calibration:* A suitable voltage calibration means shall be provided.

*2.2.5 DC Restoration:* It is highly desirable that dc

restoration at the deflection plates of the oscilloscope be employed for operational measurements on signals having changing picture content in order to prevent shifts of the trace with variations in average value of the signal. It is desirable that the time constants of such dc restoration circuits be shorter than the equivalent time constants of the ac portions of the oscilloscope amplifier to avoid shift and bounce of the base line with picture changes. At the same time, it is desirable that the time constants of the restoration circuits be as long as the above limitation allows, in order that the true low-frequency content of the signal may be exhibited.

*2.2.6 Vertical and Horizontal Centering:* Means shall be provided for adjusting the relative position of the scale and the oscilloscope image. This may consist either of electrical centering controls on the oscilloscope or of a movable scale.

## 3.0 Method of Measurement

### *3.1 Application*

Whether the oscilloscope is permanently connected to the circuit to be measured, as is the case in many operational systems, or is connected only periodically, care must be taken that the oscilloscope input circuit and the manner of connection have no adverse effect upon the signal circuit. It is essential that the circuit being measured operate with its normal source and the load impedances during the measurements.

In a transmission system the terminations may often be complex impedances, which cause the waveform to appear severely distorted when observed on an oscilloscope bridged across such a circuit. In measuring signal levels at such points, care must be exercised to properly interpret the indications. For example, where a constant-current source is used to drive a transmission system through a coupling transformer, the waveform measured directly across the transformer terminals may be so distorted as to be unusable for level measurements. It is usually preferable to connect the oscilloscope across a constant resistance point in the circuit, to which transmission from the signal origin is constant with frequency.

Low-frequency interference or distortion may seriously impair the accuracy of observation unless effective clamping means are employed. It is therefore recommended that such devices be employed wherever possible.

### *3.2 Adjustment*

In using the oscilloscope the usual precautions must be taken to insure adequate brightness, sharp nonastigmatic beam focus, and gain-control settings which allow the necessary deflection without amplifier overload.

The oscilloscope time base should normally be synchronized at either the line rate or at one half of the line rate when making level measurements, providing a convenient display of the longer duration *Blanking* and *Sync Levels* which occur during the vertical blanking interval. The oscilloscope brightness and focus should be adjusted to make these portions of the signal wave form visible and well defined.

### *3.3 Calibration*

Since, in general, the measurements will be made on a video bus or line in which the signal is to be maintained at a predetermined voltage chosen for that point in the system, it shall be standard practice to maintain an oscilloscope deflection within the appropriate calibrated boundaries of the standard scale.

In using the oscilloscope method of level measurement, accurate calibration of the oscilloscope amplifier gain is a very important aspect of the technique. Calibration is concerned with adjustment of the oscilloscope amplifier gain so that a normal signal will produce a standard oscilloscope deflection. This may conveniently be done by introducing a known calibrating voltage to the input of the oscilloscope in place of the normal input signal. The calibrating signal should be one whose principal frequency components lie within the band of uniform response of the oscilloscope. If such a calibrating signal has a peak-to-peak deflection equivalent to, for example, the *Blanking*-to-*Reference-White Level* of the standard signal, the oscilloscope gain would be adjusted so its calibrating voltage produces a deflection from 0 to 100 on the standard scale. Experience will indicate how often calibration checks should be made to maintain the desired accuracy of level measurement.

### *3.4 Interpretation*

Standardizing the response characteristic of the oscilloscope serves to minimize possible differences in interpretation of signal levels. To further insure uniformity in interpreting the oscilloscope indication, the measurement of *Sync* and *Blanking Levels* should be observed at a point in the waveform where the voltages representing these levels are substantially at their steady-state value. The longer duration signals of both *Sync* and *Blanking Levels* which occur during the vertical sync interval are suitable. A representation of the appearance of these portions is shown in Fig. 4, the measurements being made as indicated to minimize errors due to transmission distortion. For noncomposite picture signals, *Blanking Level* may be observed similarly during the vertical blanking interval. In setting picture signal levels, important information-bearing signal peaks will be normally held within the 0 to 100 scale range. Certain highlight signals may occasionally exceed this range. Where comparison measurements are being made at different points in a transmission system, it is important to insure that identical peaks are being considered.

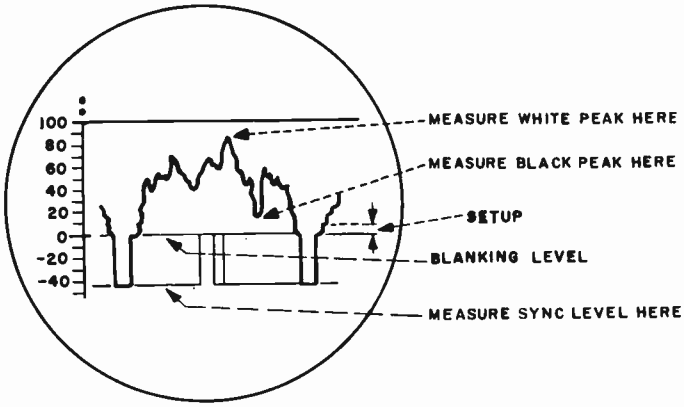


Fig. 4—Use and interpretation of IRE standard scale.

Measurements made with the IRE standard scale may be expressed as follows:

**White Peak.** 86 (meaning 86 IRE scale units or 86 per cent of the range between *Blanking* and *Reference-White Levels*).

**Black Peak.** 13 (meaning 13 IRE scale units or 13 per cent of the range between *Blanking* and *Reference-White Levels*).

**Sync Level.** −43 (meaning 43 IRE scale units or 43 per cent of the range between *Blanking* and *Reference-White Levels* but negative with respect to *Blanking Level*).

# Theory of Networks of Linearly Variable Resistances*

HAROLD LEVENSTEIN†, MEMBER, IRE

*Summary*—A network theory is derived for circuits constructed of linear rheostats driven from a common input shaft. A correspondence between these networks and *RL* networks is used to demonstrate that driving point impedances and transfer functions are real rational fractions in a real variable, the input shaft rotation. Requirements on the pole-zero characteristics of these functions are established. Methods for developing functions approximating a given input-output relation in physically realizable form are discussed. Modern methods of transfer-function realization can be applied to these fractions to synthesize the physical networks. Networks for sine and log transfer functions obtained by the technique are presented.

## Background

In the design of analog computers, the engineer often makes use of potentiometers whose output voltage is required to vary in a prescribed manner as the shaft of the potentiometer is rotated. To meet these requirements a variety of ingenious techniques and special circuits have been advised. Special potentiometers may be employed whose variation in resistance is obtained by winding on nonlinear cards, by winding different wire sizes along the length of the card, or by varying the spacing between wires. Taps may be distributed along the winding and connected to appropriate voltages from a voltage divider. The potentiometer may be loaded by connecting resistances from the slider to some reference potential.[1,2]

These and more intricate circuits all have been employed widely. It is characteristic of loading methods that a wholly empirical approach is used most often. In such methods the designer "guesses" at an appropriate circuit, takes literal values for the circuit elements, and then, by more or less sophisticated mathematics, attempts to discover numbers for the literal quantities which cause the circuit to approximate best the original prescription.

Such a technique is inefficient. It provides no basis for establishing an economical design, nor does it provide any suggestion for the improvement of the design if this is required.

From a practical point of view, the use of linear potentiometers as the basis for generating prescribed nonlinear functions of shaft rotation has considerable importance. There are several reasons for this. Linear poteniometers are considerably less expensive than nonlinear components of the same precision. They are manufactured more easily. Finally, they can be obtained commercially with an extremely high degree of linearity; at present, they can be obtained with linearity tolerances of 0.015 per cent. In this paper we present derivations of some of the significant properties of networks constructed of linearly varying rheostats. Methods for reducing data to a form appropriate to such networks are described, and some of the aspects of network synthesis are considered.

## Statement of the Problem

The problem will be formulated in the following way. Given a network with two input terminals and two out-

* Original manuscript received by the IRE, January 30, 1957; revised manuscript received, November 6, 1957.

† W. L. Maxson Corp., New York, N. Y.

[1] I. Greenwood, J. Holdam, and D. Mackae, "Electronic Instruments," McGraw-Hill Book Co., Inc., New York, N. Y.; 1946.

[2] H. Levenstein, "Generating Non-Linear Functions with Linear Potentiometers," *Trans. 1953 Natl. Conf. on Airborne Electronics.*

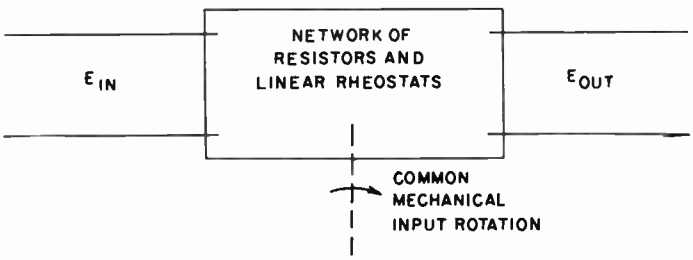


Fig. 1—The general problem.

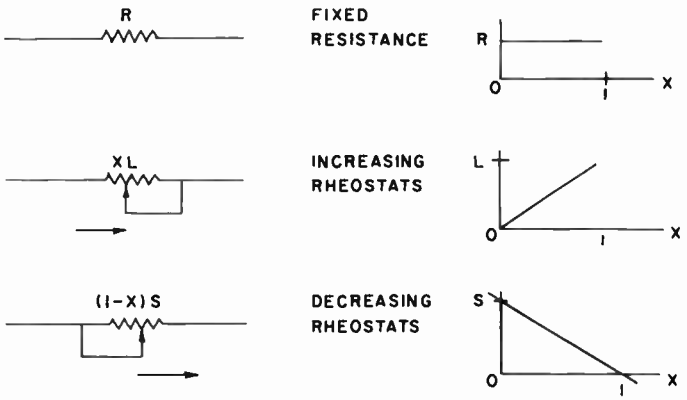


Fig. 2—The three types of elements.

put terminals and containing only fixed resistances and linear rheostats, the latter driven by a common shaft accessible from the outside, what is the relationship of the output voltage to the input voltage as a function of shaft rotation?

Note that rheostat has replaced potentiometer in this statement. Since any potentiometer can be replaced by a series connection of two rheostats, we may regard this as a more general statement of the problem.

When we have solved this problem we then can consider the problems of synthesizing networks and the problem of approximating prescribed functions. A graphic description of the problem is shown in Fig. 1.

## Basic Descriptions of Network Elements

The three types of elements which must be considered are shown schematically in Fig. 2. $R$ denotes a fixed resistance of value $R$. We take $x$, the shaft rotation, to be a variable running from zero to one, so that $x$ represents fractional shaft rotation. There are two possible connections for rheostats: resistance increasing with $x$ and resistance decreasing with $x$. If the rheostat resistance increases with $x$, its "instantaneous" resistance is $xL$, where $L$ is the total resistance. If the start and end of the winding are reversed, the resistance decreases with $x$ and can be denoted $(1-x)S$, where $S$ is the total resistance. These three cases are schematically distinguished as Fig. 2(a), 2(b), and 2(c).

## An Equivalent Circuit Theorem

So far we have described a network containing three types of elements. The present state of electric circuit


Fig. 3—Equivalent circuit for fixed resistor.

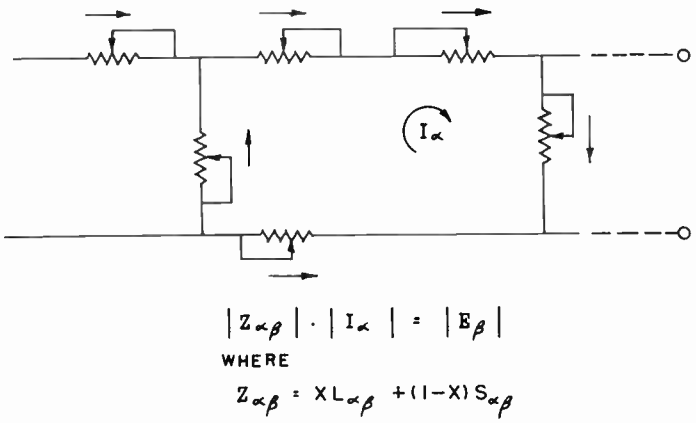


Fig. 4—Circuit relationships.

theory does not permit the complete treatment of circuits of more than two mathematically independent elements. Accordingly, we shall make note of a superficially trivial relation which permits a complete treatment of this problem. We observe that every fixed resistance $R$ can be replaced by a series connection of two rheostats of values $xR$ and $(1-x)R$. (See Fig. 3.) Thus, if we replace each fixed resistance by its equivalent circuit of two series rheostats, the network is reduced to one containing only two types of elements.

We may now refer to the general theory of such networks for a solution.

## Properties of Networks Containing Two Types of Elements

While it is not necessary to do so, we shall find it most convenient from the viewpoint of exposition to draw a close analogy between the networks we have hypothesized and networks consisting of resistors and inductors (with no mutual coupling), and to make use of the analogy to arrive at the properties of the networks.

To arrive at this analogy, we may begin by considering Fig. 4, which illustrates a typical network. Each element is either of the $x$ type or $(1-x)$ type. If we assume mesh currents and write mesh equations, we find the customary matrix relation:

$$|Z_{\alpha\beta}| \times |I_\alpha| = |E_\beta|. \tag{1}$$

Each term of $Z_{\alpha\beta}$ is generally of the form:

$$Z_{\alpha\beta} = xL_{\alpha\beta} + (1-x)S_{\alpha\beta}. \tag{2}$$

Now, if we divide every term of $Z_{\alpha\beta}$ by $x$ and multiply every current by $x$, we will have modified the elements of the matrices without modifying the matrix equation. Formally let us define

$$Z_{\alpha\beta}^* = Z_{\alpha\beta}/x \tag{3}$$

and

$$I_\alpha^* = xI_\alpha. \tag{4}$$

Then the matrix equation becomes:

$$|Z_{\alpha\beta}^*| \times |I_\alpha^*| = |E_\beta|. \tag{5}$$

The elements of the $Z^*$ matrix will now have the form:

$$Z_{\alpha\beta}^* = L + \frac{1-x}{x} S. \tag{6}$$

If we introduce a new parameter $p$ defined by (7)

$$p = \frac{1-x}{x}, \tag{7}$$

these elements become:

$$Z_{\alpha\beta}^* = L + pS. \tag{8}$$

Thus, the relations between the starred mesh currents and the voltages have the same mathematical structure as the relations which exist in a network constructed of resistances and inductances. Since the theory of these circuits has been highly developed, we may adopt it and use it to predict the properties of variable resistance networks.[3]

Accordingly, we may now make the following statements:

1) The driving-point impedance of the starred networks, the ratio of voltage to starred current, is a rational fraction in $p$. The degree of the numerator is equal to or one more than the degree of the denominator. The roots of the numerator and the denominator must be simple, real, negative, and must alternate with the least (magnitude) root of the numerator less than the least root of the denominator.

2) The transfer function of the starred network, the ratio of voltage across the load to input voltage, is a rational fraction in $p$. The order of the numerator is equal to or less than the order of the denominator. The roots of the numerator may lie anywhere in the complex $p$ plane, with the restriction that complex roots must occur in conjugate pairs. The roots of the denominator must be simple, real, and negative.

When we introduce the inverse transformation from $p$ to $x$ we can restate 1) and 2) as follows:

3) The driving point impedance of the variable resistance networks is a rational fraction in $x$. The order of the numerator may be equal to, or one, or two more than the order of the denominator. The roots of the numerator and the denominator must be simple, real, and lie outside the range of $0 < x < 1$.

Within the ranges $-\infty < x < 0$ and $1 < x < \infty$ the alternation property of the poles and zeros still holds, with the zeros of the numerator closer to 0 and 1 than the corresponding zeros of the denominator. A picture of the zero-pole distribution in the $p$ and $x$ planes is shown in Fig. 5.

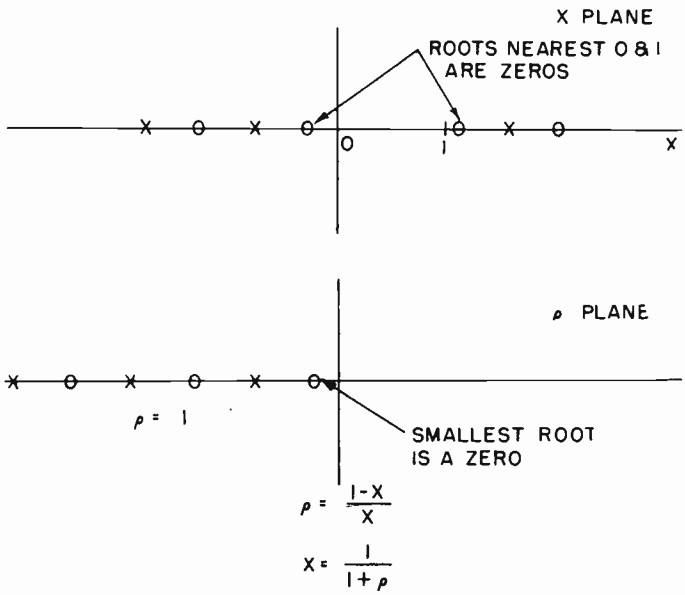


Fig. 5—Typical pole-zero distribution of driving-point impedance in $p$ plane and $x$ plane.

4) The transfer function of the variable resistance networks is a rational fraction in $x$. The order of the numerator may be equal to or less than the order of the denominator plus one. The roots of the numerator may lie anywhere in the complex plane. The roots of the denominator must be simple and real and may lie anywhere except in the range $0 \leq x \leq 1$.

In all cases, complex roots appear in complex conjugate pairs.

The derivations of the above relations appear in Appendix I.

While it is possible to deduce other related properties, these are sufficient to characterize the next phase of the problem, the approximation problem. We shall derive additional information where we require it (for example, in the synthesis phase).

It may be informative to note that the transformation of $p$ to $x$ is a mapping of the $p$ plane into the $x$ plane. While we are most often concerned with the real axes, the general character of the mapping, a bilinear transformation, is of interest when we are dealing with the complex roots of the numerator of the transfer function. Fig. 6 shows the nature of the mapping performed.

## The Approximation Problem

Since for the most part these networks are not used as impedances, we shall concern outselves primarily with methods of approximating prescribed data by functions characteristic of the transfer function. In any event, there is no serious difficulty in extending these methods to specification of impedance function.

[3] E. Guillemin, "A Summary of Modern Methods of Network Synthesis" in "Advances in Electronics," Academic Press, New York, N. Y., vol. 3, pp. 261–301; 1951.

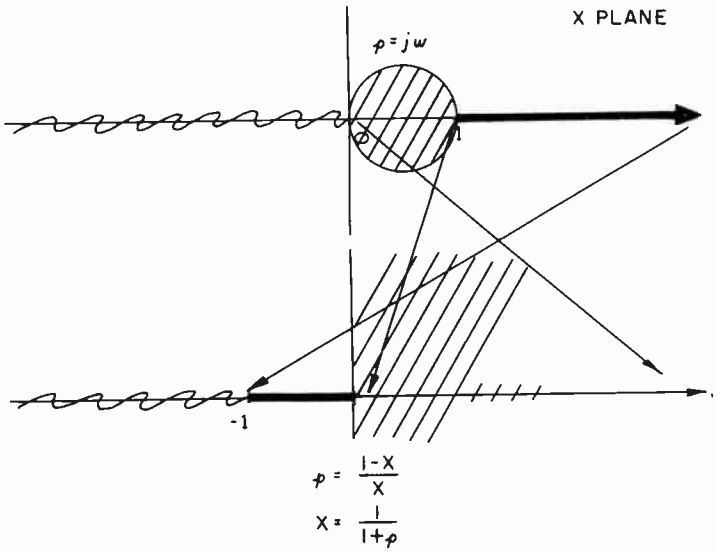


Fig. 6—Mapping between $p$ and $x$ planes.

GIVEN: $y = y_0, y_1, \cdots\cdots y_R \cdots\cdots y_N$ CORRESPONDING TO $X = X_0, X_1, \cdots\cdots X_R \cdots\cdots X_N$

FIND: $Z = N(X)/D(X)$ SUCH THAT $Z = y$ AT THE SELECTED POINTS

SOLUTION: FORM THE FOLLOWING DETERMINANT, SET EQUAL TO ZERO, AND SOLVE FOR $Z$.

$$\begin{vmatrix} 1 & y_0 & x_0 & x_0 y_0 & x_0^2 & x_0^2 y_0^2 & \cdots \\ 1 & y_1 & x_1 & x_1 y_1 & x_1^2 & x_1^2 y_1^2 & \cdots \\ \cdots & \cdots & \cdots & \cdots & \cdots & \cdots & \cdots \\ 1 & y_N & x_N & x_N y_N & x_N^2 & x_N^2 y_N^2 & \cdots \\ 1 & Z & x & xZ & x^2 & x^2 Z^2 & \cdots \end{vmatrix} = 0$$

Fig. 7—Milne's method for finding rational fraction approximation. (Milne, *op. cit.*, ch. VIII.)

The approximation problem usually is presented as follows: the desired output function $y$ shall vary with an independent parameter $z$ in a certain functional, graphical, or tabular manner. What rational fraction in $x$ shall we select to best approximate this relation between $z$ and $y$? This fraction must have the properties stated as 3).

Since the range of variation of $x$ is zero to one, we must first establish a scale factor between $z$ and $x$; sometimes, as in the case of the log function, we must shift the origin. While it is conceivable that we may select a nonlinear transformation from $z$ to $x$ (for example, in the case where the $x$ shaft carries a calibrated dial displaying the inverse transformation), we ordinarily employ a linear transformation. In any event we must first establish a relation between $y$ and $x$ over the range $0 \leq x \leq 1$.

It is not necessary to modify the scale of $y$ at this time, although it is likely that this will be necessary in synthesizing the network.

An answer to this approximation problem has been found in standard interpolation theory.[4,5] Formally, if we select $n$ values of $y$: $y_0, y_1, \cdots, y_i, \cdots, y_{n-1}$ corresponding to $x_0, x, \cdots, x_i, \cdots$, values at which we wish to make our approximation exact, we merely need to substitute them in the determinant of Fig. 7 and solve for $y$ to find an approximating rational fraction.

Unfortunately, there is no guarantee that the roots of the denominator will be of the proper nature. There is every likelihood that they will be complex.

One recourse we have is to manufacture a rational fraction with the proper denominator. An effective technique is the following:

1) Fit a polynomial in $x$ to $y$ by any suitable technique; for example, by least squares. Call it $Q(x)$.

2) Divide this by a polynomial in $x$, denoted $P(x)$, constructed of pairs of factors of the form $(x-a)(x+a-1)$. That is,

$$P(x) = \prod^{n} (x - a_i)(x + a_i - 1). \tag{9}$$

The order of $P(x)$ is $2n$ and is selected to be equal to or greater than one plus the order of $Q(x)$. The $a_i$ are all different and chosen remote from the range of interpolation. Accordingly, $P(x)$ approximates a constant over $0 \leq x \leq 1$. It is often convenient to factor $Q(x)$ first since, if it possesses a root $b_i$ which is real and outside the range of interpolation, we may make one of the $a_i$ identical with $b_i$ and thus reduce the order of $Q(x)$ and $P(x)$.

3) $Q(x)/P(x)$ is an acceptable transfer function which is physically realizable.

A further refinement of this process consists of forming the product $P(x)\,Y$ and fitting a polynomial $Q^*(x)$ to this modified datum. Generally, if $Q(x)$ and $Q^*(x)$ are of the same order, $Q^*(x)/P(x)$ more accurately fits the data than $Q(x)/P(x)$.

Another method for finding a rational fraction approximation which provides some control of the denominator is presented in Appendix II.

For the purposes of this paper, we may consider the approximation problem solved.

## The Synthesis Problem

Since network synthesis is an ever changing art with the personal preference or experience of the engineer often the dominating factor in the solution, we shall merely show how the problem is reduced to a form suitable for synthesis by any acceptable technique. Some post-synthesis considerations will be introduced.

At the conclusion of the approximation stage we

[4] W. E. Milne, "Numerical Calculus," Princeton Univ. Press, Princeton, N. J., 1949.
[5] L. M. Milne-Thompson, "Calculus of Finite Differences," Macmillan & Co., Ltd., London, Eng., pp. 106–108; 1951.

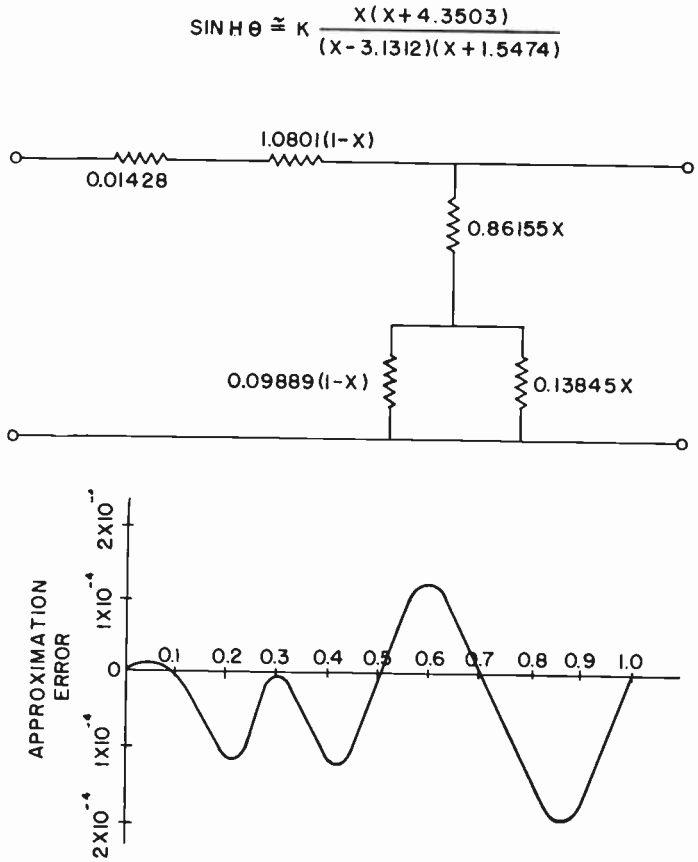


Fig. 8—Network for sinh $\theta$.

possessed a function $Y$

$$Y = Q(x)/P(x) \qquad (10)$$

which approximates $y=y(x)$ in a satisfactory manner over the range of $x$.

The substitution of $x=1/(1+p)$ into (10) provides a relation between $Y$ and $p$ identical with the transfer function of an $RL$ network. Accordingly, using the methods of Guillemin[3,6,7] or Bower and Ordung,[8] we can arrive at a network configuration and component values for this equivalent $RL$ network.

We next replace $p$ by $(1-x)/x$ in the circuit impedances. This, of course, leaves us with nothing recognizable. We must recall that the transformation into the $RL$ network also included the scaling of every component value by division by $x$. Accordingly, we multiply every component by $x$ and find that we can now interpret the network as a combination of $x$-type rheostats and $(1-x)$-type rheostats. By use of equivalent circuits we may be able to replace some of the rheostats by fixed resistors or potentiometers. Some of these equivalences are shown below (Figs. 10 and 11).

[6] J. G. Truxal, "Control System Synthesis," McGraw-Hill Book Co., Inc., New York, N. Y., ch. 3, pp. 161–220; 1955.
[7] P. M. Lewis, "The Synthesis of Voltage Transfer Functions," M.I.T., Res. Lab. of Electronics, Cambridge, Mass., Tech. Rep. 314; June, 1956.
[8] J. L. Bower and P. F. Ordung, "The synthesis of resistor capacitor networks," Proc. IRE, vol. 38, pp. 263–269; March, 1950.

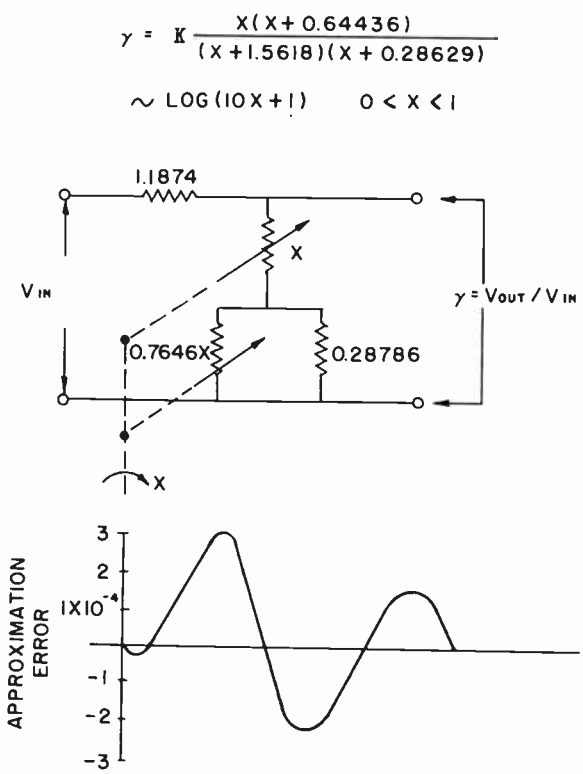


Fig. 9—Log function network.

## Two Examples

Figs. 8 and 9 show two examples of the application of the theory. In both cases it happened that it was not necessary to force the approximating functions into appropriate form. Fig. 8 shows a network for generating the hyperbolic sine over the range zero to one. Fig. 9 is a circuit for generating log $x$; it is notable for its simplicity. In each figure the error is plotted as a function of shaft rotation. The extraordinary quality of the approximating function coupled with the simplicity of the circuits is indicative of what can be accomplished when the properties of these networks are properly used.

## Some Equivalent Circuits

In Fig. 10 we have tabulated some equivalent circuits and their impedance representations in the $x$ and $p$ variables. They are intended primarily for use in recognizing standard configurations and in simplifications of the synthesized networks.

## Fields for Extension of the Theory

Several questions can be raised which indicate possible directions for extension of the theory. One important question is: what are the properties of networks in which the rheostats are turned by several independent variables? Perhaps this can be answered partly by considering what the possibilities are for networks whose driving point impedances are substantially constant over a considerable range, while possessing prescribed transfer functions. Such networks could be cascaded to obtain products of functions of independent variables.

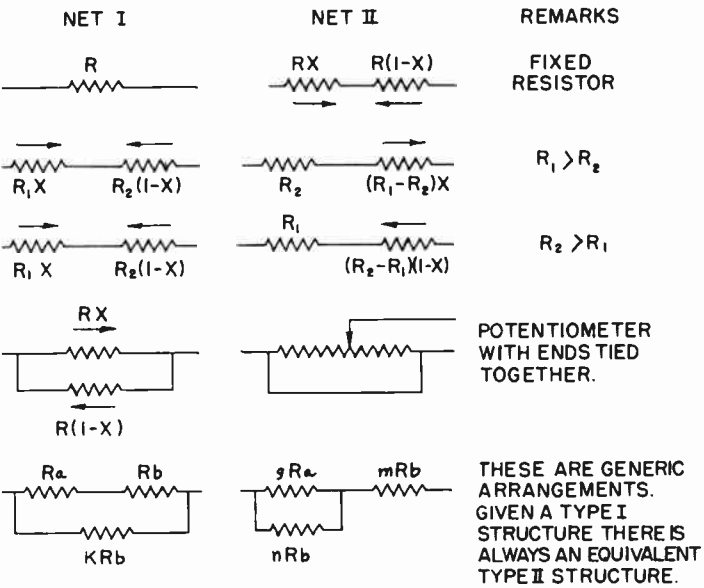


Fig. 10—Equivalent two-terminal nets.

While the discussion has been limited to linear rheostats, it is obvious that it is applicable to similar networks made up of adjustable capacitors or inductors. There may be special advantages to these circuits.

Finally, there may be some advantage in range of application to circuits constructed of some special functional rheostats which are not so readily obtained commercially. As an example, the use of sine-cosine elements may simplify some of the elaborate trigonometric relations associated with changes of coordinate reference systems in gimbal structures.

## Appendix I

## Derivation of Driving-Point Impedance and Transfer-Function Relations in the x Plane

### *Driving-Point Impedance*

In the text it is shown that the driving-point impedance can be written by means of suitable transformations in the form

$$Z = xZ^*(p). \tag{11}$$

Where $Z^*(p)$ has the form of an $RL$ network driving point impedance

$$Z^*(p) = K\frac{(p-p_1)(p-p_3)\cdots}{(p-p_2)(p-p_4)\cdots}. \tag{12}$$

In this form the $p_i$'s are negative, real, and alternate and $p_1$ is closest to the origin. The degree of the numerator may be equal to or one greater than the degree of the denominator.

By definition

$$p = \frac{1-x}{x}. \tag{13}$$

Substituting in (12) and rationalizing we have

$$Z^* = \overline{K}x^{m-n}\frac{\left(x-\frac{1}{1+p_1}\right)\left(x-\frac{1}{1+p_3}\right)\cdots}{\left(x-\frac{1}{1+p_2}\right)\left(x-\frac{1}{1+p_4}\right)\cdots} \tag{14}$$

$m$ = the degree of the denominator,
$n$ = the degree of the numerator,
$\overline{K}^*$ = a new value of $K$ appropriate to the rearranged form. Then

$$Z = xZ^* = \overline{K}x^{m-n+1}\frac{\left(x-\frac{1}{1+p_1}\right)\left(x-\frac{1}{1+p_3}\right)\cdots}{\left(x-\frac{1}{1+p_2}\right)\left(x-\frac{1}{1+p_4}\right)\cdots}. \tag{15}$$

We can now evaluate the polynomial relationships under the following possible conditions:

$$n = m$$

and

$$n = m+1$$

If $n=m$, there are the same number of roots in numerator and denominator and

$$Z = \overline{K}x\frac{N(x,n)}{D(x,n)}. \tag{16}$$

In this form the total numerator is one degree higher than the denominator.

If $n=m+1$, then

$$Z = \overline{K}\frac{N(x,n)}{D(x,n-1)}. \tag{17}$$

The numerator is again one degree higher than the denominator.

We must add to this the special case in which one of the $p_i$'s is $(-1)$. We handle all of the factors except this one as before. This factor disappears. To see this we evaluate the factor explicitly:

$$F = (p+1) = \left(\frac{1-x}{x}+1\right) = \frac{1}{x}. \tag{18}$$

Thus the contribution to $x^{m-n+1}$ appears as before but the factor disappears from $N$ or $D$, depending upon where it appeared.

Since the poles and zeros are simple, this situation can happen only once. But it can occur in either the numerator or the denominator.

In summary, the degree of the numerator may be equal to or one or two greater than the degree of the denominator.

### *Transfer Function*

We may develop the transfer function relationship in

much the same manner that we have handled the driving point impedance.

We are concerned with the ratio here of an output voltage to the input voltage as a function of $p$ first, and then $x$.

Starting with the $RL$ equivalent of the resistance network we can describe the voltage transfer function as a ratio of polynomials in $p$

$$T = K\frac{N(p)}{D(p)}. \tag{19}$$

The roots of $D(p)$ must be simple, negative, and real. The roots of $N(p)$ may be anywhere in the complex plane provided that for every complex root a conjugate root appears.

The degree of the numerator may be equal to or less than the degree of the denominator.

Note that $x$ does not appear explicitly since we are dealing with a voltage ratio only, not an impedance.

Now rewrite (19) in the form

$$T = K\frac{(p-p_1)(p-p_3)\cdots}{(p-p_2)(p-p_4)\cdots}. \tag{20}$$

No special ordering is implied here by the subscripts.

Letting $p=(1-x)/x$, and rationalizing

$$T = \overline{K}x^{m-n}\frac{\left(x-\frac{1}{1+p_1}\right)\left(x-\frac{1}{1+p_3}\right)\cdots}{\left(x-\frac{1}{1+p_2}\right)\left(x-\frac{1}{1+p_4}\right)\cdots}. \tag{21}$$

We are interested in the cases, $m=n$ and $m>n$. We must also consider the effects of a root at $p=(-1)$ which may occur simply in the denominator or multiply in the numerator.

Let $m=n$. Then the leading terms in the numerator and the denominator are both $x^m$; their degree is the same.

Let $m>n$; the leading terms are $x^m$ in both polynomials and the degree is the same, again.

Now let a simple root occur at $p=-1$ in the denominator. As before this factor will disappear from the denominator. The leading term in the numerator will be $x^m$, in the denominator $x^{m-1}$. The degree of the numerator is one higher than the degree of the denominator.

Let a multiple root of order $k$ appear at $p=-1$ in the numerator. The leading term in the numerator will be $x^{m-k}$, in the denominator $x^m$, $k$ higher than the numerator.

In summary, the degree of the numerator may be equal to or less than one plus the degree of the denominator.

*Ordering Property of the Poles and Zeros of a Driving-Point Impedance*

Poles and zeros of $Z^*(p)$ alternate on the real negative axis. A detailed examination of the way in which these roots map into the $x$ axis shows the following:

1) The alternation property is preserved. However if these roots lie outside the range $(-1<P<0)$, the relationship occurs over two regions.

The poles and zeros lying between $(-1<P<0)$ map into the corresponding range $(0<x<1)$. The root closest to $x=1$ is a zero and the poles and zeros alternate along the axis out to infinity. The ordering relationship then continues in along the negative real $x$ axis from $-\infty$ to zero.

If $m=n$ in $Z^*(p)$ there will be a zero at the origin in the $x$ plane due to the relationship

$$Z = xZ^*.$$

If $m=n-1$, the root closest to the origin in the $x$ plane along the negative $x$ axis will be a zero. Thus, in general, the alternation property holds, starting with a zero at or to the right of $x=1$, continuing to infinity and returning along the negative axis, and concluding with a zero at or to the left of the $x$ origin.

## Appendix II

### Construction of a Rational Fraction to Fit Assigned Data

Milne-Thompson[5] describes a method due to Thiele for constructing a continued fraction approximation to data. By terminating the fraction we obtain a rational fraction fitting the data at $n$ specified points. A minor modification of this method gives additional freedom to adjust the roots of the denominator so that frequently they can be made to lie in the desired ranges without increasing the complexity of the network or changing the points of fit. Since the method is direct and reasonably simple it is usually worth trying.

The continued fraction proposed has the form

$$\bar{y} = a_0 + \cfrac{(x-x_0)}{a_1 + \cfrac{(x-x_2)}{a_2 + \cfrac{(x-x_2)}{a_3+\cdots}}}. \tag{22}$$

The $x_i$'s are the points of fit, $\bar{y}$ is the approximation to $y$, the given data, and the $a_i$'s are initially unknown.

Inspection of the above equation shows that the $a$'s are readily determined in sequence.

If we set $x=x_0$, and $y=y_0$, we compute $a_0$. Then set $x=x_1$, $y=y_1$, and compute $a_1$. Setting $x=x_n$ makes the portion of the succeeding fraction identically zero, so that we can terminate the fraction at $x=x_n$ without changing the previous points of fit. The fraction can then be written in the form:

$$\bar{y} = a_0 + \cfrac{(x-x_0)}{a_1 + \cfrac{(x-x_1)}{a_2+\cdots\cfrac{(x-x_{n-2})}{a_{n-1}+\cfrac{(x-x_{n-1})}{a_n}}}}. \tag{23}$$

As we noted $\bar{y}$ is identical with $y$ at the points $x=x_0$, $x_1 \cdots x_{n-1}$. In addition, they are identical at $x=x_n$, since at that point the quantity $(x-x_n)$ is zero and would contribute nothing to the function in this form. Thus the $n+1$ coefficients characterize the function.

It is merely a matter of some algebra to rearrange this function as a rational fraction, which now approximates the data over the range $x_0 \leq x \leq x_n$.

$$\bar{y} = \frac{P(x)}{Q(x)} . \tag{24}$$

However, the roots of $Q$ may not be properly placed for $y$ to be a realizable function. So, instead of terminating the function with $a_n$ we add the term $K(x-x_n)$ where $K$ is an arbitrary parameter to be determined. Since when $x=x_n$ this term is zero, we have not changed the points of fitting.

Rearrangement of the function into a rational fraction now yields

$$\bar{y} = \frac{P(x) + K(x - x_n)P_1(x)}{Q(x) + K(x - x_n)Q_1(x)} . \tag{25}$$

This is a function which has the same points of fit as (24), but by adjustment of $K$ we have some freedom to adjust the roots of the denominator. At the most this increases the complexity of the network by one degree.

It is clear that the functions $P_1$ and $Q_1$ must be proportional to $P$ and $Q$ at all points of fit except $X_n$, where this is unnecessary.

When $Q(x)$ is of reasonable degree, say 3 or 4, the numerical work associated with finding suitable values of $K$ so that the roots of $Q$ are real, simple, and do not lie inside the $0 \leq x \leq 1$ range is not usually prohibitive.

When a suitable selection has been made, it is necessary of course to check performance between the points of fit to determine the magnitude of errors; increasing the number of points of fit will, in general, permit reduction of errors.

## Appendix III

### Characteristics of Driving-Point Impedances

Shannon and Hargelbarger[9] show the driving-point impedance of a variable resistance network must always be a convex upward function of rotation. This is accomplished through investigation of hypothetical experimental connections of the network. In the following paragraphs, we wish to prove this relation using the network theory developed in the body of this paper.

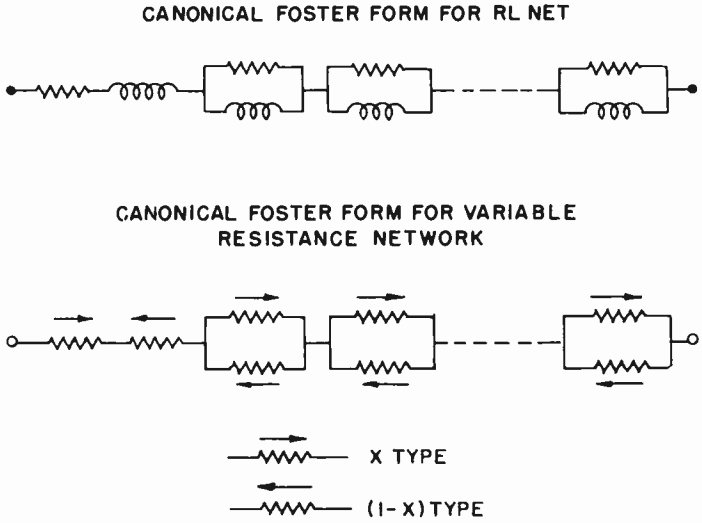


Fig. 11.

Every variable resistance network has an analog in the form of an *RL* network. Cauer's investigation of two terminal *RL* nets displays as one general canonical configuration a Foster form in which the network can be drawn as a series connection of parallel *RL* nets in series with a resistance and inductance. The series resistor and inductor may be identically zero.

The variable resistance analog of this is shown in Fig. 11.

The equation for the driving-point impedance can be written

$$Z(x) = R_{10}(x) + R_{20}(1 - x) + \sum \frac{R_{1i}R_{2i}(1 - x)x}{xR_{1i} + R_{2i}(1 - x)} .$$

Double differentiation of $Z(x)$ shows that

$$\frac{d^2Z(x)}{dx^2} \leq 0.$$

This can be verified very simply by sketching the $Z(x)$ curve of any of typical sections.

### Acknowledgment

The author is indebted to Dr. H. Hochstadt for working out the two illustrative approximating functions and to Miss M. Whitfield and Mrs. R. Waldmann for the calculations associated with them.

[9] C. E. Shannon and D. W. Hargelbarger, "Concavity of resistance functions," *J. Appl. Phys.*, vol. 27, pp. 42–43; January, 1956.

# Correspondence

## A Parametric Electron Beam Amplifier*

A new type of solid state microwave amplifier has recently been proposed by Suhl.[1] Amplification of the signal occurs by transfer of power from a local rf source at a frequency higher than the signal and can be achieved by using certain properties of ferrites.

The purpose of this note is to show that a similar amplifier can be devised using an electron beam instead of the ferrite. Such an amplifier has the possibility of very-low-noise operation. The fundamental limitations[2] of the noise performance of conventional microwave amplifiers do not apply to it. An amplifier of this type has been built and some initial experimental results are given. The term "parametric amplifier" has been used because the device works by a variation in a circuit parameter.

In the simplest form of parametric amplifier the local source of power (usually called the pump) operates at exactly twice the signal frequency. The arrangement is shown in Fig. 1, where a parallel tuned circuit is resonant to the signal. The capacity (or inductance) is modulated at twice the signal frequency $\omega/2\pi$;

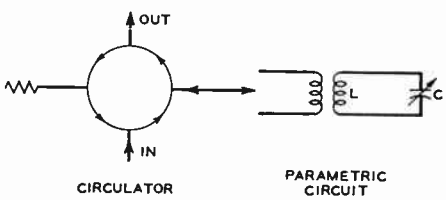


Fig. 1—Simple parametric circuit.

$$e.g.,\ C = C_0[1 + \epsilon \sin (2\omega t + \phi)]. \quad (1)$$

$\epsilon$ is a modulation coefficient with maximum value of 1.

If a signal at $\omega$ is applied to the circuit, then it can be shown that the capacity variation will inject, or extract power from the signal, depending on the value of the phase angle $\phi$. The effect is equivalent to shunting a conductance $G_p$ across the capacity where

$$G_p = -\frac{\omega C_0 \epsilon}{2} \cos \phi. \quad (2)$$

When $\phi = 0$, $G_p$ has a maximum negative value and conditions are best for feeding power into the circuit.

If $\epsilon$ is then increased until $-G_p$ equals the loaded shunt conductance $G_L$ of the circuit, oscillations will occur at frequency $\omega$ without the presence of the external signal. This condition is given by

$$G_L = -G_p = \frac{\omega C_0 \epsilon}{2}$$

or

$$\epsilon = \frac{2G_L}{\omega C_0} = \frac{2}{Q_L}, \quad (3)$$

where $Q_L$ = loaded $Q$ of circuit.

At a value of $\epsilon$ slightly less than that for oscillation, the circuit is stable and amplification can be obtained. The device acts as a regenerative amplifier like the maser and the regenerative reflex klystron amplifier. The operation of such an amplifier has been described by Gordon and White.[3] A single line is coupled to the circuit and the input and output signals are separated in a circulator. (See Fig. 1.) As well as preventing the loss of some of the output power into the input line, the circulator isolates the cavity from external load variations and enables stable operation much closer to the oscillation point with correspondingly higher gain.

Operating in this way the power gain is simply the square of the reflection coefficient ($\Gamma$) of the resonant circuit.

Power gain

$$= \Gamma^2 = \left[\frac{2}{1 + Q_E\left(\frac{1}{Q_0} - \frac{\epsilon}{2}\cos\phi\right)} - 1\right]^2, \quad (4)$$

where $Q_E$ is the external $Q$ of the loaded circuit and $Q_0$ is the unloaded $Q$ of the circuit. It will be noticed that the gain cannot exceed 1 (assuming $\cos \phi = 1$) unless $\epsilon/2 > 1/Q_0$; *i.e.*, unless the parametric variation is sufficient to make the unloaded circuit oscillate.

If the signal frequency differs slightly from half the pump frequency ($\omega_p/2\pi$), then the result can be described by a variation of the phase angle with time.

$$\phi = 2\left(\omega - \frac{\omega p}{2}\right)t. \quad (5)$$

This causes a periodic amplification and attenuation of the signal at the frequency $(\omega - \omega_p/2)/\pi$. Essentially the output signal is modulated at twice the beat between the signal and half the pump frequency, giving rise to sidebands. The actual bandwidth of the amplifier is determined by the loaded $Q$.

An electron beam can be used to produce an electronic admittance in a microwave cavity, and one way of doing this is used in klystron oscillators. Take for example the "floating drift tube" klystron. There are two equal gaps in a single cavity separated by a field free drift space. A beam of electrons passes through the cavity and is arranged to have a drift angle beteen gaps given by

$$\alpha = (2n + 3/2)\pi \text{ radians},$$

where $\alpha$ = drift angle

$$n = 0, 1, 2, 3 \cdots.$$

An electronic admittance is produced across the cavity which is a pure negative conductance. This can overcome the positive conductance of the cavity and give rise to oscillation.

If, however, the drift angle is made a quarter cycle greater or smaller than this, the electronic admittance becomes a pure susceptance shunted across the cavity. This occurs when

$\alpha = (2n + 1)\pi$ for a positive susceptance,

$\alpha = (2n + 2)\pi$ for a negative susceptance.

This susceptance will change the resonant frequency of the cavity without altering the effective losses. As seen above, however, by modulating this susceptance at twice the signal frequency, a negative conductance will be produced which can overcome the cavity losses and give oscillation or amplification of the signal.

To modulate the susceptance, the beam must be modulated. This can be done by means of a preceding cavity resonant to the pumping frequency. If this is supplied with pumping power, any degree of beam modulation up to 100 per cent can be obtained at the signal cavity. The optimum spacing between cavities is a quarter of the effective plasma wavelength. The arrangement is shown in Fig. 2.

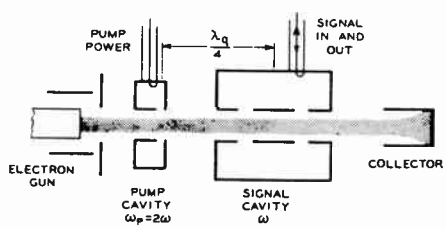


Fig. 2—Parametric beam amplifier.

The rf current (at the pump frequency) in the beam necessary to start parametric oscillations is given by

$$I_{rf} = \frac{4G_L V_0}{M^2 \alpha}, \quad (6)$$

where

$V_0$ = beam voltage;
$M$ = signal cavity gap coupling factor;
$I_{rf}$ = peak rf current on the beam.

If the beam is 100 per cent modulated,

$$I_{rf} = I_0,$$

where $I_0$ = dc beam current. It will be recognized that $I_{rf}$ is just twice the start oscillation current of a floating drift tube klystron. A parametric beam amplifier should therefore operate with reasonable values of voltage and current.

Now, consider noise currents in the beam at the signal frequency. If the drift angle between gaps is $(2n+1)\pi$ radians (corresponding to a positive susceptance) and is short

* Received by the IRE, November 8, 1957.

[1] H. Suhl, "Proposal for a ferro-magnetic amplifier in the microwave range," *Phys. Rev.*, vol. 106, p. 384; April 15, 1957.

[2] H. A. Haus and F. N. H. Robinson, "The minimum noise figure of microwave beam amplifiers," PROC. IRE, vol. 43, pp. 981–991; August, 1955.

[3] J. P. Gordon and L. D. White, "Experimental determination of the noise figure of an ammonia maser," *Phys. Rev.*, vol. 107, pp. 1728–1729; September 15, 1957.

in terms of the plasma wavelength, the currents at the two gaps are essentially equal in amplitude and are in antiphase. No noise currents will be induced into the cavity. In other words, by choosing the drift cycle to be $\pi$, $3\pi$, $5\pi$, etc., it is possible to excite a cavity to produce amplification without coupling to the noise current in the beam, at least to a first order of approximation.

A demountable tube based on Fig. 2 has been built. This operated, as far as gain and oscillation, substantially as expected. No noise measurements have yet been made. Table I shows the measured characteristics

TABLE I

| | |
|---|---|
| Signal Cavity | |
| Resonant Frequency | 4150 mc |
| Drift Angle | $3\pi$ radians |
| Pump frequency | 8300 mc |
| Beam voltage | 2450 v |
| Beam current | 18 ma |
| Pump power | 140 mw |
| Maximum observed gain | 20 db |

of the device. Fig. 3 demonstrates amplification obtained as a function of pumping power. In this figure cw power at constant frequency was used for the pump and the signal frequency was swept through the resonance of the signal cavity. In Fig. 3(a) the pumping power was zero, and the oscillation mode of the signal source klystron is seen with the resonance absorption of the signal cavity in the center (critically coupled). By increasing the pumping power to 35 mw and tuning in to twice the signal cavity frequency, some reduction in cavity loss was obtained [Fig. 3(b)]. Fig. 3(c)–3(e) shows gain with 56, 82, 140 mw of pumping power, respectively.

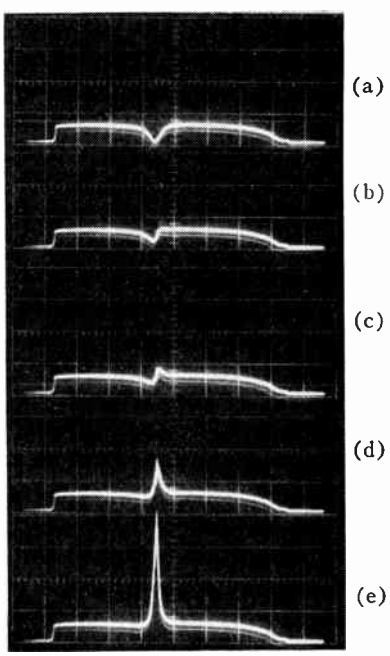


Fig. 3—Parametric amplification as function of pumping power.

Fig. 4 shows an enlarged section of the gain region. During the sweep, the phase changes periodically from that giving amplification to that giving attenuation, and this

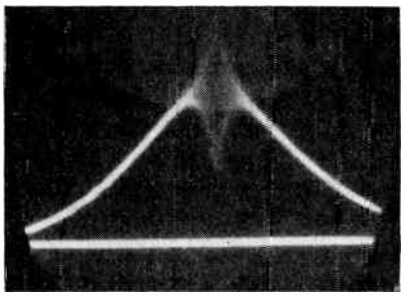

Fig. 4—Enlarged portion of Fig. 3(e).

accounts for the pattern seen in the center of the picture. The width of the pattern depends on the bandwidth of the video amplifiers used.

T. J. Bridges
Bell Telephone Labs., Inc.
Murray Hill, N. J.

## On the Earth Geometry—A Theorem*

If one chooses an arbitrary point $P$ inside of a circle other than its center, a normal $s$ upon the diameter, both through $P$, intersects the circle with $\psi$, which is the angle between $s$ and the tangent to the circle through the intersection point (Fig. 1). It can be shown analytically that $\psi$ increases if $s$ is rotated on $P$ in either sense. For the conditions stated above $\psi$ must be a minimum.

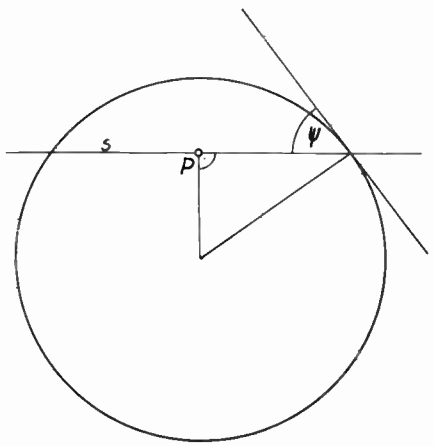


Fig. 1.

Applied to the earth geometry and to propagating radio waves which are reflected by the ionosphere, one arrives at the following conclusion: if the antenna height is zero and a radio beam is moved progressively from the zenith to the horizon, $\psi$, the angle of incidence at the reflecting layer, diminishes monotonously and reaches a minimum for zero elevation angle $\Delta$ of the beam, provided earth and ionosphere are concentric

* Received by the IRE, August 30, 1957.

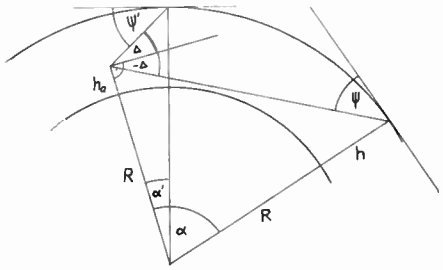


Fig. 2—The earth geometry.

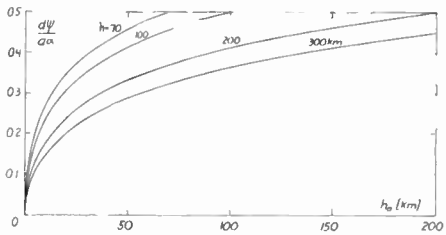


Fig. 3—$d\psi/d\alpha$ for negative elevation angles $\Delta$ as a function of antenna $h_a$ and layer height $h$.

spheres (Fig. 2). Applying the same procedure to finite antenna heights, it can be shown that $\psi$ passes through this minimum before the beam becomes tangent to the earth, *i.e.*, for a negative elevation angle $\Delta$ of the beam $d\psi/d\alpha$ is positive. For an earth whose radius is modified so as to include uniform refraction in the atmosphere $k=1.25$ and for negative values of $\Delta$, $d\psi/d\alpha$ was calculated as a function of antenna elevation $h_a$ for various heights of the reflecting layer $h$ (Fig. 3). $d\psi/d\alpha$ is less than one half for all practical cases of $h_a < h$.[1]

Kurt Toman
Geophysics Res. Directorate
Boston, Mass.

[1] Negative values of $\Delta$ correspond to the beam grazing the earth.

## Behavior of Noise Figure in Junction Transistors*

Nielsen[1] has presented a well-organized treatise on a timely subject. He has simplified van der Ziel's circuit by assuming the emitter and collector noise generators are uncorrelated. It may be of interest to see how the noise figure expressions may be modified to include the effect of partial correlation of the emitter and collector noise generators.

Van der Ziel[2,3] has determined the magnitudes of the noise generators to be

* Received by the IRE, September 13, 1957.

[1] E. G. Nielsen, Proc. IRE, vol. 45, pp. 957–963; July, 1957.

[2] A. van der Ziel, "Theory of shot noise in junction diodes and junction transistors," Proc. IRE, vol. 43, pp. 1639–1646; November, 1955.

[3] "Theory of shot noise in junction diodes and junction transistors," Proc. IRE, vol. 45, p. 1011; July, 1957.

$$\overline{e_s^2} = \frac{2kTdf(2g_e - g_0)}{g_s^2 + b_s^2} \quad (1)$$

$$\overline{i_p^2} = 4kTG_n d = 2kTdf\alpha_0 g_0\left(1 - \frac{|\alpha|^2}{\alpha_0}\right) + 2eI_{c_{sat}}df \quad (2)$$

or

$$G_n = \frac{\alpha_0 g_0}{2}\left(1 - \frac{|\alpha|^2}{\alpha_0}\right) + 20I_{c_{sat}}$$

$$e_s^* i_p = 2kTdf\alpha\left(1 - \frac{g_0}{Y_e^*}\right). \quad (3)$$

Van der Ziel sets $e_s = e_s'' + e_s'$ where $e_s''$ is uncorrelated with $i_p$, and $e_s'$ is completely correlated with $i_p$.[4]

He also sets

$$\overline{e_s''^2} = 4kTR_{ndf}, \quad (4)$$

where $R_n = r_e/2$ at low frequencies.

$$e_s' = \frac{Z_1 i_p}{\alpha} \text{ where } Z_1 = \pm R_1 \pm jX_1 \quad (5)$$

$$\therefore e_s^* i_p = \left(e_s''^* + \frac{Z_1^* i_p^*}{\alpha^*}\right) i_p = e_s''^* i_p + \frac{Z_1^* \overline{i_p^2}}{\alpha^*}. \quad (6)$$

Since $e_s''^* i_p = 0$ then, neglecting effects of collector saturated current, $I_{c_{sat}}$,

$$Z_1^* = \frac{e_s^* i_p \alpha^*}{\overline{i_p^2}} = \frac{2kTdf\alpha\left(1 - \frac{g_0}{Y_e^*}\right)\alpha^*}{2kTdf\alpha_0 g_0\left(1 - \frac{|\alpha|^2}{\alpha_0}\right)} \quad (7)$$

$$Z_1^* = \frac{|\alpha|^2\left(1 - \frac{g_0}{Y_e^*}\right)}{\alpha_0 g_0\left(1 - \frac{|\alpha|^2}{\alpha_0}\right)} = \frac{|\alpha|^2\left(\frac{1}{g_0} - \frac{1}{Y_e^*}\right)}{\alpha_0 - |\alpha|^2}. \quad (8)$$

Thus at very low frequencies $Y_e^* \to g_0$ and $Z_1 \to 0$ in the absence of If noise, and at very high frequencies $|\alpha| \to 0$ and $Z_1 \to 0$. At some intermediate frequency $Z_1$ will reach a maximum value. To find that approximate maximum value and the approximate frequency at which it occurs, the expressions for $Y_e$ and $\alpha$ derived by Pritchard[5] may be substituted into (8). $Y_e$ is the diffusion admittance of the emitter-base junction.

$$Y_e \approx \frac{qI_e}{kT}\frac{[(1 + 0.25x^2) + j0.8x]}{1 + 0.06x^2} \quad (9)$$

where

$$\frac{qI_e}{kT} = g_0, \quad x = \frac{f}{f_\alpha},$$

$f_\alpha$ = inherent alpha cutoff frequency.

$$\alpha \approx \alpha_0 \frac{[(1 - 0.25x^2) - j1.2x]}{(1 + x^2)}. \quad (10)$$

[4] G. N. Hanson and A. van der Ziel, "Noise in transistors," to be published.

[5] R. L. Pritchard, "Frequency response of theoretical models of junction transistors," IRE TRANS., vol. CT-2, pp. 183–191; June, 1955.

At this time (9) and (10) will be simplified to

$$Y_e \approx g_0(1 + jx) \quad (11)$$

$$\alpha \approx \frac{\alpha_0}{1 + jx}. \quad (12)$$

The magnitude of alpha in (12) should be within 10 per cent of the value in (10) up to twice $f_\alpha$. The magnitude of $Y_e$ in (11) is within 15 per cent of the value of (9) up to $f = 2f_\alpha$. However, there is an excess angle in (11) of 12° at $f_\alpha$ and 25° at $2f_\alpha$. With the emitter-base transition capacity assumed small compared to the diffusion capacity, then

$$Z_1 \approx \frac{\frac{\alpha_0}{g_0}\left(1 - \frac{1}{1 + jx}\right)}{(1 - \alpha_0 + x^2)}, \quad (13)$$

$$R_1 \approx \frac{\alpha_0}{g_0}\frac{x^2}{(1 + x^2)(1 - \alpha_0 + x^2)}, \quad (14)$$

$$X_1 \approx \frac{\alpha_0}{g_0}\frac{x}{(1 + x^2)(1 - \alpha_0 + x^2)}, \quad (15)$$

$$|Z_1| \approx \frac{\alpha_0}{g_0}\frac{x}{\sqrt{1 + x^2}(1 - \alpha_0 + x^2)}. \quad (16)$$

Using values of $\alpha_0 = 0.98$, $r_{e_0} = 1/g_0 = 26\Omega$ at $I_\xi = 1$ ma, (14), (15), and (16) reach maximum values at the indicated frequencies below:

$$R_{1_{max}} \approx 19.5\Omega f \approx 0.38 f_\alpha$$

$$X_{1_{max}} \approx 88.0\Omega f \approx 0.14 f_\alpha$$

$$|Z_1|_{max} \approx 90.0\Omega f \approx 0.14 f_\alpha.$$

Under those conditions of transistor amplifier operation where $Z_L$ (the load impedance across which is obtained the output signal) contains a source of thermal noise $\overline{e_{nL}^2} = 4kTR_L df$, and provided $\alpha Z_c \gg Z_e$, $\alpha Z_c \gg Z_g + Z_b$, $\alpha Z_c \gg R_L$, the common-base and common-emitter noise figures then become

$$F_b = F_e = 1 + \frac{r_b'}{R_g} + \frac{R_n}{R_g} + \frac{G_n}{R_g|\alpha|^2}|(R_g + r_b' + r_e - R_1)^2 + (x_g - x_b' - x_e - X_1)^2|, \quad (17)$$

where the complex base impedance $Z_b' = r_b' - jx_b'$. In alloy transistors $Z_b' = r_b'$.

The common collector noise figure is

$$F_c = 1 + \frac{r_b'}{R_g} + \frac{R_n + R_L}{R_g} + \frac{G_n}{R_g}\left[\left(R_g + r_b' - R_e\left[\frac{Z_1}{\alpha}\right]\right)^2 + \left(x_g - x_b' - I_m\left[\frac{Z_1}{\alpha}\right]\right)^2\right]. \quad (18)$$

It is interesting to observe that the noise figures for the common-emitter and common-base configurations are independent of $Z_L$ to the extent that the above conditions are satisfied. However, it should be noted that the common collector amplifier noise figure is degraded as $R_L$ is increased. Decreasing $R_L$ in this case to improve the noise figure will also decrease the dynamic input impedance to the stage, which may be undesirable.

Nielsen points out the noise figure of the common collector becomes fairly constant at high frequencies. However, lest one be tempted to use this configuration at frequencies above $f_\alpha$, it should be pointed out that the available power gain must inevitably decrease to zero so that the device becomes useless as a signal amplifier in spite of its lower noise figure.

The contribution to the noise figure of the correlation impedance $Z_1$ is probably negligible in Nielsen's measurements in view of the moderate value of emitter current used (1–3 ma) and the magnitude of the source resistance (around 500Ω). However, under conditions of low emitter current and low source resistance the contribution may have to be included. Also, the contribution to the noise figure from the reactive term multiplying $G_n/R_g|\alpha|^2$ may also become important when $R_g$ becomes smaller.

Finally, to those interested in the design of transistor amplifiers with the ultimate in sensitivity (hence minimum noise figure), it may be well to show how an unbypassed emitter resistance or a partially bypassed emitter resistance in the common-emitter configuration may degrade the noise figure. Let the net effective external emitter impedance be represented in the series impedance form of $Z_0 = R_0 - jx_0$. Then

$$F_e = 1 + \frac{r_b'}{R_g} + \frac{R_n + R_0}{R_g} + \frac{G_n}{|\alpha|^2 R_g}|(R_g + r_b' + r_e + R_0 - R_1) + (x_g + x_b' + x_e + x_0 - x_1)^2|. \quad (19)$$

At audio frequencies in the shot noise region $Z_1 \to 0$, $X_b' \to 0$, $x_e \to 0$. Let us assume the actual generator driving the stage is purely resistive, but let us lump the reactance of the input coupling capacitor $x_{c_1}$ into $x_g$ so that $x_g = x_{c_1}$. Then

$$F_e = 1 + \frac{r_b'}{R_g} + \frac{R_n + R_0}{R_g} + \frac{G_n}{|\alpha|^2 R_g} \cdot |(R_g + r_b' + r_e + R_0)^2 + (x_{c_1} + x_0)^2|. \quad (20)$$

Not only does $R_0$ degrade the noise figure but so does $X_0$ and $x_{c_1}$ as well. If possible, one should ground the emitter directly. Otherwise, if an external resistance is employed, use a large capacitance to reduce $R_0$ and $x_0$ to a small value. Also, $x_{c_1}$ should be made small compared to $R_g$ for minimum noise figure.

This may be a new criterion for some who have been used to making $x_{c_1}$ at some low frequency $f_l$ small, compared to generator resistance plus the input resistance to the particular stage, to help insure adequate low-frequency response down to $f_l$.

The writer would like to acknowledge helpful discussions with R. L. Watters and K. E. Mortenson of this Laboratory and with Prof. A. van der Ziel, University of Minnesota.

W. N. COFFEY
General Electric Res. Lab.
Schenectady, N.Y.

## Electrolytic Tank Design of Electron Guns with Curved Electron Trajectories*

The general problem in electron gun design is to find a set of electrode shapes which approximate along the beam edge a theoretically determined gradient and potential distribution. For guns employing rectilinear flow, the problem is relatively simple, for the equipotentials are normal to the electron trajectories and the beam edge may be simulated in an electrolytic tank by an insulating strip, a method due to Pierce.[1] Of increasing interest, however, are types of motion in which the equipotentials are not normal to the beam edge as, for example, the curved trajectory flows discussed by Meltzer[2] and Walker[3] and more recently reported on by Kirstein and Kino.[4] If an electrolytic tank is to be used for gun design in these more general cases, an alternative to the insulating strip method must be employed.

Since it is no longer practical to fix the direction of the gradient at the beam edge, the potential distribution is the logical function to specify. For the general case then, the beam edge is simulated in an electrolytic tank by a resistance card cut so that a current caused to flow from one end to the other will establish along the card a potential distribution which will match the potential distribution required along the edge electron trajectory. After cutting, the card is placed in the tank and curved so as to duplicate the electron path. With the proper voltage applied across the card, the electrode shapes and positions are adjusted until the correct angles are established between the resistance card and the equipotentials. This operation is facilitated by placing immediately adjacent to the resistance card a series of probe pairs oriented so that the direction each pair defines is appropriate to the correct equipotential at that point (see Fig. 1). Proper

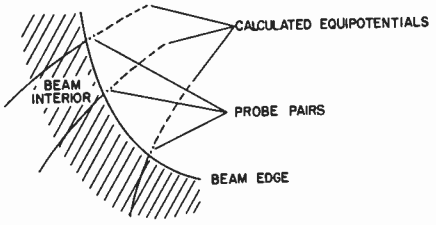


Fig. 1.

electrode design will then make the potential difference between the two probes of a given pair zero. In practice, it suffices to calculate for each pair the potential difference resulting from some allowable error in the angle of the equipotential and then settle for a design where the measured potential difference is less than or equal to this value.

To simplify the cutting of the resistance card, the potential distribution may be approximated by a series of chords and the resistance card cut, as in Fig. 2. The dotted lines indicate strands of fine wire which are


Fig. 2.

woven into the card at each discontinuity in order to keep the equipotentials on the card parallel. The conductivity of the card should be much greater than that of the electrolyte so that the current flowing into the tank from the card will not appreciably alter the potential distribution.

The device used to measure the probe pair potential differences must present identical high input impedances to each probe. In addition, each probe should be etched and coated with aqua-dag before use, in order to minimize surface effects.

The method of design just described generally is applicable to any flow which requires that a given potential and gradient be matched along a path. It has been used here quite successfully in connection with the design of electron guns which operate in the presence of a transverse magnetic field and should find additional application with the curved trajectory flows mentioned.

E. J. Cook
General Electric Research Laboratory
Schenectady, New York

* Received by the IRE, September 23, 1957.

[1] J. R. Pierce, *J. Appl. Phys.*, vol. 11, pp. 548–554; August, 1940.
[2] B. Meltzer, *Proc. Phys. Soc.*, vol. B62, pp. 813–817; December, 1949.
[3] G. B. Walker, *Proc. Phys. Soc.*, vol. B63, pp. 1017–1027; December, 1950.
[4] Kirstein and Kino, paper presented at the IRE Tube Conference, Berkeley, Calif., June, 1957.

## Space-Charge-Balanced Hollow Beam with Uniform Charge Distribution*

In 1949, Samuel[1] proposed a convergent hollow-beam electron gun with an external conductor and a special shielding magnet, which is used to divide the magnetic flux at the mouth of a focusing solenoid in such a way that the flux threading through the hole in the cathode is the flux contained within the inner beam radius. In a subsequent investigation carried out by Harris,[2] this configuration was shown to be one of a class of electron beams utilizing what has since been called *space-charge-balanced flow*; *i.e.*, the type of beam focusing in which electrons are caused to rotate about the axis in an axial magnetic field in such a way that the outward space-charge-spreading plus centrifugal forces are just balanced by the inward Lorentz force. (The well-known *Brillouin-flow* focusing is a special case, in which the magnetic field drops off to zero at the cathode.) The hollow beam in space-charge-balanced flow requires a specific radial charge distribution, given by[1]

$$\rho = 2\epsilon_0\eta A_0^2\left[1+\left(\frac{r_a}{r}\right)^4\right] \qquad (1)$$

where $A_0$ is the normalized magnetic vector potential and $r_a$ is the inner beam radius. If the radial charge distribution deviates from the form of (1), individual electrons follow stable oscillating trajectories; but as Harris has shown,[2] the angular frequency of oscillation is *not* independent of radius, so that adjacent electrons at different initial radial positions oscillate with different frequencies. Under this condition adjacent electron paths ultimately must cross, and the important laminar-flow assumption of space-charge-balanced flow analysis is violated.

The present note is a report on an analysis and experimental investigation of the case in which a deliberate deviation from the distribution of (1) is made by making $\rho$ independent of radius. The uniform charge distribution is of obvious practical interest since it would be extremely difficult to obtain any other distribution from a conventional cathode without an elaborate design of the transition region between the gun and the interaction regions.

The equation of motion for this case can be derived quite simply if it is assumed that adjacent electrons do *not* cross radially—an assumption that will be shown below to be satisfied if beam lengths are restricted to a certain range (which is, nevertheless, of considerable practical interest).

$$\ddot{r} = r_0^2\frac{\omega_p^2}{2r}\left(1-\frac{r_a^2}{r_0^2}\right)-\omega_L^2 r\left(1-\frac{r_a^4}{r^4}\right) \qquad (2)$$

where $\omega_L \equiv \eta B/2$ is the Larmor frequency, $\omega_p^2 \equiv -\eta\rho_0/\epsilon_0$ is the plasma frequency, and $\rho_0$ is the charge density inside the radius $r_0$ of a given electron. Again, (2) can be readily solved if it is assumed that electron trajectories deviate only slightly from straight paths (an assumption that likewise is justified by the results of the analysis). Then $r=r_0+\Delta$, where $\Delta \ll r_0$; $\ddot{r}=\ddot{\Delta}$; and

$$\frac{1}{r}\approx\frac{1}{r_0}\left(1-\frac{\Delta}{r_0}\right);\quad \frac{1}{r^3}\approx\frac{1}{r_0^3}\left(1-3\frac{\Delta}{r_0}\right).$$

Thus

$$\ddot{\Delta} = \alpha - \beta^2\Delta \qquad (3)$$

where

$$\alpha \equiv r_0\left[\frac{\omega_p^2}{2}\left(1-\frac{r_a^2}{r_0^2}\right)-\omega_L^2\left(1-\frac{r_a^4}{r_0^4}\right)\right]$$
$$\beta^2 \equiv \frac{\omega_p^2}{2}\left(1-\frac{r_a^2}{r_0^2}\right)+\omega_L^2\left(1+3\frac{r_a^4}{r_0^4}\right). \qquad (4)$$

Eq. (3) has the solution

$$\Delta = \gamma\cos(\beta l-\delta)+\frac{\alpha}{\beta^2} \qquad (5)$$

and the constants $\gamma$ and $\delta$ can be evaluated from the entrance conditions $\Delta=0$ and $\dot{\Delta}=\dot{r}_a$ at $t=0$, where $\dot{r}_a$ is the slope at entrance, so that finally

$$\Delta = \frac{\alpha}{\beta^2}(1-\cos\beta l)+\frac{\dot{r}_a}{\beta}\sin\beta l. \qquad (5a)$$

The value of $\alpha/\beta^2$ may be adjusted in accordance with the boundary conditions that one chooses to impose on the configuration; *e.g.*, the specification of a nonoscillating outer beam boundary ($\ddot{r}=0$ at $r_0=r_b$, the equilibrium radius of the outermost electron) leads to a generalized form of the familiar Brillouin flow equilibrium condition

* Received by the IRE, July 29, 1957; revised manuscript received, September 26, 1957. Much of this work was carried out under the sponsorship of the U. S. Navy, Army, and Air Force under Contracts N6onr 25132 and DA36-039-sc-63189.

[1] A. L. Samuel, "On the theory of axially symmetric electron beams in an axial magnetic field," PROC. IRE, vol. 37, pp. 1252-1258; November, 1949.
[2] L. A. Harris, "Axially symmetric electron beam and magnetic-field systems," PROC. IRE, vol. 40, pp. 700–708; June, 1952.

$$\frac{\omega_p^2}{2} = \omega_L^2\left(1+\frac{r_a^2}{r_b^2}\right). \tag{6}$$

It is obvious from (4) that the angular frequency of oscillation $\beta$ is not independent of $r_0$, and hence adjacent trajectories must cross, as mentioned previously. However, in the first few oscillation wavelengths, the electrons merely begin to slip past one another, and relatively little crossing takes place. As an example, consider trajectories of a hollow beam for which $\dot{r}_a=0$ (beam parallel to the axis at entrance), and the outer boundary is held at constant radius. (The inner boundary is automatically parallel to the axis, since $\alpha=0$ at $r_0=r_a$.) Two adjacent paths at radii $r_1$ and $r_2(r_1<r_2)$ will not cross if at all times $r_2+\Delta_2 \geq r_1+\Delta_1$; *i.e.*, if $\Delta_2-\Delta_1 \geq -(r_2-r_1)$, which in the limit becomes

$$\frac{d\Delta}{dr_0} \geq -1. \tag{7}$$

But from (5a), for the case $\dot{r}_a=0$,

$$\frac{d\Delta}{dr_0} = (1-\cos\beta t)\frac{d}{dr_0}\left(\frac{\alpha}{\beta^2}\right) + t\frac{\alpha}{\beta^2}\sin\beta t\frac{d\beta}{dr_0}.$$

It can be shown (perhaps most readily by means of a plot, as described below) that the term $\alpha/\beta^2$ has its maximum negative slope at $r_0=r_a$ (the equilibrium radius of the innermost electron), and that the first term of (8) consequently always is greater than $-1$, so that only the second term invalidates the inequality (7). Since this term is proportional to $t$, it is possible that the assumption of noncrossing trajectories may be satisfied if $t$ remains small (*i.e.*, if the time necessary to pass through the interaction region is small). A graphical representation of the case $r_a=\frac{2}{3}r_b$ (Fig. 1) shows that such is indeed the case. The change in angular oscillation frequency $\beta$ over the beam width is so small that virtually no crossing takes place within the first few oscillation cycles.

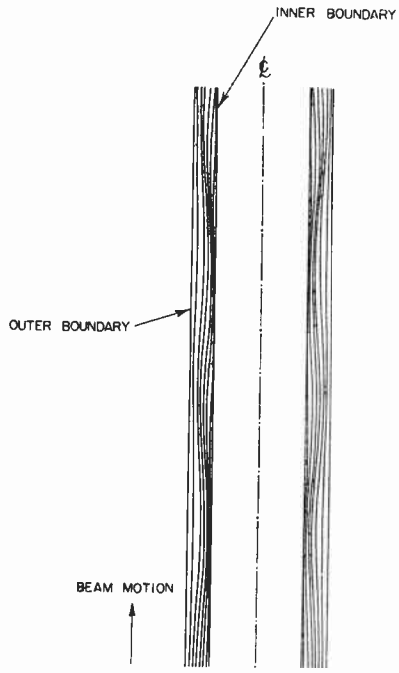


Fig. 1—Electron trajectories in a hollow beam initially parallel to the axis with uniform charge distribution under space-charge-balanced flow for $r_a=\frac{2}{3}r_b$.

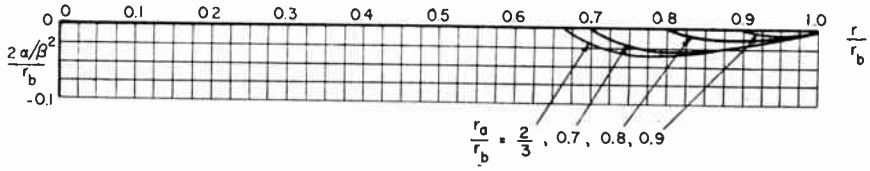


Fig. 2—Maximum deviation from initial radius (as a function of radius) for several beam thicknesses.

The amplitude of the oscillation for the present case varies with $r_0$ as $\alpha/\beta^2$ (5a) and is zero at the inner and outer edges. The maximum amplitude $2\alpha/\beta^2$ is plotted as a function of radius $r$ in Fig. 2, both normalized with regard to the outer beam radius $r_b$. The graphs show that the greatest deviation occurs near the middle between inner and outer boundary, and that the relative deviation becomes quite small for thin beams. The graphs also clearly illustrate the above statement that $\alpha/\beta^2$ has its maximum negative slope at $r=r_a$.

The angular frequency of oscillation varies from $\beta_a=2\omega_L$ (*i.e.*, a "wavelength" of $2\pi v_0/2\omega_L$ where $v_0$ is the dc beam velocity and $\omega_L$ is the Larmor frequency) at the inner boundary to $\beta_b=\omega_L\sqrt{2}[1+(r_a/r_b)^4]^{1/2}$ (*i.e.*, a wavelength of just under $2\pi v_0/\sqrt{2}\omega_L$) at the outer boundary). These values can be readily related by means of (6) to the plasma wavelength $\lambda_p=2\pi v_0/\omega_p$, where $\omega_p$ is the plasma frequency. For the present example, for instance, the oscillation "wavelength" varies from $0.423\lambda_p$ at the inner boundary to $0.556\lambda_p$ at the outer boundary.

The oscillation wavelength is thus of the order of half a plasma wavelength, and we may conclude that, even though an analysis of a hollow beam (with a uniform charge distribution) based on (2), and assuming noncrossing trajectories cannot be rigorously said to hold for arbitrary beam lengths, in practice the assumption is likely to be satisfied in a large number of actual applications in which the length of the beam is of the order of a few plasma wavelengths (*e.g.*, klystrons and most high-power traveling-wave tubes). A previously described and executed design[3] of a hollow-beam electron gun appears to bear out this conclusion.

MARVIN CHODOROW
Stanford University
Stanford, Calif.
CHARLES SÜSSKIND
University of California
Berkeley, Calif.

C. Süsskind, "A Convergent Hollow-Beam Electron Gun for Microwave Tubes," Stanford Electronics Labs. and Microwave Lab., Stanford University, Stanford, Calif., Tech. Rep. No. 450-1; June 29, 1956.

## Design of Three-Resonator Dissipative Band-Pass Filters Having Minimum Insertion Loss*

In the above paper[1] Taub and Bogner have presented a great deal of useful design information for uniformly dissipative three-resonator filters which are to be driven by a resistive generator and work into a resistive load. The desire is to maximize the ratio of the power delivered to the load to that available from the generator.

We recently have had need to design such a filter for the Butterworth response shape and took this opportunity to compare our design equations with the analytical solution developed by Dr. E. G. Fubini and given as (5) and (6) in the above paper. Unfortunately, we find the presented equations to be incorrect and, in fact, simple numerical substitution in them shows that (5d) calls for imaginary values for $k_{23}$ for even such a low-normalized decrement as 0.1.

The correct equations, arrived at by B. Sellers of the Federal Telecommunication Laboratories, Nutley, N. J., are given below:

$$\delta_1 = \frac{U_2-V_2}{2}+\delta_2 \tag{1a}$$

$$\delta_3 = \frac{U_2+V_2}{2}+\delta_2 \tag{1b}$$

$$k_{12} = \frac{U_0+V_0}{U_2+V_2} \tag{1c}$$

$$k_{23}^2 = \frac{U_0-V_0}{U_2-V_2} \tag{1d}$$

$$(P_1/P_a) = \frac{(U_0+V_0)(U_0-V_0)}{C_0^2} \tag{1e}$$

where

$$U_2 = (2-3\delta_2) \tag{2a}$$

$$U_0 = (1-2\delta_2+2\delta_2^2-\delta_2^3) \tag{2b}$$

$$V_2 = \sqrt{2B-A} \tag{2c}$$

$$V_0 = (B+A)\sqrt{(2B-A)} \tag{2d}$$

where

$$A = 1/3(4\delta_2-3\delta_2^2) \tag{2e}$$

$$B = 1/3\sqrt{(6\delta_2-8\delta_2^2)} \tag{2f}$$

$$C_0 = 1.0.$$

These solutions were obtained by using the twelve synthesis steps detailed in a previous paper.[2] These steps are one way of expressing the Darlington procedure. When performing the steps all quantities were kept literal; *i.e.*, no numerical values were used, and the following two basic points were included:

1) It was realized that, for the specific case wherein the numeric 1.0 is used in step 6 (in order that minimum insertion loss result), the resulting cubic polynomial in $(\omega/\omega_{3db})^2$ must have a positive real *double* root. Thus when step 7 is performed, we may use

* Received by the IRE, August 26, 1957.

[1] J. J. Taub and B. F. Bogner, "Design of three-resonator dissipative band-pass filters having minimum insertion loss," PROC. IRE, vol. 45, pp. 681-687; May, 1957.

[2] M. Dishal, "Two new equations for the design of filters," *Elec. Commun.*, vol. 30, pp. 324-337; December, 1953. Addendum, vol. 32, p. 178; September, 1955.

the explicit (and quite simple) closed form expressions for the roots of a cubic which is known to have a double root. Having the roots of step 7 in closed literal form enables the following steps 8 through 12 also to be performed in a literal manner.

2) The continued fraction expansion of steps 9 and 10 produces the so-called ladder-network coefficients ($a_1$, $a_2$, and $a_3$) *in terms of the left-hand termination*. To obtain the left-hand end decrement and the coefficients of coupling, it is necessary to realize that the simple relationship between the above two forms of circuit constants is as follows:[3]

$$\delta_1 = \left(\frac{1}{a_1} + \delta_0\right), \quad k_{12}^2 = \frac{1}{a_1 a_2},$$

$$k_{23}^2 = \frac{1}{a_2 a_3}, \text{ etc.}$$

Similarly, the continued fraction expansion of steps 11 and 12 produces a different set of $a$'s ($a_{111}$, $a_{11}$, $a_1$) *in terms of the right-hand termination*. This set then gives the right-hand end decrement and the coefficient of couplings as:

$$\delta_3 = \left(\frac{1}{a_{111}} + \delta_0\right), \quad k_{23}^2 = \frac{1}{a_{11} a_{111}},$$

$$k_{12}^2 = \frac{1}{a_1 a_{11}}, \text{ etc.}$$

The simplest resulting expressions then were picked to provide the design equations (1a) through (1e) of this letter.

Incidentally, as pointed out in the Taub and Bogner paper, the important (Butterworth) design chart Fig. 4(a) was obtained by "graphical" methods and not by the analytical solutions, (5), presented by them. We do agree with the values called for in Fig. 4(a), except in the region to the left of 0.2 of the abscissa. In this region of low loss the graphical solution is rather inaccurate and the design equations presented in this letter show that even with such a low-normalized decrement as 0.05 the required network values have changed from their "lossless" values more rapidly than as given in Fig. 4(a); *e.g.*, at $(\delta_2/\delta_{2\max}) = 0.05$, $\delta_1 = 0.765$, $k_{12} = 0.655$, $k_{23} = 0.780$, and $\delta_3 = 1.225$. This rapid change from the symmetrical values, called for with lossless resonators, stresses the fact that optimum filters (with respect to insertion loss) are markedly unsymmetrical—as can be seen, this is particularly true of the required end resonator decrements.

Incidentally, by comparing our solutions with those given in the Taub and Bogner paper, Sellers has found the error in the latter solutions; when corrected, they should read as follows:

$$k_{12}^2 = \delta_2^2\left[\frac{\gamma + (\beta - 2\rho)\sqrt{\alpha^2 - 4\rho}}{\alpha + \sqrt{\alpha^2 - 4\rho}}\right]$$

$$k_{23}^2 = \delta_2^2\left[\frac{\gamma - (\beta - 2\rho)\sqrt{\alpha^2 - 4\rho}}{\alpha - \sqrt{\alpha^2 - 4\rho}}\right].$$

[3] "Filters, Modern-Network-Theory Design," in "Reference Data for Radio Engineers," International Telephone and Telegraph Corp., 4th ed., pp. 187–235; 1956.

It is straightforward to obtain the closed form solutions for the end decrements and the coefficients of couplings required when uniformly lossy resonators are used and the general Tchebycheff response shape with minimum insertion loss is desired—(1) of this letter applies to this case also, but the $U$'s and $V$'s must be defined more generally as follows:

$$U_2 = (C_2 - 3d_0) \tag{3a}$$

$$U_1 = (C_1 - 2C_2 d_0 + 3d_0^2) \tag{3b}$$

$$U_0 = (C_0 - C_1 d_0 + C_2 d_0^2 - d_0^3 \tag{3c}$$

and again

$$V_2 = \sqrt{2B - A} \tag{3d}$$

$$V_0 = (B + A)\sqrt{2B - A} \tag{3e}$$

where now

$$A = 1/3(2U_1 - U_2^2) \tag{3f}$$

$$B = 1/3\sqrt{(2U_1 - U_2^2)^2 - 3(U_1^2 - 2U_2 U_0)} \tag{3g}$$

and

$$C_2 = \left(\frac{S_3}{C_3}\right)(2) \tag{3h}$$

$$C_1 = \left(\frac{S_3}{C_3}\right)^2\left(2 + \frac{0.75}{S_3^2}\right) \tag{3i}$$

$$C_0 = \left(\frac{S_3}{C_3}\right)^3\left(1 + \frac{0.75}{S_3^2}\right) \tag{3j}$$

where

$$S_3 = \sinh\left[1/3 \sinh^{-1}\left([V_\rho/V_v]^2 - 1\right)^{-1/2}\right] \tag{3k}$$

$$C_3 = \cosh\left[1/3 \cosh^{-1}\left([V_\rho/V_v]^2 - 1\right)^{-1/2}\right]. \tag{3l}$$

In the above equations, all decrements and coefficients of coupling are normalized to the 3-db down fractional bandwidth.

M. Dishal
B. Sellers
Federal Telecommun. Labs.
Nutley, N. J.

*Authors' Comment*[4]

We appreciate Dishal and Sellers pointing out an error in our paper. Upon rechecking the solution, it was found that an error was made in (5c) and (5d). The error was not in Dr. Fubini's solution. It came about in transcribing it from his notation to that used in our paper. The corrected expressions for (5c) and (5d) should read:

$$k_{12}^2 = \delta_2^2\left[\frac{-\frac{1}{2}(\alpha - \sqrt{\alpha^2 - 4\rho})(\beta - \rho) + \gamma}{\sqrt{\alpha^2 - 4\rho}}\right] \tag{5c}$$

$$k_{23}^2 = \delta_2^2\left[\frac{\frac{1}{2}(\beta - \rho)(\alpha + \sqrt{\alpha^2 - 4\rho}) - \gamma}{\sqrt{\alpha^2 - 4\rho}}\right]. \tag{5d}$$

Although not apparent, a check of these expressions and those given by Dishal and Sellers reveals that they are identical. This identity of the two solutions demonstrates that either the Darlington procedure or the direct minimization of the insertion loss, in conjunction with the three design equations, are equally valid approaches for obtaining the set of circuit constants which yield minimum midband insertion loss.

The nature of the numerical computations used in obtaining the graphical solution for the Butterworth response gave rise to errors (in the low-loss region—$\delta_2 < 0.1$) of 0.2-db maximum in the filter midband insertion loss. A recheck of the design chart, Fig. 4(a), showed agreement with the closed form solution. It therefore is recommended that the closed form solution be used in obtaining the correct deisgn parameters for $\delta_2 < 0.1$.

J. J. Taub
B. F. Bogner
Airborne Instruments Lab., Inc.
Mineola, N.Y.

[4] Received by the IRE, September 26, 1957.

## Space-Frequency Equivalence*

Correlation systems comprising a pair of widely separated antennas have been suggested for the detection of signals encompassing a wide frequency band.[1-3] The purpose of this note is twofold: 1) to observe that such wide-band correlation systems will operate equally well if the source consists of a number of discrete frequencies, and 2) to discuss the correspondence which exists between the spatial complexity of the usual single-frequency antenna system and the frequency complexity of the antenna-pair multifrequency correlation system.

Directional patterns of the two-receiver cross-correlation system are easily calculated from a consideration of the power spectrum employed and the use of Wiener's theorem which states that the correlation function is the Fourier transform of the power spectrum of the original wave. A noise band extending from zero frequency has a Fourier transform represented by $\sin x/x$ and the output of a cross-correlator at the two receivers therefore will follow a $\sin x/x$ pattern as a noise source passes through the plane equidistant from the two receivers. The Fourier transform of a limited noise band (say an octave of noise) is a $\sin x/x$ function multiplied by a cosine term. Directional patterns for noise sources of other frequency extent can be similarly determined. For the discrete frequency case, the space-frequency plot shown in Fig. 1 is of interest. The conventional single-frequency space array of discrete elements is indicated as the horizontal line of circles. The directional pattern of any radiator pair is maintained if the product of frequency and spacing is kept constant; *i.e.*, if the pair is moved along the hyperbolas shown. In this way the horizontal row of radiators is converted to a radiator pair functioning at the frequencies indicated on the two vertical rows of circles. The process can, of course, be generalized to more than two elements. Because of squaring of the cosine terms which is inherent in the cor-

* Received by the IRE, October 7, 1957.

[1] M. Ryle, "A new radio interferometer audits application to the observation of weak radio stars," *Proc. Roy. Soc. A.*, vol. 211, pp. 351–375; March 6, 1952.

[2] R. Hanbury Brown, R. C. Jennison, and M. K. DasGupta, "Apparent angular sizes of discrete radio sources—observations at Jodrill Bank, Manchester," *Nature*, vol. 170, pp. 1061–1063; December 20, 1952.

[3] J. J. Faran, Jr. and R. Hills, Jr., Acoustics Res. Lab., Harvard Univ., Cambridge, Mass., Tech. Memo Nos. 27 and 28; 1952.

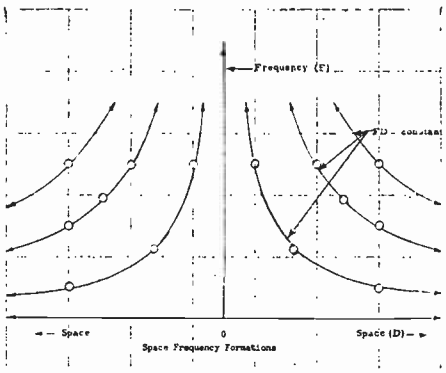


Fig. 1—The 6-element linear array operating at one frequency (top row of circles) has the same beam pattern as the correlation receiver pair detecting a source of three frequencies (two vertical rows of circles).

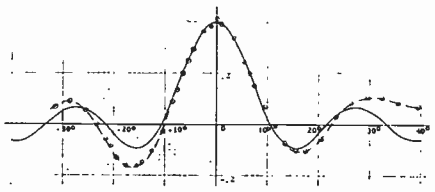

Fig. 2—Experimental test of the space-frequency equivalence indicated in Fig. 1. Dotted curve, an experimental beam pattern of the correlated outputs of two isotropic receivers spaced 21.5 inches apart against a source comprising frequencies 300, 900, and 1500 cps. Solid curve, the calculated pattern for a 6-element linear array 43 inches long against a 1500-cps source.

relation process, the pair spacing obtained by the method described must be divided by two.

Experimental verification of the concept was accomplished using sound waves. In Fig. 2 the solid curve is calculated for a 6-element array 5 wavelengths long; the dotted curve is a measured correlation pattern of a pair-array receiving three audio frequencies: 300, 900, and 1500 cps. The pair spacing was 2½ wavelengths at 1500 cps. It is observed that the correlation array is half the length of the conventional array.

We conclude that in a detection system, the space complexity and size of an antenna could be reduced by increasing the frequency complexity of the system. Such a process requires that the antennas be effective at several frequencies; however, the saving in antenna size and extent may outweigh this difficulty in certain applications. Either continuous noise bands or multiple discrete frequencies can be used to produce narrow directional patterns having low side lobes. Extensions of the concept could include 1) tapering of the intensity of the higher frequency components to reduce side lobes, 2) manipulation of the phases of individual frequencies to create shaped beams (*e.g.*, cosecant-squared beams) from a receiver pair, 3) alternate reversing of the polarity of discrete frequencies to achieve a super-directive multifrequency detection system,[4] and 4) the use of three or four receivers located in a plane with double cross-correlation to form a pencil beam.

This note has discussed mostly receiving aspects, applications of which would include radio astronomy, microwave radiometry, passive acoustic detection, and beacon tracking of moving objects. Signal-to-noise considerations, power gain evaluation, and the use of the concept in active systems will be discussed in a later paper.

W. E. Kock
J. L. Stone
Bendix Systems Division
Ann Arbor, Mich.

[4] Comparable to the single-frequency technique discussed by R. L. Pritchard, "Optimum directivity patterns for linear point arrays," *J. Acoust. Soc. Amer.*, vol. 25, pp. 879–891; September, 1953.

## Thermal Properties of Tungsten vs Copper for Electron Tube Delay Lines*

A calculational comparison has been made of the thermal load capacity of copper as against tungsten fingers in an interdigital delay line of particular, but not unrepresentative, dimensions for use in an electron tube. The finger was assumed to be a right circular cylinder of 0.050-inch diameter with a length of 10 diameters, or 0.500 inch, and was assumed to be heated uniformly along its length by electron bombardment, such as exists in tubes with a ribbon beam.

The choice of finger extremity temperatures can be made in several ways. A finger base temperature of 300°K was chosen for the problem as indicative of what can be obtained with the finger base in intimate contact with coolants at temperatures near 280°K. For the free end extremity temperature, three options are possible: 1) temperature adjusted so that the copper and tungsten delay lines have equal vapor pressures, 2) temperature adjusted so that rate of finger reduction due to evaporation is the same for the two metals, and 3) operation at the melting temperature of the metal involved. One can eliminate the third choice since the comparison ought to be made on a normal operation basis rather than on a condition tantamount to destruction of the delay line. The extremity temperatures were chosen according to option 2) based on a 1000-hour evaporation of 10 per cent of the finger mass. These values are 2680°K for tungsten and 1160°K for copper. In this case the calculated[1] vapor pressures are reasonable, $5.7 \cdot 10^{-7}$ mm Hg for copper and $1.1 \cdot 10^{-6}$ mm Hg for tungsten. Actually, options 1) and 2) give closely related extremity temperatures.

The differential equation governing the steady-state temperature distribution along the finger in the presence of radiation is,

$$Kc \frac{d^2T}{dz^2} = -\left[Pi - Kr(T^4 - C)\right] \quad (1)$$

where $Kc$ and $Kr$ are conduction and radiation "constants" (actually functions of temperature) and $Pi$ is the incident power per unit length. For tungsten, the absolute value and variation of $Kc$ have some spread in the literature, but what appeared to be the most reliable values were chosen.[2,3] Also, in the $Kr$ for tungsten, the effective radiating area is approximately 0.80 of the actual area since there is some radiation exchange between adjacent hot fingers. For copper, radiation is ineffective at the temperature achieved.

A numerical solution of (1) then yielded a permissible power input of 73 w per finger for tungsten, while the value for copper was 61 w per finger. Without radiation the tungsten value would be about 48 w.

For fingers of other diameters and length/diameter ratios, estimates can be made of their relative thermal capabilities keeping in mind that the conduction/radiation ratio is proportional to diameter/length.[2] An additional point is that increased diameters permit increased temperatures for a 1000-hour evaporation life.

Because tungsten at the chosen finger terminal temperature is an excellent thermionic emitter, some extra heating could be expected due to finger-to-finger electronic currents caused where rf power is transmitted along the delay line. Also, the average resistance of the tungsten under the assumed conditions of the problem is about 8 times that of hot copper, causing a $\sqrt{8}$ ratio of attenuation for the two lines. For tubes working at the higher microwave frequencies, a particular case shows that due to this cause about 3 extra watts/finger must be subtracted from the permissible thermal load of tungsten as against copper for a basic finger thermal load of about 36 w. Plating of the tungsten fingers with copper or silver to increase their surface conductivity is ineffective against this latter effect because of the high temperatures attained.

Roy A. Paananen
Raytheon Manufacturing Co.
Waltham, Mass.

* Received by the IRE, September 30, 1957.

[1] L. B. Loeb, "Kinetic Theory of Gases," McGraw-Hill Book Co., Inc., New York, N. Y., 2nd ed., p. 106; 1934.

[2] Forsythe and Worthing, "The properties of tungsten and characteristics of tungsten lamps," *Astrophys. J.*, vol. 61, pp. 146–185; 1925.

[3] Langmuir and Taylor, "Heat conductivity of tungsten and cooling effect of leads upon filaments at low temperatures," *Phys. Rev.*, vol. 50, pp. 68–87; 1936.

## Microwave Magnetic Field in Dielectric-Loaded Coaxial Line*

In a recent publication,[1] the authors described a probable mode configuration for a coaxial line one-half filled with a low-loss high dielectric constant material. This mode picture was based on the initial experimental results reported in that article. By additional experimental work and by subsequent theoretical considerations, it has been determined that this suggested picture should be rotated by 180° relative to the dielectric. The corrected picture is shown in Fig. 1, but this does not affect the previously re-

* Received by the IRE, April 26, 1957.

[1] B. J. Duncan, L. Swern, K. Tomiyasu, and J. Hannwacker, "Design considerations for broadband ferrite coaxial line isolators," Proc. IRE, vol. 45, pp. 483–490; April, 1957.

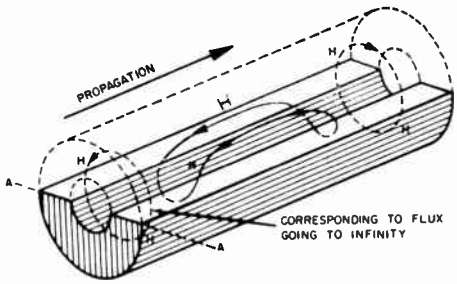


Fig. 1—Microwave $H$-field configuration in partially dielectric-loaded coaxial line.

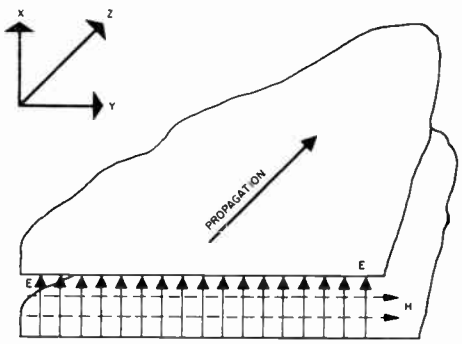


(a)

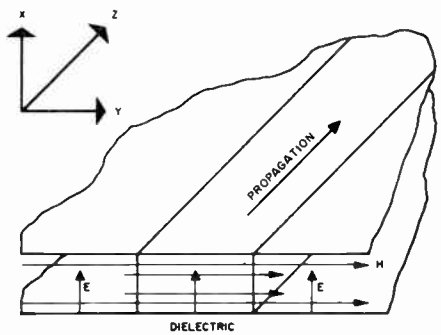


(b)

Fig. 2—(a) Microwave $E$ and $H$ fields in an air-filled plane parallel transmission line propagating the TEM mode. (b) Microwave $E$ and $H$ fields in a partially dielectric-loaded plane parallel transmission line—isometric view.

ported experimental data. That the latter picture is indeed the correct one will be demonstrated in this paper from a qualitative analysis using Maxwell's equations and by describing the additional experimental work.

An approach, to show that the strongest component of longitudinal magnetic field (Fig. 1) is in the air-filled one-half of the coax, starts with a parallel plane transmission line propagating the TEM mode [Fig. 2(a)]. As shown, only a transverse component of the microwave magnetic field $H$ exists for the air filled transmission line. Next, consider a dielectric wedge ($\epsilon' > 1$) located in the parallel plane line as depicted in Fig. 2(b). Under these conditions it will be shown that the instantaneous microwave magnetic field is as depicted in Fig. 2(b) (cross-sectional view) and Fig. 3 (top view).

The reasoning leading to this mode picture is based on several considerations. The dielectric is transparent to the microwave magnetic field due to the permeability ($\mu$) of the dielectric being unity. Also, in this region of the dielectric it can be assumed to a first-order approximation that the potential difference between the top and bottom plates [Fig. 2(b)] is a constant; *i.e.*,

$$\int E_x dx = \text{constant} \tag{1}$$

and is independent of $y$. In this equation, $E_x$ represents the $x$ component of the microwave electric field. This means that since the displacement vector ($D$) is defined by

$$D = \epsilon_0 \epsilon_m E, \tag{2}$$

where $\epsilon_0$ is the dielectric constant of free space and $\epsilon_m$ is the dielectric constant of the medium and satisfies Maxwell's divergence equation,

$$\nabla \cdot D = \rho, \tag{3}$$

where $\rho$ represents surface charge density, there must be more surface charge at the dielectric-conductor interface than at the air-conductor interface on either side. Because of the greater moving charge $\rho_m$ under the dielectric, there is a greater longitudinal current here and, hence, greater transverse field ($H_y$) as shown in Fig. 2(b) and Fig. 3. That is

$$\frac{\partial H_y}{\partial y} \neq 0.$$

Now, since away from the dielectric the longitudinal current, and hence $H_y$, becomes smaller, and since $\nabla \cdot B$ or $\nabla \cdot H$ must equal zero, there must be a longitudinal component of $B_z$ or $H_z$ near the dielectric-air interfaces to cancel out the nonzero derivative of $H_y$.

It has been demonstrated previously[2] that the change in charge distribution is not abrupt at the interface and it is reasonable to expect this for the parallel-plane case as well. This would lead, at microwave frequencies, to the picture given in Fig. 4. The kink in $E$ lines becomes essential to permit $\int E_x dx$ to remain constant, and to account for the increase in surface charge on the conductor in the region slightly removed in the transverse direction from the dielectric. This increase in surface charge and its consequent longitudinal current permits the change in $H$-flux lines shown in Fig. 3 to be gradual in the immediate vicinity of the dielectric. Since there is a kink in $E$, there is a curl of $E$. On the left side of the dielectric the curl is in the positive $z$ direction and since

$$\nabla \times E = -\frac{1}{c}\dot{B}, \tag{4}$$

this means that $B$ is increasing in the negative $z$ direction with increasing time. This result is compatible with the mode configuration of Fig. 3. Curl $E$ is oppositely oriented on opposite sides of the dielectric which also is consistent with the picture of Fig. 3.

A TEM mode coaxial line is, to a first approximation, a wrapped around version of the parallel-plane line of Fig. 2(a). Similarly, the structure of Fig. 2(b) and Fig. 3 can be wrapped around to form the coax structure of Fig. 1, thus giving rise to the TE mode configuration depicted in this same figure.

[2] D. J. Angelakos, "A coaxial line filled with two nonconcentric dielectrics," IRE TRANS., vol. MTT-2, pp. 39–44; July, 1954.

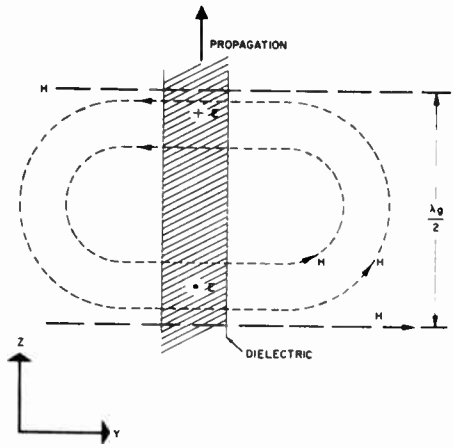


Fig. 3—Microwave $E$ and $H$ fields in a partially dielectric-loaded plane parallel transmission line—top view.

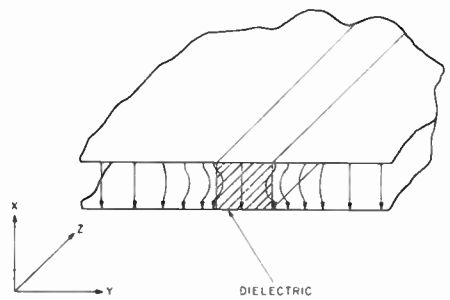


Fig. 4—Microwave $E$-field configuration in a partially dielectric-loaded plane parallel transmission line.

A similar argument can be given to show that a TM mode can, if excited, be propagated in the dielectric loaded structure. However, if a TM mode were generated it would exhibit no appreciable $H$-vector circular polarization on the dielectric surfaces and, hence, would not give rise to appreciable nonreciprocity of ferrite characteristics for the field orientation and other conditions under consideration. Since a very large nonreciprocity has been experimentally observed, most of the TEM energy incident on the dielectric loaded structure must be converted into the desired TE mode with only negligible conversion to the TM mode.

An experimental verification of the correctness of the mode picture of Fig. 1 over that previously reported can be achieved quite simply by checking the sense of circular polarization which exists on the dielectric surface under a known set of conditions.[3] This is readily apparent if it is realized that for a given direction of propagation and of transversely applied dc magnetic field along the dielectric surfaces, a 180° rotation of the mode picture changes the sense of circular polarization which exists on these surfaces.

In line with these considerations, a small diameter ferrite rod was placed on one and

[3] R. Mangiaracina and B. J. Duncan, "Nonreciprocal Ferrite Devices in TEM Mode Transmission Lines," presented at the Annual PGMTT Meeting, New York, N. Y., May 9–10, 1957.

then on the remaining flat dielectric surface of Fig. 1. The direction of propagation is as shown in the figure and a dc magnetic field of sufficient strength to produce ferrite resonance is applied along the direction from $A$ to $A'$. Under these conditions, no appreciable resonance attenuation is encountered with the ferrite located on either of the dielectric surfaces. However, when either the direction of applied magnetic field or propagation are reversed a large resonance absorption is encountered for location of the ferrite on either of the two surfaces. Therefore, it is apparent that these results are those which would be expected only for the mode configuration of Fig. 1.

B. J. Duncan
L. Swern
Sperry Gyroscope Co.
Great Neck, N. Y.
K. Tomiyasu
General Electric Microwave Lab.
Palo Alto, Calif.
(Formerly with Sperry Gyroscope Co.)

## Carrier Mobilities at Low Injection Levels*

In a recent paper,[1] Sah, Noyce, and Shockley have derived expressions for the diffusion currents flowing across a $p$-$n$ junction. They take into consideration the existence of an electric field, $E$, outside the transition layer, but they assume that the space charge due to the divergence of this field is negligible. The resulting mobility of minority carriers for any injection level is the ambipolar mobility, $\bar{\mu}=2\mu_n\mu_p/(\mu_n+\mu_p)$. The conclusion reached is that even at low injection levels the hole current injected in $n$-type material differs from the usual relation,[2] by a factor $\sqrt{\frac{1}{2}(\mu_n+\mu_p)/\mu_n}$, and implies that, under equal conditions, transit times across the bases of $n$-$p$-$n$ and $p$-$n$-$p$ transistors should be identical. We wish to point out here that the approximation used by Sah, Noyce, and Shockley is not justified.

Consider the steady-state equations:

$$J_p = q\mu_p pE - kT\mu_p \text{ grad } p, \quad (1)$$

$$J_n = q\mu_n nE + kT\mu_n \text{ grad } n, \quad (2)$$

$$\text{div } J_p = -\text{ div } J_n = -qU,$$

$$(J_p + J_n = J = \text{const}), \quad (3)$$

where the symbols have their usual meaning. Since space charge neutrality very nearly holds, $n\approx p+N$, and grad $n\approx$ grad $p$. We obtain the result of Sah, Noyce, and Shockley by adding the divergences of (1) and (2) (multiplied respectively by $-\mu_n$ and $\mu_p$) and neglecting terms containing div $E$. We shall check the validity of this procedure by computing the terms appearing in div $J_n$ in the case of low-level injection of holes in $n$-type material ($p\ll n\approx N$). From (1) and (2), using grad $n\approx$ grad $p_n$,

$$E = \frac{J - kT(\mu_n-\mu_p)\text{ grad } p}{q(\mu_p p+\mu_n n)} \approx \frac{J - kT(\mu_n-\mu_p)\text{ grad } p}{q\mu_n N}. \quad (4)$$

In the expression for div $J_n$, the terms $q\mu_n n$ div $E=-kT(\mu_n-\mu_p)\nabla^2 p$ and $kT\mu_n\nabla^2 p$ are comparable in magnitude, so that there is no justification in dropping the former term. This comes from the fact that the small factor div $E$ is multiplied by the majority carrier density. We then have

$$-\mu_n \text{ div } J_p + \mu_p \text{ div } J_n = (\mu_n+\mu_p)U = kT(\mu_n+\mu_p)\mu_p\nabla^2 p, \quad (5)$$

which leads to the correct low-level approximation.

In the same way, it can be shown that the ambipolar mobility, $\bar{\mu}$, is involved at very high-injection levels only ($n\approx p\gg N$). At intermediate levels, the effective mobility is a complicated function of the carrier densities and their gradients, as shown by Rittner.[3]

The author is indebted to Dr. R. N. Noyce and Dr. C. T. Sah for helpful discussions on this subject.

J. A. Hoerni
Fairchild Semiconductor Corp.
Palo Alto, Calif.

* Received by the IRE, October 15, 1957.

[1] C. T. Sah, R. N. Noyce and W. Shockley, "Carrier generation and recombination in $p$-$n$ junctions and $p$-$n$ junction characteristics," Proc. IRE, vol. 45, pp. 1228–1243; September, 1957.

[2] W. Shockley, "Electrons and Holes in Semiconductors," D. Van Nostrand Co., Inc., New York, N. Y., sec. 12.5; 1950.

[3] E. S. Rittner, "Extension of the theory of the junction transistor," *Phys. Rev.*, vol. 94, pp. 1161–1171; June 1, 1954.

## Hyperbolic Analogs*

To the extent to which the voltage ($V$), current ($I$), and reverse saturation current ($I_s$) of a semiconductor diode are related by the expression $I=I_s[\exp(qV/kT)-1]$, it is possible to construct circuits which provide hyperbolic relations between electrical quantities therein.

For example, if two identical semiconductor diodes are connected in series and poled to conduct in opposite directions, it is easily shown that the terminal voltage and current are related by $I=I_s\tanh(qV/2kT)$.

Two such diodes connected in parallel and oppositely poled will provide a dependence between terminal voltage and current given by $I=2I_s\sinh(qV/kT)$.

There are variations or extensions of these circuits which can be used to provide hyperbolic analog devices. For example, the diode pairs might be used as input or feedback elements in a standard operational amplifier (Fig. 1).

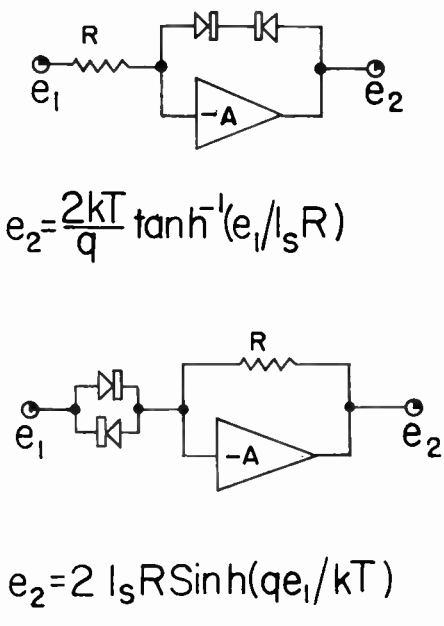


Fig. 1.

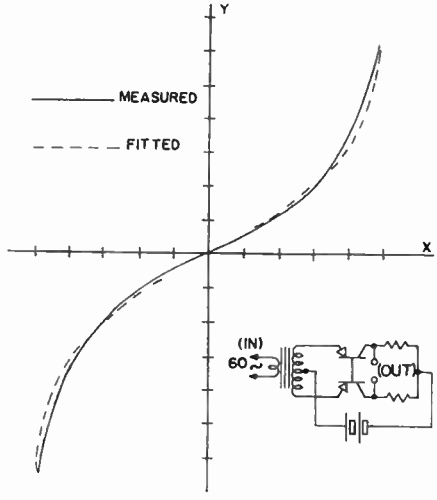


Fig. 2.

In another incorporation of these principles transistors provide both the necessary exponential characteristic and gain. A transfer characteristic measured for such a circuit is shown in Fig. 2, along with a fitted curve,

$$y=2.9\tanh^{-1}x.$$

It is also possible, although somewhat more complicated, to obtain hyperbolic cosine analogs.

Melbourne J. Hellstrom
Westinghouse Electric Corp.
Metuchen, N. J.

* Received by the IRE, September 24, 1957.

# Contributors

J. Robert Anderson (S'53–M'57) was born in New York, N. Y. on December 31, 1932. He received the B.S. degree in engineering physics from New York University in 1954. From 1954 to 1957, he was a member of the technical staff at the Electron Tube Laboratory of Hughes Aircraft Company. During part of this time, he received graduate training in physics at U.C.L.A. under a Howard Hughes Cooperative Fellowship.

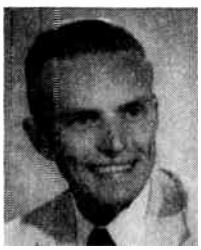

J. R. ANDERSON

Mr. Anderson presently is continuing his graduate training in electrical engineering, while holding an appointment as a research engineer in the Electron Tube Laboratory at the University of California, Berkeley, Calif.

He is a member of Tau Beta Pi, Sigma Pi Sigma, and AAAS.

❖

Elie J. Baghdady (A'52–M'57) was born in Zahleh, Lebanon, on November 10, 1930. Between 1949 and 1951, he was a British Council Scholar and recipient of the university first prize scholarship at the American University of Beirut. He received the B.A. degree with high distinction in physics in 1951.

E. J. BAGHDADY

In the summer of 1951, he came to the United States on a Georgia Institute of Technology World Student Fund Fellowship and enrolled in the Institute's graduate division of electrical engineering. In June, 1952, he joined the electrical engineering staff of the Massachusetts Institute of Technology as a graduate student and research assistant in the Research Laboratory of Electronics. He became an instructor in electrical engineering in 1955 and assistant professor in 1956. He received the M.S. and D.Sc. degrees in electrical engineering from M.I.T. in 1954 and 1956, respectively.

Dr. Baghdady's research has been mainly concerned with frequency-modulation studies, including problems of improving reception in the presence of high-level noise and interference and the analysis of network response to fm waves. Since 1954, he has taught advanced courses in radio engineering and modulation theory, mathematical methods in electrical engineering, network analysis and synthesis, electronic circuits, and transient analysis of linear electromechanical systems. Presently, he is in charge of a graduate course on modulation theory and a research project on fm.

George R. Brewer (A'43–M'49–SM'54) was born in New Albany, Ind., on September 10, 1922. He received the B.E.E. degree from the University of Louisville in 1943, and the Ph.D. degree in electrical engineering from the University of Michigan in 1952.

G. R. BREWER

Dr. Brewer has been principally engaged in research and development of electron tubes from 1943 to 1944, at the Radiation Laboratory, Massachusetts Institute of Technology; from 1944 to 1947, at the Naval Research Laboratory; and from 1947 to 1951, at the Engineering Research Institute of the University of Michigan. He now is a member of the Electron Tube Laboratory of Hughes Research Laboratories.

He is a member of the American Physical Society, Sigma Xi, and Phi Kappa Phi.

❖

T. J. Bridges (M'57) was born at Gillingham, Kent, Eng., in December, 1923. He attended London University, London, Eng., where he received the Bachelor of Science degree in engineering in 1944.

T. J. BRIDGES

He joined the Admiralty in 1945 and is a member of the Royal Naval Scientific Service at the Services Electronics Research Laboratory, Baldock, Eng. Since November, 1956, he has been on leave of absence from the Admiralty and is engaged in microwave tube research at Bell Telephone Laboratories, Murray Hill, N. J.

❖

R. C. Burgener (A'54) was born October 10, 1921 in Galion, Ohio. He received the B.S.E.E. degree from Case Institute of Technology in 1950. After graduation he was engaged in relay development at the North Electric Mfg. Co., Galion, Ohio until September, 1951. At that time he joined the Department of Electrical Engineering of The University of Tennessee as research engineer, where he was primarily concerned with development in the field of radar. He received the M.S.E.E. degree from The University of Tennessee in June, 1956. He is presently employed at Battelle Memorial Institute as a research engineer and he also is attending Ohio State University as a candidate for the Ph.D. degree.

R. C. BURGENER

He has a professional engineering license in Tennessee.

❖

Harold J. Curnow was born at Birmingham, Eng., in November, 1930. He was educated at Solihull School, Warwickshire, Eng. He also attended Birmingham University, Birmingham, Eng. He received the degree of Bachelor of Science with honors in mathematical physics from Birmingham University in 1951.

H. J. CURNOW

Since then, he has been a member of the Royal Naval Scientific Service, and at the present time is employed at the Services Electronics Research Laboratory, Baldock, Hertfordshire, Eng.

❖

E. T. Jaynes (SM'54) was born in Waterloo, Iowa, on July 5, 1922. He attended Cornell College and Iowa State University, receiving the B.A. degree in physics from the latter in 1942. He studied in the graduate school of the University of California in Berkeley and at Princeton University from which he received the M.A. degree in 1948 and the Ph.D. degree in theoretical physics in 1950.

E. T. JAYNES

From 1942 to 1946, he was engaged in microwave research and development as a project engineer at the Sperry Gyroscope Co., Garden City, N. Y., and in the combined research group of the Naval Research Laboratory.

Since 1950, he has been on the faculty of Stanford University and at present holds the titles of associate professor in the microwave laboratory and lecturer in physics.

❖

Sherwood King (S'40–A'41–SM'53) was born in Schenectady, N. Y. on August 5, 1917. He received the B.S. degree in engineering sciences from Harvard University in 1938 and the M.S.E.E. degree from Lafayette College in 1940. From 1940 until

1947, he was a member of the technical staff of Bell Telephone Laboratories, engaged in the development of sonar and radar test equipment and of mobile radio telephone systems. In 1947, he joined the staff of the Department of Electrical Engineering of the University of Tennessee as assistant professor. He became associate professor of electrical engineering in 1955. At Tennessee he was in charge of the electronics laboratories and supervisor of a research group engaged in radar development. In 1956 Mr. King became a member of the technical staff in the Ground Systems Division, Hughes Aircraft Company, and at present is head of the Studies and Analysis Section of that Division's Radar Laboratory.


S. KING

Mr. King is a member of Sigma Xi and Eta Kappa Nu.

❖

David I. Kosowsky (S'50–A'53–M'57) was born in New York, N. Y., in 1930. He received the B.E.E. degree from the College of the City of New York in 1951 and the S.M. and Sc.D. degrees from Massachusetts Institute of Technology in 1952 and 1955. He was a staff member of the Research Laboratory of Electronics (M.I.T.) from 1951 to 1955 and was engaged in research on missile systems, applications of statistical communication theory, and filter theory. He was responsible for the development of techniques for the synthesis and realization of crystal filters.


D. I. KOSOWSKY

He is presently employed by Hycon Eastern, Inc., as Director of the Crystal Filter Division. He is a member of Eta Kappa Nu, Tau Beta Pi, and Sigma Xi.

❖

Harold Levenstein (A'46–M'55) was born on June 28, 1923, in Philadelphia, Pa. He received the B.E.E. degree from Cooper Union, New York, N. Y., in 1943, and the M.E.E. degree from the Polytechnic Institute of Brooklyn in 1949. In addition to course work for the doctorate, he has been a special student in fire control systems and communications theory at Massachusetts Institute of Technology in 1949, 1953, and 1955.

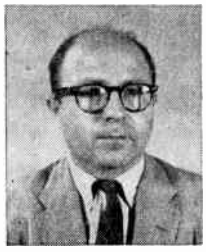
H. LEVENSTEIN

Mr. Levenstein joined Western Electric in 1943 as a test planning engineer on radar systems. In 1946, he was a member of the Sight Laboratory, Fairchild Camera and Instrument Co., working in fire control systems. From 1947 to 1950, he was employed by Fairchild Guided Missiles Division as an electronics engineer on telemetering and guidance systems for the Lark Missile. In 1950, he joined the W. L. Maxson Corp. as a senior engineer, responsible for fire control and bombing and navigation systems. He has been manager of the analysis group and the systems engineering department. In 1955, he took a leave of absence to work as a member of the M.I.T. Instrumentation Laboratory on inertial navigation systems. Since June, 1956, he has been research assistant to the Vice-President of the R&D Division of the W. L. Maxson Corp., acting as consultant in systems and control engineering and is responsible for preliminary system planning.

Mr. Levenstein is a member of Tau Beta Pi, Sigma Xi, the American Physical Society, and the American Mathematical Society.

❖

O. Thomas Purl (S'50–A'54) was born on June 5, 1924 in East St. Louis, Ill. He received the B.S. degree in general engineering from the University of Illinois in 1948. Prior to that, he was a meteorologist with the Air Force from 1943 to 1946. He was engaged in microwave tube work at the Collins Radio Co. from 1948 to 1949. In 1949, he returned to the University of Illinois, where he received the B.S.E.E., M.S.E.E., and Ph.D. degrees in 1951, 1952, and 1955, respectively. During part of this time, he was a research associate in the Electrical Engineering Research Laboratory.


O. T. PURL

Since 1955, he has been a member of the technical staff at the Hughes Electron Tube Laboratory, where he has been engaged in research and development on microwave tubes.

Dr. Purl is a member of Sigma Xi, Eta Kappa Nu, Phi Kappa Phi, and Sigma Tau.

❖

J. F. Ramsay (A'56) was born at Milngavie, Dunbartonshire, Scotland, in 1908. He received the M.A. degree in mathematics and physics from the University of Glasgow in 1934. From 1933 to 1935, he was employed by the Cosmos Lamp Works, Enfield, Eng., as assistant engineer engaged on circuit applications of receiving tubes. In 1935, he was employed by the General Electric Co., Ltd., Coventry, Eng., as radio circuit engineer on broadcast receiver problems.

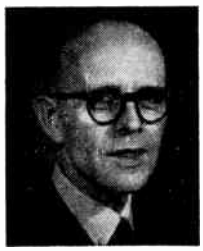
J. F. RAMSAY

In 1936, Mr. Ramsay joined the research staff of Marconi's Wireless Telegraph Co., Ltd., Chelmsford, Eng., as assistant engineer on broadcast receiver investigational work. From 1938 to 1940, he was attached to the Air Division on transmitter drive development. In 1941, he returned to research in the development of superregenerative radar: seconded to the Admiralty in the same year, Mr. Ramsay took part in war-time microwave antenna research both with Marconi's Wireless Telegraph Co., Ltd., and at Admiralty establishments. Among the antenna types with which he was associated were metal-plate lens, mirror-connected horn, squintless linear array, polyrod, channel-guide antenna, and circularly polarizing mirrors. Returning to Marconi's in 1946, he published papers on Fourier transform theory for antennas based on G. A. Campbell's memoir for circuit theory. In further antenna work, he was associated with antennas for marine radar, VOR, tv broadcasting, fm broadcasting, microwave relay, and millimetric techniques. The problems encountered in the millimeter field led to the discovery of the old microwave techniques of the 1890's. Since 1956, Mr. Ramsay has been employed by Canadian Marconi Company, Montreal, Canada.

He is a member of the IEE, London.

❖

F. V. Schultz (A'32–SM'45) was born on November 7, 1910 in Petersburg, Mich. He received the B.S.E.E. degree in 1932, the M.S.E.E. degree in 1939, and the Ph.D. degree in 1950, all from the University of Michigan. After five years in industry, primarily as a receiver development engineer, he joined the Department of Electrical Engineering of Michigan State University East Lansing. Mich., where he remained from 1937 until 1941.


F. V. SCHULTZ

During World War II, Dr. Schultz was a group leader in the Radar Laboratory of the Wright Air Development Center, where he was concerned with the development of antennas and radar beacons. From 1946 to 1950, he was research engineer in the Engineering Research Institute of the University of Michigan. During this time, Dr. Schultz was engaged in research studies on missile guidance systems and on electromagnetic wave scattering problems. From 1950 until 1956, he was professor of electrical engineering at the University of Tennessee, in charge of instruction and research in electronics. Since 1956, he has been professor of electrical engineering at Purdue University, Lafayette, Ind.

He is a member of Sigma Xi, Tau Beta Pi, Phi Kappa Phi, Eta Kappa Nu, the American Physical Society, and the American Society for Engineering Education.

# IRE News and Radio Notes

## Early Reservations Urged for IRE National Convention

Plans are all but completed for the forty-sixth annual national convention of the IRE, scheduled for the Waldorf-Astoria Hotel and the New York Coliseum, March 24–27. Fifty-five technical sessions are being set up by the Technical Program Committee with the aid of all IRE Professional Groups. Thirty-three sessions will be held at the Waldorf; the remainder, at the Coliseum. The program will feature two special symposia on the evening of March 25 in which the nation's leading experts will discuss "Electronics in Space" and "Electronics in Industry." Full program details will be published in the March issue of the PROCEEDINGS OF THE IRE.

The popular social events will open with a "get-together" cocktail party on the afternoon of March 24. The annual banquet, to be held in the Grand Ballroom of the Waldorf during the evening of March 26, will feature Robert C. Sprague, Chairman of the Board of Sprague Electric Co. and of the Federal Reserve Bank of Boston, who will speak on "The Federal Reserve and the Electronics Industry."

Since a convention attendance of 55,000 is anticipated, all members are urged to place their reservations for cocktail party tickets at $4.30 each, and banquet tickets at $15.00 with IRE Headquarters quickly.

The annual Single Sideband Dinner will be held March 25 at the Hotel New Yorker. Tickets can be obtained for $7.50 each at Single Sideband Amateur Radio Assn., 261 Madison Ave., N. Y. 16, N. Y.

## I. J. Kaar is Recipient of IRE-EIA Fall Meeting Plaque

I. J. Kaar (J'22–M'29–F'41), Vice-President of Hoffman Electronics, received the Radio Fall Meeting Plaque at the 29th meeting in Toronto, Canada. He received the award for "his many contributions to the broadcast and television receiver industry."

I. J. KAAR

Mr. Kaar was former head of the General Electric Color System Technical Project. For the previous thirty years he had been closely associated with the organization of the General Electric radio and television engineering developments.

He also served as panel chairman on receiver-transmitter coordination for the first National Television System Committee and vice-chairman of the panel on coordination for the second NTSC.

### Alois W. Graf
### 1901–1957

The following resolution was adopted by the IRE Board of Directors at a meeting on November 20, 1957.

#### Resolution

With profound sorrow the Directors of The Institute of Radio Engineers record the death of one of their friends and associates—Alois W. Graf. Mr. Graf was an IRE member for over thirty years, having joined as an Associate in 1926, advancing to Member grade in 1944, Senior Member in 1945, and Fellow in 1955. He served as a Director in 1952, 1953, and 1957.

Perhaps his most important contributions to IRE nationally were the time and effort taken from his personal law practice to devote to legal matters for IRE. A great deal of his time was spent on trade-mark applications to safeguard the IRE name, symbol, and publication titles.

Having served as the Chairman of the Constitution and Laws Committee since 1954, he believed that the Constitution and Bylaws were in need of modernization, and he undertook the tremendous task of drafting a proposal for a new Constitution and Bylaws.

Mr. Graf was very active in Professional Group administration, serving as Central Division Vice-Chairman since 1954.

He contributed vastly to the welfare of IRE on the Section level, serving as Chairman of the Chicago Section in 1946–47, and continuing thereafter, as an elder statesman, to guide the destinies of a large and flourishing Section.

The Board of Directors of The Institute of Radio Engineers desires to spread upon its records its keen sense of personal loss in Mr. Graf's death and its deep sympathy for the members of his family.

## Calendar of Coming Events and Authors' Deadlines*

**1958**

**Cleveland Elec. Conf. Masonic Audit., Cleveland, Ohio, Feb. 14–15**

**Transistor-Solid State Circuits Conf., Phil., Pa., Feb. 20–21**

**Nuclear Eng. and Science Congress, Palmer House, Chicago, Ill., Mar. 16–21**

**IRE Nat'l Convention, N. Y. Coliseum and Waldorf-Astoria Hotel, New York City, Mar. 24–27 (DL*: Nov. 1, G. L. Haller, IRE Headquarters, New York City)**

Single Sideband Dinner, Hotel New Yorker, New York City, Mar. 25

**Instruments & Regulators Conf., Univ. of Del., Newark, Del., March 31–Apr. 2**

**Conf. on Automatic Optimization, Univ. of Del., Apr. 2–4**

**Symp. on Electronic Waveguides, Eng. Soc. Bldg., New York City, Apr. 8–10**

**SW Regional Conf. & Show, Mun. Audit, San Antonio, Tex., Apr. 10–12**

**Conf. on Automatic Techniques, Statler Hotel, Detroit, Mich., Apr. 14–16**

**Spring Tech. Conf. on TV and Transistors, Eng. Soc. Bldg., Cincinnati, Ohio, Apr. 18–19**

**Elec. Components Symp., Ambassador Hotel, Los Angeles, Calif., Apr. 22–24 (DL*: Nov. 15, E. E. Brewer, Convair, Pomona, Calif.)**

**URSI Spring Mtg., Willard Hotel, Wash., D. C., Apr. 24–26**

Semiconductor Symposium of Electrochemical Society, Statler Hotel, New York City, Apr. 27–May 1

**Seventh Region Conf. & Show, Sacramento, Calif., Apr. 30–May 2**

**PGMTT Symp., Stanford Univ., Stanford, Calif., May 5–7 (DL*: Jan. 15, K. Tomiyasu, G. E. Microwave Lab., 601 California Ave., Palo Alto, Calif.)**

**Western Joint Computer Conf., Ambassador Hotel, Los Angeles, Calif., May 6–8 (DL*: Jan. 15, Tech. Program, Chairman, P. O. Box 213, Claremont, Calif.)**

**Nat'l Aero. & Nav. Elec. Conf., Dayton, Ohio, May 12–14**

IEE Convention on Microwave Values Savoy Place, London, England, May, 10–23

**PGME Mtg., Wash., D. C., May**

*DL = Deadline for submitting abstracts.

(Continued on page 506)

## Calendar of Coming Events and Authors' Deadlines*

(Continued)

**PGPT Symp., Hotel New Yorker, New York City, June 5–6**

**PGMIL Convention, Sheraton-Park Hotel, Wash., D. C., June 16–18**

**Spec. Tech. Conf. on Nonlinear Mag. and Mag. Amplifiers, Los Angeles, Calif., Aug. 6–8**

**Elec. Radio & Standards Conf., Univ. of Colo. and NBS, Boulder, Colo., Aug. 13–15**

**WESCON, Ambassador Hotel and Pan-Pacific Audit., Los Angeles, Calif., Aug. 19–22 (DL*: May 1)**

**Nat'l Symp. on Telemetering Americana Hotel, Miami Beach, Fla., Sept. 22–24**

**Indus. Elec. Conf., Detroit, Mich., Sept. 24–25**

**Nat'l Electronics Conf., Hotel Sherman, Chicago, Ill., Oct. 13–15**

**IRE Canadian Convention, Toronto, Can., Oct. 15–17**

**PGCS Symp. on Aero. Communications, Hotel Utica, Utica, N. Y., Oct. 20–22**

**Nat'l Simulation Conf., Dallas, Tex., Oct. 23–25**

**EIA-IRE Radio Fall Meeting, Sheraton Hotel, Rochester, N. Y., Oct. 27–29**

**East Coast Aero. & Nav. Elec. Conf., Lord Baltimore Hotel and 7th Regiment Armory, Baltimore, Md., Oct. 27–29**

**PGED Meeting, Shoreham Hotel, Washington, D. C., Oct. 30–Nov. 1**

**Atlanta Section Conf., Atlanta-Biltmore Hotel, Atlanta, Ga., Nov. 17–19**

Elect. Computer Exhibition, Olympia, London, Eng., Nov. 29–Dec. 4

**Eastern Joint Computer Conf., Bellevue-Stratford Hotel, Philadelphia, Pa., Dec. 3–5**

**Nat'l Symp. on Global Comm., St. Petersburg, Fla., Dec. 3–5**

**PGVC Annual Mfg., Hotel Sherman, Chicago, Ill., Dec. 4–5**

**Mid-America Elec. Convention, Mun. Audit., Kan. City, Mo., Dec. 9–11 (DL*: Aug. 1, Wilbert O'Neal, Vendo Co., 7400 E. 12, Kan. City, Mo.)**

1959

**IRE Nat'l Convention, New York City, Mar. 23–26**

**SW Regional Conf., Dallas, Tex., Apr. 16–18**

**Nat'l Aero & Nav. Elec. Conf., Dayton, Ohio, May 11–13**

**WESCON, San Francisco, Calif., Aug. 18–21**

**Nat'l Electronics Conf., Chicago, Ill., Oct. 12–14**

**East Coast Aero. & Nav. Conf., Baltimore, Md., Oct. 26–28**

**PGED Meeting, Shoreham Hotel, Washington, D. C., Oct. 29–31**

**Radio Fall Meeting, Syracuse, N. Y., Nov. 9–11**

**Eastern Joint Computer Conf., Hotel Statler, Boston, Mass., Nov. 30–Dec. 3**

* DL = Deadline for submitting abstracts.

## L. S. McDowell Is the First Woman to Become Life Member

On January 1, 1958, Louise S. McDowell (M'23–SM'43) was the first woman to become a Life Member of the IRE. The IRE bylaws provide that the Board of Directors shall waive the dues of each and every member of the IRE who has attained the age of 65 years and been a member for 35 years. These members are then designated "Life Members," and at the present time there are 131 IRE Life Members.

L. S. McDowell

Dr. McDowell is professor emeritus of physics at Wellesley College. She has been associated with Wellesley since 1909, and from 1913 until retirement in 1945 head of the physics department. Beginning in 1917, she also taught a semester course in electromagnetic waves and radio communication which offered to undergraduates experimental lectures and laboratory work as well. During 1918 and 1919 on leave from Wellesley, Dr. McDowell did physical research on crystal detectors and vacuum tube oscillators in the Radio Section of the National Bureau of Standards. In 1921, she did further research at Cruft Laboratory of Harvard University.

Dr. McDowell obtained the Ph.D. degree from Cornell University in 1909 where she had received her master's degree in 1907; her bachelor's degree from Wellesley was awarded in 1898. She is a fellow of the American Physical Society, and has had several papers published in the *Physical Review* of the American Physical Society. In 1947 she retired from active life after serving as assistant editor of *Very High Frequency Techniques*.

## MAECON Proves Successful

The IRE Mid-America Electronics Convention was held at the Municipal Auditorium in Kansas City, Mo., November 13–14, 1957, with headquarters at the Hotel Muehlebach. It was the ninth annual convention sponsored by the IRE Kansas City Section.

The convention drew approximately 1500 engineers and scientific-minded personnel, from more than 13 states.

There were 77 exhibit booths with displays of some of the latest electronic instruments, products and associated equipment. The featured exhibit was a complete technical model of America's earth satellite which was displayed by the Naval Research Laboratories.

There were ten technical sessions covered by 28 technical paper presentations. J. T. Henderson, IRE National President, gave the opening address, and also spoke on "The IRE Today" at the annual banquet. Dr. Simon Ramo, executive vice-president of the Ramo-Wooldridge Corp., was the guest banquet speaker and spoke on "The Increasing Role of Electronics in Missile Systems." The banquet was attended by nearly 300 persons.

## Temporary Memberships for Research Now Available

For the second year, the Institute of Mathematical Sciences at New York University offers temporary memberships to mathematicians and other scientists holding the Ph.D. degree who intend to study and do research in the fields in which the Institute is active. These fields include functional analysis, ordinary and partial differential equations, mathematical physics, fluid dynamics, electromagnetic theory, numerical analysis and digital computing, and various specialized branches, such as linear programming, hydromagnetics, and reactor theory. Membership will be awarded for one year, but it may be renewed. Special arrangements can be made for applicants who expect to be on leave of absence from their institutions.

Temporary members may participate freely in the research projects, the advanced graduate courses and the research seminars of the Institute, and they will have the opportunity of using the computational facilities which include an IBM 704 computer and a Univac. They will receive a stipend commensurate with their status.

Requests for information and for application blanks should be addressed to the Membership Committee, Institute of Mathematical Sciences, 25 Waverly Place, New York 3, N. Y.

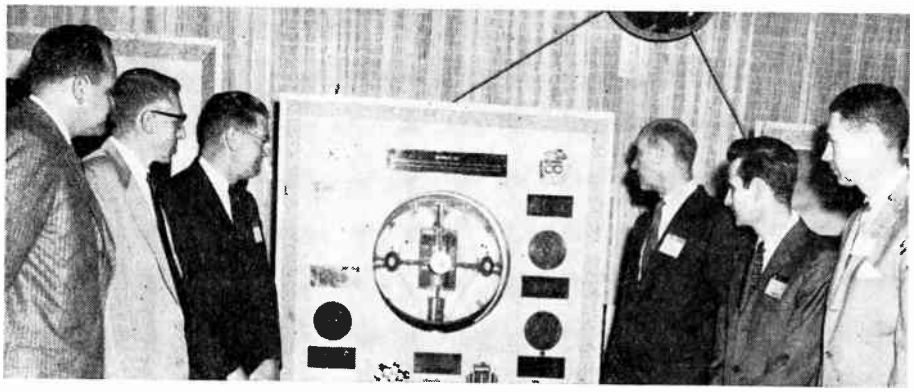

Shown at MAECON looking at a model of an earth satellite are (*left to right*): K. V. Newton, IRE Region Six Director; R. M. Somers, Bendix Aviation Corp.; L. H. Montgomery, Vanderbilt Univ.; J. T. Henderson, IRE President; P. C. Constant, Jr., IRE Kansas City Section chairman; and W. H. Ashley, Jr., convention chairman.

# 1958 Transistor & Solid State Circuits Conference

UNIVERSITY OF PENNSYLVANIA AND SHERATON HOTEL, PHILADELPHIA, PA.

FEBRUARY 20–21, 1958

## FEBRUARY 20

**9:30 a.m.–Noon**

**Irvine Auditorium**

### COMPUTER CIRCUITS

*Chairman:* T. R. Finch, Bell Tel. Labs.

*The Advantages of Linear Selection in Transistor-Core Memories*, R. E. McMahon, Lincoln Lab., M.I.T.

*Transistor Resistor Logic Circuit Analysis*, Q. W. Simkins, Bell Tel. Labs.

*Ten Megapulse Transistorized Pulse Circuits for Computer Application*, W. N. Carroll and R. A. Cooper, IBM.

*High-Speed, Graded-Base Transistor, Digital Circuit Techniques*, R. H. Baker, Lincoln Lab., M.I.T.

*Higher-Speed Computer Circuits*, A. K. Rapp and M. M. Fortini, Philco Corp.

**University Museum**

### SURVEY

*Chairman:* J. A. Rajchman, RCA.

*Noise in Semiconductors*, W. H. Fonger, RCA.

*Review of Some Novel State Devices and Their Applications*, W. H. Katz, General Electric Co.

**2:45–5:15 p.m.**

**Irvine Auditorium**

### SWITCHING

*Chairman:* P. M. Thompson, Defense Research Board, Ottawa, Canada.

*New Configurations in Nonsaturating Complementary-Current Switching Circuits*, C. M. Campbell, Jr., Burroughs Corp

*The Application of Transistors Operated in the Avalanche Mode to the Generation of Millimicrosecond Pulses*, G. B. B. Chaplin, United Kingdom Atomic Energy Authority, England.

*The Use of Junction Transistors as a Three-Terminal Temporary Memory for Digital Circuits*, G. H. Perry, Royal Radar Research Establishment, England.

*Transistor Bilateral Switches*, W. M. Cook and P. I. Bargellini, RCA.

*A Two-Transistor Gate for Time-Division Switching*, J. D. Johannesen and P. B. Myers, Bell Tel. Labs.

**3:15–5:15 p.m.**

**University Museum**

### NEW TECHNIQUES

*Chairman:* H. E. Tompkins, Univ. of Pennsylvania.

*Low-Level, High-Speed Voltage Comparator*, J. W. Higginbotham and H. H. Douglass, Martin Co.

*A High-Speed Analog Multiplier with a Linearity Better than +0.3 Per Cent*, R. J. Bibby and P. M. Thompson, Defense Research Board, Ottawa, Canada.

*A Semiconductor Voltage Regulator for Rotating Generators*, J. L. Jensen, Minneapolis-Honeywell Regulator Co.

*A Transistorized Overload-Proof Electronic Regulator—TOPER*, P. A. Dodge, General Electric Co.

## FEBRUARY 21

**9:00 a.m.–Noon**

**Irvine Auditorium**

### LINEAR APPLICATION

*Chairman:* J. G. Linvill, Stanford Univ.

*Methods of Cascading Unneutralized Tuned Transistor Amplifiers*, R. M. Frazier, Jr., Westinghouse Electric.

*Transistor 70-MC IF Amplifier*, V. R. Saari, Bell Tel. Labs.

*Optimum Noise Performance of Transistor Input Circuits*, R. D. Middlebrook, Calif. Inst. of Technology.

Paper to be announced by J. T. Paupin and/or H. T. Mooers, Minneapolis-Honeywell Regulator Co.

*Dielectric Modulators Using Space-Charge Capacitance of Junction Diodes*, Carl Hurtig, M.I.T.

**University Museum**

### SURVEY ON SWITCHING and POWER CONTROL

*Chairman:* J. J. Suran, General Electric Co.

*Switching*, Gary Clark, Burroughs Corp.

*Power Control with Semiconductors*, Louis Bright, Westinghouse.

**2:00–4:30 p.m.**

**Irvine Auditorium**

### NEW DEVICES

*Chairman:* George Royer, IBM.

*Operation of a Low-Temperature Memory Element*, C. J. Kraus, IBM.

*The Application of the Dynister Diode to Off-On Controllers*, P. F. Pittman, Westinghouse Electric.

*Diode Amplifiers*, H. W. Abbott and L. D. Wechsler, General Electric Co.

*Magnetoresistive Amplifiers and Second Harmonic Modulators*, H. N. Putschi, General Electric Co.

*Photoelectronic Circuit Applications*, S. K. Ghandhi, General Electric Co.

# Books

### Microwave Measurements by E. L. Ginzton

Published (1957) by McGraw-Hill Book Co., 330 W. 42 St., N. Y. 36. N. Y. 476 pages+21 index pages +17 pages of appendix+xvii pages. Illus. 9¼×6¼. $12.00.

The author has successfully consolidated a multitude of basic microwave techniques into a book which can serve both as a basic text to a first year graduate course in microwave measurements and as a reference text to microwave engineers. Topics are carefully selected, clearly described, and very well integrated into a valuable unity. The impedance concept, transmission-line theory, and the equivalent-circuit approach are fully treated and utilized in the development of methods suitable for microwave measurements.

The first chapter delves into sources of microwave power, presents a practical discussion of klystrons, microwave triodes, and traveling-wave tubes, and includes the need and devices for isolating laboratory oscillators. Also considered are standard signal and harmonic generators. Chapters 2 and 3 contain a comprehensive evaluation of methods for detecting and measuring microwave power. Bolometers are extensively covered.

An excellent exposition of the impedance concept is developed in Chapter 4, with stress on graphical procedures. It is followed by a chapter on impedance measurements, which includes an elaborate treatment on the standing-wave detector and practices for achieving precision measurements. The behavior of microwave circuits and equivalent representations are discussed in Chapter 6.

Topics relating to the measurement of wavelength and frequency are dealt with in Chapters 7 and 8. The presentation is extended to wavemeter techniques and frequency standards. Chapters 9 and 10 concern resonant-cavity characteristics and the evaluation of the important parameters, $Q$ and $R$. The final chapter investigates the measurement of attenuation and describes the power-ratio, substitution, cavity-resonance and scattering-coefficient methods.

There are many figures, footnotes and experimental data coherently introduced into the text. Perhaps the bibliography may be considered to be rather limited although a large number is not really required. All in all, the book reflects much credit on those concerned with it and will prove to be of great value for any one who desires to become thoroughly familiar with microwave measurements.

A. B. GIORDANO
Polytechnic Institute of Brooklyn
Brooklyn 1, N. Y.

### Analytical Design of Linear Feedback Controls by G. C. Newton, Jr., L. A. Gould and J. F. Kaiser

Published (1957) by John Wiley & Sons, Inc., 440 Fourth Ave., N. Y. 16, N. Y. 282 pages+3 index pages+130 pages of appendix+3 pages of bibliography+xi pages. Illus. 9¼×6¼. $12.00.

This book covers the theory of the design of linear feedback control systems by the process of minimizing the integral of error squared for step and ramp inputs, or minimizing rms error for stochastic (random) in-

puts to linear mathematical models of the actual systems. Lagrangian multipliers are used to account for certain restraints, such as those placed on the amplitude of signals in order to maintain essentially linear operation.

The minimization procedure leads to a form of the Wiener-Hopf integral equation. The solution of this equation supplies the data for design of the compensating element, and for calculating the minimum possible rms error. This information is intended to be used as a guide in the trial and error design for the actual system.

The book is intended for readers who have had some graduate study in control systems, or are prepared to do collateral reading. It is assumed that the reader has already obtained an insight into the conventional frequency approach, and to the practical design of feedback control systems. There is a brief coverage of basic material in the appendices.

The book is terse. The basic thesis is developed in 286 pages. Of necessity the development is mathematical, and the description of the minimization procedure involves complicated integral expressions. Essentially there is no deviation from the basic thesis, and no exposition on practical aspects. Where examples are used, they are stripped to mathematical models in all cases except that of the example which makes up Chapter 9. However, the authors are careful to point out the assumptions they introduce and the restrictions on the methods they advocate.

There is little reference to somewhat similar work done by others, such as the work on minimization of the integral of time-weighted absolute value of error response to step inputs done by R. C. Lathrop and D. Graham.

It is felt that development of the minimization expressions in the frequency domain rather than the time domain would have resulted in expressions more readily interpreted by control people. The end results would have been the same, providing that key expressions were transformed back to the time domain.

The book is recommended for reading by every person wishing to be sophisticated in the area of feedback controls. The presentation is straightforward and clean cut. It provides a unified coverage of material not available elsewhere except in scattered journal reports.

A. M. Hopkin
Univ. of Calif.
Berkeley 4, Calif.

### Nomograms of Complex Hyperbolic Functions, 2nd ed., by Jorgen Rybner

Published (1955) by Jul. Gjellerups Forlag, Copenhagen, Denmark. 99 pages. 12×8½. Dan. Kr. 44.00.

The second edition of this book incorporates a number of improvements over the first edition, as well as some additional nomograms. The notation of complex arguments has been changed to the common English usage. The ring binding has been changed from the top to the side, making the book more convenient to use.

Thirteen separate nomograms for cosh $(A+jB)=p+jq$ cover the range $0\leq A\leq 4$, $0\leq B\leq \pi/2$. With one exception, the scales for $A$ are given in both nepers and decibels, while $B$ is expressed in both radians and degrees. sinh $(A+jB)=p+jq$ is treated similarly in thirteen nomograms.

tanh $(A+jB)=r\angle\theta$ is treated in twenty separate nomograms covering the range $0\leq A\leq 3$, $0\leq B\leq \pi/2$, $A$ in nepers and decibels, $B$ in radians, and $\theta$ in degrees.

In addition, nomograms are given for conversion of complex numbers from rectangular to polar form, and vice versa, for reflection loss and reflection phase shift in networks, new nomograms for interaction loss and phase shift, and for resonance circuits and filters. An introductory section of 39 pages discusses the use of the nomograms, and gives a collection of formulas for circular and hyperbolic functions, and for four-terminal networks and transmission lines. The text is given in both Danish and English.

This book will be found of value in transmission line, wave propagation, filter and other problems which involve complex hyperbolic functions. Their accuracy in unusually high, insuring at least three-figure accuracy over much of the range. Some spot checks gave errors of only a few parts in $10^{-4}$. The accuracy and convenience of these nomograms should make them a useful addition to the library of the electronics engineer.

Martin Katzin
Electromagnetic Research Corp.
Washington, D. C.

### Solid State Physics, Vol. IV, ed. by F. Seitz and D. Turnbull

Published (1957) by Academic Press Inc., 111 Fifth Ave., N. Y. 3, N. Y. 521 pages+19 index pages +xiv pages. Illus. 9½×6½. $12.00.

This is Volume IV of the series of texts covering advances in research and applications in solid state physics edited by F. Seitz and D. Turnbull. The topics selected for this volume are "Ferroelectrics and Antiferroelectrics" by Werner Kanzig; "Theory of Mobility of Electrons in Solids" by F. J. Blatt; "The Orthogonalized Plane-Wave Method" by T. O. Woodruff; "Bibliography of Atomic Wave Functions" by R. S. Knox; and "Techniques of Zone Melting and Crystal Growing" by W. G. Pfann.

Kanzig has attempted to present a systematic review of the field of ferroelectricity as seen by the solid state physicist with principal emphasis on the behavior of single crystals. This monograph is quite long, containing nearly 200 pages and subdivided into 13 chapters. These chapters include the "Phenomenological Behavior of Ferroelectrics: Experimental," "Thermodynamic Theory of Ferroelectric Crystals," "Optical Properties of Ferroelectrics in the Visible Range," "Domain Structure and Hysteresis," "Thermodynamic Behavior of Antiferroelectrics," "Thermodynamic Theory of Antiferroelectrics," "Optical Properties of Antiferroelectrics," "Antiferroelectric Domains," "The Static and Dynamic Structure of Ferroelectric and Antiferroelectric Crystals," "Isotope Effects," "Ferroelectricity and Antiferroelectricity of Solid Solutions," and a chapter on "Molecular Models."

This review is comprehensive, systematic and authoritative. It refers to 378 articles in the literature. It is well organized, well illustrated and represents a valuable reference for workers in the field.

The monograph on the "Theory of Mobility of Electronics in Solids" by F. J. Blatt is also very long. It contains 167 pages and 328 references to original literature. The article is broken down into 6 chapters including an introductory chapter, a chapter each on "Statistics of Free Electrons," "Boltzmann Equation," "Solution of the Boltzmann Equation for Nonspherical Energy Surfaces and Anisotropic Relaxation Times," "Scattering Mechanisms," and "Effects Arising from Lack of Thermal Equilibrium."

The emphasis in this article is primarily on the theoretical approach but a certain amount of experimental work is cited in order to establish the validity of the theoretical deductions. It is concerned primarily with transport phenomena and the effects of electric and magnetic fields and of thermal gradients separately and simultaneously. The one electron approximation neglecting correlation and exchange effects is employed throughout. This review is unusually good and will serve as a valuable reference for workers in the field.

The article on "The Orthogonalized Plane-Wave Method" by T. O. Woodruff is primarily an elaboration of Part X of an article in the first volume of this series by Reitz. This article contains 44 pages and three chapters. The first chapter is devoted to a description of the method, the second to a survey of some applications of the method, and the third is a calculation of an example in which this method is applied to the silicon crystal. The principal merit of this article is in its detailed outline of the calculation of the specific solid state problem by a method of approximation which has shown promise of giving quantitative results with reasonably rapidly convergent solutions. This article will prove useful to those concerned with the calculations of wave functions and energy eigenvalues of an electron in an arbitrary crystal potential.

The article "Bibliography of Atomic Wave Functions" by R. S. Knox is a compilation of references to the literature on atomic wave functions which have been computed. This compilation makes use of five earlier compilations which have been corrected, expanded and brought up to date. The article includes an alphabetical list of atoms and ions with the literature references. 117 articles in the literature have been employed in this compilation.

The article on "Techniques of Zone Melting and Crystal Growing" by W. G. Pfann contains nearly 100 pages and 187 literature references. It is organized in eight chapters including "Distribution and Coefficient and Normal Freezing," "Principles of Zone Refining," "Practice of Zone Refining," "Zone Leveling," Methods of Perturbing the Concentration," "Temperature-Gradient Zone Melting," and "Crystal Growth and Dislocations."

This is an article describing techniques employed by research men in the preparation of crystalline materials for research purposes. It discusses the techniques in a manner rarely found in standard texts and highly desirable from the point of view of the research man. Pfann has done an outstanding job in compiling in a very readable form material which is difficult to obtain and organize from the literature.

Volume IV is a very welcome addition to this highly interesting series of monographs on special topics in solid state physics.

L. T DeVore
Stewart-Warner Electronics
Chicago, Ill

# Scanning the Transactions

It has been suggested that the average IRE member, although he is not interested in reading highly specialized papers outside his own field, would nevertheless, welcome a report on some of the significant or unusual work that is going on in other fields which appears in IRE publications he does not normally see.

With this objective in mind we are hereby inaugurating a new monthly feature in which the Managing Editor, with the aid of TRANSACTIONS editors, will single out and interpret for the general reader, appropriate papers appearing in current issues of the TRANSACTIONS of the 28 IRE Professional Groups. Further information about the issues from which these papers are selected will be found in the "Abstracts of IRE TRANSACTIONS" section that immediately follows.

The title of this new section is actually incomplete. We plan to cover not only the TRANSACTIONS but the STUDENT QUARTERLY and the WESCON and NATIONAL CONVENTION RECORDS as well. As a case in point we refer readers to the first item below.

Comments from readers on the utility (or futility) of this endeavor will be welcomed by the IRE Editorial Board.—*The Editor*

**Life in a laboratory** was revealed to the surprised readers of the STUDENT QUARTERLY in the most unusual form yet to appear in an IRE publication. Twelve verses, ranging over the laboratory scene from Conferences to Applied Mathematics, indicate that the author, already distinguished as a leading engineer, as a past Editor of the IRE and as a prolific and articulate writer of science fiction and nonfiction, must now take a bow as a poet of no small talent. The verses were so delightful and stimulating that we feel compelled to offer a sample below. (J. R. Pierce, "Life in a laboratory," IRE STUDENT QUARTERLY, December, 1957.)

### Bosses

Bosses are people up a fantastic tree
Which stretches rootlets into the fertile earth
And bears some fragrant blossoms at its top.
Well-digested achievement upward flows,
And what flows down? Dirty jobs from on high
Sediment themselves among the mucky roots
And interrupt the uneven course of thought.
But bosses have the dirty end as well:
The men who can't do better, God help them;
The unhappy ones (who isn't?) who blame the boss;
The happy ones, who need more things and men
To make their little millennium in a year,
The ones in a rut, who go on and on and on,
And who can stop what he has once set going?
And the bosses themselves, who wonder if they are right—
That is, good bosses do.
And then, the endless splicing of red tape
To see that all is done as is allowed,
And things are run to please yet higher bosses,
Or bosses dead, whose muddled thoughts are sacred,
Or The Machine, transcending all the bosses,
With meshed parts, plant men, accountants, et cetera, such
As grind along how no one understands
Nor dares to interrupt.

### Credit

You can seek credit. Maybe you can get it.
Don't bother whether for your work or others';
Credit is credit; never mind the source.
Getting things done is a different kettle of fish.
If you want another to do it, he'll do it faster
With your ideas a part of his very substance,
Digested flesh of his brain, grown fruit of his labor.
If you want another to help you, he'll do it better
If he believes that his is the greater part.
Besides which, credit itself may be overrated;
Do reputations grow on credit alone?
Only when the seeker of credit is clever.
And why quibble about his reputation then?

### Direction

Every one needs good advice; a few men want it,
But how can one get it? That is the troublesome question.
You can't go by quantity. I've met some great advisers
Whose advice was neither pertinent nor right.
Can the boss advise? He doesn't know the details,
And sometimes misses the problem quite as much,
And yet, he may have an inner feeling for things
Which can be translated hardly into sense;
If you are clever, there may be advice in the boss—
If he's a good boss; that is, if he's a good man.
And that is the point. Advice is where you find it.
Choose the good, I say, from any source.
But if you know the good when once you see it,
After all, do you really need advice?

**Sending signals backwards** offers intriguing possibilities as a means of self-correcting the delay distortion that occurs in transmission circuits. Suppose that a magnetic tape recorder is placed at the midpoint of a transmission system to record the signals that have traversed the first half of the route. Suppose further that the recorded signals are then played backwards into the second half of the system. The delay distortion of the two halves of the system would then cancel, since the components of the signal delayed the most in the first half of the circuit would get a head start when they are fed into the second half. If necessary, a second time-reversing recorder could be installed at the terminus of the system to revert the segments of the signal to their original sequence. This ingenious scheme is of particular interest in the use of standard telephone circuits for data transmission and slow-speed television, where delay distortion requirements are much more severe than for the voice transmissions for which the circuits were originally designed. Bell Laboratories has used this time-reversal technique in experimental transmissions of slow-speed pictures over a 5-kilocycle 16,000-mile loop between Murray Hill and Los Angeles with impressive results. Perhaps the network theorists will soon be adding time inverters to their bag of analytical tools, and the circuit designers, magnetic recorders to their supply of standard circuit elements. (B. P. Bogert, "Demonstration of delay distortion correction by time reversal techniques," IRE TRANS. ON COMMUNICATION SYSTEMS, December, 1957.)

**Unionization of engineers** has come up for discussion for the first time in any IRE publication. Two articles, one presenting the union viewpoint and the other written by a management representative in labor relations, point up the fact that approximately 11 per cent of the country's more than 500,000 engineers are represented in collective bargaining by unions and that their numbers will, in all likelihood, continue to increase. Both are agreed as to why there are engineering unions today. They trace it directly to the widespread growth

of vast engineering organizations within individual companies since World War II, coupled with the more recent scrambling for hard-to-find engineers at rapidly increasing salaries. In some instances this has led to salary inequities, a diminishing of the engineer's accustomed identity and treatment as an individual and a professional, and a hardening or impairment of the traditional communication arteries which held the engineer in close and direct contact with management. Missing from the discussion, though, were the views of those opposed to engineering unions. (J. Amann, "Unionization of engineers—I," IRE TRANS. ON ENGINEERING MANAGEMENT, December, 1957. H. H. Rains, "Unionization of engineers—II," *loc. cit.*)

**Steinmetz,** whose life is the subject of an absorbing article in the December STUDENT QUARTERLY, was one of the great mathematical wizards of his era. For those readers with a similar bent, we offer a problem posed to him by an associate who was trying to stump him: If you bore a hole two inches in diameter through the side of a circular solid rod two inches in diameter, how much material is removed? The answer, which Steinmetz gave without hesitation after jotting a few figures on a pad, is given below.[1] (C. D. Wagoner, "Steinmetz revisited: The myth and the man," IRE STUDENT QUARTERLY, December, 1957.)

**Coded pictures** have been proposed as a means of speeding up digital facsimile transmissions over telephone circuits. The coding scheme has its basis in the fact that most documents that are transmitted, whether they be pictures, drawings or printed matter, have substantial patches of all-white or all-black in them. Therefore, a run of all-white or all-black dots in part of a scanning line could be represented by a simple code which indicated the number of dots in the sequence and whether they were black or white. The number of binary digits required for this code would on the average be less than if each dot were transmitted individually in the customary fashion. Thus, simple documents could be automatically handled faster than the complex ones. The equipment required for this, although it has not been built, has been given enough thought to prove that it would be feasible, although more complex. This proposal represents an interesting engineering application of information theory which, in its ramifications, conceivably could find use in special types of television systems, as well. (W. S. Michel, W. C. Fleckenstein, and E. R. Kretzmer, "A coded facsimile system," 1957 IRE WESCON CONVENTION RECORD, Part 2.)

**The impact of computers on network theory** may well prove to be revolutionary. Not only can a computer solve problems faster, cheaper and more reliably than a man armed with a slide rule and desk calculator, but it promises to eliminate what has heretofore been the major restrictions in the application of network theory to practical design problems. No longer does the designer have to avoid using a difficult method he doesn't understand or that isn't "practical" to solve. The chances are good that the computer programming staff will be able to code it, making it immediately available to all. The result will be a virtual elimination of the frustrating 20-year lag between theory and application, and a flourishing of complex techniques that might otherwise be considered purely academic. Even more important, circuit theory as we know it today will in time disappear, to become part of a broader field which we might call system theory. The engineer of the future, instead of tinkering with this and that circuit or component and then trying to fit them all together somehow, will set out with yet unborn techniques to design the entire system as a whole with the aid of a computer. In a broader sense, the computer will require that engineering schooling and training place an increasingly greater emphasis on creativity and fundamental knowledge, as the standardized details and specialized techniques are relegated more and more to punch cards. The machine, rather than replacing man, will require that he be more of a man and less of a machine. (T. R. Bashkow and C. A. Desoer, "Digital computers and network theory," 1957 IRE WESCON CONVENTION RECORD, Part 2.)

**Aluminum,** which is being used these days in everything from house sidings to automobile brakes, is now being used to boost the power handling capabilities of very high power germanium transistors. A fabrication scheme has been devised for evaporating aluminum and condensing it on a hot germanium wafer to form an aluminum emitter or collector junction. The evaporated aluminum technique is superior for high power applications to the standard fused indium junctions because aluminum provides higher conductivities and emitter injection efficiencies. Moreover, it is possible to obtain more accurate control of certain important dimensional characteristics of the junction when it is formed by an evaporation process. Transistors with aluminum junctions are capable of switching currents of 10 amperes with a power handling capacity of 500 watts, which bodes well for the future of the transistor in the industrial control field. (H. W. Henkels and G. Strull, "Very high-power transistors with evaporated aluminum electrodes," IRE TRANS. ON ELECTRON DEVICES, October, 1957.)

**The information-handling capacity of humans** has been the subject of some novel tests to determine how fast a person can read aloud. Some details of the tests were reported here last year.[2] The tests showed that the highest capacity of a human as an information channel was about 43 bits per second, and that this figure represents a fundamental mental limitation of the human being and not a physical limitation connected with the speed of uttering words. These reading-rate tests are a first small step in efforts to measure the least information rate necessary in order to transmit a signal, such as a speech or picture signal, well enough so as to be perfectly satisfactory to a hearer or viewer. At present, a channel capacity of 50,000 bits per second is used in sending voice signals over a telephone circuit, and 50,000,000 bits per second in sending television signals. However, no one is suggesting that anything like 43 bits per second are all that is necessary, since innumerable other factors that cannot be determined by reading rates are also involved. As an interesting sidelight, the tests showed that reading rates were about the same for different languages. Also, some small comfort can be taken in the finding that engineers are faster readers than porters. (J. R. Pierce and J. E. Karlin, "Reading rates and information rates of a human channel," 1957 IRE WESCON CONVENTION RECORD, Part 2, p. 60.)

**Transistor circuits.** If anyone needs to be convinced of the important impact that transistors are having on network theorists, they need only to look at the 236-page September issue of the CIRCUIT THEORY TRANSACTIONS, the second largest issue ever produced by a Professional Group. In the opening editorial of the issue, PGCT Chairman, H. J. Carlin, quoted a statement by E. W. Herold that has appeared twice before in the PROCEEDINGS,[3,4] Nevertheless it bears repeating: "The chemical synthesis of an improved compound can do more to revolutionize the performance of an electronic system than years of painstaking circuit work." To which Carlin adds, "The circuit theorist recognizes this situation but is prepared to take the new elements given him by materials scientists and to modify his methods to exploit these elements in an optimum manner." That the network specialist is indeed modifying his methods because of the transistor, and to good

[1] The answer is 5.333 cubic inches.

[2] J. R. Pierce and J. E. Karlin, "Information rate of a human channel," PROC. IRE, vol. 45, p. 368; March, 1957.

[3] "Poles and Zeros," PROC. IRE, vol. 45, p. 1457; November, 1957.

[4] E. W. Herold, "Future circuit aspects of solid-state phenomena," PROC. IRE, vol. 45, p. 1463; November, 1957.

advantage, is attested to by this impressive group of 31 papers.

**Ferrite mixers** for microwave frequencies, which have been the subject of some theoretical speculation during the last two years, have now undergone experimental tests, with the best conversion efficiencies ranging from about −15 db for the sum frequency output to −47 db for the difference frequency. While this doesn't match the −6 db figure reported for ferrites when used as frequency doublers,[5] further improvements can be expected as the technique is refined. Indeed, the first ferrite frequency doublers showed only a −60 db efficiency. In any event, this experimental verification should give added stimulus to the use of ferrites for mixing and doubling, especially at high power levels where they promise to prove superior to crystals. (P. N. Vartanian and E. N. Skomal, "Mixing in ferrites at microwave frequencies," 1957 IRE WESCON CONVENTION RECORD, Part 1.)

**X-raying germanium wafers** has been proposed as a simple and straightforward method to determine how thick they are. X-ray absorption measurements can reveal the thickness of a 2-mil (0.002-inch) wafer to within 0.1 mil. Conceivably, this method could be used to control an electrolytic etching operation so as to cut off the electrolysis automatically at the correct thickness. The scheme, while by no means revolutionary, is nevertheless an interesting example of the many ways in which the absorption of waves (whether they be electromagnetic or ultrasonic) can be used to determine important physical characteristics of materials. (A. R. Moore, "A method of accurate thickness determination of germanium wafers suitable for transistor production," IRE TRANS. ON ELECTRON DEVICES, October, 1957.)

[5] J. L. Melchor, W. P. Ayres, P. H. Vartanian, "Microwave frequency doubling from 9 to 18 kmc in ferrites," PROC. IRE, vol. 45, pp. 643–646; May, 1957.

# Abstracts of IRE Transactions

**The following issues of "Transactions" have recently been published, and are now available from the Institute of Radio Engineers, Inc., 1 East 79th Street, New York 21, N. Y. at the following prices. The contents of each issue and, where available, abstracts of technical papers are given below.**

| Sponsoring Group | Publication | Group Members | IRE Members | Non-Members* |
|---|---|---|---|---|
| Circuit Theory | Vol. CT-4, No. 3 | $2.50 | $3.75 | $7.50 |
| Communications Systems | Vol. CS-5, No. 3 | 0.95 | 1.40 | 2.85 |
| Electron Devices | Vol. ED-4, No. 4 | 0.80 | 1.20 | 2.40 |
| Engineering Management | Vol. EM-4, No. 4 | 0.70 | 1.05 | 2.10 |

* Public libraries and colleges may purchase copies at IRE Member rates.

## Circuit Theory

### VOL. CT-4, NO. 3, SEPTEMBER, 1957

**Pandora's Black Boxes**—H. J. Carlin (p. 60)

**Abstracts of Active-Network Papers** (p. 62)

**Foreword to Active-Network Papers**—J. G. Truxal (p. 69)

**Survey of Some Properties of Linear Networks**—E. F. Bolinder (p. 70)

An attempt is made to give a brief exposé of some modern works on linear network properties. The concepts treated are the following: passivity, stability, efficiency, and nonreciprocity; $n$-terminal-pair networks and two-terminal-pair networks in particular are studied at a fixed frequency.

**Active RC Networks**—R. D. Thornton (p. 78)

If all available amplifying devices can be approximated by linear models with capacitive, terminal, energy storage, there are bounds on the allowed natural frequencies of circuits constructed from these devices. These bounds are readily determined from the eigenvalues of a frequency matrix and can be related to the maximum power that can be dissipated by the device per unit energy stored in the terminal capacity. Synthesis of unilateral and constant-$k$ amplifiers is considered, and concepts such as the gain-bandwidth product and the maximum frequency of oscillation are related to the bounds on allowed natural frequencies.

**About Such Things as Unistors, Flow Graphs, Probability, Partial Factoring, and Matrices**—S. J. Mason (p. 90)

The purpose here is to point out three things. 1) Topological circuit analysis, in which we look for trees, and topological flow-graph analysis, in which we look for loops, are intimately related, since both have to do with simultaneous linear algebraic equations. The intimate relationship becomes an identity when we deal with Markoff probability diagrams, for which the circuit model of the problem and the flow-graph model of the problem are one and the same. 2) The expression for a flow-graph transmission in terms of the branch transmissions can often be made much more compact by a process called partial factoring. Fortunately, this process has a simple topological interpretation, so that the compact form is obtainable by inspection of the flow-graph. 3) Simultaneous linear matrix equations may be conveniently expressed in flow-graph form, whereupon the solution is obtainable by standard flow-graph reduction techniques.

**Multipole Analysis of Active Networks**—L. A. Zadeh (p. 97)

To replace the conceptual framework of network theory as based on the building blocks of two-terminal elements, a framework is suggested that is built on the premise that a network element is a black box with finitely many—but not necessarily two—accessible terminals. The greater generality and abstractness of the multipole method give it a considerably broader range of applicability than that possessed by the two-pole method.

**Transformation Theory Applied to Linear Active and/or Nonbilateral Networks**—E. A. Guillemin (p. 106)

A nonpassive and/or nonbilateral (linear) network can be represented analytically as a passive bilateral one in which the variables are subjected to an appropriate linear transformation. In contrast to the "dependent source" method of analysis, transformation theory offers not only a very general and elegant way of dealing with both the nonbilateral as well as the active character of devices, but through the existence of a considerable number of interpretive mechanisms such as geometric visualization in multidimensional spaces and the concept of normal coordinate transformations, it represents a relatively untapped storehouse of manipulative artifices that may ultimately provide a clearer understanding of this broader class of networks.

**Separation Transformations for Square Matrices**—H. E. Meadows, Jr. and B. J. Dasher (p. 111)

A class of transformations of square matrices which may be regarded as a generalization of matrix transposition and complex conjugation is defined by a set of five postulates. These transformations, termed "separation transformations," make evident certain characteristics of form for square matrices by resolving every square matrix into two additive component matrices called the "consonant" and "dissonant" parts. This property may be valuable in the study of active linear networks since the impedance matrices, for example, of these networks may display no obvious special characteristic of form.

Separation transformations and the related consonant and dissonant parts of square matrices have some interesting manipulative properties. These properties lead to an extension of the concept of orthogonality of matrices.

An example to illustrate the possible use of the relations derived for separation transformations shows a generalization of Mason's invariant for active linear networks subjected to lossless, linear, reciprocal coupling.

**The $A$ Matrix, New Network Description**—T. R. Bashkow (p. 117)

Both the loop and node methods of network analysis produce a system of second-order differential equations. A method of analysis is proposed which produces a set of first-order differential equations. With this method, the network equations obtained can be expressed in the form $F+dy/dt=Ay$, where $F$ and $y$ are column matrices and $A$ is a square matrix. The variables, $y$, are currents through inductances and voltages across capacitances; the forcing functions $F$ are proportional to voltage and current sources. The elements of $A$ are inductances, capacitances, and resistances, or combinations thereof. Characteristic roots (natural frequencies) of the network are identical with the eigenvalues of the $A$ matrix.

**Some Simplifications for Analysis of Linear Circuits**—G. L. Matthaei (p. 120)

Any linear, passive, or active two-terminal pair network is describable in terms of six, interrelated "characteristic polynomials." A method for finding them is presented which requires less labor than is usually involved in finding a set of the conventional circuit param-

in detail, and design procedures set up for these schemes. A comparison is made of the various schemes; in particular, direct and feedback stabilization are compared on the basis of battery drain, ac gain, and variation of operating point with battery voltage.

The stabilization of direct-coupled stages is also discussed, and the design of a bias circuit for a two-stage direct-coupled pair is taken up in detail.

Nonlinear techniques for temperature stabilization are also discussed. These are useful in special applications such as high-power output stages, where the temperature changes are extreme, or in low-level circuits where extremely stable operation is required, *e.g.*, in oscillators.

**Thermal Stability of Junction Transistors and Its Effect on Maximum Power Dissipation**—H. C. Lin (p. 202)

When the junction temperature of a transistor increases, the collector current increases, as a result of increases in 1) saturation currents and 2) dc conductances. Thermal instability occurs when junction temperature and collector current increase in regenerative and uncontrollable fashion. The limit depends on factors both within and external to the transistor. The internal factors are the thermal resistance, the current amplification factor, and the base lead resistance. The external factors are ambient temperature, collector voltage, circuit resistances, and the thermal coupling between the transistor and temperature compensation elements, if any. Circuits with greater temperature stability permit a higher maximum power dissipation. The factors are discussed which determine the thermal stability and consequently, the maximum dissipation of transistors. The criteria for stability are derived mathematically and some thermal compensation techniques are treated.

**A Survey of Magnetic and Other Solid-State Devices for the Manipulation of Information**—J. A. Rajchman (p. 210)

A review is made of the art of manipulating digital information by means of magnetic devices. Also included are some remarks on other solid-state devices. There is a brief introductory discussion of semiconductor diodes and of the unique properties of the transistor. The storage and switching capabilities of magnetic cores made of square hysteresis loop materials are discussed with some detail. This discussion includes: random access memories made of individual cores or ferrite apertured plates, various types of decoding and encoding switches, shift registers, current and voltage driven circuits, the principle of current steering, transistor coupled circuits, the principle of the transfluxor, the application of the transfluxor to nondestructive read-out memories and channel commutators, the principle of transfluxor current steering, and some examples of multiapertured transfluxors. The potentialities of some phenomena as yet not widely exploited are discussed: ferroelectric, electro-optical and magnetoresistive effects.

**Counting Circuits Employing Ferroelectric Devices**—R. M. Wolfe (p. 226)

A new type of counting circuit utilizing ferroelectric devices has been developed. This circuit, although similar to the older energy storage type of counter, overcomes most of the disadvantages of the older circuit. Whereas the older circuit required standardization of the input pulse to stabilize the counting ratio, *i.e.*, the number of input pulses per output pulse, the use of a ferroelectric device to meter charge removes the need for such standardization. A second ferroelectric device used to integrate the packets of charge developed by the first removes the lower bound on the repetition rate of pulses to be counted.

Circuits have been built with counting ratios up to 40 to 1. They have operated satisfactorily under conditions of changing voltage, temperature, and pulse spacing. Several counters may be connected in cascade to provide higher counting ratios.

**A High-Speed Two-Winding Transistor-Magnetic-Core Oscillator**—A. J. Meyerhoff and R. M. Tillman (p. 228)

Recent articles in the literature have described voltage-controlled square-wave oscillators using transistors and square-loop magnetic cores and generally incorporating four windings. These oscillators give output frequency directly proportional to applied voltage; hence they are useful as solid-state dc to dc converters, telemetering oscillators, and many other devices. Each application is based on the fact that the volt seconds applied to a core are proportional to the flux switched, which is essentially constant for the core.

This paper is primarily devoted to the fundamentals and applications of a novel two-winding transistor-core oscillator and derived circuits. The two-winding circuit is capable of true square-wave output at 700 kc, the upper frequency limit being determined by the present state of the art of transistor and core development.

A review is given first of the usual four-winding oscillator, tracing its operating cycle step by step and showing the circuit to be derivable directly from a fundamental transistor-core switching circuit.

Then the two-winding oscillator is discussed. With this circuit, the two separate base windings are eliminated through cross-coupling of each collector to the base of the opposite transistor. During switching time, the collector winding of the OFF transistor supplies the necessary regenerative voltage to the base of the ON transistor. A parallel RC in each base circuit speeds up the turn-off action by application of inverse current to the ON base. Direct electrical cross-connection from the ON base to the OFF collector means that at switch-over the inverse transient voltage, due to flyback, will momentarily place the OFF transistor into inverse saturated conduction, thereby presupplying it with holes so that it can take on its load in the forward direction extremely rapidly when the ON transistor shuts off. In this circuit, self-starting is inherent, due to the direct connections from base to negative supply.

The circuit operation is analyzed in detail and worst-case design equations are derived. A bibliography of the literature is included.

**Millimicrosecond Transistor Current Switching Circuits**—H. S. Yourke (p. 236)

If transistor switching circuits are to have response times limited by the bandwidths of the transistors operating as amplifiers and by diffusion or transit time delay, it becomes necessary to avoid operation in saturation. Since a low collector to base voltage, or operation near saturation, has a detrimental effect on transistor bandwidth, it is desirable to avoid this operating region as well.

Where nonsaturating circuits are used with transistors having cutoff frequencies of several hundred megacycles, transistor and circuit capacitances become the primary limitation on speed. To minimize the delays due to capacitance, it is desirable to operate with voltage swings as small as reliability consideration will permit.

A new mode of operation has been developed whereby well-specified currents can be switched reliably with small voltage swings. The complementary current switching technique described provides a means of constructing relatively simple logical circuits in which transistors are operated well out of saturation in a region of maximum bandwidth. This technique offers several advantages besides high-speed switching. The resulting logical circuits have complemented outputs, and reset their own levels. There is no requirement on the upper limit of $\alpha$ and dc stability factors are essentially unity. The circuits are simple and relatively noise free. A few basic circuits and working examples are presented in the paper. Application and extension of this current switching technique results in a large body of new and useful logical circuits.

**Some New Transistor Bistable Elements for Heavy Duty Operation**—N. F. Moody and C. D. Florida (p. 241)

Bistable elements of fast switching speed (0.2 $\mu$sec), capable of delivering load currents up to 100 ma and having a low-output impedance, are required in many electronic circuits. Such an element is particularly useful in digital computers employing passive routing.

The paper shows that circuits which use both $p$-$n$-$p$ and $n$-$p$-$n$ transistors are well suited for such duties. It also describes both nonsaturated and saturated forms.

Part I devotes itself to nonsaturated circuits, and the analysis is mathematical in approach. The general properties thus deduced are applicable to all members of the circuit family.

Part II turns to the problems introduced by saturation and is a general theoretical discussion of wide application. It leads to a concept denoted controlled saturation; this is applied to switching circuits in order to minimize the penalty of lost speed which saturation can cause.

Part III applies the theoretical work of the preceding parts to a fast trigger circuit in which saturation is permitted. It concludes by showing that this basic saturated circuit can be developed into a variety of forms.

**A Decade Ring Counter Using Avalanche-Operated Junction Transistors**—J. E. Lindsay (p. 262)

The avalanche mode of operation for junction transistors is encountered at higher-than-normal collector voltages. In this avalanche region of operation the electrical character of the junction transistor is profoundly altered because of a voltage sensitive current-multiplication occurring at the collector junction. Current controlled $N$-type negative resistance characteristics suitable for bistable operation are obtained. Important features of these characteristics can be treated analytically to obtain results suitable for design purposes.

Twelve experimental avalanche-operated junction transistors have been used in a decade ring counter and driver. This represents a saving of two-to-one in semiconductor devices, as contrasted to the use of conventionally operated junction transistors for the same function. A like saving of other components is obtained. The ring counter uses a new method of count transfer which provides improved reliability and higher counting speed capability. The driver and counter achieve operation to 500 kilocycles using transistors having a frequency of $\alpha_e$ cutoff in the range 30 to 40 kilocycles for conventional operation. The counter operates to 300 kilocycles over a temperature range from below $-50°$ to 50°C without compensation or optimized design.

**Transient Response Characteristics of Unijunction Transistors**—J. J. Suran and B. K. Eriksen (p. 267)

Carrier transport in unijunction transistors is due primarily to electric fields rather than diffusion gradients. Thus, the high-frequency and transient response characteristics of unijunction transistors are considerably different from the characteristics associated with diffusion type devices.

The high-frequency and transient response characteristics of silicon unijunction transistors are described. A previously published solution of the electrodynamic equations, taking into account field and recombination effects, is used to calculate theoretical frequency and transient response characteristics which are subsequently compared to experimental measurements.

It is shown that:

1) Electric field effects lead to resonance characteristics which are somewhat similar to those encountered in wave interference phenomena.

2) The frequency response characteristics of unijunction transistors are predominantly determined by the electric field gradient for high fields and by recombination effects for low fields.

3) The large-signal transient response of unijunction transistors is characterized by at least two time constants, one related to transit time and the other to minority carrier lifetime.

4) The maximum large-signal switching speeds and minimum trigger energy of regenerative unijunction transistor circuits depend upon both the electric field and lifetime characteristics of the device.

**An Improved Square-Wave Oscillator Circuit**—J. L. Jensen (p. 276)

Inductively coupled square-wave transistor oscillators using a saturating output transformer subject the transistor to rather severe transient conditions and require an expensive transformer. The improved circuit, however, uses a separate saturating feedback transformer and a conventional output transformer. The described circuit has improved performance with less severe duty on the transistors, permits the use of inexpensive transformers, and allows the adaption to a variety of operating requirements.

**A Phase-Regulated Transistor Power Supply**—D. E. Deuitch and H. J. Paz (p. 279)

Transistors have been utilized effectively for class A regulation of power supplies. However, the power-handling capacity and high-temperature performance of these power supplies are basically restricted because of the power-temperature limitation of transistors.

This paper describes a type of regulated transistor power supply in which the dissipation in the regulator transistors is extremely small. This enables low-power transistors to control large amounts of power and permits substantial improvement of power supply capabilities at high temperature over that of the Class A regulated supply.

The principle of operation of this supply is similar to that used in thyratron regulation. The regulator transistors are operated as rectifying switches whose conduction period is varied in phase with respect to the ac input. Regulation is obtained by controlling the conduction phase of the transistors in response to load and input voltage variation.

A transistor switch circuit for this power supply is described together with general design and operating considerations for its power supply application. The performance of a 12-volt, 0- to 1-ampere developmental phase regulated power supply is discussed.

**Abstracts of Transistor Conference Papers Not in This Issue** (p. 66)

**Correction** (p. 284)

**Correspondence** (p. 285)

**Reviews of Current Literature—Finite Duration Signals With Maximum Filtered Energy**—J. A. Ville and J. Bouzitat (in French) (p. 293)

**Mode Conversion Phenomena in the Case of Multilayer Conductors and its Effect on the Transmission Through Individual or Through Connected Partial Sections**—Horst-Edgar Martin (in German) (p. 293)

**Experimental Study of Tapped Delay-Line Filters**—D. W. Lytle (p. 294)

**Piecewise-Linear Network Theory**—T. E. Stern (p. 294)

**Double Tuned Filter Circuits for Wide Relative Pass-Band**—F. Carassa (in Italian) (p. 294)

**Analysis of Electric Circuits Containing Nonlinear Resistance**—L. A. Pipes (in English) (p. 294)

**Wave Dispersion in Disk Transmission Lines**—Gerhard Piefke (in German) (p. 294)

**Concerning the Chain Connection of Two Multipoles**—W. Ruppe (in German) (p. 294)

**Calculation of Current Distribution in a Linear Network**—Joannis Vratsanos (in German) (p. 294)

## Communications Systems

### Vol. CS-5, No. 3, December, 1957

**20/20 Visualization**—J. E. Schlaikjer (p. 1)

**Demonstration of Delay Distortion Correction by Time-Reversal Techniques**—B. P. Bogert (p. 2)

Experiments relating to methods of correcting delay distortion by time-reversal have been made utilizing a slow-speed picture transmission system. The improvements in picture quality by phase correction of a 3 kc telephone loop 30.4 miles long and a 5 kc loop from Murray Hill, N. J., to Los Angeles, Calif., and back are demonstrated. The total distance that the signal was transmitted over the 5 kc loop was 16,600 miles and there were 16 type L carrier links involved. By way of an introduction, the improvement in the impulse response of networks and transmission circuits is discussed.

**Quadruple-Diversity Tropospheric Scatter Systems**—W. G. Long and R. R. Weeks (p. 8)

**Operations Research and Communications Systems Planning**—R. V. Higdon (p. 20)

A discussion is presented outlining the general concept of operations research for those who are not familiar with it. A necessarily brief description is given of efforts to apply these concepts to specifying effective communications for complex organizations or weapons systems.

**High-Speed Frequency-Shift Keying of LF and VLF Radio Circuits**—H. G. Wolff (p. 29)

Present VLF transmitters are limited in transmission speed to approximately 20 words per minute because of the bandwidth limitations of the High-$Q$ antenna circuit. To permit an increase in transmission speed, an unique method has been developed which makes use of the variation of reactance of the antenna circuit in synchronism with frequency shift modulation of the carrier. The method makes possible the transmission of teletype or high speed Morse signals at speeds of 100 words per minute or more. This increase by a significant factor in present traffic handling capabilities of VLF stations can be accomplished by increasing the cost of the station less than ten per cent.

**An Electronic Multicoupler and Antenna Amplifier for the VHF-Range**—K. Fischer (p. 43)

A single-stage distributed amplifier for the frequency range from 25 to 223 mc/s may be used as an antenna amplifier for compensation of cable-attenuation or, in connection with a divider network, as a multicoupler for feeding six receivers from a common antenna. Single-stage amplification results in not only low noise level due to the parallel tube circuitry employed but also in a low cross-modulation figure. Second order distortions are minimized by special push-pull operation without doubling the number of tubes. Another advantage of the distributed amplifier is its reliability, which is further improved by dividing the power supply into two independent sections.

**Contributors to This Issue** (p. 49)

## Electron Devices

### Vol. ED-4, No. 4, October, 1957

**Very High-Power Transistors with Evaporated Aluminum Electrodes**—H. W. Henkels and G. Strull (p. 291)

The principles involved in the design of high-power and very high-power transistors are considered in brief. The important factors in high-gain, high-current transistor design are the emitter-injection efficiency, the emitter and collector planarity, and the base-bias high-current falloff. The fabrication techniques involved in the production of transistors to maximize the injection efficiency and planarity (by evaporation of aluminum electrodes) and minimize base bias drop (by choice of optimum emitter geometry), are discussed. The characteristics of devices capable of handling currents in the range from 1 to 10 amperes at very high common-emitter current gains ranging from 50 to above 300 are described.

**An Eqnivalent Circuit for Microwave Noise at the Potential Minimum**—A. E. Siegman and S. Bloom (p. 295)

It has been suggested that an inductive element should be added to Watkins RC equivalent circuit for the microwave noise current fluctuations at the potential minimum of a diode, and that this added element gives closer agreement with more recent work which shows a pronounced peak in noise current near the plasma resonance, $a=\frac{1}{2}$. This paper presents an approximate analytical argument for the inclusion of an inductive element, based on the density-function method of analysis, which predicts the proper value for the inductance and yields a curve of reduction factor vs frequency in agreement with more detailed theories. The value of the inductance is such as to resonate with the capacitance of the potential minimum at $a=\frac{1}{2}$. A discussion of the linearity of the potential minimum and of the idealized potential-minimum model is also included.

**A Novel Approach to Microwave Duplexer Tube Design**—L. Gould, E. V. Edwards, and I. Reingold (p. 300)

An encapsulated input window with an independent gas fill has been incorporated in the design of a broad-band duplexer tube. This design has been effective in separating the interdependence of the high-power characteristics of the tr tube. Recovery time and arc loss are determined predominantly by the input window design, whereas spike leakage energy and flat leakage power are determined by the tube body design. The two portions of the tube are designed independently for optimum performance. The effects of gas pressure and nature of the gas on the behavior of the high-power characteristics have been investigated. The factors determining adequate tube operation are discussed, and experimental data are presented to verify the advantages of the encapsulated structure.

**Multicolor Storage Tube**—C. D. Beintema, S. T. Smith, and L. L. Vant-Hull (p. 303)

Multicolor storage tubes for applications with low frame rates have been built by modification of direct-viewing storage tubes. A perforated shadow mask is placed between the three writing guns and the storage surface. This shadow mask allows electrons from each writing gun to strike discrete storage areas, each containing a single aperture in register with a color dot on the view plate. In this way, it is possible to write and store electrical signals independently in adjacent color areas. Factors causing color impurity are described, together with the steps taken to minimize their effects. A tube has been built that shows good color purity in a 6-inch-diameter circle; it has 75 total color dots per inch resolution, 8 foot-lamberts brightness, and about 1-minute persistence. Other possible multicolor storage tube designs are discussed.

**Experimental Notes and Techniques** (p. 309)

**Contributors** (p. 311)

**Index to IRE Transactions on Electron Devices—Volume ED-4, 1957** (follows p. 313)

## Engineering Management

### Vol. EM-4, No. 4, December, 1957

**The Climate of Research in the University**—C. W. Gartlein (p. 109)

**Unionization of Engineers—I**—Joseph Amann (p. 113)

**Unionization of Engineers—II**—H. H. Rains (p. 116)

**The Nation's Need for Greater Scientific and Technical Strength—Means for its Attainment**—M. J. Kelly (p. 122)

**Dynamic Project-Orientated Industrial Organization**—Henry Imus (p. 128)

**The Establishment and Operation of a Semiautonomous Field Organization**—J. D. Finley (p. 132)

# Abstracts and References

Compiled by the Radio Research Organization of the Department of Scientific and Industrial Research, London, England, and Published by Arrangement with that Department and the *Electronic and Radio Engineer*, incorporating *Wireless Engineer*, London, England

**NOTE: The Institute of Radio Engineers does not have available copies of the publications mentioned in these pages, nor does it have reprints of the articles abstracted. Correspondence regarding these articles and requests for their procurement should be addressed to the individual publications, not to the IRE.**



The Index to the Abstracts and References published in the PROC. IRE from February, 1956 through January, 1957 is published by the PROC. IRE, May, 1957, Part II. It is also published by *Electronics and Radio Engineer*, incorporating *Wireless Engineer*, and included in the March, 1957 issue of that journal. Included with the Index is a selected list of journals scanned for abstracting with publishers' addresses.

The number in heavy type at the upper left of each Abstract is its Universal Decimal Classification number and is not to be confused with the Decimal Classification used by the United States National Bureau of Standards. The number in heavy type at the top right is the serial number of the Abstract. DC numbers marked with a dagger (†) must be regarded as provisional.

### U.D.C. NUMBERS

Extensions and changes in U.D.C. numbers published in P.E. Notes, up to and including P.E. Note 609, will be introduced in Abstracts and References where applicable, notably the subdivisions of 621.372.8 waveguides published in P.E. Note 594. U.D.C. publications are obtainable from The International Federation for Documentation, Willem Witsenplein 6, The Hague, Netherlands, or from The British Standards Institution, 2 Park Street, London, W.1, England.

### JOURNAL REFERENCES

References to Russian publications will henceforth be based on the Russian title which will be abbreviated on the principles of The World List of Scientific Periodicals. The main changes are as follows:

Dokl. Ak. Nauk S.S.S.R. (formerly C.R. Acad. Sci. U.R.S.S.),

Izv. Ak. Nauk S.S.S.R. (formerly Bull. Acad. Sci. U.R.S.S.).

## ACOUSTICS AND AUDIO FREQUENCIES

534.2–13:536.3 1

**Effect of Heat Radiation on Sound Propagation in Gases**—P. W. Smith, Jr. (*J. Acoust. Soc. Amer.*, vol. 29, pp. 693–698; June, 1957.)

534.21–8–14 2

**Ultrasonic Propagation Measurement in Sea Water up to 400 kc/s**—T. Hashimoto and Y. Kikuchi. (*J. Acoust. Soc. Amer.*, vol. 29, pp. 702–707; June, 1957.) Methods of measurement for horizontal and for vertical propagation are described. Measured values of absorption were 10–20 db/km at 28 kc increasing to 120 db/km at 400 kc.

534.23 3

**Sound Transmission through Thin Cylindrical Shells**—P. W. Smith, Jr. (*J. Acoust. Soc. Amer.*, vol. 29, pp. 721–729; June, 1957.) An analysis of the impedance presented by a thin cylindrical elastic shell to a pressure or normal stress as a function of the axial wavelength and the angular dependence of the forces.

534.23:537.227 4

**Vibrations of Ferroelectric Cylindrical Shells with Transverse Isotropy: Part 1—Radially Polarized Case**—J. F. Haskins and J. L. Walsh. (*J. Acoust. Soc. Amer.*, vol. 29, pp. 729–734; June, 1957.) Expressions for the coupled mechanical vibrations and electrical admittance of ferroelectric tubes having transverse isotropy are derived and the results supported by experimental data.

534.232 5

**Experimental Investigation of Conical Horns Used with Underwater Sound Transducers**—W. R. Owens and C. M. McKinney. (*J. Acoust. Soc. Amer.*, vol. 29, pp. 744–748; June, 1957.) A simple conical horn lined with pressure-release material is very effective in increasing the axial sensitivity of transducers and improving directivity. Design curves are given.

534.232:534.24 6

**Effect of a Reflecting Plane on the Power Output of Sound Sources**—U. Ingard and G. L. Lamb, Jr. (*J. Acoust. Soc. Amer.*, vol. 29, pp. 743–744; June, 1957.) The effect of a rigid reflecting plane on the output from a sound source above it is expressed as a "power amplification factor." This is calculated for a number of elementary sound sources and power output is determined as a function of source height.

534.414 7

**Accoustic Impedance of a Helmholtz Resonator at Very High Amplitude**—D. A. Bies and O. B. Wilson, Jr. (*J. Accoust. Soc. Amer.*, vol. 29, pp. 711–714; June, 1957.) A Helmholtz resonator terminating a 10-inch diameter tube has been investigated for sound pressure levels 100–170 db. With increasing sound pressure the same general rise in acoustic resistance and resonance frequency was observed for two different mountings.

534.612 8

**Acoustical Radiation Pressure due to Incident Plane Progressive Waves on Spherical Objects**—G. Maidanik. (*J. Acoust. Soc. Amer.* vol. 29, pp. 738–742; June, 1957.)

534.75 9

**On the Fusion of Sounds Reaching Different Sense Organs**—D. E. Broadbent and P. Ladefoged. (*J. Acoust. Soc. Amer.*, vol. 29, pp. 708–710; June, 1957.) Experiments with synthetically produced speech show that fusion occurs when the first formant is presented to one ear and the second formant to the other, but not if the formants are given different fundamental frequencies.

534.78 10

**Constant-Ratio Rule for Confusion Matrices in Speech Communication**—F. R. Clarke. (*J. Acoust. Soc. Amer.*, vol. 29, pp. 715–720; June, 1957.) "Three experiments are reported which give support to an empirical rule which may be used for predicting the entries in a closed confusion matrix for any subset of items drawn from a master set of items with a known confusion matrix."

534.78 11

**The Intelligibility of Synthetic Speech**—O. Warns. (*Frequenz*, vol. 11, pp. 169–175; June, 1957.) The results of subjective tests on the intelligibility of synthetic logatoms are analyzed. For the German language 700–1100 interchangeable speech elements would be adequate, requiring an information rate of 40 bits per second.

621.395.625.3:621.397.5 12

**Video Tape Recorder Design**—(See 294.)

## ANTENNAS AND TRANSMISSION LINES

621.315.212 13

**The Characteristic Impedance of Coaxial Cables**—F. Raggi. (*Note Recensioni Notiz.*, vol. 6, pp. 174–188; March/April, 1957.) Note summarizing the factors which determine the characteristic impedance of coaxial cables.

621.315.212:621.397.24 14

**A New 4-Mc/s Coaxial Line Equipment—C.E.L. No. 6A**—M. E. Collier and W. G. Simpson. (*P.O. Elec. Eng. J.*, vol. 50, Pt. 1, pp. 24–34; April, 1957.) The equipment described is suitable for the transmission of either 16 telephony supergroups (960 circuits) or a 405-line television signal.

621.315.212:621.397.24 15

**A 4-Mc/s Coaxial Line Equipment—C.E.L. No. 4A**—E. Davis. (*P.O. Elec. Eng. J.*, vol. 50, Pt. 2, pp. 92–97; July, 1957.) A description of

equipment suitable for the transmission of either 17 telephony supergroups (1020 circuits) or a television signal of 3-mc video bandwidth. See also 14 above.

621.372.2 16
**Return Loss: Part 1**—T. Roddam. (*Wireless World*, vol. 63, pp. 521–524; November, 1957.) The use of the concept of return loss instead of standing wave ratios is recommended in dealing with reflections of short pulses on long loss-free incorrectly terminated lines.

621.372.8:621.372.5 17
**Noisy and Noise-Free Two-Port Networks Treated by the Isometric Circle Method**—E. F. Bolinder. (PROC. IRE, vol. 45, pp. 1412–1413; October, 1957.)

621.372.823 18
**Circular Electric Wave Transmission through Serpentine Bends**—H. G. Unger. (*Bell Sys. Tech. J.*, vol. 36, pp. 1279–1291; September, 1957.) An analysis of the propagation in a circular waveguide with equally spaced discrete supports and deformed elastically into a serpentine bend under its own weight.

621.372.831.4 19
**Slots in an Imperfectly Conducting Waveguide**—B. Chatterjee. (*Indian J. Phys.*, vol. 40, pp. 278–282; May, 1957.) The shunt conductance of a slot initially increases with departure from perfect conductivity of the guide wall but decreases rapidly in almost direct proportion to further decreases in conductivity.

621.372.852.21 20
**Theory of Curved Circular Waveguide containing an Inhomogeneous Dielectric**—S. P. Morgan. (*Bell Sys. Tech. J.*, vol. 36, pp. 1209–1251; September, 1957.) General equations are derived for all modes in a curved circular waveguide containing an inhomogeneous dielectric. The results are applied to the problem of preventing mode conversion from $TE_{01}$ to $TM_{11}$. Design equations are given for various compensators with criteria for keeping the power level of spurious modes at a minimum.

621.372.853.1 21
**Circular Electric Wave Transmission in a Dielectric-Coated Waveguide**—H. G. Unger. (*Bell Sys. Tech. J.*, vol. 36, pp. 1253–1278; September, 1957.) The mode conversion from the $TE_{01}$ wave to the $TM_{11}$ wave in a curved circular waveguide may be reduced by applying a thin uniform dielectric coating to the inner wall. Design curves are given for both uniform bends of small radius and for large bending radii which may occur in a normally straight guide.

621.372.853.1 22
**Normal Mode Bends for Circular Electric Waves**—H. G. Unger. (*Bell Sys. Tech. J.*, vol. 36, pp. 1292–1307; September, 1957.) The $TE_{01}$-$TM_{11}$ degeneracy is removed by a thin dielectric coating, and a further reduction in the mode conversion at a bend is obtained by tapering the curvature along the guide. Details are given of the bend loss for $\lambda = 5.4$ mm. See also 21 above.

621.396.674:621.396.93 23
**A Versatile Multiport Biconical Antenna**—R. C. Honey and E. M. T. Jones. (PROC. IRE, vol. 45, pp. 1374–1383; October, 1957.) This antenna can be used as a wide-band direction finder, as it excites in the feeding waveguide modes whose ratios are azimuth dependent. It also has uses as a multiplexer.

621.396.677 24
**Bi-directional F.M. Antennas**—H. B. Dent. (*Wireless World*, vol. 63, pp. 534–536; November, 1957.) Description of stacked horizontal half-wave dipoles which are simple to construct and erect.

621.396.677.43 25
**Rhombic Antennas**—F. J. Norman and J. F. Ward. (*Electronic Radio Eng.*, vol. 34, pp. 398–403; November, 1957.) "The design of aperiodic rhombic antennas is examined and a method derived whereby a set of charts of open scale yields all the antenna parameters of practical significance for high-frequency operation. The angle of fire and the gain with respect to a dipole in free space are displayed for an adequate range of antenna side lengths and included angles. Corrections are given for the height above ground and a simple method to find the shape of the main lobe is suggested."

621.396.677.8:523.16 26
**The Mullard Radio Astronomy Observatory, Cambridge**—Ryle. (See 107.)

621.396.677.833:523.16 27
**World's Largest Radio Telescope**—(See 108.)

621.396.677.85 28
**Calculated Intensity and Phase Distribution in the Image Space of a Microwave Lens**—G. W. Farnell. (*Can. J. Phys.*, vol. 35, pp. 777–783; June, 1957.) Intensity and constant-phase contours and an energy-flow diagram are shown for a 3.2-cm-$\lambda$ lens with exit pupil of 25-cm radius distant 105 cm from the image point. Calculations are based on scalar diffraction theory. Results of measurements show close agreement.

621.396.677.85 29
**Study of Optical Diffraction Images at Microwave Frequencies**—M. P. Bachynski and G. Bekefi. (*J. Opt. Soc. Amer.*, vol. 47, pp. 428–438; May, 1957.) "Experimental investigations of the intensity distribution in the region of the focus of microwave lenses are described. The circularly symmetric lenses, made from polystyrene plastic, were illuminated by a linearly polarized beam of radiation of 1.25-cm wavelength. Most of the measurements are presented in the form of intensity contours in planes both containing the principal ray and lying perpendicular to it. Images formed by nearly perfect optical systems and by systems suffering from various third-order monochromatic aberrations were examined. In most cases the results are compared with calculations made from the scalar-diffraction theory of optical systems. In general, good agreement between theory and experiment is found."

## AUTOMATIC COMPUTERS

681.142 30
**Controlling the Digital Computer**—R. W. Hamming. (*Sci. Mon.*, vol. 85, pp. 169–175; October, 1957.) A nonmathematical discussion of the programming and application of computers for scientific purposes.

681.142 31
**An Experimental 50-Mc/s Arithmetic Unit**—R. M. Walker, D. E. Rosenheim, P. A. Lewis, and A. G. Anderson. (*IBM J. Res. Devel.*, vol. 1, pp. 257–278; July, 1957.) Detailed description of a unit which performs a repetitive multiplication program and checks the results for errors.

681.142 32
**The Design of the Ferranti Pegasus Computer: Part 2**—G. Emery. (*Electronic Eng.*, vol. 29, pp. 420–425; September, 1957.) The detailed engineering aspects of the design problem are discussed. Part 1: 3753 of 1957 (Braunholtz).

681.142 33
**A 32000-Word Magnetic-Core Memory**—E. Foss and R. S. Partridge. (*IBM J. Res. Devel.*, vol. 1, pp. 102–109; April, 1957.) The storage matrix consists of $128 \times 256 \times 36$ ferrite cores and has a read-write cycle of 12 $\mu$sec. Its construction is described, together with the driver and sense amplifier circuits.

681.142 34
**A Positive-Integer Arithmetic for Data Processing**—R. W. Murphy. (*IBM J. Res. Devel.*, vol. 1, pp. 158–170; April, 1957.)

681.142 35
**Irredundant Disjunctive and Conjunctive Forms of a Boolean Function**—M. J. Ghazala (Gazale). (*IBM J. Res. Devel.*, vol. 1, pp. 171–176; April, 1857.) A thorough algebraic method is described for determining the complete set of irredundant normal and conjunctive forms. The procedure is mechanical and the method can be applied for programming computers.

681.142 36
**Electronic Computers**—W. Taeger. (*Frequenz*, vol. 11, pp. 185–191; June, 1957.) The application of analog computers to the solution of control-system problems is discussed.

681.142 37
**Approximating Nonlinear Functions by Shunt-Loading Tapped Potentiometers in Analogue Computing Machines**—D. W. C. Shen. (*Electronic Eng.*, vol. 29, pp. 434–439; September, 1957.)

681.142:621.314.7 38
**The Multipurpose Bias Device: Part 1—The Commutator Transistor**—B. Dunham. (*IBM J. Res. Devel.*, vol. 1, pp. 116–129; April, 1957.) A study of the application of the Rutz commutator transistor to three-input, one-output logical problems for handling by automatic computer systems. The Rutz commutator is a single-emitter amplitude-sensitive device with three separate input wires applied to the emitter. Its design will be detailed in a subsequent paper.

681.142:621.314.7 39
**Two-Collector Transistor for Binary Full Addition**—Rutz. (See 315.)

681.142:621.395.625.3 40
**A Mathematical Model for Determining the Probabilities of Undetected Errors in Magnetic Tape Systems**—M. Schatzoff and W. B. Harding. (*IBM J. Res. Devel.*, vol. 1, pp. 177–184; April, 1957.)

681.142:621.395.625.3 41
**The Magnetic Tape Store for Pegasus**—T. G. H. Braunholtz and D. Hogg. (*Electronic Eng.*, vol. 29, pp. 484–489; October, 1957.)

681.142:621.395.625.3 42
**The Recording of Digital Information on Magnetic Drums**—D. G. N. Hunter and D. S. Ridler. (*Electronic Eng.*, vol. 29, pp. 490–496; October, 1957.) "Methods of representing binary digital information on magnetic drums are discussed with regard to their reliability, cost, and technical merits."

## CIRCUITS AND CIRCUIT ELEMENTS

621.3:061.3 43
**International Components Symposium**—(*Electronic Radio Eng.*, vol. 34, pp. 428–431; November, 1957.) Summary of papers read at the Royal Radar Establishment, Malvern, in September, 1957. Reliability, efficient use of space, liquid cooling techniques, and optimum component shapes for automatic assembly are discussed.

621.3.011.3 44
**Calculation of Inductance of Toroids with Rectangular Cross Section and Few Turns**—R. F. Schwartz. (PROC. IRE, vol. 45, pp. 1416–1417; October, 1957.)

621.3.049.7:621.39.03:061.3 45
**"Solid Circuits"**—(*Wireless World*, vol. 63, pp. 516–517; November, 1957.) Discussion of the International Symposium on Electronic Components held at Malvern, England. A "solid circuit" forming the equivalent of several transistors connected by resistors and capacitors is obtained by depositing films of conductive, resistive, and dielectric materials on a small block of semiconductor material. The solution of problems regarding the operation of components at high temperatures is mentioned.

621.3.049.75 46
**Printed Circuits in Receiver Construction**—W. I. Flack. (*J. Telev. Soc.*, vol. 8, pp. 176–185; January/March, 1957.) Outline of development of the printed circuit, and description of modern production techniques.

621.3.049.75 47
Pro and Con on Seven Different Methods of Printed Wiring—A. E. Stones. (*Electronic Inds. Tele-Tech.*, vol. 16, pp. 64–66, 158; March, 1957.) The basic techniques for each method are described and compared. A table of relevant U.S. patents is included.

621.314.6 48
**A General Circuit Theorem on Rectification**—J. W. Gewartowski. (PROC. IRE, vol. 45, p. 1410; October, 1957.) Nonlinear capacitors and inductors cannot effect rectification unless nonlinear resistance is present in the circuit.

621.318.424 49
**New Method of Evaluating Ferro-inductors**—W. J. Polydoroff. (*Electronic Inds. Tele-Tech.*, vol. 16, pp. 78–79, 150; April, 1957.) Formulas for calculating the insertion loss and the resistance increase due to the iron core are derived. The practical factors governing optimum coil design are investigated.

621.318.57:621.387 50
**Cold-Cathode Voltage-Transfer Circuits**—J. H. Beesley. (*GEC Telecommun.*, no. 23, pp. 6–19; February, 1957.) Practical techniques used in the application of cold-cathode triodes are given in detail. A number of circuit diagrams are included.

621.319.4:537.311.33 51
**Charge and Discharge of a Non-linear Condenser through a Linear Nondissipative Inductance**—A. Mozumder. (*Z. angew. Math. Phys.*, vol. 8, pp. 261–280; July 25, 1957.) Macdonald (*J. Chem. Phys.*, vol. 22, pp. 1317–1322; August, 1954) has shown that for a capacitor with a semiconductor as dielectric the capacitance is proportional to $\sinh \alpha V/\alpha V$ where $V$ is the voltage across the capacitor and $\alpha$ is a constant. A circuit is analyzed in which such a capacitor is connected in series with a lossless inductance and a direct-voltage source, and a comparison is made with an exponential capacitor ($C\alpha \exp |\alpha V|$). Applications to the generation of rectangular and triangular waveforms are indicated. See also 958 of 1955 (Macdonald and Brackman).

621.319.42:621.3.049.75 52
**Evaluating Base Materials for Printed Capacitors**—J. J. Logan. (*Electronic Inds. Tele-Tech.*, vol. 16, pp. 72–73., 160; August, 1957.) Definition of terms specifying the losses of base materials used for printed circuits which affect the size and $Q$ factor of printed capacitors.

621.372.412.002.2:549.514.51:621.793.14 53
**A Vacuum Plant for the Frequency Calibration of Quartz Vibrators**—J. Green, L. Holland, and B. D. Power. (*Electronic Eng.*, vol. 29, pp. 440–444; September, 1957.) See also 503 of 1956 (Awender, *et al*).

621.372.5 54
**A Network Theorem**—E. Green. (*Marconi Rev.*, vol. 20, pp. 35–38; 2nd Quart., 1957.) The impedance level of half a symmetrical network can be changed without altering the frequency response; the use of this theorem for the solution of network problems is discussed and illustrated by an example.

621.372.5:621.372.8 55
**Noisy and Noise-Free Two-Port Networks Treated by the Isometric Circle Method**—Bolinder. (PROC. IRE, vol. 45, pp. 1412–1413; October, 1957.)

621.372.5:621.375.2.018.75 56
**On the Design of Four-Terminal Interstages for Pulse Applications**—A. K. Choudhury and N. B. Chakrabarti. (*Indian J. Phys.*, vol. 40, pp. 193–210; April, 1957.) The limits set by the input and output capacitance on the time response and the conditions for no overshoot are determined. Methods for achieving the necessary pole distributions are described and circuit networks suggested.

621.372.52:621.314.7 57
**The Mathematical Treatment of Transistor Feedback Circuits**—W. Glaser. (*Nachr-Tech.*, vol. 7, pp. 159–162; April, 1957.) Formulas are tabulated giving in convenient form the parameters of transistor networks for four types of feedback circuit.

621.372.54.029.64 58
**Design and Development of Strip-Line Filters**—E. H. Bradley. (IRE TRANS., vol. MTT-4, pp. 86–93; April, 1956. Abstract, PROC. IRE, vol. 44, p. 956; July, 1956.)

621.372.543.2:538.652 59
**Concentric-Shear-Mode 455-kc/s Electromechanical Filter**—R. W. George. (*RCA Rev.*, vol. 18, pp. 186–194; June, 1957.) An experimental filter of simplified design is described which consists of four magnetostrictive ferrite disk resonators.

621.372.55:621.396.4:621.376.3 60
**A Broad-Band Variable Group-Delay Equalizer**—R. Hamer and R. C. Wilkinson. (*P.O. Elec. Eng. J.*, vol. 50, Pt. 2, pp. 120–123; July, 1957.) The equalizer has been developed for use in fm microwave systems. It is inserted in the 70-mc IF signal path in long radio-relay systems. The performance is adequate for the transmission of frequency-division-multiplex telephony of at least 600 channels, or subcarrier color-television transmission.

621.373.029.64:538.569.4 61
**Comments on Frequency Pulling of Maser Oscillators**—C. H. Townes. (*J. Appl. Phys.*, vol. 28, pp. 920–921; August, 1957.) The physical origin is illustrated of the theoretically predicted reduction in frequency pulling with increasing number of beam molecules, and reasons are given for its failure to occur in practice.

621.373.029.64:538.569.4:538.221 62
**A Solid-State Microwave Amplifier and Oscillator using Ferrites**—M. T. Weiss. (*Phys. Rev.*, vol. 107, p. 317; July 1, 1957.) Experimental results obtained with an oscillator based on the proposal by Suhl (3076 of 1957). The active element is a piece of magnetized ferrite at room temperature.

621.373.421 63
**Sensitivity of a Self-Excited Oscillator**—I. S. Shpigel', M. D. Raĭzer, and E. A. Myae. (*Zh. Tekh. Fiz.*, vol. 27, pp. 387–390; February, 1957.) Theoretical and experimental investigation of the characteristics of a tube feedback oscillator suitable for nuclear resonance detection.

621.373.5:621.396.621 64
**Crystal Oscillators in Communication Receivers**—A. G. Manke. (IRE TRANS., vol. PGVC-7, pp. 10–15; December, 1956. Abstract, PROC. IRE, vol. 45, p. 258; February, 1957.)

621.373.52:621.373.431.1 65
**Unijunction Transistor forms Flip-Flop**—E. Keonjian and J. J. Suran. (*Electronics*, vol. 30, pp. 165–167; September 1, 1957.) The construction and performance are described of a multivibrator circuit for a stable or monostable operation (see also 2878 of 1955). Its active element is the double-base diode, a 3-terminal $p$-$n$ junction device [see 3562 of 1956 (Suran)].

621.373.52.018.756 66
**Pulse Generator uses Junction Transistors**—E. J. Fuller. (*Electronics*, vol. 30, pp. 176–179; September 1, 1957.) A transistor circuit is described giving pulses of 1 to 10-$\mu$sec. duration at repetition rates of 50–5000 pulses per second with internal delays of 1–100 $\mu$sec.

621.373.52.018.78 67
**Distortion in Transistor Amplifiers**—P. Tharma. (*Mullard tech. Commun.*, vol. 3, pp. 62–64; March, 1957.) An analysis of the distortion in low-level grounded-emitter stages are due to input-circuit nonlinearity and to variations of collector-to-base current gain.

621.373.52.029.4 68
**Low-Frequency Transistor Oscillators**—L. G. Gripps. (*Mullard tech. Commun.*, vol. 3, pp. 44–58; March, 1957. *Electronic Applic. Bull.*, vol. 17, pp. 113–128; May, 1957.) Theoretical treatment of a junction-transistor oscillator for frequencies of a few kc. Frequency and amplitude stability, conversion efficiency and the conditions governing starting, are considered. A practical circuit design is derived and experimental results are given.

621.374.32 69
**Build-Up of Large Signals with Elimination of Reflections in Magnetostrictive Storage Lines**—D. Maeder. (*Z. angew. Math. Phys.*, vol. 8, pp. 326–327; July 25, 1957.) Greater reliability and increased storage capacity are obtained by substituting twelve energizing coils for the usual one. With this arrangement, a steel-wire delay line can be used. See also 2385 of 1957.

621.374.33:621.314.7 70
**A Transistor Gating Matrix for a Simulated Warfare Computer**—W. H. MacWilliams, Jr. (*Bell Lab. Rec.*, vol. 35, pp. 94–99; March, 1957.) Brief description of a circuit, devised in 1949, which used a matrix of 4×10 point-contact transistors. Amplification of signals was also achieved.

621.374.5 71
**Signal-Enhanced Delay Line**—T. I. Humphreys. (*Electronic Inds. Tele-Tech.* vol. 16, pp. 70–71, 167; August, 1957.) To maintain pulse shape the high-frequency response of the delay line described is improved by selective amplification.

621.374.5:621.396.962.3 72
**Pulse Compression**—R. Krönert. (*Nachr-Tech.*, vol. 7, pp. 148–152, 162; April, 1957.) A method is described for compressing frequency-modulated rf pulses, *i.e.*, shortening them and increasing their amplitude by passing them

through a delay-distortion network consisting of a chain of lattice quadripoles. The theory outlined is based on work by Cauer, published posthumously. Its practical application in the field of radar should result in higher resolving power for a given snr.

621.375:621.372.51 73
**Minimizing Mismatch Loss**—H. E. Hollmann. (*Electronic Inds. Tele-Tech.* vol. 16, pp. 74–75, 165; August, 1957.) Simple formulas and curves are given.

621.375.2+621.375.4 74
**Upper Limits of Output Power in Vacuum-Tube and Transistor A.C. Amplifiers**—L. M. Vallese. (*Commun. and Electronics*, no. 29, pp. 87–92; March, 1957.) Simple analysis and comparison based on idealized characteristics.

621.375.2 75
**Stacked Valve Circuits**—J. B. Earnshaw. (*Electronic Radio Eng.*, vol. 34, pp. 404–406; November, 1957.) An analysis by means of feedback theorems and modified equivalent circuits. Application of the method to the cascade amplifier and the cathode-follower circuits is given in detail.

621.375.2.029.3 76
**Single-Ended Push-Pull Output Stages**—(*Electronic Applic. Bull.*, vol. 17, pp. 81–106; May, 1957.) The development of low-dc-resistance pentodes and high-resistance moving-coil loudspeakers has made possible the construction of transformerless output stages several types of which are described. The paper is based on the work of W. Aschermann and J. Rodrigues de Miranda (see 3727 of 1957).

621.375.2.029.4 77
**A Low-Frequency Selective Amplifier**—C. K. Battye. (*J. Sci. Instr.*, vol. 34, pp. 263–265; July, 1957.) The frequency is variable in steps from 1 to 1000 cps. The selectivity can be set up to $Q = 100$. The amplifier is dc coupled; a twin-T network shunted by a capacitor acts as a selective network in the negative feedback line.

621.375.2.029.55 78
**PT-15 P.A. Unit**—J. N. Walker. (*Short Wave Mag.*, vol. 14, pp. 624–630; February, 1957.) Description of a band-switching rf amplifier for 80, 40, and 20 m, which uses a pair of tubes Type PT 15 in parallel.

621.375.221.029.62:621.396.4:621.376.3 79
**A Broad-Band Intermediate-Frequency Amplifier for Use in Frequency-Modulation Microwave Radio-Relay Systems**—R. Hamer and C. H. Gibbs. (*P.O. Elec. Eng. J.*, vol. 50, Pt. 2, pp. 124–126; July, 1957.) A 70-mc amplifier is described which is suitable for the transmission of 600-channel frequency-division-multiplex telephony or subcarrier color-television signals in fm microwave radio-relay systems. A test-tone/noise ratio of 70 db is not significantly degraded after transmission through five amplifiers in tandem.

621.375.227.029.3 80
**400-Watt Audio Amplifier**—G. R. Woodville. (*Wireless World*, vol. 63, pp. 543–546; November, 1957.) The circuit described includes small output tubes in parallel push-pull connection.

621.375.3 81
**Self-Balancing Magnetic Amplifiers of the Differential-Feedback Type**—W. A. Geyger. (*Commun. and Electronics*, no. 29, pp. 39–46; March, 1957.) A 60-cps magnetic amplifier for extending the range of a moving-coil ink recorder is described.

621.375.4.029.3:629.13 82
**The Use of Transistors in Airborne Audio Equipment**—V. P. Holec. IRE TRANS., vol. AU-4, pp. 90–93; July/August, 1956. Abstract, PROC. IRE, vol. 44, p. 1641; November, 1956.)

621.375.43.029.3:621.314.7 83
**Negative-Feedback Transistor Amplifiers**—H. R. Lowry. (*Radio Ü Telev. News*, vol. 57, pp. 55–58, 109; May, 1957.) Design data are given for high-fidelity af amplifiers.

621.375.9.029.64:538.569.4 84
**Microwave Amplification by MASER Techniques**—W. V. Smith. (*IBM J. Res. Devel.*, vol. 1, pp. 232–238; July, 1957.) Elementary analysis of maser operation, including its application to wide-band, short-transit-time amplification.

621.376:621.316.7.078 85
**Demodulator-Limiter for Control System Signals**—N. L. Johanson. (*Electronics*, vol. 30, p. 155; September 1, 1957.) Description of transistor circuit for automatic control systems which acts as limiter during modulation or demodulation.

621.376.239 86
**Magnetically Keyed, Phase-Sensitive Demodulators**—R. B. Mark, W. X. Johnson, and P. R. Johannessen. (*Commun. and Electronics*, no. 29, pp. 1–6; March, 1957.) The operation and performance of a pulse-shaping circuit using magnetic reactors is described. The properties of three types of phase-sensitive demodulator are compared. Diode demodulators have linear characteristics, magnetic amplifier demodulators have high input impedance, and transistor demodulators combine good linearity with low noise level.

621.376.4:621.314.7 87
**Transistorized Phase Discriminators**—A. N. De Sautels. (*Commun. and Electronics*, no. 29, pp. 19–26; March, 1957.) Half-wave and full-wave phase discriminators are described with two- or three-terminal dc outputs. An analysis of the operating characteristics of transistors in discriminator circuits is given; temperature stability and power limitations are discussed.

## GENERAL PHYSICS

535.33–1 88
**Interferometry for the Far Infrared**—J. Strong. (*J. Opt. Soc. Amer.*, vol. 47, pp. 354–357; May, 1957.)

535.61–1 89
**Infrared Radiation and its Detection**—(*Electronic Radio Eng.*, vol. 34, pp. 412–415; November, 1957.) A comparison of the sensitivity and time constant of available detectors of infrared radiation. Thermal detectors of thermocouple, bolometer, and pneumatic type and photoelectric detectors are discussed.

537.311.1:536.21:537.311.33 90
**The Lorenz Number**—P. J. Price. (*IBM J. Res. Devel.*, vol. 1, pp. 147–157; April, 1957.) The theory of the Lorenz number of a conducting crystal is developed for the "band" and "one-electron" models of the electron assembly. With certain approximations, the Lorenz number is found to be equal to the mean square fluctuation of the thermoelectric power.

[537.311.1+536.212.2]:539.13 91
**Some Scattering Problems in Conduction Theory**—P. G. Klemens. (*Can. J. Phys.*, vol. 35, pp. 441–450; April, 1957.) An expression derived for the scattering of electrons by inhomogeneous slowly varying strain fields is applied to scattering by dislocations and stacking faults.

537.5 92
**Free-Path Formulae for the Coefficient of Diffusion and Velocity of Drift of Electrons in Gases**—L. G. H. Huxley. (*Aust. J. Phys.*, vol. 10, pp. 118–129; March, 1957. Correction, *ibid.*, vol. 10, p. 329; June, 1957.)

537.5:538.6 93
**Type of Plasma Oscillations in a Magnetic Field**—S. I. Braginski. (*Dokl. Ak. Nauk S.S.S.R.*, vol. 115, pp. 475–478; July 21, 1957.) Mathematical analysis based on a model of ideal electron and ion gases.

537.5:538.63 94
**Free-Path Formulae for the Electronic Conductivity of a Weakly Ionized Gas in the Presence of a Uniform and Constant Magnetic Field and a Sinusoidal Electric Field**—L. G. H. Huxley. (*Aust. J. Phys.*, vol. 10, pp. 240–245; June, 1957.) "A general free path formula is given for the drift velocity of electrons in a weakly ionized gas in a sinusoidal electric field. Most special cases of interest, including the magnetic deflection of an electron stream in a gas, are readily derivable from the general formula. The results find application in microwave and ionospheric studies of the motion of electrons in gases as well as in experiments on the magnetic deflection of an electron stream." See also 92 above.

537.525.8 95
**Oscillations in Direct-Current Glow Discharges**—A. M. Pilon. (*Phys. Rev.*, vol. 107, pp. 25–27; July 1, 1957.) Experimental results are given concerning the stable oscillations with the same period which occur in the current and in the light emitted by the positive column.

538.244.2 96
**Magnetization in the Presence of Magnetic Viscosity**—M. I. Rozovski. (*Zh. Tekh. Fiz.*, vol. 27, pp. 355–359; February, 1957.) A mathematical expression is derived for solving problems of magnetization of magnetically viscous samples, in particular those of cylindrical shape. See also 3697 of 1956 (Tikhonov and Samarski).

538.566:535.42 97
**Diffraction of Electromagnetic Waves by Ribbon and Slit: Part 1**—Y. Nomura and S. Katsura. (*J. phys. Soc. Japan*, vol. 12, pp. 190–200; February, 1957.) Rigorous solutions are presented for a wave incident on a plane normal to the edge of the ribbon or slit, but with arbitrary angles of incidence and polarization. For diffraction by circular plate and hole, see 3235 of 1955.

538.566:535.422]+534.26 98
**Diffraction of a Spherical-Wave Pulse by a Half-Plane Screen**—J. R. Wait. (*Can. J. Phys.*, vol. 35, pp. 693–696; May, 1957.) Fourier-integral treatment for a point source.

538.569.4 99
**Distortions of Magnetic Resonances by Additional and Excessive Oscillatory Fields**—H. R. Lewis, A. Pery, W. Quinn, and N. F. Ramsey. (*Phys. Rev.*, vol. 107, pp. 446–449; July 15, 1957.) A theoretical explanation is given of the shift of the resonance frequency which occurs as a result of the presence of an extraneous rf electric field. See also 1386 of 1956 (Ramsey).

538.569.4:539.15.098 100
**The Dependence of the Amplitude of the First Harmonic of Nuclear-Magnetic-Resonance Absorption on the Amount of Detuning**

—I. S. Shpigel', M. D. Raizer, and E. A. Myae. (*Zh. Tekh. Fiz.*, vol. 27, pp. 351–354; February, 1957.)

538.569.4:546.171.1 101
**Equivalence between the Line Width and the Rate of Energy Relaxation in the Inversion Spectrum of Ammonia**—K. Tomita. (*Progr. theoret. Phys.*, vol. 17, pp. 513–515; March, 1957.)

538.6 102
**On the Equilibrium Configurations of Oblate Fluid Spheroids under the Influence of a Magnetic Field**—S. P. Talwar. (*Proc. nat. Inst. Sci. India*, Pt. A, vol. 22, pp. 316–323; September 26, 1956.)

538.6 103
**Toroidal Oscillations of a Spherical Mass of Viscous Conducting Fluid in a Uniform Magnetic Field**—K. Stewartson. (*Z. angew. Math. Phys.*, vol. 8, pp. 290–297; July, 25 1957.) See also 3352 of 1956.

539.1:541.124 104
**Theoretical Treatment of the Kinetics of Diffusion-Limited Reactions**—T. R. Waite. (*Phys. Rev.*, vol. 107, pp. 463–470; July 15, 1957.) The diffusion-limited reaction $A+B \rightarrow AB$ has been solved for a random initial distribution of $A$ and $B$ particles.

## GEOPHYSICAL AND EXTRATERRESTRIAL PHENOMENA

523.16:551.510.535 105
**Radio-Star Ridges**—M. Dagg. (*J. Atmos. Terr. Phys.*, vol. 11, no. 2, pp. 118–127; 1957.) The distinctive amplitude variations known as "ridges" can probably be explained in terms of divergent-lens effects in the E region. See also 2058 of 1956 (Wild and Roberts).

523.16:551.510.535 106
**A Consideration of Radio-Star Scintillations as Caused by Interstellar Particles Entering the Ionosphere: Part 1—Daily and Seasonal Variations of the Scintillation of a Radio Star. Part 2—The Accretion of Interstellar Particles as a Cause of Radio-Star Scintillations**—G. A. Harrower. (*Can. J. Phys.*, vol. 35, pp. 512–535; May, 1957.) An analysis is made of measurements of scintillations of the rf source in Cassiopeia recorded at Ottawa during 1954 at a frequency of 50 mc. The data show certain daily maxima occurring at solar times dependent on the date of the year and grouped unsymmetrically in a way which suggests that they are due to the infall of interstellar particles from outside the solar system. The velocities of certain of these particles are derived by simple applications of vector addition employing the known velocity of the earth. See 2116 of 1957.

523.16:621.396.677.8 107
**The Mullard Radio Astronomy Observatory, Cambridge**—M. Ryle. (*Nature, London*, vol. 180, pp. 110–112; July 20, 1957.) The observatory was formally opened in July, 1957. Two instruments then under construction were a radio-star interferometer for 1.7 mλ, and a pencil-beam system for investigating continuous galactic radiation at 7.9 mλ. The aperture synthesis technique applied in the two systems is described. See also 3749 of 1957.

523.16:621.396.677.833 108
**World's Largest Radio Telescope**—(*Overseas Eng.*, vol. 31, pp. 15–18; August, 1957.) An illustrated description of the design and construction of the 250-foot fully steerable paraboloid of the Jodrell Bank instrument with details of the driving system and drive control equipment.

523.5 109
**The Distribution of the Orbits of Sporadic Meteors**—A. A. Weiss. (*Aust. J. Phys.*, vol. 10, pp. 77–102; March, 1957.) Radio observations at Adelaide during 1952–1956, are analyzed. A distribution of orbits is derived which is consistent with radar and visual observations in the northern hemisphere.

523.5:621.396.11.029.62 110
**Variations in the Intrinsic Strength of the 1956 Quadrantid Meteor Shower**—C. O. Hines and E. L. Vogan. (*Can. J. Phys.*, vol. 35, pp. 703–711; June, 1957.) Analysis of the occurrence rate of meteoric signals detected on a vhf forward-scatter east-west path in Canada. See also 3392 of 1955 (Forsyth and Vogan).

523.5:621.396.11.029.62:551.510.535 111
**A Theory of Long-Duration Meteor-Echoes based on Atmospheric Turbulence with Experimental Confirmation**—L. A. Manning and V. R. Eshleman. (*J. Geophys. Res.*, vol. 62, pp. 367–371; September, 1957.) Comments on 1417 of 1957 (Booker and Cohen). The experimental evidence is examined with the conclusion that the theory does not accurately represent the properties of meteoric echoes.

523.5:621.396.96 112
**Meteor Activity in the Southern Hemisphere**—A. A. Weiss. (*Aust. J. Phys.*, vol. 10, pp. 299–309; June, 1957.) Activity and radiants of meteor showers are discussed and compared with similar data for the northern hemisphere. See also 109 above and 2938 of 1955.

523.74:551.510.535 113
**Ionospheric Indices of Solar Activity**—W. J. G. Beynon and G. M. Brown. (*J. Atmos. Terr. Phys.*, vol. 11, no. 2, pp. 128–131; 1957.) It is suggested that a simple index based on E-layer measurements at a single station is adequate, and that the additional effort required to provide the index $I_F$ based on $F_2$-layer measurements at three stations is not justified. See also 1397 of 1956 (Minnis).

523.75 114
**Observation of a New Type of Flare**—R. J. Bray, R. E. Loughhead, V. R. Burgess, and M. K. McCabe. (*Aust. J. Phys.*, vol. 10, pp. 319–323; June, 1957.) A mass of very bright material was ejected from a flare about 28° from the sun's limb. Except for the velocity, the mass possessed all the properties of a small flare.

550.372 115
**The Effective Electrical Constants of Soil at Low Frequencies**—J. R. Wait. (PROC. IRE, vol. 45, pp. 1411–1412; October, 1957.) A possible explanation is presented for the large apparent dielectric constants ($\approx 10^3$) which occur at frequencies of the order of 15 kc.

550.389.2 116
**I. G. Y. Rocket Program**—N. W. Spencer. (*Sci. Mon.*, vol. 85, pp. 130–142; September, 1957.) An outline of the work of the IGY subcommittee of the U.S. Technical Panel for Rocketry. A table is given listing organizations participating and their objectives.

551.510.52:551.510.535 117
**A Possible Troposphere-Ionosphere Relationship**—S. J. Bauer. (*J. Geophys. Res.*, vol. 62, pp. 425–430; September, 1957.) A relation is suggested between $F_2$-layer characteristics and the passage of meteorological fronts through the troposphere. An hypothesis for dynamical coupling between the two regions is outlined.

551.510.53 118
**Electric Field Measurements in the Stratosphere**—C. G. Stergis, G. C. Rein, and T. Kangas. (*J. Atmos, Terr. Phys.*, vol. 11, no. 2, pp. 77–82; 1957.) Above the exchange layer the field decreases monotonically up to the limit (90,000 feet) of measurements made in 1955 and 1956. The measured and calculated values are in good agreement.

551.510.53:551.594.21 119
**Electric Field Measurements above Thunderstorms**—C. G. Stergis, G. C. Rein, and T. Kangas. (*J. Atmos. Terr. Phys.*, vol. 11, no. 2, pp. 83–90; 1957.) In measurements at heights of 70,000 to 90,000 feet above central Florida a positive upward-flowing current of about 1.3 a was found.

551.510.535 120
**Models of the Lower Ionosphere as may be Inferred from Absorption Results**—P. Bandyopadhyay. (*Indian J. Phys.*, vol. 31, pp. 297–308; June, 1957.) Values of deriative and nondeviative absorption and their variations with cos χ are calculated for the D-region models of Nertney (2306 of 1953), Piggott (unpublished), and Mitra (see 2087 of 1954) and for the E-region model of Jones (1661 of 1955). Satisfactory agreement with experimental results is found for Mitra's model of the D region but not for Jones's model of the E region.

551.510.535 121
**A Study of "Spread-F" Ionospheric Echoes at Night at Brisbane: Part 3—Frequency Spreading**—D. G. Singleton. (*Aust. J. Phys.*, vol. 10, pp. 60–76; March, 1957.) Diurnal and seasonal variations in spreading of the penetration frequency are compared with similar world-wide data. The observations are interpreted in terms of scattering from clouds of enhanced ionization near the $F_2$-layer maximum and a seasonal vertical movement of these clouds is suggested, the extent of which increases with latitude. Parts 1 and 2: 119 of 1957 (McNicol, *et al.*).

551.510.535 122
**Severe Ionospheric Storm**—(*Wireless World*, vol. 63, p. 553; November, 1957.) Notes on the disturbances of August 29–September 6, 1957.

551.510.535:523.75:621.396.11.029.62 123
**Disturbances in the Lower Ionosphere Observed at V.H.F. following the Solar Flare of 23 February 1956 with Particular Reference to Auroral-Zone Absorption**—D. K. Bailey. (*J. Geophys. Res.*, vol. 62, pp. 431–463; September, 1957.) The effects of the flare on ionospheric-scatter links in the band 30–40 mc at high latitudes are reported. An abrupt increase in oblique-incidence signal intensity, occurring almost simultaneously with the arrival of cosmic rays, was followed during the next three days by abnormally high levels at night and low levels during the day. Background cosmic noise measurements showed increased absorption at night and greatly increased absorption during daylight. The penetration into the D region of moderately heavy solar atomic ions is suggested as an explanation of the absorption phenomena.

551.510.535:523.78 124
**Solar Eclipse of 30th June 1954 and its Effect upon the Ionosphere**—S. N. Mitra. (*Indian J. Phys.*, vol. 31, pp. 309–323; June, 1957.) The investigations at Delhi reported include vertical-incidence ionospheric measurements, the recording of variations of sw and mf signals, and the recording of solar noise on 204 mc. Evidence of three distinct "corpuscular eclipses" was obtained both on the ionization density of the F layer and on the absorption in the nondeviating region. These were found to occur 2, 4, and $6\frac{1}{2}$ hours before the optical eclipse. Theoretical arguments and past observations indicate that these corpuscular

emissions may have originated from the so-called M region of the sun.

551.510.535:523.78:621.396.11 125
**Ionospheric Research**—A. P. Dale. (*RSGB Bull.*, vol. 32, pp. 499–501; May, 1957.) Note on signal-strength changes during the annular solar eclipse on December 25, 1954, and the control days for transmitters both in South Africa and in other countries.

551.510.535:550.385 126
**Disturbances in the $F_1$ and E Regions of the Ionosphere Associated with Geomagnetic Storms**—T. Sato. (*J. Geomag. Geoelect.*, vol. 9, pp. 57–60; March, 1957.) The E- and $F_1$-layer variations which occur during geomagnetic disturbances are examined for different phases of the solar cycle and for a number of latitudes. The data are discussed in relation to the electron drifts associated with geomagnetic disturbances. See also 127 below.

551.510.535:550.385 127
**Disturbances in the Ionospheric $F_2$ Region associated with Geomagnetic Storms: Part 2—Middle Latitudes**—T. Sato. (*J. Geomag. Geoelect.*, vol. 9, pp. 1–22; March, 1957.) Disturbances at middle latitudes are divided into negative and positive types, characteristic of high and low latitudes, respectively. These results are discussed in terms of vertical drift of electrons and the disturbance daily variations in the geomagnetic field. The bearing of the *Sq* dynamo current on seasonal and latitude variations of disturbances is discussed. Part 1: 3139 of 1957.

551.510.535:621.396.812.3 128
**Ionospheric Irregularities Causing Random Fading of Very Low Frequencies**—Bowhill. (See 251.)

551.510.535:621.396.9:523.3 129
**Ionospheric Studies by the Lunar Technique**—B. C. Blevis. (*Nature, London*, vol. 180, pp. 138–139; July 20, 1957.) Equipment operating near Ottawa comprises a 10-kw 488-mc transmitter, keyed "on" for 2 seconds and "off" for 4 seconds, feeding a 28-foot paraboloid via a horn, and orthogonal dipoles with a similar reflector feeding a dual-conversion receiver (IF 32 and 4 mc). Synchronous detection is used to give an af output signal equal in frequency to the Doppler shift of the signal reflected from the moon. Preliminary results indicate the presence of fading due to libration, long- and short-period Faraday rotation, and long-term fading without Faraday rotation.

551.594.21/.25 130
**The Electrification of Precipitation and Thunderstorms**—R. Gunn. (Proc. IRE, vol. 45, pp. 1331–1358; October, 1957.) A review article. Cosmic rays, radioactivity, and other agencies produce ion pairs which are transferred to cloud droplets or ice crystals and establish a droplet charge distribution greatly influenced by differences in conductivity for positive and negative ions. Rain formed from these droplets may be electrified, usually both positive and negative drops being present. Processes are considered which charge this rain and may eventually lead to a lightning stroke. The conditions necessary to establish gross free charge distributions by regeneration are specified and shown to be met under frequently occurring meteorological situations. Forty-seven references.

551.594.5 131
**Rotational Temperatures Measured in Aurorae at Churchill, Manitoba**—R. Montalbetti. (*Can. J. Phys.*, vol. 35, pp. 831–836; August, 1957.) The measurements indicate there is no latitude effect. A vertical temperature gradient of 6°K/km is deduced. See also 3871 of 1957 (Montalbetti and Jones).

551.594.6:523.745 132
**A Study of the Audio-Frequency Radio Phenomenon Known as "Dawn Chorus"**—G. McK. Allcock. (*Aust. J. Phys.*, vol. 10, pp. 286–298; June, 1957.) Experimental evidence supports the hypothesis that "dawn chorus" signals are generated by the entry into the ionosphere of clouds of positively charged particles of solar origin. Propagation appears to take place in the extraordinary magnetoionic mode along the earth's magnetic lines of force.

## LOCATION AND AIDS TO NAVIGATION

621.396.932 133
**Electronic Clock-Coder for Marine Radio Beacons**—A. C. MacKellar and A. J. B. Baty. (*Brit. Commun. Electronics*, vol. 4, pp. 476–477; August, 1957.) Crystal control is used to give more reliable service.

621.396.932.2 134
**The TALBE: a V.H.F. C.W. Radio Aid for Air/Sea Rescue**—W. Kiryluk. (*J. Brit. IRE*, vol. 17, pp. 489–500; September, 1957.) Describes the development and construction of a "talk-and-listen beacon," together with prior work on an unmodulated dinghy transmitter.

621.396.932.2 135
**An Introduction to Radio Aids to Air/Sea Rescue**—G. W. Hosie. (*J. Brit. IRE*, vol. 17, pp. 481–488; September, 1957.) Developments since 1940, are surveyed, and the mf, cw, and vhf radar beacons in general use during the war are discussed, together with post-war equipment. A crystal-controlled vhf beacon of low duty cycle is suggested, and also a crash location beacon.

621.396.962.3:621.374.5 136
**Pulse Compression**—Krönert. (See 72.)

621.396.965.8 137
**Optimizing the Dynamic Parameters of a Track-While-Scan System**—J. Sklansky. (*RCA Rev.*, vol. 18, pp. 163–185; June, 1957.)

## MATERIALS AND SUBSIDIARY TECHNIQUES

535.215:546.48.241.1 138
**Preparation and Photoconductive Properties of Cadmium Telluride Films**—G. G. Kretschmar and L. E. Schilberg. (*J. Appl. Phys.*, vol. 28, pp. 865–867; August, 1957.) A thin film gave a high dark resistance, falling by 10 to 200 times with 2-foot candle illumination. A film prepared in indium vapor gave a dark resistance of 1–10 mΩ falling to a few hundred kΩ.

535.37 139
**Critical Comment on a Method for Determining Electron Trap Depths**—C. H. Haake. (*J. Opt. Soc. Amer.*, vol. 47, pp. 649–652; July, 1957.) "A critical analysis of Garlick and Gibson's method (3421 of 1948) based on a mathematical determination of the applicable temperature range and on experimental evidence shows that the trap depths obtained are lower than those found by other methods. Especially the frequency-of-escape constants calculated subsequently contrast strongly to those determined by separate measurements."

535.37 140
**Energy Transport by Cascade and Resonance Processes in Doubly Activated Phosphors**—E. W. Claffy and C. C. Klick. (*J. Electrochem. Soc.*, vol. 104, pp. 445–447; July, 1957.)

535.376 141
**Review of Articles on Luminescence for 1955–1956**—G. R. Fonda. (*J. Electrochem. Soc.* vol. 104, pp. 524–530; August, 1957.) Review covering articles published in English, German, and French. One-hundred and fifty-six references.

535.376:546.472.21 142
**Electroluminescence of ZnS Single Crystals**—G. F. Neumark. (*Sylvania Technologist*, vol. 10, pp. 29–34; April, 1957.) Electroluminescence in ZnS depends on the number and type of traps in the crystal. Impact ionization appears to be the predominant mechanism for the excitation. Thirty-one references.

537.226/.228.1:546.431.824–31:534.232 143
**An Investigation of some Barium Titanate Compositions for Transducer Applications**—D. Schofield and R. F. Brown. (*Can. J. Phys.*, vol. 35, pp. 594–607; May, 1957.) The addition of Co to 5 per cent Ca, 95 per cent Ba titanate compositions, produces a large reduction in the dielectric loss in high electric fields without significant effect on the piezoelectric characteristics. Preliminary results were given earlier (3160 of 1957).

537.226/.227:534.1.087 144
**The Use of Ferroelectric Ceramics for Vibration Analysis**—R. C. Kell, G. A. Luck, and L. A. Thomas. (*J. Sci. Instr.*, vol. 34, pp. 271–274; July, 1957.)

537.227:546.431.824–31 145
**Preparation of $BaTiO_3$ Single Crystals in Coal Gas Atmosphere**—K. Kawabe and S. Sawada. (*J. phys. Soc. Japan*, vol. 12, p. 218; February, 1957.)

537.227:546.431.824–31 146
**Heating Effects in Single Crystal Barium Titanate**—D. S. Campbell. (*J. Electronics Control*, vol. 3, pp. 330–338; September, 1957.) The coercive field inccreases with frequency up to a certain limiting frequency above which it falls due to heating effects. This gives a criterion for the maximum frequency at which crystals can be expected to operate in a matrix storage system.

537.227:546.431.824–31 147
**Quasi-static Hysteresis in Barium-Titanate Single Crystals**—K. Zen'iti, K. Husimi, and K. Kataoka. (*J. phys. Soc. Japan*, vol. 12, p. 432; April, 1957.)

537.227:546.431.824–31 148
**On the 180°-Type Domain Wall of $BaTiO_3$ Crystal**—W. Kinase and H. Takahasi. (*J. phys. Soc. Japan*, vol. 12, pp. 464–476; May, 1957.) At room temperature the domain width is about $10^{-4}$ cm and its energy is 1.4 erg/cm² The structure of the domains and their reversing process are also discussed.

537.228.5:546.36 149
**Stark Effect on Caesium-133 Hyperfine Structure**—R. D. Haun, Jr and J. R. Zacharias. (*Phys. Rev.*, vol. 107, pp. 107–109; July 1, 1957.) The change of the hyperfine-structure separation energy caused by an electric field has been measured in $^{133}Cs$ by the atomic-beam magnetic-resonance method and is compared with other experimental and theoretical data.

537.311.33 150
**Generation of an E.M.F. in Semiconductors with Nonequilibrium Current Carrier Concentrations**—J. Tauc. (*Rev. mod. Phys.*, vol. 29, pp. 308–324; July, 1957.) A general formulation of the problem is presented. Solutions are obtained for two special cases for which the impurity-concentration change occurs over a distance either long or short

compared with the diffusion length of current carriers; these are bulk and barrier-layer photovoltaic effects, respectively. Practical implications are discussed. One-hundred and two references.

537.311.33 151
**Statistics of the Charge Distribution for a Localized Flaw in a Semiconductor**—W. Shockley and J. T. Last. (*Phys. Rev.*, vol. 107, pp. 392–396; July 15, 1957.) The charge situation is described by a set of energy levels which are independent of the Fermi level but are temperature-dependent. The charge of the flaw increases by one electron unit of negative charge as the Fermi level is raised successively above each level of the set and, conversely, as it is lowered.

537.311.33 152
**Scattering of Current Carriers in Semiconductors with Ionic Type of Bond**—T. A. Kontorova. (*Zh. Tekh. Fiz.*, vol. 27, pp. 269–274; February, 1957.) The scattering of carriers in the optical and acoustic modes is investigated and their free path is calculated. Approximate formulas for the carrier mobility are derived. The dependence of mobility on temperature is examined.

537.311.33 153
**High-Frequency Relaxation Processes in the Field-Effect Experiment**—C. G. B. Garrett. (*Phys. Rev.*, vol. 107, pp. 478–487; July 15, 1957.) A theoretical treatment is given of two dispersion phenomena in the semiconductor field-effect experiment [see, *e.g.*, 3532 of 1951 (Montgomery)]: 1) dispersion arising from the finite time required to generate minority carriers, and 2) relaxation of the fast surface states.

537.311.33:538.632 154
**On the Electrical Properties of Degenerate Semiconductors**—E. Haga. (*J. phys. Soc. Japan*, vol. 12, p. 217; February, 1957.) Theoretical derivation of quantitative data on resistivity and the Hall coefficient.

537.311.33:538.632 155
**Resistivity and Hall Coefficient of Semiconductors**—K. Shogenji and S. Uchiyama. (*J. phys. Soc. Japan*, vol. 12, p. 434; April, 1957.) Calculations assuming scattering of current carriers by acoustic and optical modes of lattice vibration, but neglecting scattering by impurity centers.

537.311.33:546.23:621.314.6 156
**The Surface Potential of Selenium and its Relation to the Rectification and the Photovoltaic Effects**—U. Yoshida and A. Suzuki. (*J. phys. Soc. Japan*, vol. 12, pp. 459–463; May, 1957.) The changes with time of the surface potential and the rectification ratio after heat treatment are reduced by coating with a thin film of synthetic resin.

537.311.33:546.24 157
**Electrical Properties of Tellurium at the Melting Point and in the Liquid State**—A. S. Epstein, H. Fritzsche, and K. Lark-Horovitz. (*Phys. Rev.*, vol. 107, pp. 412–419; July 15, 1957.) The experimental results show that semiconductor properties persist in the liquid state, but as the temperature is raised a gradual transition to metallic behavior occurs.

537.311.33:546.27 158
**Electrical Properties of Boron Single Crystals**—W. C. Shaw, D. E. Hudson, and G. C. Danielson. (*Phys. Rev.*, vol. 107, pp. 419–427; July 15, 1957.) The electrical resistivity, Hall coefficient, and thermoelectric power of microscopic crystals have been measured as functions of temperature. A value of $1.55 \pm 0.05$ ev is deduced for the energy gap.

537.311.33:546.28+546.289 159
**Expansions in Reactor Irradiated Germanium and Silicon**—M. C. Wittels. (*J. Appl. Phys.*, vol. 28, p. 921; August, 1957.) The lattice expansions observed were greater in Ge than Si, as expected from theory. The retained damage in Ge was dependent on the irradiation temperature.

537.311.33:546.28 160
**Donor Electron Spin Relaxation in Silicon**—E. Abrahams. (*Phys. Rev.*, vol. 107, pp. 491–496; July 15, 1957.) The effects of spin-orbit coupling on the relaxation time for donor electron spins are considered.

537.311.33:546.28 161
**Damage to Silicon Produced by Bombardment with Helium Ions**—U. F. Gianola. (*J. Appl. Phys.*, vol. 28, pp. 868–873; August, 1957.) Helium ions at $3 \times 10^4$ ev were used. The surface layer was found to be converted to a quasi-stable amorphous form, which becomes partially crystalline on annealing. The amorphous material is soluble in aqueous hydrofluoric acid and has about 1/10th the thickness of the affected Si.

537.311.33:546.28 162
**Oxygen Content of Silicon Single Crystals**—W. Kaiser and P. H. Keck. (*J. Appl. Phys.*, vol. 28, pp. 882–887; August, 1957.) The oxygen content of pulled Si crystals is correlated with the infrared absorption at 9 microns. Methods of altering the oxygen concentration are discussed.

537.311.33:546.289 163
**Study of the Minority-Carrier Mobility in Germanium**—M. Shtenbek and P. I. Baranski. (*Zh. Tekh. Fiz.*, vol. 27, pp. 221–232; February, 1957.) Report of investigation on *n*-type single-crystal Ge. The transit time, the mobility, and the coefficients of longitudinal and transverse diffusion of minority carriers are calculated.

537.311.33:546.289 164
**Experimental Investigation of the Correlation between Peltier Effect and Thermo-e.m.f. in Germanium**—M. Shtenbek and P. I. Baranski. (*Zh. Tekh. Fiz.*, vol. 27, pp. 233–237; February, 1957.) This correlation is investigated in the impurity and intrinsic conduction bands for samples of *n*- and *p*-type Ge of differing specific resistance.

537.311.33:546.289 165
**Nature of Recombination Centres in Germanium Originated by Low-Temperature Heat Treatment**—T. V. Mashovets and S. M. Ryvkin. (*Zh. Tekh. Fiz.*, vol. 27, pp. 238–241; February, 1957.) See also 2794 of 1956.

537.311.33:546.289 166
**Probability of Capture by Carrier Recombination at Frenkel-Type Defects in n-Type Germanium**—L. S. Smirnov and V. S. Vasilov. (*Zh. Tekh. Fiz.*, vol. 27, pp. 427–429; February, 1957.) Bombardment of Ge crystals with electrons of energy over 500 kev produces at room temperature stable dislocations of crystal structure, called Frenkel defects, corresponding to several levels in the forbidden zone, which act as effective recombination centers of holes and electrons.

537.311.33:546.289 167
**Electrical Properties of Nickel-Doped Germanium at Low Temperatures**—Y. Kanai and R. Nii. (*J. phys. Soc. Japan*, vol. 12, pp. 125–133; February, 1957.) Anomalous behavior was found at temperatures in the range 120–170°K, the resistivity increasing as the temperature was reduced. The electrical properties could be explained by use of the model proposed by Hung (*Phys. Rev.*, vol. 79, pp. 727–728; August 15, 1950.)

537.311.33:546.289 168
**Peripheral Inhomogeneities of the Alloyed Germanium *p-n* Junction**—M. Kikuchi. (*J. phys. Soc. Japan*, vol. 12, pp. 133–139; February, 1957.) The local photocurrent exhibits peaks, the positions of which depend on the bias voltage. A model for the junction is proposed.

537.311.33:546.289 169
**Observation of the Drift of Germanium Surface by Field-Effect Experiment**—M. Kikuchi. (*J. phys. Soc. Japan*, vol. 12, p. 436; April, 1957.) The surface conductance and photoconductance were measured at various time intervals after the etching of *n*-type Ge.

537.311.33:546.289 170
**Alloying Properties of Germanium Free of Edge Dislocations**—C. W. Mueller. (*RCA Rev.*, vol. 18, pp. 205–212; June, 1957.) The main factors involved in alloying In on dislocation-free Ge are considered. The controlled alloying method described gives extremely flat and uniform junctions.

537.311.33:546.289 171
**The Dissolution of Germanium by Molten Indium**—B. Goldstein. (*RCA Rev.*, vol. 18, pp. 213–220; June, 1957.) Experimental results of an investigation of dissolution as a function of crystal axis orientation, temperature, and amount of Ge already contained in the molten In solvent.

537.311.33:546.289 172
**Preferential Diffusion of Sb along Small-Angle Boundaries in Ge and the Dependence of this Effect on the Direction of the Dislocation Lines in the Boundary**—F. Karstensen. (*J. Electronics Control*, vol. 3, pp. 305–307; September, 1957.) Experiment shows that preferential diffusion occurs if the grain boundary contains dislocation lines parallel to the direction of diffusion, but does not occur if these are perpendicular to it.

537.311.33:546.289 173
**Diffusion of Antimony out of Germanium and some Properties of the Antimony-Germanium System**—R. C. Miller and F. M. Smits. (*Phys. Rev.*, vol. 107, pp. 65–70; July 1, 1957.) Experimental Sb distributions are shown to be consistent with a rate limitation or potential barrier at the Ge/ambient interface. Introduced external rate limitations provide data for calculating partition and sticking coefficients for the system and estimating the binding energy of Sb in Ge. See also 1478 of 1957.

537.311.33:546.289 174
**Distribution and Cross-Sections of Fast States on Germanium Surfaces in Different Gaseous Ambients**—A. Many and D. Gerlich. (*Phys. Rev.*, vol. 107, pp. 404–411; July 15, 1957.) Simultaneous measurements of surface recombination velocity and trapped charge density in the fast states as a function of surface potential show that the energy distribution of the fast states consists of four discrete sets of levels. Only one of these sets is significant in the recombination process.

537.311.33:546.289 175
**The Depth of Surface Damage Produced by Lapping Germanium Monocrystals**—D. Baker and H. Yemm. (*Brit. J. Appl. Phys.*, vol. 8, pp. 302–303; July, 1957.) The depth of damage is estimated from the variation of the effective diffusion distance of minority carriers as the disturbed layer is removed by etching.

537.311.33:546.289:534.13-8 176
**Ultrasonic Attenuation by Free Carriers in Germanium**—G. Weinreich. (*Phys. Rev.*, vol. 107, pp. 317–318; July 1, 1957.) The close re-

lationship with the acoustoelectric effect is noted and the amount of attenuation is predicted from the observed magnitude of this effect. See also 2499 of 1957 (Blatt).

537.311.33:546.289:537.32 177
**Magnetic Field Dependence of the Seebeck Effect in Germanium**—M. C. Steele. (*Phys. Rev.*, vol. 107, pp. 81–83; July 1, 1957.) The thermoelectric power of *n*-type Ge single crystals increases with magnetic field at temperatures from 78° to 278°K. The thermal conductivity is constant for magnetic fields between zero and 11500 oersteds.

537.311.33:546.289:538.6 178
**Investigation of Thermomagnetic Effects in *p*-Type Germanium**—I. V. Mochan, Yu. N. Obraztsov, and T. V. Krylova. (*Zh. Tekh. Fiz.*, vol. 27, pp. 242–259; February, 1957.) The transverse and longitudinal Nernst-Ettingshausen and Hall effects are measured on samples of *p*-type Ge of specific resistance 69 Ω cm at room temperature, in the impurity conduction band. In the temperature range 80°–240°K and a field of 5000 G the transverse Nernst-Ettingshausen effect appears to be due to hole transfer by phonons.

537.311.33:546.289:538.63 179
**On the Measurements of the Galvanomagnetic Effect in Semiconductors at Microwave Frequencies**—T. Fukuroi and M. Date. (*Sci. Rep. Res. Inst. Tohoku Univ., Ser. A.*, vol. 9, pp. 190–195; June, 1957.) The resonant cavity method is used to make measurements at 9800 mc at temperatures down to 1.5°K. The results obtained for the magnetoresistance of pure Ge are compared with those of Fritzche (153 of 1956).

537.311.33:546.289:538.632 180
**Galvanomagnetic Theory for *n*-Type Germanium and Silicon: Hall Theory and General Behaviour of Magnetoresistance**—L. Gold and L. M. Roth. (*Phys. Rev.*, vol. 107, pp. 358–364; July 15, 1957.) The magnetoresistance $\Delta\rho/\rho$, and Hall coefficient $R_H$ for *n*-type Ge and Si are calculated from the resistivity tensor. The angular dependence of $\Delta\rho/\rho$ is compared with experimental data. The field dependence of $\Delta\rho/\rho$ and of $R_H$ are considered for various current and field orientations.

537.311.33:546.289:539.1 181
**Diffusion-Limited Annealing of Radiation Damage in Germanium**—T. R. Waite. (*Phys. Rev.*, vol. 107, pp. 471–478; July 15, 1957.) The theory given in 104 above has been applied to experimental data [see, *e.g.*, 1469 of 1954 (Brown, *et al.*)]; reasonable agreement was found.

537.311.33:546.682.19:535.215 182
**Photoelectromagnetic Effect in Indium Arsenide**—J. R. Dixon. (*Phys. Rev.*, vol. 107, pp. 374–378; July 15, 1957.) Experimental studies on *n*- and *p*-type single crystals at room temperature are described. The dependence of the photoelectromagnetic short-circuit current on magnetic induction is consistent with the theory of Kurnick and Zitter (2429 of 1956). Bulk lifetimes are found to be about $6\times10^{-8}$ for *n*-type, and $5\times10^{-10}$ for *p*-type material; estimates of surface recombination velocity for *n*-type material are 0–$10^3$ cm for an etched surface, and $10^5$ cm for a ground surface.

537.311.33:621.3.049.7 183
**Technique for Connecting Electrical Leads to Semiconductors**—C. L. Anderson, H. Christensen, and P. Andreatch. (*J. Appl. Phys.*, vol. 28, p. 923; August, 1957.) Two techniques are described which give adhesion between certain soft metals and semiconductors at temperatures well below the eutectic point.

537.311.33:621.314.63 184
**Minority Carrier Lifetime in *p-n* Junction Devices**—M. Byczkowski and J. R. Madigan. (*J. Appl. Phys.*, vol. 28, pp. 878–881; August, 1957.) Minority-carrier lifetime is conveniently determined by studying the switching time in junction diodes. Some theoretical and experimental results are given.

537.533:546.883 185
**Electrostatic Emission from Tantalum Single Crystals**—N. A. Gorbatyĭ, L. V. Reshetnikova, E. P. Sytaya, and G. N. Shuppe. (*Zh. Tekh. Fiz.*, vol. 27, pp. 296–298; February, 1957.) Field emission patterns for Ta single crystals appear identical to those obtained for W and Mo.

538.22 186
**Effective Gyromagnetic Ratio for Triangular Ferrimagnetic States**—A. Eskowitz and R. K. Wangsness. (*Phys. Rev.*, vol. 107, pp. 379–380; July 15, 1957.)

538.22 187
**Magnetic Properties of Perovskites Containing Strontium: Part 1—Strontium-Rich Ferrites and Cobaltites**—H. Watanabe. (*J. phys. Soc. Japan*, vol. 12, pp. 515–522; May, 1957.) Magnetic susceptibilities and electrical conductivities for samples sintered in vacuo differ from those sintered in oxygen. An interpretation of experimental results is given.

538.22:538.569.4:546.763–31 188
**Antiferromagnetic Resonance in $Cr_2O_3$**—E. S. Dayhoff. (*Phys. Rev.*, vol. 107, pp. 84–91; July 1, 1957.) Theory and experimental data are given for the antiferromagnetic resonance spectrum of single-crystal $Cr_2O_3$ for 12-2.8 mmλ and magnetic field intensities from zero to 30,000 oersteds.

538.22:538.613 189
**Magnetography—the Microscopy of Magnetism**—F. G. Foster. (*Bell Lab. Rec.*, vol. 35, pp. 175–178; May, 1957.) The Kerr magneto-optical effect is applied to the microscopy of magnetic domain structure.

538.221 190
**Transverse Impedance Transformation for Ferromagnetic Media**—F. R. Morgenthaler. (PROC. IRE, vol. 45, p. 1407; October, 1957.) The transformation relates to media magnetized transversely, and is valid for $TE_{m0}$ modes with the magnetization in the *E*-field direction.

538.221 191
**Domain Wall Orientations in Silicon-Iron Crystals**—C. D. Graham, Jr., and P. W. Neurath. (*J. Appl. Phys.*, vol. 28, pp. 888–891; August, 1957.) The stable orientation of a 180° ferromagnetic domain wall in a cubic crystal is calculated and the results are compared with experimentally determined orientations.

538.221:538.122 192
**Experimental Investigation of the Magnetic Field Distribution due to Artificial Surface Defects in Ferromagnetic Substances**—N. N. Zatsepin. (*Zh. Tekh. Fiz.*, vol. 27, pp. 368–373; February, 1957.)

538.221:539.23 193
**Magnetization Reversal in Thin Films at Low Fields**—R. L. Conger and F. C. Essig. (*J. Appl. Phys.*, vol. 28, pp. 855–858; August, 1957.) Statistical theory is presented for reversing fields less than the anisotropy field under the assumption that reversal takes place by domain wall motion; experimental data supporting the theory are given. See also 1513 of 1957.

538.221:[621.318.124+621.318.134 194
**Dielectric Spectroscopy of Ferromagnetic Semiconductors**—P. A. Miles, W. B. Westphal, and A. von Hippel. (*Rev. mod. Phys.*, vol. 29, pp. 279–307; July, 1957.) Methods of measuring the electric and magnetic spectra, within the range from dc to optical frequencies, are described and results discussed. In addition to a general review some new experimental data including the rf spectra of a single-crystal Ni ferrite are presented.

538.221:[621.318.124+621.318.134 195
**On the Origin of the Magnetic Anisotropy Energy of Ferrites**—K. Yosida and M. Tachiki. (*Progr. Theoret. Phys.*, vol. 17, pp. 331–359; March, 1957.) The anisotropy energy for Ni ferrites comes mainly from $Fe^{3+}$ ions for magnetite from $Fe^{2+}$ and $Fe^{3+}$ ions and for Mn ferrites from $Fe^{3+}$ and $Mn^{3+}$ ions. The large anisotropy energy of Co ferrites arises from the pseudo-quadrupole and anisotropic exchange reactors among Co and Fe ions.

538.221:[621.318.124+621.318.134 196
**A Theory of the Uniaxial Anisotropy Induced by Magnetic Annealing in Ferrites**—S. Taniguchi. (*Sci. Rep. Res. Inst. Tohoku Univ., Ser. A*, vol. 9, pp. 196–214; June, 1957.)

538.221:621.318.134 197
**Magnetic and Magnetostrictive Properties of Magnesium-Nickel Ferrites**—P. O. Hoffmann. (*J. Amer. Ceram. Soc.*, vol. 40, pp. 250–252; July 1, 1957.) A study of mixed Ni-Mg ferrites of various compositions shows them to be inferior to Ni ferrite.

538.221:621.318.134 198
**Magnetic Properties and Associated Microstructure of Zinc-Bearing Square-Loop Ferrites**—G. G. Palmer, R. W. Johnston, and R. E. Schultz. (*J. Amer. Ceram. Soc.*, vol. 40, pp. 256–262; August 1, 1957.) A series of Mn-Mg ferrites in which Zn is substituted for Mg has been prepared and tested in a successful attempt to obtain a material having a lower coercive force and higher magnetic saturation than standard rectangular-loop ferrites used extensively in digital computers.

538.221:621.318.134:538.6 199
**Rotation of the Plane of Polarization in a Longitudinal Magnetic Field (Faraday Effect) in the Millimetre Wavelength Range**—D. I. Mash. (*Zh. Tekh. Fiz.*, vol. 27, pp. 360–363; February, 1957.) Results of tests on ferrites are summarized and discussed.

538.632 200
**Temperature Dependence of the Hall Coefficients in some Silver Palladium Alloys**—F. E. Allison and E. M. Pugh. (*Phys. Rev.*, vol. 107, pp. 103–105; July 1, 1957.)

666.1.037.5 201
**Fundamentals of Glass-to-Metal Bonding: Part 3—Temperature and Pressure Dependence of Wettability of Metals by Glass**—R. M. Fulrath, S. P. Mitoff, and J. A. Pask. (*J. Amer. Ceram. Soc.*, vol. 40, pp. 269–274; August 1, 1957.) Part 2: 3576 of 1957 (Mitoff).

## MATHEMATICS

512.25 202
**A Least-Squares Solution of Linear Equations with Coefficients Subject to a Special Type of Error**—J. K. Mackenzie. (*Aust. J. Phys.*, vol. 10, pp. 103–109; March, 1957.)

## MEASUREMENTS AND TEST GEAR

529.786+531.711 203
**The Units of Time and Length**—L. Essen. (*Nature, London*, vol. 180, pp. 137–138; July 20, 1957.) Difficulties in an ideal system using an atomic frequency standard to define the unit of time are discussed. A practical solution would be to define time in terms of the caesium

line and length in terms of the radiation of a suitable light source. A system in which time interval is based on an atomic unit and epoch on astronomical measurements has been satisfactory during two years of operation at the National Physical Laboratory.

529.786 204
**The Caesium Resonator as a Standard of Frequency and Time**—L. Essen and J. V. L. Parry. (*Phil. Trans. A.*, vol. 250, pp. 45–69; August 8, 1957.) The construction, operation, and testing of the standard are described. The present experimental model can be used to define frequency with a standard deviation of $\pm 1$ part in $10^{10}$. The design of a resonator with sharper reasonance less than 100 cps wide appears possible and should improve the definition. See also 2471 of 1956.

529.786:538.569.4 205
**Recent Developments in Measurement of Time**—C. H. Townes. (*Nuovo Cim.*, vol. 5, Supplement No. 1, pp. 222–229; 1957. In English.) The use of the molecular oscillator described in 100 of 1955 (Gordon, *et al.*) as a frequency standard is discussed.

621.3.018.41(083.74)+529.786]:538.569.4 206
**Precise Frequency of the 3,3 Inversion Line of Ammonia**—K. Shimoda. (*J. phys. Soc. Japan*, vol. 12, p. 558; May, 1957.)

621.3.018.41(083.74):621.385.029.6 207
**A New Microwave Frequency Standard by Quenching Oscillator Control**—N. Sawazaki and T. Honma. (IRE TRANS., vol. MTT-4, pp. 116–121; April, 1956. Abstract, PROC. IRE, vol. 44, pp. 956–957; July, 1957.)

621.317.1.087:519.24 208
**The Automatic Classification and Storage of Measurement Results**—H. J. Vogt and E. Zimmer. (*Elektronik*, vol. 6, pp. 191–197; July, 1957.) Description of methods and electronic equipment for use in the statistical analysis of manufacturing processes with particular reference to applications in the textile industry.

621.317.3:537.311.33 209
**Direct-Reading Minority-Carrier-Lifetime Measuring Apparatus**—A. R. Engler and C. J. Kevane. (*Rev. Sci. Instr.*, vol. 28, pp. 548–551; July, 1957.) The decay of optically injected excess minority carriers is compared with voltage decay in a *RC* circuit, and lifetimes ($>10$ $\mu$sec) are read directly from a calibrated dial.

621.317.3:538.63 210
**Geometrical Effects in Transverse Magnetoresistance Measurements**—J. R. Drabble and R. Wolfe. (*J. Electronics Control*, vol. 3, pp. 259–266; September, 1957.) "The effect of finite length-to-width ratio and of probe positions on measurements of resistivity in a transverse magnetic field is investigated for various Hall angles. Wick's method (3161 of 1954) is extended to include the case of measurements made between probes symmetrically placed at various distances from the ends. Graphs are included which give the fractional change of resistance for various probe positions and Hall angles for specimens of any length-to-width ratio greater than two."

621.317.3:538.632 211
**Experimental Use of Hall-Effect Linear Detector for Measurements**—V. N. Bogomolov and V. D. Vasil'ev. (*Zh. Tekh. Fiz.*, vol. 27, pp. 260–261; February, 1957.) The circuit described incorporates an *n*-type Ge plate as the Hall detector; an experimental application is briefly described.

621.317.3:621.314.63 212
**Measurements of Crystal Impedances at Low Levels**—H. N. Dawirs and E. K. Damon. (IRE TRANS., vol. MTT-4, pp. 94–96; April, 1956. Abstract, PROC. IRE, vol. 44, p. 956; July, 1956.)

621.317.3:621.314.7 213
**Transistor Tests Predict High-Frequency Performance**—R. L. Pritchard. (*Electronic Inds. Tele-Tech.*, vol. 16, pp. 62–63, 144; March, 1957.) Methods are described for measuring the alpha cutoff frequency, the ohmic base resistance and the collector-base capacitance from which parameters the high-frequency performance may be determined.

621.317.3:621.396.822:621.396.62.029.6 214
**Absolute Measurement of Receiver Noise Figures at U.H.F.**—E. Maxwell and B. J. Leon. (IRE TRANS., vol. MTT-4, pp. 81–85; April, 1956. Abstract, PROC. IRE, vol. 44, p. 956; July, 1956.)

621.317.331:621.316.993 215
**Measuring Earth Conductivity**—M. Strohfeldt. (*Electronic Radio Eng.*, vol. 34, pp. 425–427; November, 1957.) Measurements at an "ideal" site by radio methods gave a much lower value than those obtained by electrode methods. Some correlation exists between measurements by the two methods when applied to the variation of conductivity with distance.

621.317.335.3.029.64 216
**A Rod Method of Measuring Dielectric Constants. Application to $(NH_4)_2H_3IO_2$ at 3-cm Wavelength**—H. Gränicher and W. Schurter. (*Z. angew. Math. Phys.*, vol. 8, pp. 382–400; September 25, 1957.) A modified version of the method described by Le Bot and Le Montagner (2067 of 1953) was adopted to measure the complex permittivity of rod specimens. The experimental results are discussed.

621.317.34.029.63/.64 217
**Automatic Microwave Transmission Measuring Equipment**—J. B. Linker, Jr. and H. H. Grimm. (*Rev. Sci. Instr.*, vol. 28, pp. 559–563; July, 1957.) The phase of a 200-kc heterodyne is compared with that of a phase-coherent 200-kc reference source by a null-seeking servo phase discriminator, and loss is measured by a commercial ratio meter. A traveling-wave tube produces the phase-coherent 200-kc frequency offset which is passed through a waveguide containing the ferrite or other material to be measured.

621.317.343.029.6 218
**V.H.F. Line Measurements**—F. J. Charman. (*Electronic Eng.*, vol. 29, pp. 499–503; October, 1957.) A method is described of using a single loop directional coupler by which the impedance or admittance of an unknown load may be obtained graphically. The method is compared with that of the impedometer [155 of 1950 (Parzen)]; the parameters measured by the new device are not directly applicable to a Smith chart.

621.317.351:621.397 219
**Equipment for the Oscillographic Display of the Phase and Amplitude Characteristics of Video and I.F. Networks**—W. Kroebel and L. A. Wegner. (*Rundfunktech. Mitt.*, vol. 1, pp. 37–44; April, 1957.) In the equipment described parameters representing phase shift and amplitude distortion are displayed on two cr tubes as a function of modulation frequency in the range 0.1–6.0 mc, together with an electronically produced graticule. Special methods of phase measurements are described and some test results are reproduced.

621.317.353.1 220
**A New Method of Measuring Nonlinear Distortion**—O. Henkler. (*Nachr-Tech.*, vol. 7, pp. 145–147; April, 1957.) The "combination-factor" method outlined is more suitable, particularly for application to carrier-frequency systems, than the conventional distortion-factor and difference-tone methods. Two test signals of equal amplitude are used with a frequency difference depending on the application. The "combination factor" obtained is the ratio of the amplitude of a certain intermodulation product to that of one of the test signals.

621.317.382 221
**A Wide-Band Level-Measuring Set**—R. C. Bolt. (*A.T.E.J.*, vol. 13, pp. 151–156; April, 1957.) The instrument is suitable for power measurements at various input impedances, in the frequency range 200 cps–612 kc at levels from $-50$ to $+40$ db relative to 1 mw.

621.317.444:621.385 222
**Rectilinearity of Electron-Beam Focusing Fields from Transverse Component Determinations**—P. P. Cioffi. (*Commun. and Electronics*, no. 29, pp. 15–19; March, 1957.) An accurate method of measuring the transverse component of the magnetic focusing field using a small search coil is described. The longitudinal field component produced by errors in positioning of the coil is eliminated. For a description of the recording fluxmeter used, see 3174 of 1952.

621.317.733.025 223
**Component Testing Bridge**—C. D. Lindsay. (*Wireless World*, vol. 63, pp. 549–550; November, 1957.) Design of an ac comparator working at 50 cps.

621.317.755 224
**Calibrated D.C. Oscilloscope**—B. Pearce. (*Wireless World*, vol. 63, pp. 539–542; November, 1957.) Design details are given.

621.317.755:621.397.5 225
**Oscillographs for Television Work**—O. H. Davie. (*J. Telev. Soc.*, vol. 8, pp. 225–233; April/June, 1957.) A description of the design and application of ancillary equipment required when using a general-purpose oscilloscope for television measurements.

621.317.79.029.64 226
**A Focused Spectrometer for Microwave Measurements**—E. G. A. Goodall and J. A. C. Jackson. (*Marconi Rev.*, vol. 20, pp. 51–59; 2nd Quart., 1957.) Two variants of spectrometer are described for X-band frequencies. Measurements of transmission and reflection characteristics for incident angles of 15° to 70° on single sandwich-type radome samples are presented.

621.317.79.029.64:538.569.4 227
**A Frequency-Modulated Microwave Spectrometer for Electron-Resonance Measurements**—A. C. Rose-Innes. (*J. Sci. Instr.*, vol. 34, pp. 276–278; July, 1957.) The instrument is designed for use in the 3-cm band. Frequency modulation allows spectra to be recorded with simple equipment; details are given of a special technique for increasing the sensitivity. The instrument is especially suitable for measurements at low temperatures and for recording wide lines.

621.317.794 228
**Comparison of Subtraction-Type and Multiplier-Type Radiometers**—J. Galejs. (PROC. IRE, vol. 45, pp. 1420–1422; October, 1957.)

621.317.794.029.64 229
**A Calibration Procedure for Microwave Radiometers**—R. N. Whitehurst, F. H. Mitchell, and J. Copeland. (PROC. IRE, vol. 45, pp. 1410–1411; October, 1957.) A procedure allowing for the antenna side lobes in estimating radiation from a stellar source. Three measurements are made: one with the fixed antenna

pointing to the west of the source, one towards it, and one with the forward lobes absorbed. See also 2739 of 1957.

621.317.799:621.385.832 230
**An Electrostatic Cathode-Ray Tube Tester**—R. B. Hale. (*Brit. Commun. Electronics*, vol. 4, p. 496; August, 1957.)

## OTHER APPLICATIONS OF RADIO AND ELECTRONICS

621.373.52:612 231
**A Simple Physiological Stimulator, using a Transistor Oscillating Circuit**—W. T. Catton, L. Molyneux, and B. Schofield. (*Electronic Eng.*, vol. 29, pp. 496–498; October, 1957.)

621.373.52.029.3:53.087.25:616 232
**Monitoring of Low-Frequency Phenomena**—C. F. Rothe and M. W. Street. (*Science*, vol. 126, pp. 77–78; July 12, 1957.) A transistor regenerative oscillator has been adapted to convert subaudio frequencies into af for monitoring phenomena such as the electrical activity of the heart in a way more convenient than visual observation of instruments.

621.387:654.924.56 233
**The Ionization Fire-Alarm. Electronics in the Service of Fire Protection**—H. P. Halm. (*Elektronik*, vol. 6, pp. 205–207; July, 1957.) The apparatus described uses an ionization chamber in which the presence of combustion gases causes a change in the normal ionization produced by a radioactive source. Some recent refinements are discussed.

621.387.4:621.374.3 234
**Some Electronic Instruments used in Nuclear Spectroscopic Investigations**—B. Åström. (*Ark. Fys.*, vol. 12, Pt. 3, pp. 215–236; 1957.) A description is given of two complete sets of equipment: 1) an automatic scintillation spectrometer comprising scintillation detector and single channel pulse height analyzer, 2) an $\alpha$-particle spectrometer comprising ionization chamber and 50-channel pulse-height analyzer of stacked discriminator type. To facilitate maintenance and improve cooling, all tubes are mounted horizontally and concentrated in a ventilated space.

621.398:551.508.822 235
**Telemetering System is Balloon Borne**—E. K. Novak. (*Electronics*, vol. 30, pp. 158–164; September 1, 1957.) Description of fm/AM telemetry system for a weather radiosonde. It provides a 1680-mc carrier with three simultaneous channels one of which is time-multiplexed into 12 additional channels with sampling rate of one sample per minute; the maximum range is approximately 360 miles.

## PROPAGATION OF WAVES

621.396.11 236
**A New Solution of the Problem of Propagation over a Flat Earth**—G. Boudouris. (*Nuovo Cim.*, vol. 5, Supplement No. 1, pp. 71–91; 1957. In French.) Simplifications of classical theory are introduced in fixing the boundary conditions for the problem. This "method of approximate boundary conditions" is more convenient for practical applications.

621.396.11 237
**Electromagnetic Fields due to Current Flowing Parallel to Interface of Two Different Media**—K. Horiuchi. (*J. phys. Soc. Japan*, vol. 12, pp. 170–176; February, 1957.) Integral equations are established for various configurations. The results have applications in problems of wave propagation over an inhomogeneous earth, or through a stratified atmosphere.

621.396.11 238
**Fading of Radio Waves Scattered by Dielectric Turbulence**—R. A. Silverman. (*J. Appl. Phys.*, vol. 28, p. 922; August, 1957.) Note of corrections to 3274 of 1957.

621.396.11 239
**Short-Range Echoes Observed on Ionospheric Recorders**—R. L. Dowden. (*J. Atmos. Terr. Phys.*, vol. 11, no. 2, pp. 111–117; 1957.) Echoes from the 20–100-km region observed at ionospheric stations near the sea are found to arrive at very low angles of elevation with vertical polarization. They are due to coherent back scatter from sea waves of length $\lambda/2$.

621.396.11:551.510.52 240
**A New Technique for the Study of Scatter Propagation in the Troposphere**—J. H. Chapman, W. S. Haikkila, and J. E. Hogarth. (*Can. J. Phys.*, vol. 35, pp. 823–830; August, 1957.) Fluctuations of received field strength may be considered to have the characteristics of noise. Measurements on 500-mc near-optical links show the "propagations noise" power varies as $1/f^2$ for 0.1 cps$<f<$10 cps, $f$ being the difference between carrier and side-band frequencies.

621.396.11:551.510.535 241
**Refractive Corrections to Scatter Propagation**—A. D. Wheelon. (*J. Geophys. Res.*, vol. 62, pp. 343–349; September, 1957.) An examination of the role of the mean electron density of the ionosphere in scatter propagation. Correlations between the field strength of F-layer scattered signals and the maximum usable frequency for classical propagation along the path are studied.

621.396.11:551.510.535 242
**A Method for Obtaining L.F. Oblique-Incidence Reflection Coefficients and its Application to 135.6-kc/s Data in the Alaskan Area**—J. E. Bickel. (*J. Geophys. Res.*, vol. 62, pp. 373–381; September, 1957.)

621.396.11:551.510.535 243
**The Relation of Forward Scattering of Very High Frequency Radio Waves to Partial Reflection of Medium Frequency Waves at Vertical incidence**—J. B. Gregory. (*J. Geophys. Res.*, vol. 62, pp. 383–388; September, 1957.) Some characteristics of vhf forward scatter, such as temporal variations and the region of the ionosphere responsible, are shown to be similar to those of vertical-incidence reflection at 1.75 mc. It is considered that the two phenomena have a common origin.

621.396.11:551.510.535 244
**Studies of Transequatorial Ionospheric Propagation by the Scatter-Sounding Method**—O. G. Villard, Jr., S. Stein, and K. C. Yeh. (*J. Geophys. Res.*, vol. 62, pp. 399–412; September, 1957.) Long-delay echoes on a hf radar are interpreted as ground back scatter propagated by two or more successive reflections from the F region without intermediate ground reflection. Ionospheric tilts could lead to this type of propagation, which occurs regularly in equatorial regions.

621.396.11:551.510.535 245
**Self-Distortion of Radio Waves in the Ionosphere, near the Gyro Frequency**—F. H. Hibberd. (*J. Atmos. Terr. Phys.*, vol. 11, no. 2, pp. 102–110; 1957.) The theory described in 2198 of 1956 is extended to include the effect of the geomagnetic field near the gyro frequency. The reduction in modulation depth varies slowly with frequency and shows no resonance-like variation. The reduction is proportional to radiated power and decreases rapidly as the modulation frequency is increased.

621.396.11:551.510.535 246
**Ionospheric Demodulation of Radio Waves at Vertical Incidence**—G. J. Aitchison. (*Aust. J. Phys.*, vol. 10, pp. 204–207; March, 1957.) Agreement between observations and theory indicates that demodulation occurs in the E layer, affecting the wave on both upward and downward paths. The actual mechanism of the demodulation requires further investigation. See also 3070 of 1955 (Aitchison and Goodwin).

621.396.11:551.510.535:523.78 247
**Ionospheric Research**—Dale. (See 125.)

621.396.11.029.6 248
**Radio Propagation above 40 Mc/s over Irregular Terrain**—J. J. Egli. (Proc. IRE, vol. 45, pp. 1383–1391; October, 1957.) The available statistical wave-propagation data on terrain effects as a function of frequency, antenna height, polarization, and distance are analyzed and expressed by empirical formulas and in the form of nomographs and correction curves.

621.396.11.029.6:551.510.535 249
**Delayed Signals in Ionospheric Forward-Scatter Communication**—G. W. Luscombe. (*Nature, London*, vol. 180, p. 138; June 20, 1957.) Long-delay multipath effects observed at Slough in the reception of 37-mc pulsed transmissions from Gibraltar indicate that the signal with the largest delay was due to round-the-world propagation and that ground back scatter was not involved. See 1217 of 1957 (Crow, *et al*).

621.396.11.029.62:551.510.535:523.75 250
**Disturbances in the Lower Ionosphere Observed at V.H.F. following the Solar Flare of 23 February 1956 with Particular Reference to Auroral-Zone Absorption**—Bailey. (See 123.)

621.396.812.3:551.510.535 251
**Ionospheric Irregularities Causing Random Fading of Very Low Frequencies**—S. A. Bowhill. (*J. Atmos. Terr. Phys.*, vol. 11, no. 2, pp. 91–101; 1957.) An investigation, based on measurements at 75 and 150 kc, into the two component sources of random fading of signals reflected from the ionosphere: 1) scattering in the reflecting layer, 2) diffraction during propagation down to the ground.

## RECEPTION

621.376 252
**Intermodulation Products for $\nu$-Law Biased Wave Rectifier for Multiple-Frequency Input**—E. Feuerstein. (*Quart. appl. Math.*, vol. 15, pp. 183–192; July, 1957.) The intermodulation products obtained by passing the same of $N+1$ sinusoids of amplitudes $P_1, \ldots, P_N$ through a rectifier of characteristic

$$I=\begin{cases}10 & V<B\\ 1a(V-B)^{\nu} & V>B \quad \nu>0\end{cases}$$

have been expressed in terms of contour integrals involving products of Bessel functions [see, *e.g.*, 2169 of 1945 (Rice) and 3506 of 1947 (Bennett)]. These integrals are rewritten as improper integrals on the real line plus constant terms. These integrals converge fast enough in many cases to be useful in numerical integration.

621.376.23:621.396.822 253
**Optimum vs. Correlation Methods in Tracking Random Signals in Background Noise**—R. C. Davis. (*Quart. appl. Math.*, vol. 15, pp. 123–138; July, 1957.) A comparison of the use of statistical methods of analysis in estimating unknown parameters of probability distribution with the use of correlation methods previously applied to the problem of obtaining maximum snr.

621.376.332 254
**An Improved F. M. Discriminator**—V. B. Hulme. (*Electronic Eng.*, vol. 29, pp. 416–419; September, 1957.) Details are given of a constant-area type circuit which provides a relation to 0.1 per cent between input frequency and output voltage over the range 100 kc–1 mc.

621.396.62.029.6:621.396.822:621.317.3 255
**Absolute Measurement of Receiver Noise Figures at U.H.F.**—E. Maxwell and B. J. Leon. (IRE TRANS., vol. MTT-4, pp. 81–85; April, 1956. Abstract, PROC. IRE, vol. 44, p. 956; July, 1956.)

621.396.621 256
**Receiver Selectivity**—B. J. Rogers. (*RSGB Bull.*, vol. 32, pp. 444–448; April, 1957.) Some modern methods of improving the selectivity of communication receivers are described.

621.396.621 257
**F.M./A.M. "Second Set"**—G. D. Browne. (*Mullard tech. Commun.*, vol. 3, pp. 38–43; March, 1957.) Design suggestions for a simple and economical receiver in which all tubes are operative in both systems of reception.

621.396.621:621.314.7 258
**Design Considerations in the First Stage of Transistor Receivers**—L. A. Freedman. (*RCA Rev.*, vol. 18, pp. 145–162; June, 1957.) Noise performance of transistor rf stages using capacitive antennas and mixer stages with loop antennas is discussed with examples. Comparisons are made between transistor stages and corresponding tube stages.

621.396.621:621.314.7 259
**Circuit Techniques associated with Transistor Broadcast Receivers**—J. N. Barry. (*Electronic Eng.*, vol. 29, pp. 408–415 and 478–483; September and October, 1957.) A discussion of transistor circuit problems and their solution. The various stages of the receiver are considered and the economic aspects of using transistors are discussed with reference to the performance of 6 commercial-type portable and car receivers.

621.396.621:621.314.7 260
**The Thunderbird—a New Transistorized Portable Radio**—T. Vanacore. (*Sylvania Technologist*, vol. 10, pp. 35–37; April, 1597.)

621.396.621:621.376 261
**A New Method of Demodulation for Phase, Frequency and Amplitude**—P. Knudu. (*Indian J. Phys.* vol. 40, pp. 231–234; April, 1957.) Limiting and differentiating a modulated sinusoidal wave produces pulses with leading edges separated by an amount dependent upon the instantaneous phase of the modulated wave, and upon its amplitude if the limiting level is above the zero axis. The pulses are converted to variable-amplitude sawtooth waves and passed through a low-pass filter to reproduce the modulating signal. See also 551 of 1956.

621.396.621:621.396.822 262
**Receiver Detects Signals below Noise Level**—W. L. Blair. (*Electronics*, vol. 30, pp. 168–171; September 1, 1957.) The integrating receiver described uses a modified form of Dicke's technique (475 of 1947) with a comparison switching rate of 500 cps and a counter display.

621.396.621.029.63/.64 263
**Design for a Broadband Microwave Receiver**—B. Rosen and R. Saul. (*Electronic Inds. Tele-Tech.*, vol. 16, pp. 81–82, 170; March, 1957.) Brief description of a receiver covering the frequency range 950–11260 mc in four bands. It is suitable for AM, fm, and pm reception and for use as a microwave power meter.

621.396.8:621.3.018.41(083.74) 264
**Doppler Shift of the Received Frequency from the Standard Station Reflected by the Ionosphere**—I. Takahashi, T. Ogawa, M. Yamano, A. Hirai, and M. Takiuchi. (PROC. IRE, vol. 45, p. 1408; October, 1957.) Equipment for recording frequency continuously is described, and results of Doppler-shift measurements made on waves reflected from the E region on 4 mc over a 400-km path are given.

621.396.8:621.396.931.029.62/.63 265
**Propagation Tests of Frequencies for V.H.F. Mobile Radio**—E. Shimizu, T. Morinaga, T. Kawano, S. Sato, and M. Hirasaki. (*Rep. elect. Commun. Lab., Japan*, vol. 5, pp. 13–16; January, 1957.) Measurements are given of signal and noise received at a mobile station from fixed transmitters in Tokyo operating at 60, 200, and 470 mc. Less fluctuation was observed than in comparable U. S. measurements, and this is attributable to the wooden houses normal in Japan.

621.396.812.3:621.396.666.029.64 266
**Some Results with Frequency Diversity in a Microwave Radio System**—F. H. Willis. (*Commun. and Electronics*, no. 29, pp. 63–67; March, 1957.) The results of tests with 240-mc frequency separation and an appreciable switching differential are discussed.

## STATIONS AND COMMUNICATION SYSTEMS

621.39.001.11:621.372.012 267
**Signal-Flow Graphs and Random Signals**—L. A. Zadeh and W. H. Huggins. (PROC. IRE, vol. 45, pp. 1413–1414; October, 1957.) Comments on 1227 of 1957 and author's reply.

621.394.3:621.394.828 268
**Distortion Correction of Teleprinter Signals by Electronic Means**—E. K. Aschmoneit. (*Elektronik*, vol. 6, pp. 199–203 and 244–245; July and August, 1957.) The principles and circuits of some electronic distortion-correcting and regenerative repeaters are described.

621.396.41:621.396.324:621.314.7 269
**Transistorized Multiplex Radio-Teletypewriter**—P. G. Wray. (*Electronics*, vol. 30, pp. 150–154; September 1, 1957.) Lightweight four-channel time-division multiplex equipment for use on board ship is described. Ring counter and digital synchronizer circuits using transistors give an operating speed of 100 words per minute.

621.396.41.029.63 270
**Ultra-high-Frequency Radio Equipment for 60 Speech Circuits**—(*GEC Telecommun.*, no. 22, pp. 34–49; August, 1956.) The Type-SPO 5500 equipment described uses fm and operates in the band 1700–2300 mc. Up to three rf channels each carrying 60 speech channels can be arranged in multiplex.

621.394.441 271
**An Electronic Error-Correcting Multiplex Telegraph System**—(*P.O. Elec. Eng. J.*, vol. 50, Pt. 1, p. 44; April, 1957.)

621.396.5.029.6:621.396.822 272
**Noise Considerations on Toll Telephone Microwave Radio Systems**—T. A. Combellick and M. E. Ferguson. (*Commun. and Electronics*, no. 29, pp. 67–70; March, 1957.) The noise level requirements for microwave radio equipment to be used in multichannel telephone systems are discussed. The magnitude of and relation between the noise generated in the transmitter, in the receiver, or by intermodulation, are examined.

621.396.71.029.55 273
**The Rugby "B" High-Frequency Transmitting Station**—A. Cook and L. L. Hall. (*P.O. Elec. Eng. J.*, vol. 50, Pt. 1, pp. 15–23; April, 1957.) The layout and technical facilities of the station are described. There are 28 hf transmitters of 30-kw power rating in operation and some 70 antennas on a site of 700 acres. See also 2538 of 1956 (Booth and MacLarty).

621.396.74:621.397.743 274
**Frequency Transposers as Very-Low-Power Transmitters**—A. Kolarz. (*Rundfunktech. Mitt.*, vol. 1, pp. 53–57; April, 1957.) A 50-mw relay transmitter for providing a local television service is described. The transposition from received to transmitted frequency is made without the use of an IF. See also 1927 of 1957.

621.396.74.029.62:621.376.3 275
**Investigation of Coverage Facilities with Frequency-Offset U.S.W. F.M. Operation**—E. Belger, E. Paulesn, and L. Dahrendorf. (*Rundfunktech. Mitt.*, vol. 1, pp. 58–64; April, 1957.) The limitations and advantages of this method of obtaining regional coverage are discussed with reference to experimental results. See also 1869 of 1956 (Belger and von Rautenfeld).

621.396.931 276
**Radio Communication in Railroad Tunnels**—H. S. Winbigler. (*Bell Lab. Rec.*, vol. 35, pp. 57–60; February, 1957.) Radiation from a continuous length of twin transmission line suspended from the tunnel wall is received satisfactorily up to 5000 feet from the transmitter, using frequencies in the 159–162-mc band.

621.396.932 277
**Ships and Coast Stations**—P. N. Spooner. (*Short Wave Mag.*, vol. 14, pp. 636–639; February, 1957.) Details of systems, procedure, operating frequencies, and general organization.

621.396.945 278
**The Guided Radio Telephone**—W. H. Hill. (*A.T.E.J.*, vol. 13, pp. 113–118; April, 1957.) This communication system uses currents induced in metallic conductors by the transmitter. A satisfactory portable transmitter/receiver is described for use in coal mines.

## SUBSIDIARY APPARATUS

621.3–71 279
**Removal of Heat from Sealed Miniature Equipment**—E. P. Newell. (*Brit. Commun. Electronics*, vol. 4, pp. 468–475; August, 1957.) Experimental investigation has shown that the most satisfactory way of dissipating the heat generated internally is by providing thermal conduction paths from the heat sources to the front panel.

621.311.6:537.311.33:535.215 280
**Utilizing the Sun's Energy**—(*Elec. J.*, vol. 159, pp. 1256–1257; November 1, 1957.) Report on progress in the development of solar batteries of the Si *p-n*-junction type with description of experimental installations in England.

621.311.6:621.314.7 281
**A Stabilized D.C. Power Supply using Transistors**—T. H. Brown and W. L. Stephenson. (*Electronic Eng.*, vol. 29, pp. 425–428; September, 1957.) A mains-operated unit is described which provides an output voltage variable from 0 to 30 v at currents of up to 1 a.

621.314.63:546.289 282
**Germanium Rectifiers as Electronic Components**—J. T. Cataldo. (*Electronic Inds.*

*Tele-Tech.*, vol. 16, pp. 61–63, 168; August, 1957.) Discussion of advantages and applications. Cooling methods and overload characteristics are considered.

621.316.722.1:621.314.7 283
**A Low-Voltage Stabilizer employing Junction Transistors and a Silicon Junction Reference Diode**—D. Aspinall. (*Electronic Eng.*, vol. 29, pp. 450–454; September, 1957.)

621.316.722.1:621.314.7 284
**Voltage Regulator uses Multivibrators**—W. A. Scism. (*Electronics*, vol. 30, pp. 184–186; September 1, 1957.) Voltage changes vary the frequency of an astable transistor multivibrator and the average value of the load voltage is thus kept constant.

621.396.662.029.5 285
**Multichannel Drives for Transmitters and Receivers in the H.F. Band**—D. J. Fewings. (*Marconi Rev.*, vol. 20, pp. 60–76; 2nd Quart., 1957.) Methods of tuning accurately to a prescribed frequency are described, as applied to 1) a diversity oscillator with manual tuning, 2) an automatically tuned airborne receiver /transmitter drive.

621.396.664:621.376 286
**Monitoring the Modulator**—P. M. Carment. (*Short Wave Mag.*, vol. 14, pp. 631–632; February, 1957.) A circuit for monitoring the output of a high-power modulator on a pair of headphones.

## TELEVISION AND PHOTOTELEGRAPHY

621.397:628.93 287
**Techniques of Television Lighting**—D. Thayer. (*J. Soc. Mot. Pict. Telev. Eng.*, vol. 66, Pt. 1, pp. 212–216; April, 1957.)

621.397.2:621.372.55 288
**Error-Predicting D.C.-Restoring Circuits for Television Signals**—E. L. C. White. (*Electronic Eng.*, vol. 29, pp. 472–477; October, 1957.) The performance of direct and negative-feedback types of dc restoring circuit is analyzed. By a combination of slope equalization and error prediction the low-frequency cutoff of the circuit prior to dc restoration may be raised by a large factor. Some experimental results are given.

621.397.24 289
**Performance of the A2A Video Transmission System**—R. W. Edmonds. (*Bell Lab. Rec.*, vol. 35, pp. 85–88; March, 1957.) Design considerations and performance details of a broadband local wire transmission system for monochrome and color television.

621.397.24:621.315.212 290
**A New 4-Mc/s Coaxial Line Equipment—C. E. L. No. 6A**—Collier and Simpson. (See 14.)

621.397.24:621.315.212 291
**A 4-Mc/s Coaxial Line Equipment—C.E.L. No. 4A**—E. Davis. (See 15.)

621.397.242 292
**Television Terminals for the L3 System**—J. J. Jansen. (*Bell Lab. Rec.*, vol. 35, pp. 179–183; May, 1957.) 600 telephone channels and a 4.2-mc television channel may be transmitted by the coaxial cable system the terminal equipment of which is described.

621.397.5:535.623 293
**Some Alternatives to the N.T.S.C. Colour Television System**—E. L. C. White. (*J. Telev. Soc.*, vol. 8, pp. 191–206; January/March, 1957.) The NTSC system is compared with the two-subcarrier, the French L.E.P. "3 double-message," and the Valensi systems. For a three-gun picture tube, the first system seems most satisfactory. The signal requirements of single-gun tubes, such as the chromatron and "apple" tubes, are then discussed; here a symmetrical ratio system may be better.

621.397.5:621.395.625.3 294
**Video Tape Recorder Design**—(*J. Soc. Mot. Pict. Telev. Eng.*, vol. 66, Pt. 1, pp. 177–188; April, 1957.) Three papers, describing equipment incorporating a system of four magnetic recording heads on a revolving drum for recording transverse tracks on tape traveling at 15 inches per second. See also 4018 of 1957 (Snyder).

**Comprehensive Description of the Ampex Video Tape Recorder**—C. P. Ginsburg (pp. 177–182).

**The Modulation System of the Ampex Video Tape Recorder**—C. E. Anderson (pp. 182–184).

**Rotary-Head Switching in the Ampex Video Tape Recorder**—R. M. Dolby (pp. 184–188).

621.397.5(083.74) 295
**Comparison of Four Television Standards**—R. D. A. Maurice. (*Electronic Radio Eng.*, vol. 34, pp. 416–421; November, 1957.) "The resolutions of four CCIR standard television systems are compared, some account being taken of the effects of the asymmetric side-band reception. The extent to which some of the distortions may be due to nonlinearity of the phase-frequency characteristic is briefly mentioned."

621.397.611:778.5 296
**The Limits of Optical Compensation by Polygonal Prisms in relation to Freedom from Flicker, Registration and Relative Aperture**—H. Grabke. (*Rundfunktech. Mitt.*, vol 1, pp 65–72; April, 1957.) Theoretical treatment of the problem based on earlier experiments with film scanning equipment (1227 of 1956). The design of a "polygon-ring scanner" is discussed and data for calculating tolerances and color correction of the system are given. The manufacture of such a scanner with 40–60 faces appears feasible; it should produce satisfactory pictures comparable to those obtained by other flying-spot scanners.

621.397.621.2 297
**Television Frame Pulse Separator**—H. D. Kitchin. (*Wireless World*, vol. 63, pp. 554–559; November, 1957.) A single-pulse circuit for accurate interlacing is described.

621.397.621.2 298
**The Return of Electrostatic Focusing**—R. R. Pearce. (*J. Telev. Soc.*, vol. 8, pp. 237–248; April/June, 1957.) A survey of the developments in post-war television tubes and techniques with a detailed discussion of the characteristics and relative merits of modern electrostatic guns.

621.397.82 299
**The Visibility of Sinusoidal Interference in Television Images**—H. Grosskopf and R. Suhrmann. (*Rundfunktech. Mitt.*, vol. 1, pp. 45–52; April, 1957.) The nature of interference patterns is reviewed and the effects of interference due to frequencies which are specially related to line or frame frequency are examined. Curves for evaluating some of these effects are given and the requisite "safe" frequency spacing between adjacent transmitters is compared with that recommended by CCIR.

## TRANSMISSION

621.396.61.029.6:621.396.662 300
**Transmitter Tuned by Distortion Indicator**—C. R. Ellis, K. Owen, and G. R. Weatherup. (*Electronics*, vol. 30, pp. 180–183; September 1, 1957.) The system described gives harmonic distortion of less than 3 per cent rms over the range 200 cps–20 kc when the transmitter is operated at 225–400 mc, with 80 per cent AM of a 1-kw carrier.

621.396.61.072.9 301
**A New Device for the Automatic Radio-Frequency Synchronization of Common-Frequency Broadcasting in the Medium-Wave Band**—A. Karaminkov. (*Nachr-Tech.*, vol. 7, pp. 163–166; April, 1957.) In the system proposed synchronization is carried out by radio transmission during breaks in the program. During these interruptions of about 12-seconds duration which are intentionally introduced at intervals of about 1 hour, the carrier of the local transmitter is stopped so that the distant master transmitter can be received for the automatic frequency correction of the local carrier. Using quartz oscillators with long-term stability 1 part in $10^6$ an hourly stability within about 1 part in $10^8$ can be achieved.

## TUBES AND THERMIONICS

621.314.63:621.317.3 302
**Measurements of Crystal Impedances at Low Levels**—H. N. Dawirs and E. K. Damon. (IRE TRANS., vol. MTT-4, pp. 94–96; April, 1956. Abstract, PROC. IRE, vol. 44, p. 956; July, 1956.

621.314.63:621.372.632 303
**The Frequency Dependence of Noise Temperature Ratio in Microwave Mixer Crystals**—M. E. Sprinks, G. T. G. Robinson, and B. G. Bosch. (*Brit. J. Appl. Phys.*, vol. 8, pp. 275–277; July, 1957.) A discussion with experimental results of the contribution of the noise temperature ratio of the mixer to the over-all noise factor of the receiver. The latter has an intermediate frequency in the range 10–60 mc.

621.314.7 304
**Some Aspects of Transistor Progress**—H. W. Loeb. (*A.T.E.J.*, vol. 13, pp. 119–134; April, 1957.) Reprint. See 295 of 1957.

621.314.7 305
**Heat Sinks for Power Transistors**—O. J. Edwards. (*Mullard tech. Commun.*, vol. 3, pp. 59–61; March, 1957.) Sinks of mild steel and aluminum are examined and the effects of thickness, area, and surface treatment are discussed.

621.314.7 306
**Design Theory for Depletion-Layer Transistors**—W. W. Gärtner. (PROC. IRE, vol. 45, pp. 1392–1400; October, 1957.) This new type of high-frequency transistor uses maximum attainable carrier velocities in solids by injecting electrons or holes into the high electric fields prevailing in properly designed depletion layers of reverse-biased *p-n* junctions. Low- and high-frequency performance, small-signal behavior, power gain, and stability are discussed in a particular theoretical design. The short transit times should be important for solid-state microwave amplification.

621.314.7 307
**Design for an Improved High-Frequency Transistor**—C. Thornton, J. Roschen, and T. Miles. (*Electronic Inds. Tele-Tech.*, vol. 16, pp. 47–49, 124; July, 1957.) The construction and properties of the Type L-6100 silicon surface-alloy transistor are described. It has a base width of $7\times10^{-5}$ inches and a maximum oscillation frequency of about 16 mc.

621.314.7 308
**The Junction Transistor as a Charge-Controlled Device**—R. Beaufoy and J. J. Sparkes. (*A.T.E.J.*, vol. 13, pp. 310–327; October, 1957.) Transistor operation is described in terms of the charge in the base region so that the transistor performance is defined in the form of time constants (pc/$\mu$a). The analysis was developed for large-signal opera-

tion but yields complete expressions for small-signal admittance parameters. Methods of measurement are outlined.

621.314.7 309
**Flow Line Analysis**--R. B. Hurley. (*Electronic Inds. Tele-Tech.*, vol. 16, pp. 52–54, 140; April, 1957.) A pictorial representation of the expressions derived by Ebers and Moll (884 of 1955) to analyze transistor behavior in various types of switching circuit.

621.314.7:546.289 310
**Influence of Surface Oxidation on Alpha$_{cb}$ of Germanium *p-n-p* Transistors**—J. T. Wallmark. (*RCA Rev.*, vol. 18, pp. 255–271; June, 1957.) Oxidation of the Ge surface is shown to be a major factor influencing surface recombination and thereby the slow decay of the current transfer ratio $\alpha_{cb}$ in *p-n-p* transistors. An outline of the underlying processes is given.

621.314.7:621.317.3 311
**Transistor Tests Predict High-Frequency Performance**—Pritchard. (See 213.)

621.314.7:621.318.57 312
**Determination of Transient Response of a Drift Transistor using the Diffusion Equation**—H. B. von Horn and W. Y. Stevens. (*IBM J. Res. Devel.*, vol. 1, pp. 189–191; April, 1957.) The one-dimensional diffusion equation is solved to give the time required for the collector current to reach a steady value in response to a step function of emitter current.

621.314.7:621.373.51 313
**Unique Properties of the Four-Layer Diode**—W. Shockley. (*Electronic Inds. Tele-Tech.*, vol. 16, pp. 58–60, 165; August, 1957.) Description of a new bistable two-terminal semiconductor device and details of some of its applications. See also 3899 of 1956 (Moll, *et al*).

621.314.7:681.142 314
**The Multipurpose Bias Device: Part 1—The Commutator Transistor**—Dunham. (See 38.)

621.314.7:681.142 315
**Two-Collector Transistor for Binary Full Addition**—R. F. Rutz. (*IBM J. Res. Devel.*, vol. 1, pp. 212–222; July, 1957.) Two versions of a two-collector transistor are described, one using point contacts, and the other using *p-n* "hook" junctions as collectors. The function of such a transistor as a binary adder and its circuit characteristics are discussed. See also 38 above.

621.314.7(083.7) 316
**Semiconductor Symbols**—P. M. Thompson and J. Bateson. (*Wireless World*, vol. 63, pp. 525–528; November, 1957.) A logical system for diodes, transistors, and other junction devices is proposed.

621.383.27 317
**Photomultiplier Tubes**—J. Sharpe. (*Brit. Commun. Electronics*, vol. 4, pp. 484–492; August, 1957.) The design and applications of the various types of photomultiplier tube are described. A table of representative tubes available in the U. K. is given.

621.383.27:621.387.464 318
**Improved Performance of Photomultipliers in Scintillation Counters**—A. Ashmore, B. Collinge, and S. K. Sen. (*Indian J. Phys.*, vol. 40, pp. 261–264; May, 1957.) A cathode follower reduces the effective capacitance to earth of the collecting electrode of a photomultiplier, enabling bigger voltage pulses to be obtained for the same degree of nonlinearity in the photomultiplier.

621.383.4:535.371.07 319
**An Improved High-Gain Panel Light Amplifier**—B. Kazan. (PROC. IRE, vol. 45, pp. 1358–1364; October, 1957.) A grooved photoconductor light-amplifying picture panel is described, whose gain is more than 10 times greater than any previous amplifier and whose threshold for input light is reduced. See also 933 of 1956 (Kazan and Nicoll).

621.385:621.317.321 320
**A Survey of Methods Used to Determine Contact Potentials in Receiving Tubes**—E. R. Schrader. (*RCA Rev.*, vol. 18, pp. 243–254; June, 1957.)

621.385:621.317.444 321
**Rectilinearity of Electron-Beam Focusing Fields from Transverse Component Determinations**—Cioffi. (See 222.)

621.385.029.6 322
**Investigation of a Special Type of Reflex Klystron**—W. N. Shevchik, S. A. Suslov, and Yu. D. Zharkov. (*Zh. Tekh. Fiz.*, vol. 27, pp. 377–386; February, 1957.) A theoretical and experimental investigation of a reflex klystron operating with a large transit angle ($>2\pi$) in the interaction space is described. Good agreement is found between the theoretical evaluation of the tube efficiency and the experimental results.

621.385.029.6 323
**On the Nonlinear Behavior of Electron-Beam Devices**—F. Paschke. (*RCA Rev.*, vol. 18, pp. 221–242; June, 1957.) The nonlinear space-charge-wave equation is derived and reduced by third-order successive approximation to three simultaneous linear differential equations which are solved for the case of a velocity-modulated electron beam. Nonlinear phenomena in traveling-wave tubes can be treated similarly.

621.385.029.6 324
**Electron Beam Focusing in Three-Anode Guns for Travelling-Wave Tubes**—T. S. Chen and L. Kovach. (*J. Electronics Control*, vol. 3, pp. 287–304; September, 1957.) The electron trajectory in the accelerating region is solved and beam rippling in the drift region discussed. The principle of compensated three-anode guns is developed in the form of design formulas and curves. Experiments confirm that compensated guns result in a reduction of the focusing magnetic field for parallel-flow beams.

621.385.029.6 325
**The Large-Signal Behaviour of Crossed-Field Travelling-Wave Devices**—J. Feinstein and G. S. Kino. (PROC. IRE, vol. 45, pp. 1364–1373; October, 1957.) The limits of validity of the conventional small-signal theory are obtained theoretically, and the analysis is extended to follow the interaction to power saturation. Forward-wave and backward-wave amplifiers and a backward-wave oscillator are considered. In the amplifier tubes the gain is inherently low, and suggestions for improving this deficiency are examined.

621.385.029.6 326
**An Experimental High-Power Pulsed Travelling-Wave Tube**—J. F. Gittins, N. H. Rock, and A. B. J. Sullivan. (*J. Electronics Control*, vol. 3, pp. 267–286; September, 1957.) A high-impedance slow-wave structure with good thermal dissipation and suitable for a 100-kv electron beam is used. A saturated efficiency of 34 per cent, power output of 3 mw, and a gain of 35 db are obtained.

621.385.029.6:621.372 327
**Interdigital and other Slow-Wave Structures**—J. C. Walling. (*J. Electronics Control*, vol. 3, pp. 239–258; September, 1957.) A method of calculating the properties of structures consisting of arrays of parallel conductors is developed and a table of numerical values is presented. This is applied to obtain dispersion characteristics, input and beam-coupling impedances for the Karp structure, interdigital line, and tape helix.

621.385.029.6:621.376 328
**The Modulation of Travelling-Wave Tubes**—G. F. Steele. (*Electronic Eng.*, vol. 29, pp. 429–433; September, 1957.) "The simple theory of traveling-wave tube modulation is discussed and some expressions derived for the cases of phase and amplitude modulation. Details are given of the experimental procedure used to measure phase shift and the side-band power resulting from a 60-mc modulation."

621.385.029.64 329
**Velocity-Jump Amplification at 10000 Mc/s**—B. V. Dore. (*Can. J. Phys.*, vol. 35, pp. 742–752; June, 1957.) Description of a vm tube based on an earlier design [2068 of 1951 (Field, *et al*)]. Theory previously developed for space-charge-wave amplifiers is applied to its operation and conclusions are drawn regarding the operation of coupling helices and the effect of small gaps in the amplifying section of the tube. See also 3721 of 1954 (Agdur).

621.385.832:621.317.799 330
**An Electrostatic Cathode-Ray-Tube Tester**—R. B. Hale. (*Brit. Commun. Electronics*, vol. 4, p. 496; August, 1957.)

## MISCELLANEOUS

621.39(091) 331
**Fifty Years of the Institution of Post Office Electrical Engineers**—(*P.O. Elec. Eng. J.*, vol. 49, Pt. 3, pp. 147–274; October, 1956.) A number of papers surveying the history and activities of the Institution and detailing its achievements in all fields of telecommunications.